METHODS IN MOLECULAR MEDICINE™

Tumor Necrosis Factor

Methods and Protocols

Edited by

Angelo Corti
Pietro Ghezzi

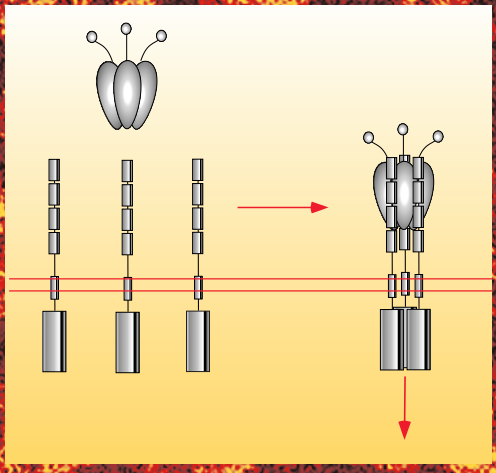

HUMANA PRESS

1

Tumor Necrosis Factor as a Pharmacological Target

Pietro Ghezzi and Anthony Cerami

Summary

Tumor necrosis factor (TNF) was originally described as a molecule with antitumor properties released by macrophages stimulated with bacterial products. Almost at the same time that TNF was cloned, it was found to be identical to cachectin, a mediator of cachexia. After the finding of this second aspect of TNF action, several studies demonstrated its role as a proinflammatory cytokine. These studies led to the use of anti-TNF molecules in rheumatoid arthritis and Crohn's disease. The various strategies used to inhibit TNF are summarized.

Key Words: Pharmacology; cachexia; sepsis; endotoxin.

1. History of TNF

1.1. The Era of Soluble Mediators and the Magic Bullets Against Cancer

The 1970s and 1980s were the golden age of cytokines, during which the biochemical nature of several soluble mediators was clarified. Cellular immunologists then identified macrophage-derived mediators that activate lymphocytes (lymphocyte-activating factors, or LAFs), along with lymphocyte-derived mediators that activate macrophages (macrophage-activating factors, or MAFs). These molecules added to the list of mediators defined as growth factors, which include hematopoietic growth factors (that now retain those names: G-CSF, GM-CSF, EPO), and interferons (described as antiviral factors in the late 1950s). One particularly active field was the research of soluble mediators that could kill tumor cells or boost anticancer defenses. Along this line, earlier studies focused on a lymphocyte-derived cytotoxin termed *lymphotoxin (LT)*, and research led to the discovery of a serum factor capable of inducing hemor-

From: *Methods in Molecular Medicine, Vol. 98: Tumor Necrosis Factor*
Edited by: A. Corti and P. Ghezzi © Humana Press Inc., Totowa, NJ

rhagic necrosis of tumors in vivo and of killing tumor cells in vitro. This factor was termed tumor necrosis factor (TNF) and was shown to be mainly a macrophage product, as opposed to LT. In 1985 several groups reported the cloning of human and mouse TNF and the ability of recombinant TNF to induce hemorrhagic necrosis of tumors in mice. It would not have been easy, 15 years ago, to predict that the main clinical application of the discovery and characterization of TNF would consist of the administration of anti-TNF molecules for the therapy of rheumatoid arthritis and Crohn's disease. In fact, TNF turned out to be a key pathogenic mediator with pleiotropic activities, and its history and path, from immunity to inflammation, was very similar to that of interleukin (IL)-1. The fact that the characterization of the inflammatory action of TNF stemmed from studies on models of sepsis was also unexpected.

1.2. From Cancer and Immunity to Endotoxic Shock and Septic Shock

Studies on the molecular basis of cachexia associated with sepsis led to the finding that macrophages activated with endotoxin and used to reproduce settings of septic shock, release a factor that is cachectogenic in vivo and inhibits ipogenesis in cultured adipocytes. We termed this factor "cachectin," and then we purified it, we found that it was identical to TNF.

These earlier studies pointed out a pathogenic role for TNF in sepsis and inflammation, which was confirmed by earlier clinical trials with rTNF in cancer patients showing toxicity in phase I and II studies. The first studies of neutralization of endogenous TNF have shown that this cytokine is a lethal mediator associated with toxicity of endotoxin ***(1)*** and septic shock induced by live bacteria ***(2)***. These studies have pointed at the possible use of anti-TNF antibodies in the therapy of septic shock. However, the clinical trials conducted so far have not indicated a clear efficacy of anti-TNF in septic shock.

Indeed, after a period of great enthusiasm, during which septic shock was considered the prototypic cytokine-mediated disease, most of the big pharmaceutical companies became daunted by the complexity of this pathological condition, which is associated with other diseases such as cancer, trauma, or burn injury. Some attempts have been toward a narrower definition of the component of septic shock, including acute respiratory distress syndrome (ARDS) and multiple organ failure (MOF), in which cytokines play an important role. In 1992 the American College of Chest Physicians and the Society of Critical Care Medicine Consensus Conference introduced the term "systemic inflammatory response syndrome" (SIRS) ***(3)***. Despite these difficulties, the scientists working in the field of cytokines and inflammation have continued using the models of lipopolysaccharide (LPS) toxicity as a means of inducing a systemic inflammatory response (to stick to the above definition).

1.3. Lipopolysaccharide Toxity As a Model of Inflammation

Studies of the role of TNF and IL-1 in septic shock have stimulated a large amount of research on these cytokines in several models of inflammation. Effects of TNF administration have been demonstrated in various models in vivo and in vitro, and increased TNF production has been reported in patients or animal models of diseases including rheumatic diseases.

Soon after cytokines were characterized, their involvement in arthritis was suggested. In the same years that TNF was cloned, J. M. Dayer et al. ***(4)*** and J. Saklatvala et al. ***(5)*** reported that TNF was able to induce prostaglandin and collagenase production by synovial cells and to stimulate resorption in cartilage, and they suggested its pathogenic role in rheumatoid arthritis.

The development of anti-TNF antibodies was the first strategy to inhibit TNF (*see* **Subheading 1.2.**) Anti-TNF antibodies, then soluble TNF receptors (*see* **Subheading 2.1.**), and, more recently, IL-1ra are now approved drugs for the therapy of rheumatoid arthritis and/or Crohn's disease.

Retrospectively, one can say that the models of LPS toxicity in vivo have been predictive of an anti-inflammatory action in diseases where inflammation is induced in the absence of sepsis.

2. Endogenous TNF Inhibitors and Inhibitory Pathways

It is impossible to cite all the molecules that have been shown to inhibit TNF production or action. The endogenous inhibitors of TNF are particularly interesting from the perspective of basic research and immunopathology, but they are also of pharmacological interest. One inhibitor, sTNFR, which is now a widely used anti-TNF drug, is of particular interest.

2.1. Soluble Receptors

As early as 1988, J. M. Dayer et al. reported the existence of a TNF inhibitor in human urine ***(6)***, which was soon identified as a soluble form of the TNF receptor ***(7,8)***. As a consequence of these studies, administration of recombinant soluble TNF receptor, both the native molecule and an engineered Fc fusion protein developed to increase the plasma half-life, were tested in models of disease and are at the basis of the current use of these molecules in patients with inflammatory diseases.

2.2. Glucocorticoids and the Neuroendocrine System

Glucocorticoids were the first inhibitors of TNF production reported ***(9)***. Their action is mediated by the glucocorticoid (GC) receptor and reversed by the GC-receptor antagonist mifepristone ***(10)***. It should be noted that other

steroids, namely neurosteroids, inhibit TNF production by a GC-receptor-independent mechanism ***(11)***.

Endogenous glucocorticoids probably represent the most important feedback system to limit TNF production, as demonstrated by the augmentation of TNF-mediated endotoxic shock in adrenalectomized mice, which has been known for a long time ***(12,13)***, and by similar results obtained with mifepristone ***(14,15)***. It is now recognized that TNF increases serum GC levels through activation of the hypothalamus pituitary adrenal axis ***(16)***.

2.3. Prostaglandins and Cyclic AMP

The inhibitory effect of the phosphodiesterase inhibitors on TNF production was described soon after the discovery of TNF. In particular, pentoxifylline and rolipram have been widely used to inhibit TNF production in several animal models. Their inhibition is mediated by the increase in intracellular cyclic AMP (cAMP). Likewise, other agents that augment intracellular cAMP (particularly prostaglandin E_2) inhibit TNF production.

In fact, prostaglandin E_2 is another very important feedback inhibitor of TNF production (and that of other cytokines) because inhibitors of prostaglandin synthesis augment cytokine production in most models ranging from in vitro systems ***(17)*** to human volunteers injected with LPS and in vivo tests ***(18,19)***. (The cyclooxygenase inhibitors are also known as nonsteroidal anti-inflammatory drugs, or NSAIDs.) This effect demonstrates that prostaglandin E2 endogenously produced during inflammation effectively switches off TNF synthesis.

Based on these findings, several clinical trials have been initiated using phosphodiesterase inhibitors to augment intracellular cAMP, such as rolipram or pentoxyfilline. Clearly, this approach is not specific for TNF.

2.4. "Anti-inflammatory Cytokines"

IL-10 and IL-4 are the prototypic "anti-inflammatory cytokines" and inhibit TNF production in vitro and in vivo ***(20–22)***. This effect was later demonstrated with IL-13 ***(23)*** and other cytokines of the so-called IL-10 family ***(24)***. These anti-inflammatory cytokines are being investigated as possible anti-inflammatory drugs. (According to PubMed, the term anti-inflammatory cytokine was actually first used for IL-4; *see* **ref. *22***.)

2.5. The Cholinergic Anti-Inflammatory Pathway

Studies by K. J. Tracey et al. ***(25,26)*** using vagotomized animals or electrical stimulation of the vagus nerve have shown that efferent activity in this nerve inhibits TNF production and has anti-inflammatory actions.

This pathway has been termed the "cholinergic anti-inflammatory pathway" because inhibition of TNF synthesis is mediated by acetylcholine acting on

nicotinic-bungarotoxin-sensitive acetylcholine receptors on macrophages. This finding provides a new means of inhibiting TNF production by electrical or chemical methods.

3. Other TNF Inhibitors

It is no surprise that the effectiveness of recombinant proteins acting as TNF inhibitors has prompted the investigation of small-molecular-weight drugs that might be administered orally to act as inhibitors of TNF production or action.

Several classes of drugs have been reported to act in this context, but none, as far as we know, are specific for TNF. In particular, no small TNF-receptor antagonists have been described to the best of our knowledge. A (partial) list of drugs, or classes of drugs, that reportedly inhibit either TNF production or TNF action and that have been shown to be efficacious in animal models of inflammation are presented in the subsections below.

3.1. Inhibitors of NF-κB

Nuclear factor-kappa B (NF-κB) is a transcription factor implicated in the expression of several inflammatory genes, including TNF, and it is regarded as a major pharmacological target for anti-inflammatory drugs. A long list of well-known molecules were reported to inhibit NF-κB, including antioxidants ***(27)***, glucocorticoids ***(28)***, aspirin, and salicylates ***(29)***.

3.2. Metalloprotease Inhibitors

TNF α is synthesized as a membrane-anchored translation product. It is processed to mature TNF, which is then released, by TNF-α-converting enzyme (TACE), a membrane protease in the class of the ADAM proteases (which contain *a d*isintegrin and *a m*etalloprotease domain). Inhibitors of TACE are thus potential anti-TNF molecules, and some have been shown active in various animal models of TNF-mediated pathologies ***(30)***.

3.3. Thalidomide

This older drug was shown to inhibit TNF production in 1991 ***(31,32)***. It is now considered for rheumatoid arthritis and Crohn's disease, and the search for analogs without the teratogenic properties of this drug is being actively pursued.

3.4. p38 Mitogen-Activated Protein Kinase (MAPK) Inhibitors

Unlike the cAMP pathways, the p38 MAPK pathway has been identified only after the discovery of TNF and IL-1. This kinase was originally described by J. C. Lee et al. ***(33)***. By studying the mechanism of action of a new series of compounds acting as cytokine synthesis inhibitors, the authors identified p38

MAPK by photoaffinity labeling. This kinase was soon identified as a key step in the pathway leading to cytokine production and action.

Another compound that was described as an inhibitor of TNF production and was then found to act probably by inhibiting p38 MAPK is the guanylhydrazone CNI-1493 ***(34,35)***. CNI-1493 showed promising activity in patients with Crohn's disease ***(36)***.

4. Conclusions: Back to Immunity and Host Defense?

Although this short historical overview has focused on the inflammatory actions of TNF and on anti-TNF strategies, it is important to remember that TNF is also a notable mediator in host defense and innate immunity.

These characteristics are probably exemplified by the increased incidence of infections in arthritis patients given anti-TNF molecules, an observation that is now incorporated in the prescription information for these drugs, advising to avoid use in patients with underlying sepsis. Although this finding is not totally unexpected, in that other drugs, namely methotrexate and glucocorticoids, are by definition immunosuppressive drugs, it reinforces the animal data showing that TNF is a key molecule in innate immunity to infection. Nevertheless, the successful therapeutic application of anti-TNF molecules for a variety of diseases stresses the deleterious effects of its overproduction.

References

1. Beutler, B., Milsark, I. W., and Cerami, A. C. (1985) Passive immunization against cachectin/tumor necrosis factor protects mice from lethal effect of endotoxin. *Science* **229,** 869–871.
2. Tracey, K. J., Fong, Y., Hesse, D. G., Manogue, K. R., Lee, A. T., Kuo, G. C., et al. (1987) Anti-cachectin/TNF monoclonal antibodies prevent septic shock during lethal bacteraemia. *Nature* **330,** 662–664.
3. American College of Chest Physicians/Society of Critical Care Medicine Consensus Conference: definitions for sepsis and organ failure and guidelines for the use of innovative therapies in sepsis. (1992) *Crit. Care Med.* **20,** 864–874.
4. Dayer, J. M., Beutler, B., and Cerami, A. (1985) Cachectin/tumor necrosis factor stimulates collagenase and prostaglandin E2 production by human synovial cells and dermal fibroblasts. *J. Exp. Med.* **162,** 2163–2168.
5. Saklatvala, J. (1986) Tumour necrosis factor alpha stimulates resorption and inhibits its synthesis of proteoglycan in cartilage. *Nature* **322,** 547–549.
6. Seckinger, P., Isaaz, S., and Dayer, J. M. (1988) A human inhibitor of tumor necrosis factor alpha. *J. Exp. Med.* **167,** 1511–1516.
7. Seckinger, P., Zhang, J. H., Hauptmann, B., and Dayer, J. M. (1990) Characterization of a tumor necrosis factor alpha (TNF-alpha) inhibitor: evidence of immunological cross-reactivity with the TNF receptor. *Proc. Natl. Acad. Sci. USA* **87,** 5188–5192.

8. Engelmann, H., Novick, D., and Wallach, D. (1990) Two tumor necrosis factor-binding proteins purified from human urine. Evidence for immunological cross-reactivity with cell surface tumor necrosis factor receptors. *J. Biol. Chem.* **265,** 1531–1536.
9. Beutler, B., Krochin, N., Milsark, I. W., Luedke, C., and Cerami, A. (1986) Control of cachectin (tumor necrosis factor) synthesis: mechanisms of endotoxin resistance. *Science* **232**, 977–980.
10. Busso, N., Collart, M., Vassalli, J. D., and Belin, D. (1987) Antagonist effect of RU 486 on transcription of glucocorticoid-regulated genes. *Exp. Cell Res.* **173,** 425–430.
11. Di Santo, E., Sironi, M., Mennini, T., Zinetti, M., Savoldi, G., Di Lorenzo, D., et al. (1996) A glucocorticoid receptor-independent mechanism for neurosteroid inhibition of tumor necrosis factor production. *Eur. J. Pharmacol.* **299,** 179–186.
12. Swingle, W. W. and Remington, J. W. (1944) Role of adrenal cortex in physiological processes. *Physiol. Rev.* **24,** 89–127.
13. Abernathy, R. S., Halberg, F., and Spink, W. W. (1957) Studies on mechanism of chloropromazine protection against *Brucella* endotoxin. *J. Lab. Clin. Med.* **49,** 708–715.
14. Lazar, G. and Agarwal, M. K. (1986) The influence of a novel glucocorticoid antagonist on endotoxin lethality in mice strains. *Biochem. Med. Metab. Biol.* **36,** 70–74.
15. Lazar, G. J., Duda, E., and Lazar, G. (1992) Effect of RU 38486 on TNF production and toxicity. *FEBS Lett.* **308,** 137–140.
16. Perlstein, R. S., Whitnall, M. H., Abrams, J. S., Mougey, E. H., and Neta, R. (1993) Synergistic roles of interleukin-6, interleukin-1, and tumor necrosis factor in the adrenocorticotropin response to bacterial lipopolysaccharide in vivo. *Endocrinology* **132,** 946–952.
17. Kunkel, S. L., Spengler, M., May, M. A., Spengler, R., Larrick, J., and Remick, D. (1988) Prostaglandin E2 regulates macrophage-derived tumor necrosis factor gene expression. *J. Biol. Chem.* **263,** 5380–5384.
18. Spinas, G. A., Bloeash, D., Keller, U., Zimmerli, W., and Cammisuli, S. (1991) Pretreatment with ibuprofen augments circulating tumor necrosis factor-a, interleukin-6, and elastase during acute endotoxemia. *J. Infect. Dis.* **163,** 89–95.
19. Martich, G. D., Danner, R. L., Ceska, M., and Suffredini, A. F. (1991) Detection of interleukin 8 and tumor necrosis factor in normal humans after intavenous endotoxin: the effect of anti-inflammatory agents. *J. Exp. Med.* **173,** 1021–1024.
20. Gérard, C., Bruyns, C., Marchant, A., Abramowicz, D., Vandenabeele, P., Delvaux, A., et al. (1993) Interleukin 10 reduces the release of tumor necrosis factor and prevents lethality in experimental endotoxemia. *J. Exp. Med.* **177,** 547–550.
21. de Waal-Malefyt, R., Abrams, J., Bennet, B., Figdor, C., and de Vries, J. E. (1991) Interleukin-10 (IL-10) inhibits cytokine synthesis by human monocytes: an autoregulatory role of IL-10 produced by monocytes. *J. Exp. Med.* **174,** 1209–1220.

22. Gautam, S., Tebo, J. M., and Hamilton, T. A. (1992) IL-4 suppresses cytokine gene expression induced by IFN-gamma and/or IL-2 in murine peritoneal macrophages. *J. Immunol.* **148,** 1725–1730.
23. de Waal-Malefyt, R., Figdor, C. G., Huijbens, R., Mohan-Peterson, S., Bennett, B., Culpepper, J., et al. (1993) Effects of IL-13 on phenotype, cytokine production, and cytotoxic function of human monocytes. Comparison with IL-4 and modulation by IFN-gamma or IL-10. *J. Immunol.* **151,** 6370–6381.
24. Dumoutier, L. and Renauld, J. C. (2002) Viral and cellular interleukin-10 (IL-10)-related cytokines: from structures to functions. *Eur. Cytokine Netw.* **13,** 5–15.
25. Borovikova, L. V., Ivanova, S., Zhang, M., Yang, H., Botchkina, G. I., Watkins, L. R., et al. (2000) Vagus nerve stimulation attenuates the systemic inflammatory response to endotoxin. *Nature* **405,** 458–462.
26. Tracey, K. J. (2002) The inflammatory reflex. *Nature* **420,** 853–859.
27. Staal, F. J., Roederer, M., and Herzenberg, L. A. (1990) Intracellular thiols regulate activation of nuclear factor kappa B and transcription of human immunodeficiency virus. *Proc. Natl. Acad. Sci. USA* **87,** 9943–9947.
28. Auphan, N., DiDonato, J. A., Rosette, C., Helmberg, A., and Karin, M. (1995) Immunosuppression by glucocorticoids: inhibition of NF-kappa B activity through induction of I kappa B synthesis. *Science* **270,** 286–290.
29. Kopp, E. and Ghosh, S. (1994) Inhibition of NF-kappa B by sodium salicylate and aspirin. *Science* **265,** 956–959.
30. Moss, M. L., White, J. M., Lambert, M. H., and Andrews, R. C. (2001) TACE and other ADAM proteases as targets for drug discovery. *Drug Discov. Today* **6,** 417–426.
31. Sampaio, E. P., Sarno, E. N., Galilly, R., Cohn, Z. A., and Kaplan, G. (1991) Thalidomide selectively inhibits tumor necrosis factor alpha production by stimulated human monocytes. *J. Exp. Med.* **173,** 699–703.
32. Moreira, A. L., Sampaio, E. P., Zmuidzinas, A., Frindt, P., Smith, K. A., and Kaplan, G. (1993) Thalidomide exerts its inhibitory action on tumor necrosis factor alpha by enhancing mRNA degradation. *J. Exp. Med.* **177,** 1675–1680.
33. Lee, J. C., Laydon, J. T., McDonnell, P. C., Gallagher, T. F., Kumar, S., Green, D., et al. (1994) A protein kinase involved in the regulation of inflammatory cytokine biosynthesis. *Nature* **372,** 739–746.
34. Bianchi, M., Bloom, O., Raabe, T., Cohen, P. S., Chesney, J., Sherry, B., et al. (1996) Suppression of proinflammatory cytokines in monocytes by a tetravalent guanylhydrazone. *J. Exp. Med.* **183,** 927–936.
35. Cohen, P. S., Schmidtmayerova, H., Dennis, J., Dubrovsky, L., Sherry, B., Wang, H., et al. (1997) The critical role of p38 MAP kinase in T cell HIV-1 replication. *Mol. Med.* **3,** 339–346.
36. Hommes, D., van den Blink, B., Plasse, T., Bartelsman, J., Xu, C., Macpherson, B., et al. (2002) Inhibition of stress-activated MAP kinases induces clinical improvement in moderate to severe Crohn's disease. *Gastroenterology* **122,** 7–14.

2

Production and Characterization of Recombinant Human and Murine TNF

Flavio Curnis and Angelo Corti

Summary

Here we describe the methods for the expression of human and murine soluble tumor necrosis factor (hTNF and mTNF) in *Escherichia coli* cells and for their extraction, purification, and characterization. The expression and purification procedure takes about 2 wk. Human and murine TNF can be purified from crude extracts with high yields (>50 mg from 1 L of fermentation) by hydrophobic-interaction chromatography, ion-exchange chromatography, and gel-filtration chromatography. The purity and the identity of the final products can be checked by SDS-PAGE, ELISA, Western blot, analytical gel-filtration chromatography, mass spectrometry, and lipopolysaccharide assay. The biological activity of both human and murine TNF is assessed by in vitro cytolytic assays using murine L-M cells. Purified hTNF and mTNF can be used for in vitro and in vivo studies in animal models.

Key Words: TNF; plasmids; *E. coli* expression; purification; characterization; cytolytic assay.

1. Introduction

Tumor necrosis factor (TNF) is a cytokine produced by several cell types (macrophages, subsets of T cells, B cells, mast cells, eosinophils, endothelial cells, cardiomyocytes, and so on). It is expressed as a 26-kDa integral transmembrane precursor protein from which a 17-kDa mature TNF protein is released by proteolytic cleavage ***(1)***. Soluble, bioactive TNF is a homotrimeric protein that slowly dissociates into inactive, monomeric subunits at picomolar levels ***(2)***. Biological activities are induced upon interaction of trimeric TNF with two distinct cell surface receptors (p55-TNFR and p75-TNFR).

From: *Methods in Molecular Medicine, Vol. 98: Tumor Necrosis Factor*
Edited by: A. Corti and P. Ghezzi © Humana Press Inc., Totowa, NJ

Although limited amounts of TNF can be obtained from natural sources, relatively large quantities of bioactive, soluble TNF, for structural and functional studies, can be easily obtained by recombinant DNA technology. For instance, human and murine TNF cDNA has been successfully expressed in *Escherichia coli* ***(3,4)*** and has been recovered as soluble homotrimeric protein with high yields ***(5)***. Several mutants of TNF have also been successfully expressed in *E. coli* ***(5,6)***. Here we describe the methods for the expression of human and murine soluble TNF (hTNF and mTNF) in *E. coli*, for their extraction, purification, and characterization. Purified TNF, obtained according to this method, can be used for in vitro and in vivo studies in animal models.

2. Materials

2.1. cDNA Cloning and Expression

1. Enzymes for DNA manipulations.
2. Oligonucleotide primers.
3. RAW 264.7 cell line (clone TIB-71, ATCC).
4. *Salmonella minnesota* lipopolysaccharide (Sigma-Aldrich).
5. *E. coli* strain BL21(DE3) and DH5α (Novagen).
6. pET11b expression plasmid (Novagen).
7. Electrophoresis equipment for DNA analysis.
8. Ampicillin.
9. Autoclaved Luria broth (LB): freshly prepared by mixing 1% tryptone, 0.5% yeast extract, and 1% NaCl, pH 7.0, with 10 *N* NaOH.
10. Glycerol.
11. IPTG (isopropyl-β-D-thio-galactopyranoside).
12. Disposable 0.45-μm and 0.2-μm filters.
13. 2.5-L and 100-mL flasks for bacteria culture.
14. Extraction buffer: 20 m*M* Tris-HCl, 2 m*M* EDTA, pH 8.0.
15. Endonuclease.
16. Sonicator.
17. Sodium dodecyl sulfate-polyacrylamide gel electrophoresis (SDS-PAGE) equipment.

2.2. Protein Purification

1. Chromatography equipment.
2. Phenyl-Sepharose (low sub) Fast Flow (Amersham Biosciences Europe GmbH).
3. DEAE-Sepharose (low sub) Fast Flow (Amersham Biosciences Europe GmbH).
4. HR Sephacryl S-300 (Amersham Biosciences Europe GmbH).
5. Superdex 75 HR column (Amersham Biosciences Europe GmbH).
6. Dialysis tubing (cut-off, 12,000 Da).
7. TA buffer: 100 m*M* Tris-HCl, 1*M* $(NH_4)_2SO_4$, 5% methanol, pH 8.0, ice cold.
8. 2X TA buffer: 200 m*M* Tris-HCl, 2*M* $(NH_4)_2SO_4$, 10% methanol, pH 8.0, ice cold.

9. TB buffer: 100 m*M* Tris-HCl, pH 8.0, 70% ethylene glycol, 5% methanol, ice cold.
10. TA1 buffer: 20 m*M* Tris-HCl, pH 8.0, ice cold.
11. TB 2 buffer: 20 m*M* Tris-HCl, pH 8.0, 1*M* NaCl, ice cold.
12. PBS buffer: 150 m*M* NaCl, 50 m*M* NaH_2PO_4, pH 7.2, cooled at 4°C.

All solutions must be prepared with sterile and endotoxin-free water.

2.3. TNF Cytolytic Assay

1. L-M murine fibroblast cell line (clone CCL-1.2; ATCC).
2. 96-well flat-bottom plate for cell culture.
3. DMEM medium supplemented with 2 m*M* glutamine, 100 U/mL penicillin, 100 μg/mL streptomycin, 0.25 μg/mL amphotericin-B, and 10% fetal bovine serum (complete medium).
4. Actinomycin D: prepare a stock solution at 200 μg/mL in DMEM complete medium and store at –20°C.
5. MTT solution: 3-(4,5-dimethyl-2-thiazolyl)-2,5-diphenyl-2H-tetrazolium bromide, freshly prepared at 5 mg/mL in PBS.
6. Dimethyl sulfoxide.

2.4. Quantification of mTNF by ELISA

1. PVC microtiterplates (Becton Dickinson, cod. 3912).
2. Rat anti-mTNF, mAb V1q (kindly supplied by Dr. D. Mannel, University of Regensburg, Germany).
3. Nonfat dry milk powder.
4. Bovine serum albumin (BSA).
5. Tween-20.
6. Normal goat serum (NGS).
7. Assay buffer: 3% nonfat dry milk powder, 1% BSA in PBS containing 1% NGS.
8. Rabbit anti-mTNF, IgGs.
9. Goat anti-rabbit IgG-HRP.
10. *O*-phenylenediamine tablets (5 mg/tablet).
11. 36% hydrogen peroxide solution.

3. Methods

The methods described below outline (1) the preparation of cDNA coding for hTNF and mTNF, (2) the construction of expression plasmids, (3) the expression of hTNF and mTNF in *E. coli* cells, (4) the purification, and (5) the characterization of both proteins.

3.1. Preparation of cDNA Coding for mTNF and hTNF

DNA manipulations were performed by standard recombinant DNA methods.

The cDNA coding for murine TNF was prepared by RT-PCR, starting from a poly-A^+ mRNA obtained from 4×10^7 murine macrophage cells (RAW 264.7 cell line) stimulated for 16 h with 100 ng/mL of lipopolysaccharide, using the following primers:

5' TGCCTCACATATGCTCAGATCATCTTCTC 3' (5' *Nde*I primer);

5' CTGGATCCTCACAGAGCAATGACTCCAAAG 3' (3' *BamH*I primer).

The primers were designed to amplify the cDNA sequence coding for mature murine $TNF_{1–156}$.

The 5' *Nde*I primer contains the *Nde*I restriction site (underlined), necessary for cloning, and the translation starting codon ATG (bold). The 3' *BamH*I primer, corresponding to the antisense strand, contains the *BamH*I restriction site (underlined) and the stop codon.

The cDNA coding for mouse Met-$TNF_{1–156}$ and human Met-$TNF_{1–157}$ (generated using the same strategy) were 476 bp and 479 bp long, respectively, after digestion with *Nde*I-*BamH*I enzymes.

3.2. Construction of Expression Plasmids

The following subsections describe the expression vectors and the cloning strategy exploited for the production of hTNF and mTNF.

3.2.1. pET11b Expression Vector

The pET System is a system developed for cloning and expression of recombinant proteins in *E. coli* *(7)*. Target genes are cloned in pET plasmids under control of strong bacteriophage T7 transcription and translation signals; expression can be induced by the addition of IPTG. The pET11b plasmid translation vector contains the highly efficient ribosome-binding site from phage T7 major capsid protein. Sequences inserted into the cloning site can be expressed as T7-Tag fusion proteins to facilitate detection, purification, or solubilization of the target protein. However, expression of the recombinant protein lacking the T7-Tag can be accomplished by removing the coding T7-Tag region by digestion with *Nde*I and *BamH*I. The pET11b vector contains an ampicillin-resistance gene for selection.

3.2.2. Cloning Strategy

The pET11b plasmid was digested with *Nde*I-*BamH*I enzymes to remove the sequence coding for the T7-Tag, dephosphorylated, and ligated with the TNF cDNAs obtained as described in **Subheading 3.1.** Both ligation products were used to transform *E. coli* DH5α cells by standard methods *(8)*. Transformed *E. coli* DH5α cells were plated on LB plates containing ampicillin (100 μg/mL) and incubated overnight at 37°C. Single colonies were selected and

grown overnight in LB ampicillin. The plasmids, named hTNF-pET11 and mTNF-pET11, were then isolated, analyzed by agarose gel electrophoresis after digestion with *Nde*I and *BamH*I and sequenced (*see* **Note 1**).

3.3. Expression of mTNF and hTNF in E. coli

The entire process (expression and purification) takes about 10 d. The methods described below outline (1) the preparation of glycerol stocks, and (2) the fermentation process. The protocol refers to 1 L of fermentation.

3.3.1. Preparation of Glycerol Stocks

1. Transform BL21(DE3) *E. coli* strain with hTNF-pET11 or mTNF-pET11 using standard protocols ***(8)***.
2. Plate cells on LB plates containing ampicillin (100 μg/mL) and incubate overnight at 37°C.
3. Select single colonies and grow them in 20 mL of LB containing 100 μg/mL ampicillin until the optical density (OD) at 600 nm is about 0.6 units.
4. Add 4 mL of autoclaved glycerol (20% final concentration), mix well, and prepare several cryovials.
5. Quickly freeze the cryogenic vials in liquid nitrogen and transfer at –80°C (*see* **Note 2**).

3.3.2. Preparation of Preinoculum

1. Streak transformed cells from one cryogenic vial and transfer to a 100-mL flask containing 20 mL of LB containing 100 μg/mL ampicillin. Incubate at 37°C under shaking (200 rpm) until the OD at 600 nm is about 1.0 unit (about 6 h).
2. Transfer the preinoculum into a 50-mL tube and store overnight at 4°C.
3. The next day, spin the product (3500*g*, 10 min, 4°C), discard the supernatant, and gently resuspend the pellet in 20 mL of LB containing 100 μg/mL ampicillin.

3.3.3. Cell Culture and Protein Expression

1. Fill two flasks (void volume, 2500 mL each) with 500 mL of LB containing 100 μg/mL ampicillin, and add an amount of preinoculum giving an OD at 600 nm of 0.03 units.
2. Incubate at 37°C under vigorous shaking (200 rpm) until the OD at 600 nm is about 0.7–0.8 units and induce protein expression by adding IPTG (final concentration, 1 m*M*). Let the cells grow for 3.5 h.
3. Centrifuge the culture (4000*g*, 20 min, 4°C).
4. Discard the supernatant and recover the bacterial pellet.
5. Freeze the bacterial pellet at –20°C (*see* **Note 3**).

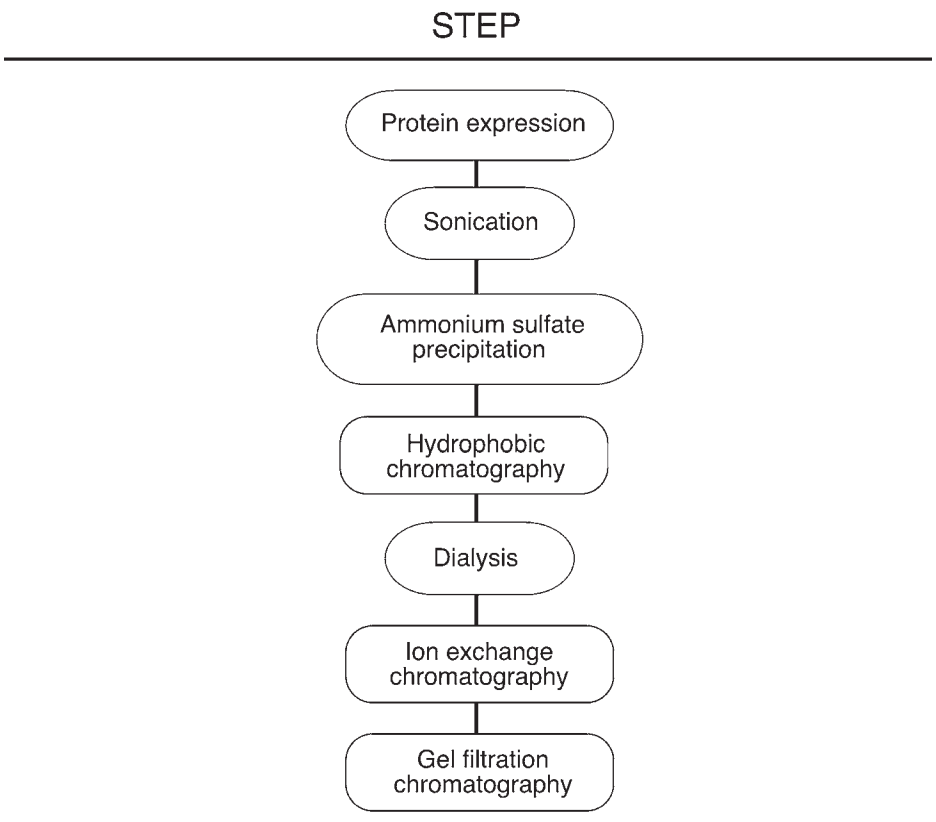

Fig. 1. Flow chart of hTNF and mTNF purification.

3.4. Purification of mTNF From E. coli *Extracts*

The flow chart of the purification method is shown in **Fig. 1**. The entire procedure takes about 7 d. The steps described in **Subheadings 3.4.1.** and **3.4.2.** outline the procedure for extracting mTNF from *E. coli* cells as a soluble protein. The steps described in **Subheadings 3.4.3.** to **3.4.6.** outline the procedure for mTNF purification from soluble crude extracts. During the extraction and purification process each fraction is stored on ice. All centrifugation steps are performed at 15,000*g* for 20 min at 4°C.

3.4.1. Disruption of Bacteria by Sonication

1. Resuspend the bacterial pellet with 50 mL of extraction buffer and add 40 U/mL endonuclease.

2. Lyse the bacterial suspension by sonication (*see* **Note 4**).
3. Centrifuge the sonicated material, recover the soluble fraction and discard the pellet (*see* **Note 5**).

3.4.2. Ammonium Sulfate Precipitation

1. Add the amount of ammonium sulfate necessary to obtain 30% saturation to the soluble fraction obtained in **Subheading 3.4.1.** and incubate for 1 h at 4°C under stirring.
2. Centrifuge and recover the soluble fraction; discard the pellet.
3. Add ammonium sulfate to the soluble fraction (65% saturation) and incubate overnight at 4°C under stirring.
4. The next day, centrifuge and discard the soluble fraction. Gently resuspend the pellet by adding 15 mL of sterile water, then slowly add 15 mL of 2X TA buffer and incubate on ice for 10 min.
5. Centrifuge and discard the pellet. Filter the soluble fraction (SM-HIC) using a 0.45 μm filter.

3.4.3. Hydrophobic Chromatography

1. Load the product (SM-HIC) onto a 16 × 250 mm phenyl-sepharose column, equilibrated with TA buffer, using a peristaltic pump (4 mL/min).
2. Wash the column with 160 mL TA and elute the protein using the following gradient: 20–70% TB (301 mL); 70–100% TB (1 mL); 100% TB (150 mL); flow rate 3 mL/min.
3. Collect fractions of 10 mL and analyze them by SDS-PAGE. Pool fractions, trying to discard those fractions containing impurities in high proportion (Pool HIC). Store the pooled fractions at 4°C until the next step.

3.4.4. Dialysis

1. Dialyze the product (Pool HIC) against 23 volumes of 2 m*M* EDTA, 20 m*M* Tris-HCl, pH 8.0 (2 h, 4°C).
2. Repeat this step twice and dialyze the product for 60 h at 4°C. Filter the product (Pool HIC-f) using a 0.22-μm filter (*see* **Note 6**).

3.4.5. Ion-Exchange Chromatography

1. Load the product (Pool-HIC-f) onto a 16 × 320 mm DEAE-sepharose column, equilibrated with TA1 buffer, using a peristaltic pump (2 mL/min).
2. Wash the column with 510 mL TA1 and elute the protein using the following gradient: 0–50% TB1 (180 mL); 50–100% TB1 (2 mL); 100% TB1 (92 mL); flow rate 2 mL/min.
3. Collect fractions of 5 mL and analyze them by SDS-PAGE. Pool fractions, trying to discard impurities (Pool DEAE). Store the pooled fractions at 4°C until the next step.

Table 1
Purification of mTNF From *E. coli* Extract (1 L of Fermentation)

Fractions	Volume (mL)	TNF antigen[a] (mg)	Protein[b] (mg)	Purity antigen/protein (%)	Yield (%)
Crude extract	55	180	450	40	100
Hydrophobic interaction chromatography	155	123	190	65	68
Ion-exchange chromatography	15	61.4	66	93	34.1
Gel-filtration chromatography	50	51	52	98	28.3

[a]By ELISA.
[b]By BCA protein assay kit (Pierce).

3.4.6. Gel Filtration Chromatography

1. Gel-filter the product (Pool DEAE) through a 50 × 600 mm HR Sephacryl S-300 column, pre-equilibrated with PBS.
2. Elute the protein with PBS (flow rate 2 mL/min), collect the first 400 mL of effluent in a bottle and then collect 40 fractions of 12.5 mL each.
3. Analyze each fraction by SDS-PAGE and pool the fractions with the highest protein content and purity.
4. Filter the pooled fractions (Pool GF) under a sterile hood using 0.22-μm filters, aliquot, and store at –20°C (*see* **Note 7**).

3.5. Purification of hTNF From E. coli *Extracts*

We have successfully used the same protocol for the purification of hTNF, with minor modification: In **Subheading 3.4.2.** we use 35% saturated ammonium sulfate concentration instead of 30%.

3.6. Biochemical and Biological Characterization of hTNF and mTNF

The protein content and the immunoreactivity of the chromatographic fractions and the final products can be determined by commercial protein detection and TNF-ELISA kits. **Table 1** shows the yield of each step of mTNF purification. Typically, more than 50 mg of purified material can be recovered from 1 L of fermentation.

The purity and the identity of the final products can be estimated using the following analytical procedures: (1) SDS-PAGE, (2) Western blot, (3) analytical gel filtration, and (4) mass spectrometry. The results of SDS-PAGE of purified mTNF and hTNF, under reducing and nonreducing conditions are shown in **Fig. 2**. A single band of 17–18 KDa, with purity greater than 98%, should be observed. The hydrodynamic volumes, estimated by analytical gel filtration,

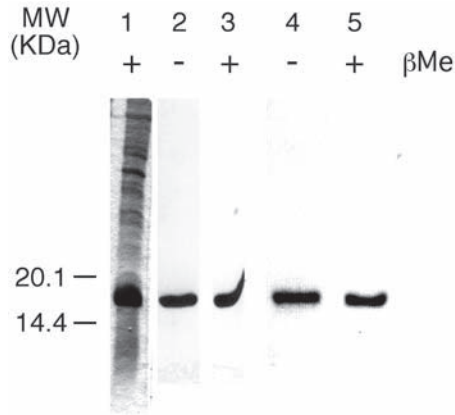

Fig. 2. SDS-PAGE analysis of mTNF and hTNF. Lane 1: Soluble crude extract of mTNF after sonication; Lanes 2 and 3: purified mTNF; Lanes 4 and 5: purified hTNF. The samples were analyzed under reducing (+) and nonreducing (–) conditions on 12.5% SDS-PAGE stained with Coomassie R250. MW: molecular markers.

correspond to proteins of 40 KDa (**Fig. 3**). The discrepancy between the theoretical molecular weight (about 50 KDa) and the observed hydrodynamic behavior (40 KDa) is likely because TNF is a compact trimer ***(9)*** with a small hydrodynamic volume ***(2)***. The expected molecular masses of $hTNF_{1–157}$ and $mTNF_{1–156}$ subunits are 17,350.7 Da and 17,386.7 Da, respectively. Electrospray ionization mass spectrometry (ESI-MS) analysis of hTNF shows a heterogeneous product consisting of a major peak of 17,349 Da, corresponding to mature $TNF_{1–157}$, and a minor peak of 17,481 Da, corresponding to the mass expected for human Met-$TNF_{1–157}$. Typically, in our preparations this product is about 20% of total (**Fig. 4**). The molecular mass of mTNF, by ESI-MS, is 17,386 Da, corresponding to the mass expected for murine Met-$TNF_{1–156}$. Many in vitro and in vivo applications of TNF require low endotoxin contamination. The amount of lipopolysaccharide in our preparations is typically approx 0.1 U/μg of purified protein, as measured by quantitative chromogenic *Limulus* amebocyte lysate (LAL) test. The in vitro cytotoxic activities of hTNF and mTNF are about 5×10^7 and 8×10^7 U/mg of protein, respectively, as determined by standard cytolytic assay with murine L-M mouse fibroblasts (*see* **Subheading 3.7.**).

3.7. Cytolytic Assay

Here, we describe a cytolytic assay for the quantitative detection of TNF, based on murine fibroblast L-M cells, and a dose-response curve in the range of 3–3000 pg/mL (**Fig. 5**). L-M cell are cultured in DMEM medium supplemented with 2 m*M* glutamine, 100 U/mL penicillin, 100 μg/mL streptomycin,

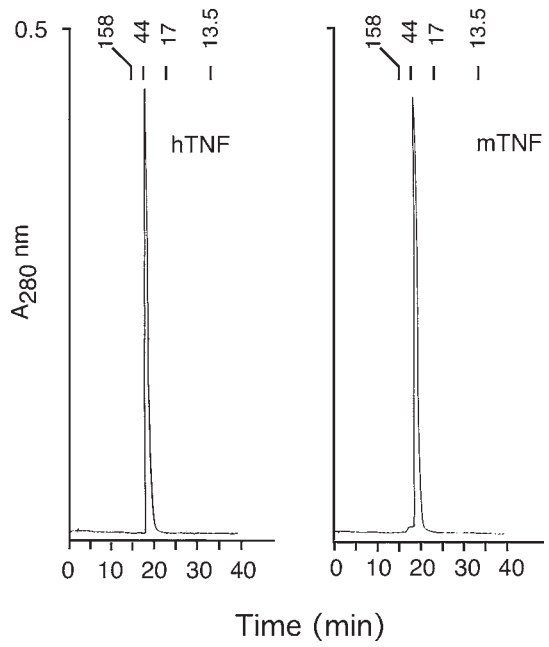

Fig. 3. Analytical gel filtration chromatography of hTNF and mTNF (Superdex 75 HR column). The column was equilibrated with PBS and calibrated with the following proteins: thyroglubulin (670 KDa), IgG (158 KDa), ovalbumin (44 KDa), myoglobin (17 KDa) and B_{12} vitamin (1.35 KDa).

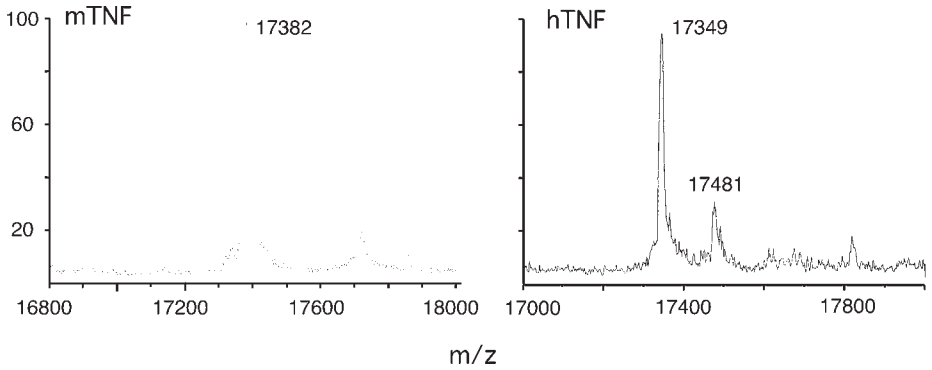

Fig. 4. Analysis of purified hTNF and mTNF by electrospray ionization mass spectrometry (ESI-MS).

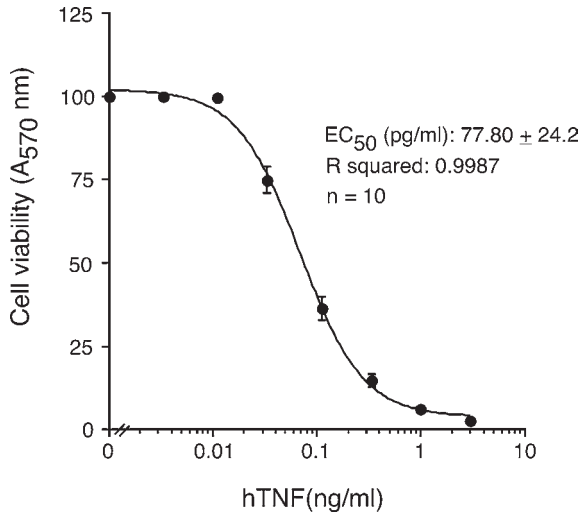

Fig. 5. Calibration curve of the hTNF cytolytic assay. L-M cells (30,000 cell/well) were incubated with 2 μg/mL of actinomycin D and increasing amount of hTNF. Similar results can be obtained with mTNF.

0.25 μg/mL amphotericin-B and 10% fetal bovine serum (*see* **Note 8**). The cells are detached with a trypsin-EDTA solution and expanded three times per week. The protocol described below takes about 3 d to be performed and can be used for both hTNF and mTNF. Other, more sensitive bioassays have been described using different cell lines ***(10–13)***.

1. Plate 30,000 cells/well (100 μL/well, 96-well flat-bottom plate) in DMEM medium and incubate overnight at 37°C under 5% CO_2.
2. Prepare various solutions of standard TNF (3–3000 pg/mL, final concentration) and samples in "complete medium" (*see* **Note 9**).
3. Add to each well 50 μL of actinomycin-D (2 μg/mL final concentration) and 50 μL of TNF solutions, then incubate 24 h at 37°C under 5% CO_2.
4. Add to each well 10 μL of MTT solution and incubate 3 h at 37°C under 5% CO_2 (*see* **Note 10**).
5. Remove the supernatant using a Pasteur pipet connected to a vacuum pump, and add 200 μL of dimethyl sulfoxide to dissolve the formazan crystals.
6. Measure the absorbance at 540 nm or at 570 nm.

3.8. mTNF Quantification by ELISA

1. Coat PVC microtiterplates with mAb V1q (10 μg/mL in PBS), 50 μL/well, and incubate overnight at 4°C.
2. After washing three times by emptying and filling with PBS, incubate the plate with 3% nonfat dry milk powder, 1% BSA in PBS containing 0.05% Tween-20, 200 μL/well, for 2 h at 37°C, and then wash again three times with PBS.

3. Fill the wells with 50 μL of mTNF standard solutions (0.010–10 ng/mL), or samples diluted in "assay buffer" (*see* **Subheading 2.4.**), and incubate for 2 h at room temperature.
4. Wash the plate eight times by emptying and filling with PBS containing 0.05% Tween-20 (PBS-TW).
5. Add to each well 50 μL of anti-mTNF IgGs (10 μg/mL final concentration) diluted in "assay buffer" and incubate for 1.5 h at room temperature.
6. After washing eight times with PBS-TW, add to each well 50 μL of goat anti-rabbit IgG-HRP diluted 1:1000 in "assay buffer" and incubate for 45 min at room temperature.
7. Wash again with PBS-TW and fill each well with 75 μL of *o*-phenylenediamine solution (1 tablet in 7.5 mL of distilled water containing 10 μL of 36% hydrogen peroxide) and incubate for 30 min.
8. Block the chromogenic reaction by adding 10% sulfuric acid (75 μL/well). The absorbance at 490 nm of each well is then measured using an ELISA plate reader.

A dose-response curve in the 20–1000 pg/mL range can be obtained with this protocol.

4. Notes

1. Another very efficient method for screening recombinant clones exploits the cytolytic activity of TNF (*see* **Subheading 3.7.**). Given that TNF cDNA is not toxic to BL21(DE3), the product of ligation can be directly used to transform these cells. The clones obtained can then be inoculated in 100 μL of LB containing 100 μg/mL ampicillin, in a 96-well plate, and incubated at 37°C under shaking (make a master plate of the picked colonies). When the culture is slight turbid, the plate is centrifuged (820*g* for 10 min), the supernatant is discarded, and the bacterial pellet is resuspended with 100 μL/well of LB containing 100 μg/mL ampicillin and 1 m*M* of IPTG. After 3 h of induction at 37°C under shaking, the plate is centrifuged (2500*g* for 10 min), the supernatant is eliminated, and the bacteria are lyzed by adding 30 μL/well of B-PER Reagent for 10 min (Pierce). Then add 70 μL of PBS to each well and centrifuge (2500*g* for 10 min) to remove the bacterial debris. Analyze the supernatant (containing the soluble fraction protein) by cytolytic assay. The clones able to kill the cells are isolated and sequenced. With this protocol hundreds of clones can be screened in 2 d.
2. Glycerol stocks of BL21(DE3) containing TNF-coding plasmids are very stable (up to 5 yr).
3. Alternatively, the frozen pellet can be stored at –80°C for several days (up to 3 mo).
4. During the sonication process, store the sample on ice to avoid overheating. To assess the bacterial lysis during sonication, remove 10 μL of the sonicated sample, centrifuge 5 min at 13,000*g*, dilute the supernatant 1:100 with extraction buffer, and measure the absorbance at 280 nm. Repeat the sonication step until the absor-

bance at 280 nm is stable. Typically, 7 cycles are sufficient to obtain a final absorbance at 280 nm of about 100 units.

5. The crude extract can be stored –80°C for several days (up to 3 mo).
6. During dialysis the sample volume may increase one-third. Thus, to avoid the rupture of tubing, leave some air between sample and clamp.
7. Purified TNF can be stored at –80°C for several years. Also, diluted TNF (1–5 μg/mL) can be stored for several years, with minor loss of activity, provided it is diluted in the presence of carrier proteins. For instance, TNF can be stored in DMEM containing 5–10% of serum at –20°C. Storing highly diluted TNF solution (less then 10 ng/mL) at >4°C should be avoided, as it may dissociate to inactive monomers ***(2)***.
8. L-M cells must be mycoplasma free. Infection causes marked loss of assay detectability.
9. Diluted TNF solutions should be added to the plate within 1 h (*see also* **Note 7**).
10. Remove any particulate by filtration through a 0.22-μm filter.

References

1. Grell, M., Douni, E., Wajant, H., Lohden, M., Clauss, M., Georgopulos, S., et al. (1995) The transmembrane form of tumor necrosis factor is the prime activating ligand of the 80 kDa tumor necrosis factor receptor. *Cell* **83,** 793–802.
2. Corti, A., Fassina, G., Marcucci, F., Barbanti, E., and Cassani, G. (1992) Oligomeric tumour necrosis factor alpha slowly converts into inactive forms at bioactive levels. *Biochem. J.* **284,** 905–910.
3. Pennica, D., Nedwin, G. E., Hayflick, J. S., Seeburg, P. H., Derynck, R., Palladino, M. A., et al. (1984) Human tumor necrosis factor: precursor, structure, expression and homology to lymphotoxin. *Nature* **321,** 724–729.
4. Marmenout, A., Fransen, L., Tavernier, J., Van der Heyden, J., Tizard, R., Kawashima, E., et al. (1985) Molecular cloning and expression of human tumor necrosis factor and comparison with mouse tumor necrosis factor. *Eur. J. Biochem.* **152,** 515–522.
5. Gase, K., Wagner, B., Wagner, M., Wollweber, L., and Behnke, D. (1991) Expression and subcellular location of native and mutant hTNF alpha proteins in Escherichia coli. *FEMS Microbiol. Lett.* **68,** 259–265.
6. Ito, R., Matsumoto, H., Uchida, K., Kubo, T., Tsukii, Y., Endo, T., et al. (1991) Novel muteins of human tumor necrosis factor alpha. *Biochim. Biophys. Acta* **1096,** 245–252.
7. Studier, F. W. and Moffatt, B. A. (1986) Use of bacteriophage T7 RNA polymerase to direct selective high-level expression of cloned genes. *J. Mol. Biol.* **189,** 113–130.
8. Sambrook, J., Fritsch, E. F., and Maniatis, T. *Molecular Cloning: A Laboratory Manual*, Cold Spring Harbor Laboratory, Cold Spring Harbor, NY, 1989.
9. Smith, R. A. and Baglioni, C. (1987) The active form of tumor necrosis factor is a trimer. *J. Biol. Chem.* **262,** 6951–6954.

10. Meager, A., Leung, H., and Woolley, J. (1989) Assays for tumour necrosis factor and related cytokines. *J. Immunol. Meth.* **116,** 1–17.
11. Kramer, S. M. and Carver, M. E. (1986) Serum-free in vitro bioassay for the detection of tumor necrosis factor. *J. Immunol. Meth.* **93,** 201–206.
12. Blagosklonny, M. V. and Neckers, L. M. (1993) Sensitive and simple bioassay for human tumour necrosis factor-alpha. *Eur. Cytokine Net.* **4,** 279–283.
13. Espevik, T. and Nissen-Meyer, J. (1986) A highly sensitive cell line, WEHI 164 clone 13, for measuring cytotoxic factor/tumor necrosis factor from human monocytes. *J. Immunol. Meth.* **95,** 99–105.

3

Purification of TNF Binding Proteins

Hartmut Engelmann, Dani Aderka, and David Wallach

Summary

The finding that the two tumor necrosis factor receptors (TNFR) exist in soluble form in various body fluids not only has substantiated the paradigm of naturally existing soluble cytokine receptors but also has represented a milestone on the road to the biochemical and biological characterization of the two TNFRs. This chapter gives a simple, basic protocol for the purification of the two soluble TNFRs. The protocols found here may be easily adapted for the purification of various other soluble cytokine receptors. The purified proteins may be used in biological experiments or for the generation of specific research tools such as polyclonal or monoclonal antibodies.

Key Words: Soluble TNF receptors; TNF binding proteins; TBP; ligand affinity chromatography; reversed-phase HPLC.

1. Introduction

With the cloning of the first cytokine genes in the early and mid-1980s the hunt for their cell surface receptors began. Because of their low abundance, purification and molecular characterization with traditional biochemical methods turned out to be difficult in many cases. This situation changed with the discovery that many cytokine receptors exist not only in membrane-bound form but also in soluble form. Soluble cytokine binding proteins for human growth hormone (HGH) ***(1,2)***, interleukin (IL)-2 ***(3)***, nerve growth factor (NGF) ***(4)***, tumor necrosis factor (TNF) ***(5–7)***, IL-1 ***(8)***, IL-6, and interferon (IFN)-γ ***(9)*** were identified and purified to homogeneity. Thus, molecular probes for the cloning of the corresponding genes became available, and the further molecular and functional characterization was facilitated. However, soluble cytokine receptors are not simply the soluble counterparts of their membrane-bound form. As evidenced by the sIL-6 receptor (sIL-6R), the soluble Fas/Apo1,

From: *Methods in Molecular Medicine, Vol. 98: Tumor Necrosis Factor*
Edited by: A. Corti and P. Ghezzi © Humana Press Inc., Totowa, NJ

IL-18 binding protein (IL-18bp), or osteoprotegerin (OPG), they may also exert important regulatory functions by acting as cytokine buffers or even as mediators of cytokine function ***(9–13)***. Therefore, it is important to know these receptors' exact functions as well as the modes and the circumstances under which they are made in our body. For those cytokines which mediate tissue damage and disease, such as TNF in rheumatoid arthritis, the soluble receptor proteins have also gained great therapeutic importance as natural cytokine-neutralizing drugs (reviewed in ***ref. 14***).

This chapter provides a protocol for the purification of the soluble TNF receptors. Appropriately adapted, these protocols may also be utilized for the purification of several other soluble cytokine receptors found in biological fluids.

2. Materials

1. If available, approx 40 L urine from febrile (septic) patients (handle under the appropriate biosafety precautions) or 1–2 L of ascites from a patient with ovarian carcinoma.
2. U-937 (ATCC CRL-1593.2), HL-60 (ATCC CCL-240), K-562 (ATCC CCL-243), or RPMI-1788 cells (ATCC CCL-156).
3. RPMI medium, fetal calf serum, penicillin, and streptomycin (Gibco).
4. TNF Receptor ELISA (e.g., from Hofmann-LaRoche Applied Science or from Bender MedSystems GmbH).
5. Phorbol myristate acetate (PMA) (Sigma-Aldrich).
6. Phytohemagglutinin (PHA) (Sigma-Aldrich).
7. Phenymethylsulfonyl fluoride (PMSF) (Sigma) or Pefabloc SC (Hoffmann-LaRoche Applied Sciences).
8. Ascites from patients with ovarial carcinoma ***(15)***.
9. Rotary or peristaltic pump with high capacity (up 100 mL/min).
10. Tangential filtration systems such as the Helicon® or Pellicon® (Millipore).
11. At least 2 mg (better 3–5) recombinant TNF or 2–3 mg of anti-TNFR antibody.
12. 1 mL AffiGel10 (Bio-Rad) or CNBr-activated Sepharose™ (Amersham Biosciences).
13. 5-mL column cartridge (e.g., from BioRad).
14. HPLC pumps equipped with UV detector and fraction collector.
15. Aquapore RP300 C8 reverse-phase HPLC column (Brownlee Labs).
16. Chromatography-grade acetonitrile.
17. Chromatograpy-grade trifluoroacetic acid (Merck).

3. Methods

3.1. Source

Several sources have been used for the purification of soluble TNFRs (*see* **Note 1**). Initially both TNFRs were found in high concentrations in various

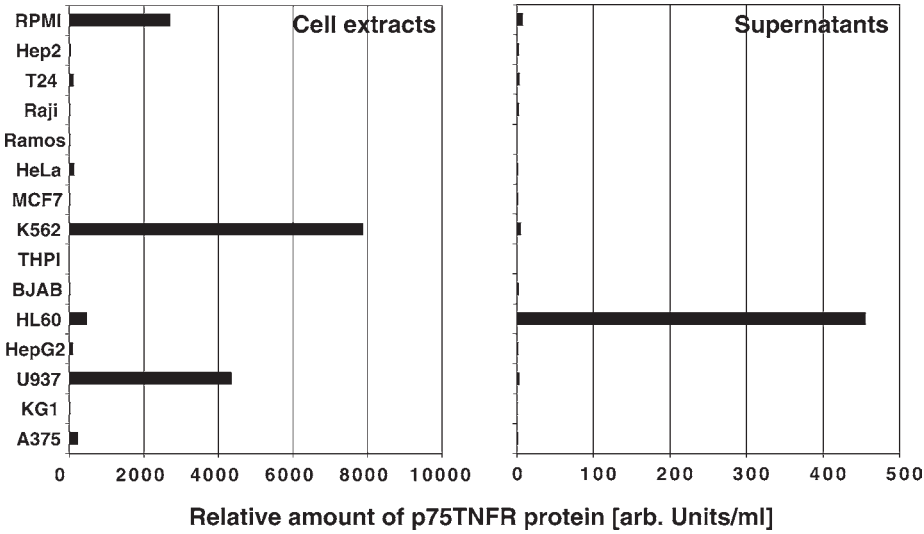

Fig. 1. Comparison of total cellular p75-TNFR expression versus spontaneous release of soluble p75-TNFR in relation to total p75-TNFR protein content. The indicated cell lines were grown to confluency in DMEM supplemented with 5% FCS. Supernatants (SN) and cells were harvested, and cells were lysed in 1% Triton X-100 in phosphate buffered saline. Lysates and SN were normalized on the basis of cell numbers, and p75-TNFR concentration was measured by ELISA. The signal found with RPMI cells was arbitrarily defined as 2700 Units per mL.

body fluids such as urine ***(5–7)***, serum, or ascitic fluid ***(16)***. Another possible source is the supernatant fluid of tissue-cultured cells ***(17)***. Soluble cytokine receptor secretion may differ greatly from cell line to cell line, as is shown in **Fig. 1** for the soluble p75-TNFR. The optimal cell line and conditions for sTNFR production may be easily determined with commercially available ELISA systems. It is advisable to test the available starting material for the presence of the soluble receptor of interest before investing time and effort on purification. For the purpose of purifying microgram amounts of soluble TNFR (p55-TNFR or p75-TNFR) the most practical source is the supernatant of PMA-treated U937, K562, or HL60 cells. These cell lines may be obtained from cell banks such as ATCC, and no special facilities or knowledge is required to propagate them. To enhance the production of soluble TNFR, the cells should be grown under optimal conditions and then be stimulated in serum-free or low-serum conditions with PHA and PMA. The supernatant may be collected up to three times per culture and should be harvested approx 1 d after the addition of PMA. In order to protect the soluble receptors in the crude protein mixture from proteolytic degradation the addition of protease inhibitors such as

phenymethylsulfonyl fluoride (PMSF) or Pefabloc SC (Hoffmann-LaRoche Applied Sciences) is recommended.

For 50 to 100 μg of soluble TNFR protein a minimum of 20 L of cell supernatant will be needed. Roller bottles or 100 cm^2 Petri dishes are preferred.

1. Grow cells under optimal conditions (with 5–10% fetal calf serum in the medium) in the logarithmic phase to a density of 10^6 cells per mL.
2. Harvest and resuspend at a density of 2×10^6 cells per mL in serum-free RPMI medium containing 5 μg of PHA and 10 ng of PMA per mL.
3. Harvest the supernatant after 20–24 h.

This procedure may be repeated up to three times (by centrifugation at 1500*g* for 10 min), i.e., at 24, 48, and 72 h after start of the culture. After addition of protease inhibitors (PMSF at 2 m*M* or Pefabloc at 1 m*M*), the supernatant may be kept frozen until further use at –20°C.

Before starting the purification each batch of supernatant should be tested for soluble TNFRs by ELISA. Alternatively, the TNF neutralizing activity may be evaluated in a standard TNF cytotoxicity assay ***(18)***. Briefly, the procedure is as follows:

1. L929 cells (ATCC CCL1) are seeded in 96-well microtiter plates at a density of 25,000 to 30,000 cells per well (the assay should be adjusted for optimum density in a pilot experiment).
2. After 24 h serial dilutions of the tested supernatants are applied together with 1 to 2 U/mL TNF and 50 μg/mL cycloheximide (Sigma). (The optimal TNF concentration should be determined in a pilot experiment and should result in approx 70 to 90% cell death.)
3. After an incubation period of 18 to 20 h neutral red in medium is applied on the cells for 2 h. A 100-fold concentrated stock solution is available from Sigma (cat. no. N 2889).
4. The microtiter plates are then washed three times with phosphate buffered saline containing $CaCl_2$ (0.9 m*M*) and $MgCl_2$ (0.5 m*M*) to remove the excess neutral red and cell debris.
5. The neutral red is then extracted from the viable cells with a 1:1 (v/v) mixture of 95% ethanol and Soerenson buffer (0.1 *M* disodium-citrate buffer and 0.1 *M* HCl mixed at a ratio of 61.2:38.8 (v/v), pH 4.2).
6. The microtiter plates are then read in an ELISA reader at 450 nm.

3.2. Concentration

Tangential filtration systems such as the Helicon® or Pellicon® (Millipore) are ideally suited to concentrate the volumes needed to obtain sufficient amounts of soluble TNFR. Alternatively, hollow fiber filtration systems may be used. The molecular weight cut off should be in the range of 10 kDa.

1. Depending on the ultra-filtration system the starting material should be precleared from particulate matter or cell debris. This may be done by centrifugation or by the use of a preclearing membranes available for most tangential filtration systems.
2. The cell supernatant is concentrated to a volume of 0.5 to 1.0 L.
3. The concentrate is transferred into phosphate buffered saline. This step may be conveniently performed with the concentration device by diluting the retentate 3× with 3.0 L of PBS followed by reconcentration to the desired final volume.

3.3. The TNF Affinity Column

Due to the low concentration of soluble TNFR in the starting material, it is almost mandatory to use a ligand-affinity step for the purification. This step may become a cost factor because recombinant TNF is in the range of $1400 to $2000 per mg. Alternatively, a monoclonal antibody against the sTNFR of interest may be used (price ranges between $400 and $600 per mg of purified Ig). The first approach has the advantage that both sTNFRs bind to a TNF column and may be enriched simultaneously, with the disadvantage that the TNF column is unstable and may be used only three to five times. Affinity chromatography with anti-TNFR antibodies offers higher column stability, however, at the expense of being able to purify only one of the two sTNFRs.

TNF-Sepharose (or TNF-AffiGel) columns are constructed according to the instructions included with the preactivated slurry. It is critical to keep the TNF (or the mAbs) in buffers free of primary amines, such as PBS (freshly prepared), and to use them at the highest possible protein concentration (i.e., at concentrations greater than 2 mg/mL). Thus, if only 1 mg TNF is available, it should be concentrated into a volume of 0.4 to 0.5 mL. This approach will ensure a high coupling efficiency.

TNF is a noncovalently linked homotrimer. Therefore, TNF affinity columns have a strong tendency to bleed the coupled TNF, leading to a limited lifespan (three to five runs at most). In view of this problem, it is recommended that the TNF-gel be prewashed only once briefly with the intended elution conditions, followed by immediate neutralization with PBS. As an elution buffer, 50 m*M* citric acid, pH 2.0, containing 100 m*M* NaCl proved to be the best solution. This buffer elutes the bound sTNFRs without intolerable TNF bleeding from the column.

3.4. Ligand Affinity Chromatography (see *Fig. 2*)

1. Fill a small column cartridge (available from BioRad) with the TNF sepharose and apply the concentrated starting material at a flow rate of 0.5 to 0.75 mL/min.
2. Take a sample of the starting material and the first mL of the "flow through" in order to evaluate the performance of the column.

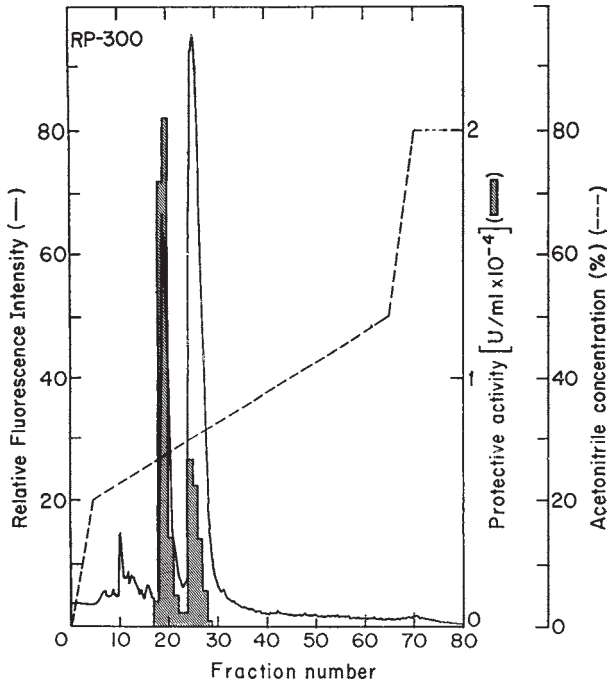

Fig. 2. Reverse-phase HPLC of ligand-affinity purified TNF binding proteins. The ligand (TNF) affinity column eluate was applied on an Aquapore RP 300 column. Elution was performed with the indicated gradient of acetonitrile in 0.1% aqueous trifluoroacetic acid (---). Fractions were examined for bioactivity (▒) and protein content (—).

3. After loading the column is washed with 50 mL PBS and then eluted stepwise with 8 column volumes elution buffer (50 m*M* citric acid buffer, pH 2.0, 100 m*M* NaCl). For optimal elution 0.5 mL elution buffer is applied on the column, and the flow is stopped for 5 min before the elution proceeds in 1 mL portions.
4. The two soluble TNFRs elute in the first three fractions, peaking in fraction 2.
5. After elution the column should be immediately neutralized with PBS.

When affinity columns constructed with anti-TNFR antibodies are used, the purification should be done in an analogous manner. The citric acid elution buffer also works with most antibody columns; however, the affinity of an mAb may be such that more stringent elution conditions must be applied. In such cases, an increase of the NaCl concentration up to 1*M* may be useful. Alternatively, elution at high pH (i.e., pH 9.0–10.0) or chaotropic salts such as urea may be tried. Note that for the latter elution conditions it is mandatory to transfer into buffer systems that are compatible with the chemistry of the HPLC column used in the next step.

3.5. Reverse-Phase HPLC

Purification of the two TNFRs to homogeneity is most conveniently achieved by reverse-phase HPLC. The proteins eluting from the TNF affinity column are pooled and separated on a C8 reverse-phase HPLC column such as the Aquapore RP300 (Brownlee Labs).

1. Pre-equilibrate the column with 0.1% aqueous TFA (buffer A), and apply the eluate from the TNF affinity column.
2. Wash the column with buffer A until the signal at the detector returns to baseline.
3. Elute with a gradient from 0 to 20% acetonitrile in 5 min, followed by a gradient from 20 to 50% acetonitrile in 60 min.

The two soluble TNFRs elute at 28 to 29% acetonitrile and 31 to 32% acetonitrile, respectively. The purity is sufficient to sequence the resulting proteins according to Edman. The biological activity is preserved, and specific activities in a range of 300,000 U/mL for the soluble p55-TNFR and 50,000 for the soluble p75-TNFR should be expected. One unit is defined as the amount of TNFR needed to obtain a statistically significant protection from an LD_{50} dose of TNF (approx 1–2 U/mL) in the standard TNF cytotoxicity assay using L929 cells as target. The use of very harsh conditions in elution from the affinity column, such as 3*M* urea or pH 12, may reduce the bioactivity.

4. Notes

1. Whereas the molecular weight of the soluble p55-TNFR is invariably in the range of 30 kDa, it should be noted that there are two forms of the soluble p75-TNFR, one of approx 30 kDa and a second of approx 42 kDa. Depending on the source, either form may be prevalent. Thus in urine of healthy donors the 30 kDa form is more common ***(19)***. From U937 supernatant, in contrast, mainly the 42-kDa form will be purified ***(17)***. Another notable difference between the two soluble TNFRs is the biological activity. When tested in the classical TNF bioassay, the soluble p55-TNFR has an approx 50-fold higher TNF neutralizing activity than the soluble p75-TNFR.

   Depending on the source, the yield may differ greatly. A healthy donor's urine yields approx 0.5 μg/L soluble p55-TNFR and up to 1.5 μg soluble p75-TNFR. Urine from febrile patients as well as U937 supernatants give better yields, in particular for the soluble p75-TNFR.

References

1. Ymer, S. I. and Herington, A. C. (1984) Water-soluble hepatic growth hormone receptors: structural studies using gel chromatography and chemical cross-linking. *Endocrinology* **114,** 1732–1739.
2. Leung, D. W., Spencer, S. A., Cachianes, G., Hammonds, R. G., Collins, C., Henzel, W. J., et al. (1987) Growth hormone receptor and serum binding protein: purification, cloning and expression. *Nature* **330,** 537–543.

3. Rubin, L. A., Kurman, C. C., Fritz, M. E., Biddison, W. E., Boutin, B., Yarchoan, R., et al. (1985) Soluble interleukin 2 receptors are released from activated human lymphoid cells in vitro. *J. Immunol.* **135**, 3172–3177.
4. DiStefano, P. S. and Johnson, E. M., Jr. (1988) Identification of a truncated form of the nerve growth factor receptor. *Proc. Natl. Acad. Sci. USA* **85,** 270–274.
5. Engelmann, H., Aderka, D., Rubinstein, M., Rotman, D., and Wallach, D. (1989) A tumor necrosis factor-binding protein purified to homogeneity from human urine protects cells from tumor necrosis factor cytotoxicity. *J. Biol. Chem.* **264,** 11,974–11,980.
6. Olsson, I., Lantz, M., Nilsson, E., Peetre, C., Thysell, H., and Grubb, A. (1989) Isolation and characterization of a tumor necrosis factor binding protein from urine. *Eur. J. Haematol.* **42,** 270–275.
7. Seckinger, P., Isaaz, S., and Dayer, J.-M. (1989) Purification and biologic characterization of a specific tumor necrosis factor α inhibitor. *J. Biol. Chem.* **264,** 11,966–11,973.
8. Symons, J. A., Eastgate, J. A., and Duff, G. W. (1990) A soluble binding protein specific for interleukin 1 beta is produced by activated mononuclear cells. *Cytokine* **2,** 190–198.
9. Novick, D., Engelmann, H., Wallach, D., and Rubinstein, M. (1989) Soluble cytokine receptors are present in normal human urine. *J. Exp. Med.* **170,** 1409–1414.
10. Novick, D., Cohen, B., and Rubinstein, M. (1994) The human interferon alpha/beta receptor: characterization and molecular cloning. *Cell* **77,** 391–400.
11. Knipping, E., Krammer, P. H., Onel, K. B., Lehman, T. J., Mysler, E., and Elkon, K. B. (1995) Levels of soluble Fas/APO-1/CD95 in systemic lupus erythematosus and juvenile rheumatoid arthritis. *Arthritis Rheum.* **38,** 1735–1737.
12. Novick, D., Kim, S. H., Fantuzzi, G., Reznikov, L. L., Dinarello, C. A., and Rubinstein, M. (1999) Interleukin-18 binding protein: a novel modulator of the Th1 cytokine response. *Immunity* **10,** 127–136.
13. Simonet, W. S., Lacey, D. L., Dunstan, C. R., Kelley, M., Chang, M. S., Luthy, R., et al. (1997) Osteoprotegerin: a novel secreted protein involved in the regulation of bone density [see comments]. *Cell* **89,** 309–319.
14. Fernandez-Botran, R., Crespo, F. A., and Sun, X. (2002) Soluble cytokine receptors in biological therapy. *Expert Opin. Biol. Ther.* **2,** 585–605.
15. Gatanaga, T., Hwang, C., Kohr, W., Cappuccini, F., Lucci, J. A. I., Jeffes, E. W. B., et al. (1990) Purification and characterization of an inhibitor (soluble tumor necrosis factor receptor) for tumor necrosis factor and lymphotoxin obtained from the serum ultrafiltrates of human cancer patients. *Proc. Natl. Acad. Sci. USA* **87,** 8781–8784.
16. Schall, T. J., Lewis, M., Koller, K. J., Lee, A., Rice, G. C., Wong, G. H., et al. (1990) Molecular cloning and expression of a receptor for human tumor necrosis factor. *Cell* **61,** 361–370.
17. Kohno, T., Brewer M. T., Baker S. L., Schwartz P. E., King M. W., Hale K. K., et al. (1990) A second tumor necrosis factor receptor gene product can shed a natu-

rally occurring tumor necrosis factor inhibitor. *Proc. Natl. Acad. Sci. USA* **87,** 8331–8335.

18. Wallach, D. (1984) Preparations of lymphotoxin induce resistance to their own cytotoxic effect. *J. Immunol.* **132,** 2464.
19. Corti, A., D'Ambrosio, F., Marino, M., Merli, S., and Cassani, G. (1995) Identification of differentially glycosylated forms of the soluble p75 tumor necrosis factor (TNF) receptor in human urine. *Eur. Cytokine Netw.* **6,** 29–35.

4

Production and Characterization of Receptor-Specific TNF Muteins

Paul Ameloot and Peter Brouckaert

Summary

Tumor necrosis factor (TNF) is a pleiotropic cytokine with a wide range of biological activities including cytotoxicity, immune-cell proliferation, and mediation of inflammatory responses. Mutational analysis of mature TNF has been facilitated by the high expression levels that were obtained in *Escherichia coli* cells. Furthermore, the fact that mature TNF does not form inclusion bodies, but remains soluble in bacterial extracts, allows a fast and easy characterization. We describe an efficient method for the introduction of a specific mutation in mature murine TNF making use of double-stranded plasmid DNA and two oligonucleotides. Two in vitro protocols are given that allow assessment of the binding of wild-type TNF and/or TNF muteins to TNF receptors (TNFR) (radioligand competition binding and Biacore). The biological activity of wild-type TNF and/or TNF muteins can be assessed in cellular assays. TNF-induced cytotoxicity toward murine L929s cells and human Kym39A6 cells is mediated by interaction with cellular TNFR-I, whereas TNF-induced proliferation of murine CT6 cells is mediated by triggering of cellular TNFR-II.

Key Words: Tumor necrosis factor; mutagenesis; oligonucleotide; iodination; competition binding; Biacore; cytotoxicity assay; cell proliferation assay; L929s; Kym39A6; CT6; MTT.

1. Introduction

Tumor necrosis factor (TNF) is a pleiotropic cytokine with a wide range of biological activities including cytotoxicity, immune cell proliferation, and mediation of inflammatory responses. It is produced as a transmembrane protein, and enzymatic cleavage of the extracellular part can give rise to mature, soluble TNF protein. Transmembrane as well as mature TNFs form homotrimeric molecules and are biologically active. Activity is mediated by the interaction with two types of TNF receptors, i.e., TNFR-I and TNFR-II. As

From: *Methods in Molecular Medicine, Vol. 98: Tumor Necrosis Factor*
Edited by: A. Corti and P. Ghezzi © Humana Press Inc., Totowa, NJ

well TNFR-I as TNFR-II bind to the intrasubunit grooves of a trimeric TNF molecule.

Mutational analysis of mature TNF has been facilitated by the high expression levels that were obtained in *Escherichia coli* cells. Furthermore, the fact that mature TNF does not form inclusion bodies, but remains soluble in bacterial extracts, allows a fast and easy purification and characterization. Studying the influence of site-specific mutations in recombinant TNF, it has become clear that it is possible to block specifically the interaction of TNF with one type of receptor ***(1–3)***.

In this chapter we describe the introduction of a specific mutation in mature murine TNF. The method works by simultaneously annealing two oligonucleotide primers to one strand of a denatured double-stranded plasmid. One primer introduces the desired mutation, and the second restores antibiotic resistance to the expression plasmid. In order to characterize a mutant TNF protein, one has to compare its binding to both types of TNF receptors with that of wild-type TNF and to analyze its activity in biological assays. In this chapter we describe two in vitro protocols to assess the binding of TNF mutein to TNF receptors, and three cellular assays to assess the biological activity of TNF muteins. TNF-induced cytotoxicity toward murine L929s cells and human Kym39A6 cells is mediated by interaction with cellular TNFR-I; TNF-induced proliferation of murine CT6 cells is mediated by triggering of cellular TNFR-II. Although wild-type human TNF is active in the murine L929s cytotoxicity assay, muteins interacting specifically with human TNFR-I or TNFR-II were inactive in this assay ***(4)***. Therefore, the Kym39A6 cytotoxicity assay is more suited for the characterization of human TNF muteins. Because of the great specificity and affinity of the interaction between TNF and its receptors, and due to the fact that the sensitivity of these cellular assays for TNF is not influenced by the presence of bacterial endotoxins, crude bacterial lysates containing recombinant mature TNF mutein can also be used for an initial characterization of the effects of a given mutation on the interaction with TNF receptors in these assays.

2. Materials

2.1. Mutagenesis of the TNF Expression Plasmid

1. Expression plasmid pMaTrpMTNF (*see* **Note 1**).
2. Phosphorylated chloramphenicol selection primer:
   5' C CAG CTa AAC GGT C 3' (lowercase, altered nucleotide; underlined, *Pvu*II site deleted) (*see* **Note 2**).
3. Phosphorylated mutagenic primer:
   5' TCA TAC CAG acG AAA GTt AAC CTC 3' (lowercase, altered nucleotides; underlined, *Hpa*I site) (*see* **Note 3**).

4. 10X annealing buffer: 200 m*M* Tris-HCl, pH 7.5, 100 m*M* $MgCl_2$, 500 m*M* NaCl.
5. 10X synthesis buffer: 100 m*M* Tris-HCl, pH 7.5, 5 m*M* dNTPs, 10 m*M* ATP, 20 m*M* DTT.
6. T4 DNA polymerase (4 U/μL) and T4 DNA ligase (4 U/μL).
7. *E. coli* strains, WK6mutS (*see* **Note 4**) and MC1061.
8. Luria bertani (LB) medium: 10 g/L bacto-tryptone, 5 g/L bacto-yeast extract, 10 g/L NaCl. Autoclave to sterilize.
9. LB plates containing antibiotics: Add 15 g/L agar to LB medium and autoclave. Allow autoclaved media to cool to 55°C before adding antibiotics and pouring plates (Petri dishes). Store the plates at 4°C.
10. STET buffer: 8% sucrose, 5% Triton X-100, 50 m*M* Tris-HCl, pH 8.0, 50 m*M* EDTA. Filter-sterilize (0.22 μm). Store at 4°C.
11. Lysozyme/RNase mix: 10 mg/mL lysozyme, 1 mg/mL RNase, 50 m*M* Tris-HCl, pH 8.0. Store at –20°C in small aliquots.
12. 5*M* ammonium acetate.
13. TE buffer: 10 m*M* Tris-HCl, pH 7.5, 1 m*M* EDTA.
14. Ampicillin: 100 mg/mL (1000X) stock solution in water.
15. Chloramphenicol: 25 mg/mL (1000X) stock solution in ethanol. Store at –20°C.
16. Minimal medium: 100 m*M* HEPES-HCl, pH 6.4, 1X M9 salts, 0.5% casamino acids, 0.5% glucose, 1 m*M* $MgCl_2$, 0.1 m*M* $CaCl_2$. Prepare by dilution from the following stock solutions: 1 *M* HEPES-HCl, pH 6.4 (autoclaved), 10X M9 salts: 6 g/L Na_2HPO_4, 3 g/L KH_2PO_4, 1 g/L NH_4Cl, 0.5 g/L NaCl (autoclaved), 10% casamino acids (DIFCO Laboratories) (autoclaved), 20% glucose (filter-sterilized), 200 m*M* $MgCl_2$ (autoclaved), and 200 m*M* $CaCl_2$ (autoclaved).
17. Lysis buffer: 10 m*M* Tris-HCl, pH 8.0, 5 m*M* EDTA, 2 m*M* PMSF, 10 m*M* benzamidine, 200 U/mL aprotinine, 0.1 mg/mL lysozyme.
18. Ultrasonic cell disruptor (Branson Sonifier).

2.2. In Vitro Assays for TNF Receptor Binding

1. IODO-GEN (Pierce).
2. Borax buffer: 0.1 *M* boric acid-borax, pH 7.5.
3. PBS (phosphate-buffered saline): 4.3 m*M* Na_2HPO_4, 1.4 m*M* KH_2PO_4, pH 7.3, 137 m*M* NaCl, 2.7 m*M* KCl.
4. PBS/gelatine: PBS containing 0.25% gelatine. Heat at 65°C to dissolve gelatine.
5. Glass tube: 12 × 75 mm test tube.
6. Chloroform.
7. $Na^{125}I$ in NaOH solution for protein iodination, 4 GBq/mL (107 mCi/mL). Store at ambient temperature (*see* **Note 5**).
8. NAP-10 gel filtration column (Amersham Pharmacia Biotech).
9. Recombinant mouse TNF (*see* **Note 6**).
10. γ-counter.
11. Purified recombinant soluble mTNF receptors (*see* **Note 7**).
12. 96-well Breakapart microtiter strips (Nunc).
13. PBS/BSA: PBS containing 0.1% bovine serum albumin. Store at 4°C.

14. Biacore 2000 apparatus (Biacore AB).
15. CM5 sensor chip (Biacore AB).
16. HBS: 10 m*M* HEPES-NaOH, pH 7.4, 150 m*M* NaCl, 3 m*M* EDTA.
17. NHS: 11.5 mg/mL *N*-hydroxysuccinimide in water. Store at –20°C.
18. EDC: 75 mg/mL 1-ethyl-3-(3-dimethylaminopropyl) carbodiimide hydrochloride in water. Store at –20°C.
19. Ethanolamine: 1 *M* ethanolamine hydrochloride-NaOH, pH 8.5. Store at 4–8°C.
20. Regeneration buffer: 10 m*M* glycine-HCl, pH 2.5.

2.3. Cellular Assays for TNF Biological Activity

1. Murine fibrosarcoma cell line L929s.
2. DMEM complete: DMEM containing 10% fetal calf serum, 2 m*M* L-glutamine, 100 U/mL penicillin, and 100 μg/mL streptomycin.
3. MTT solution: 5 mg/mL 3-(4,5-dimethylthiazol-2-yl)-2,5-difenyltetrazolium bromide in PBS, and sterilized on a 0.22-μm filter. Store at 4°C, protected from light.
4. SDS/HCl: 10% SDS in 0.01*N* HCl.
5. Trypsin/EDTA: 2.5 g/L of trypsin and 0.38 g/L of EDTA•4Na in Hanks balanced salt solution.
6. Actinomycin D: 1 mg/mL stock solution in 70% ethanol. Store at –20°C. Prepare working stock by dilution 1:100 in medium.
7. 96-well microtiter plate (flat bottom).
8. Microplate reader.
9. Humidified incubator with 5% CO_2 in air.
10. Human rhabdomyosarcoma cell line Kym39A6 ***(5)***.
11. RPMI complete: RPMI containing 10% fetal calf serum, 2 m*M* L-glutamine, 1 m*M* sodium pyruvate, 0.05 m*M* 2-mercaptoethanol, 100 U/mL penicillin, and 100 μg/mL streptomycin.
12. Cell dissociation buffer, enzyme free, PBS based (Gibco).
13. Murine CT6 cell line ***(6)***.
14. ^{3}H-thymidine: 1 mCi/mL. Prepare working stock by 1:20 dilution in medium.
15. EL4-supernatant (*see* **Note 8**).
16. Filtermate Harvester and microplate scintillation counter (Packard).
17. Microtiter plate with bonded GF/C filter.
18. Plate Sealer and adhesive tape (Packard).
19. MicroScint-O (Packard).

3. Methods

3.1. Mutagenesis of TNF Expression Plasmid

3.1.1. Denaturation of Plasmid DNA and Annealing of Primers to the DNA Template

1. Prewarm a water bath to boiling (100°C).
2. Prepare the primer/plasmid annealing reaction in a microcentifuge tube: 2 μL

10X annealing buffer, 2 μL plasmid pMaTrpMTNF (0.05 μg/μL), 2 μL phosphorylated chloramphenicol selection primer (0.05 μg/μL), 2 μL phosphorylated mutagenic primer (0.05 μg/μL), sterile deionized water to a final volume of 20 μL.
3. Incubate the DNA mix at 100°C for 3 min.
4. Chill immediately in an ice-water bath for 5 min.

3.1.2. Synthesis of the Mutant Strand

1. To the primer/plasmid solution add the following: 3 μL 10X synthesis buffer, 1 μL T4 DNA polymerase, 1 μL T4 DNA ligase, 5 μL sterile, deionized water (final volume 30 μL).
2. Incubate at 37°C for 2 h.
3. Stop the reaction by heating at 70°C for at least 5 min.
4. Let the tube cool to room temperature and proceed with transformation or store at 4°C.

3.1.3. First Transformation

1. Add 5–10 μL of the plasmid/primer DNA solution to a 10-mL tube containing 100 μL competent WK6mutS cells, and incubate for 20 min on ice (*see* **Note 9**).
2. Transfer tube to 42°C water bath for 1 min.
3. Add 1 mL of LB medium to tube and incubate for 60 min at 37°C with shaking at 220 rpm.
4. To assess the efficiency of the mutagensis reaction, spread 100 μL of the transformation mixture onto an LB plate containing chloramphenicol and ampicillin, and incubate at 37°C overnight.
5. Add the transformation mixture (use 100 μL and 800 μL) to 4 mL LB containing chloramphenicol and ampicillin, and incubate the cultures at 37°C overnight with shaking at 220 rpm.

3.1.4. Isolation of the Plasmid Pool Using the Boiling-Lysis Method

1. Transfer 2 mL of the overnight culture to a 2.5 mL microcentrifuge tube and centrifuge at 1200*g* for 3 min at room temperature.
2. Aspirate supernatant and resuspend the cell pellet in 200 μL of STET buffer.
3. Add 10 μL of lysozyme/RNase mix.
4. Transfer tubes to a 100°C water bath for 3 min.
5. Centrifuge tubes at 12,000*g* for 10 min.
6. Transfer the supernatant to a fresh 1.5 mL microcentrifuge tube.
7. Add 200 μL of 5*M* ammonium acetate solution and 400 μL of isopropanol.
8. Mix well by inverting the tube and centrifuge at 12,000*g* for 2 min at room temperature.
9. Aspirate supernatant carefully and wash pellet with 70% ethanol (centrifugation and aspiration of supernatant).
10. Air-dry the pellet for 5–10 min, until the remaining ethanol has evaporated.
11. Dissolve DNA pellet in 100 μL TE buffer. (The normal yield should be approx 1–3 μg.)

3.1.5. Second Transformation

1. Add 2 μL of the plasmid DNA to a 10-mL tube containing 100 μL competent MC1061 cells, and incubate for 20 min on ice.
2. Transfer tube to a 42°C water bath for 1 min.
3. Add 1 mL of LB medium to the tube and incubate for 60 min at 37°C with shaking at 220 rpm.
4. Set up a serial dilution of the transformed cells in LB medium (undiluted and diluted 1:10 and 1:100).
5. Spread out 100 μL of each dilution on LB plates containing chloramphenicol and ampicillin (three plates each).
6. Incubate the plates at 37°C overnight.
7. Store the plates at 4°C until characterization of the individual colonies.

3.1.6. Characterization of Individual Colonies

1. Single colonies can be picked with toothpicks and used to inoculate in sequence a plate and a 2-mL liquid culture containing LB with antibiotics.
2. Incubate at 37°C overnight.
3. Seal the plate with parafilm and store at 4°C.
4. Use the liquid culture for the isolation of the plasmid DNA and characterize it by restriction enzyme digestions ***(7)*** and DNA sequencing ***(8,9)***.

3.1.7. Bacterial Expression of TNF Mutein

1. Pick an individual colony of MC1061 that contains the desired pMacTrpMTNF-x plasmid from a plate, and grow overnight in LB containing ampicillin and chloramphenicol at 37°C with shaking at 220 rpm.
2. Dilute culture 1:100 in 10 mL minimal medium containing ampicillin and chloramphenicol, and incubate for 24 h at 30°C with shaking at 220 rpm (*see* **Note 10**).
3. Collect the cells by centrifugation at 4000*g* for 10 min at 4°C.
4. Resuspend cells in 0.9 mL of lysis buffer.
5. Disrupt bacteria with an ultrasonic cell disruptor 2 times for 2 min at maximal output on ice.
6. Centrifuge for 15 min at 14,000*g* at 4°C, and collect supernatant and pellet.
7. Analyze supernatant and pellet by electrophoresis on a 15% sodium dodecyl sulfate polyacrylamide gel followed by staining with Coomassie brilliant blue ***(7)*** to confirm the presence and the approximate amount of recombinant TNF protein.
8. Filter-sterilize supernatant (0.22 μm) and store at –20°C in aliquots.

3.2. In Vitro Assays for TNF Receptor Binding

3.2.1. Iodination of Murine TNF

1. Weigh out IODO-GEN powder and dissolve in chloroform at a concentration of 250 μg/mL.

2. Add 40 μL of IODO-GEN solution to a glass tube and evaporate chloroform under a nitrogen stream.
3. Wash the tube with 40 μL of borax buffer (add and remove).
4. Add 36 μL of ice-cooled borax buffer and 4 μL $Na^{125}I$.
5. Incubate on ice for 10 min to generate iodine radicals.
6. Transfer this solution to a microcentrifuge tube containing 4 μg murine TNF (in less than 5 μL) and leave on ice for 15 min.
7. Add 200 μL of ice-cooled PBS/gelatine, and apply the reaction mixture to a NAP-10 gel filtration column, equilibrated with PBS/gelatine.
8. Elute TNF with PBS/gelatine: add 500 μL and let sink in completely, change sample tube, and add again 500 μL.
9. Collect 8 fractions of 500 μL and count 2-μl aliquots of each fraction in a gamma counter.
10. Pool the 2 fractions with the highest counts, normally fractions 2–3 (this is the runthrough), count 2-μL aliquots in a gamma counter, and store at 4°C.

3.2.2. Solid-Phase Radioligand Competition-Binding Assay

1. Coat breakapart strips with soluble murine TNFR at a concentration of 1 μg/mL in PBS at 4°C overnight (use 100 μL/well).
2. Block each well with 150 μL of PBS containing 2% BSA for 2 h at room temperature.
3. Wash wells twice with 100 μL of PBS/BSA.
4. Dilute unlabeled TNF (mutein) in PBS/BSA using 10-fold dilution so the final concentrations are from 10^2 to 10^{-5} μg/mL.
5. To 50 μL of this dilution series add 50 μL of a solution containing 20 ng/mL ^{125}I-TNF, and apply this mixture to the wells coated with TNFR.
6. Incubate for 3 h at room temperature.
7. Wash wells at least three times with PBS/BSA; aspirate and collect radioactive liquid waste.
8. Break off wells from strip and count each well individually in a γ-counter.
9. Plot bound ^{125}I-TNF (cpm) vs concentration of unlabeled TNF (mutein) and determine IC50 (concentration for 50% inhibition).

3.2.3. TNF Receptor Binding Assay Using BIAcore 2000

3.2.3.1. Immobilization of TNF Receptors on Chip

1. Dock a new CM5 sensor chip on the apparatus and prime it with HBS.
2. Start a sensorgram selecting for detection on the four channels, and set flow rate at 10 μL/min.
3. Change flow path to channels 1 and 2, and inject 50 μL of a freshly prepared mixture of NHS and EDC (1:1).
4. Change flow path to channel 2, and inject 50 μL of TNFR-II at a concentration of 25 μg/mL in 10 m*M* sodium acetate, pH 4.0.
5. Change flow path to channel 3, and inject 50 μL of NHS/EDC mixture.

6. Inject 50 μL of TNFR-I, 25 μg/mL in 10 m*M* NaAc, pH 4.0, over channel 3.
7. Change flow to channel 1, 2, and 3, and inject 50 μL of ethanolamine.
8. Determine the net immobilized protein for the different channels by setting report points after injection of NHS/EDC (reference point) and after injection of ethanolamine.
9. Stop sensorgram.

3.2.3.2. Interaction Analysis

1. Dock the CM5 sensor chip prepared under **Subheading 3.2.3.1.** on the apparatus.
2. Start a sensorgram selecting for detection on the 4 channels, and set flow to channels 1–3, with a flow rate of 25 μL/min.
3. Dilute murine TNF in HBS at a concentration of 15 μg/mL and inject 125 μL with a dissociation time of 5 min (*see* **Note 11**).
4. Change flow rate to 10 μL/min.
5. Inject 25 μL of a regeneration solution two times to remove all TNF from the chips.
6. Start a new cycle and repeat **steps 2–5**, changing the concentration of the TNF solution (**step 3**). A complete interaction analysis involves a concentration range from 15 μg/mL to 154 ng/mL TNF (in steps of 1:2.5).
7. Stop sensorgram and open data file in BIAevaluation program in order to calculate the affinity and/or the kinetic parameters of the interaction between TNF (mutein) and its receptors.

3.3. Cellular Assays for TNF Biological Activity

3.3.1. L929s Cytotoxicity Assay

3.3.1.1. Maintenance of L929s Cells

Grow cells in DMEM complete. Subculture cells every 3–4 d as follows:

1. Aspirate medium and wash the cell layer with PBS.
2. Add 2 mL of trypsin/EDTA (for a 25-cm^2 tissue culture flask) and aspirate.
3. Add 5 mL of trypsin/EDTA and incubate at 37°C until all cells have detached from plastic (normally 5–10 min; check with an inverted microscope).
4. Wash cells once with DMEM complete by centrifugation for 5 min at 200*g*.
5. Reseed tissue culture flasks with dilution 1:10 or 1:20 in DMEM complete.

3.3.1.2. L929s Cytotoxicity Assay

1. Seed L929s cells at 20,000 cells/well (in 80 μL) on 96-well microtiterplates (flat bottom) and incubate for 16 h at 37°C in a humidified incubator under 5% CO_2 in air.
2. Add 20 μL Actinomycin-D into each well (final concentration 1 μg/mL).
3. Dilute TNF (mutein) in DMEM using threefold dilution so the final concentrations are from 20 ng/mL to 0.5 pg/mL.
4. Transfer 100 μL from this dilution series to the wells containing the cells.
5. Incubate for 18 h at 37°C in the incubator.

6. Add 20 µL of MTT solution and incubate for 4–6 h at 37°C (*see* **Note 12**).
7. Add 80 µL SDS/HCl and incubate at 37°C overnight to lyse the cells and to dissolve the formazan crystals.
8. Measure absorbance in a microplate reader at λ1 595 nm, with λ2 655 nm as reference.
9. Plot absorbance (OD) versus concentration of TNF (in *x*-axis) and determine TNF (mutein) concentration needed to kill 50% of the cells. By definition, a TNF solution that kills 50% of the cells corresponds to 1 U/mL (*see* **Note 13**).

3.3.2. Kym39A6 Cytotoxicity Assay

3.3.2.1. Maintenance of Kym39A6 Cells

Grow cells in RPMI complete. Subculture cells every 2–3 d, using cell dissociation buffer (enzyme free) to detach the cells, and reseed at dilution 1:10 or 1:20 in RPMI complete.

3.3.2.2. Kym39A6 Cytotoxicity Assay

1. Seed Kym39A6 at 10,000 cells/well (in 100 µL) on 96-well microtiterplates (flat bottom) and incubate for 16 h at 37°C in a humidified incubator under 5% CO_2 in air.
2. Dilute TNF (mutein) in DMEM using threefold dilution so the final concentrations are from 20 ng/mL to 0.5 pg/mL.
3. Transfer 100 µL from the dilution series to the wells containing the cells.
4. Incubate for 18 h at 37°C in the incubator.
5. Add 20 µL of MTT solution and incubate overnight at 37°C.
6. Add 80 µL SDS/HCl and incubate at 37°C for 48 h (*see* **Note 14**).
7. Measure absorbance in a microplate reader at λ1 595 nm, with λ2 655 nm as reference.
8. Plot absorbance (OD) vs concentration of TNF (in *x*-axis) and determine the concentration of TNF (mutein) needed to kill 50% of the cells.

3.3.3. CT6 Proliferation Assay

3.3.3.1. Maintenance of CT6 Cells

Grow cells in RPMI complete supplemented with 10% EL4-supernatant (as source for murine IL-2) at 37°C. Subculture cells every 2–3 d at 5×10^4 to 5×10^5 cells/mL. Harvest the cells in the culture supernatant as well as the adhering cells, using cell dissociation buffer (enzyme free). Precipitate cells by centrifugation for 8 min at 500*g*.

3.3.3.2. Cell Proliferation Assay

1. Subculture cells at 10^5 cells/mL in RPMI complete, containing 5% EL4 supernatant for 3 d.
2. Collect the cells in the supernatant and the adhering cells by treatment with cell dissociation buffer.

3. Wash cells twice in RPMI complete (without EL4 supernatant) by centrifugation at 500*g* for 8 min.
4. Incubate cells for 1 h in RPMI complete at 37°C on a rotating wheel.
5. Wash cells once in RPMI complete, and seed 96-well plate at 5×10^4 cells/well (in 100 μL).
6. Add TNF solution (100 μL) and incubate for 24 h at 37°C.
7. Pulse cells with ^{3}H-thymidine (10 μL of working stock; 0.5 μCi/well) and incubate for 6 h.
8. Place the microtiter plate at –20°C overnight to detach/lyse the cells.
9. Transfer the cells from the microtiter plates to 96-well microplates with bonded GF/C filter using a Filtermate Harvester.
10. Wash the microtiter plates 5 times with water and finally with ethanol, passing all wash solutions over the filter plate.
11. Dry filter completely at 45°C and seal the bottom of the filter plate with adhesive tape on a Plate Sealer.
12. Add 20 μL of MicroScint-O to each well of the filter plate and seal the filter plate with adhesive tape.
13. Measure bound radioactivity in a microplate scintillation counter.
14. Plot incorporated ^{3}H-thymidine (cpm) vs TNF concentration (*see* **Note 15**).

4. Notes

1. In the bacterial expression plasmid pMaTrpMTNF the coding information for mature murine TNF is placed under control of the inducible *trp* promoter and translation initiation is guided by the *trp* ribosome binding site ***(3)***. Induction of the promoter is achieved by starvation of the cells for L-trp upon growing in minimal medium. The plasmid carries the β-lactamase gene that confers resistance to ampicillin and a mutated chloramphenicol acetyl transferase gene (CAT). Because the codon for Gln-38 (CAG) of the CAT gene is replaced by a stop codon (UAG), this plasmid does not confer resistance to chloramphenicol in (translation termination) suppressor-negative strains of *E. coli*, such as WK6mutS and MC1061.
2. The pMa58-derived plasmids contain an inactivated CAT gene ***(10).*** The chloramphenicol selection primer reverts the mutant stop codon in the CAT gene to Gln. The primer used is complementary to the coding strand because the CAT gene is inserted counterclockwise in the plasmid. The plasmid with a reverted CAT gene confers resistance to chloramphenicol (and also to ampicillin), and is therefore annotated as pMacTrpMTNF.
3. To rapidly check for the presence of the mutation by restriction enzyme analysis, an oligonucleotide was synthesized in which the codon mutation (Glu89Thr; GAG>ACG) was accompanied by the formation of a new restriction site for *Hpa*I (silent mutation of Val 91: GTC>GTT) in the TNF gene. Generally, the following considerations should be made for designing a mutagenic primer: (1) 6–13 nucleotides of uninterrupted, matched sequences on both ends of the primer (flanking the mismatched sites) give sufficient annealing stability, (2) optimally,

the mismatched bases should be placed in the center of the primer sequence, (3) optimally, the primer should start and end with a G or a C, (4) the annealing strength of the mutagenic primer should be greater than (or equal to) that of the selection primer, and (5) mutagenic and selection primers must anneal to the same strand of the plasmid.

4. This strain carries a Tn10 insertion in *mutS*. This insertion causes a repair-deficiency phenotype (preventing undesirable repair of the mutant DNA strand during the first transformation) as well as tetracycline resistance. To maintain the repair-deficiency phenotype, this strain must be grown on medium containing 25 μg/mL tetracycline. Tetracycline hydrochloride stock: 12.5 mg/mL in ethanol/water (1:1), store at –20°C.
5. ^{125}I accumulates in the thyroid and is a potential health hazard. The $^{125}I_2$ formed during oxidation of $Na^{125}I$ is volatile. Work in an approved chemical fume hood when exposing the $Na^{125}I$ to an oxidizing reagent such as IODO-GEN (iodination and subsequent gel filtration). To prevent the formation of volatile $^{125}I_2$ in ^{125}I-containing liquid waste, add 1 volume of NaI solution to 5 volumes of waste. Shield all forms of the isotope with lead. Consult the local radiation safety office for further guidance in the appropriate use and disposal of radioactive materials. NaI solution: 0.1 *M* NaOH, 0.1 *M* $Na_2S_2O_3 \cdot 5H_2O$, 10 g/L NaI.
6. Use recombinant TNF that is free of protein carrier.
7. Use recombinant TNF receptor that is free of protein carrier.
8. The mouse thymoma cel line, EL4, secretes IL-2 upon induction with phorbol 12-myristate 13-acetate (PMA, Sigma-Aldrich). Grow EL4 cells in DMEM containing 5% fetal calf serum, 2 m*M* L-glutamine, 1 m*M* sodium pyruvate, 100 U/mL penicillin, and 100 μg/mL streptomycin at 37°C in roller bottles. Subculture every 2–3 d at 10^5 cells/mL. IL-2 induction: Add 20 ng/mL PMA to a culture of 10^6 cells/mL and incubate for 4 h. Wash the cells and reseed in fresh medium with 2% fetal calf serum. Harvest medium after 72 h and store it at –20°C.
9. Grow a bacterial culture of WK6mutS overnight at 37°C with shaking at 220 rpm in LB containing tetracycline (25 μg/mL). Add 1 mL of the overnight culture to 100 mL LB and grow to OD_{600} 0.25–0.5. (This usually takes 2–3 h.) Chill on ice for 10 min and centrifuge for 10 min at 4000*g* at 4°C. Resuspend the cell pellet in 50 mL of an ice-cold solution of 100 m*M* $MgCl_2$. Centrifuge this suspension and resuspend the cell pellet in 50 mL of ice-cold 100 m*M* $CaCl_2$. Incubate for 20 min on ice. Pellet cells by centrifugation and resuspend with 5 mL of an ice-cold solution of 100 m*M* $CaCl_2$. Incubate for 20 min and finally add 1.76 mL of glycerol. Dispense 100-μL aliquots in 10-mL tubes and store at –80°C. As competent cells are very sensitive to variations in temperature, keep the cells on ice during aliquoting and upon the preparation for transformation with plasmid DNA.
10. Growing the bacterial cells at lower temperature often enhances the expression of TNF muteins and minimizes breakdown of the protein ***(11)***.
11. The kinject command determines a low dispersion sample injection that is ideal for kinetic applications. During the association phase, TNF solution passes over the channels with the immobilized receptors, and the accumulation of TNF on

the chip due to specific binding with a receptor can be followed on the sensorgram. During the dissociation phase, HBS buffer is injected, and the release of TNF (mutein) from receptors immobilized on the chip can be measured.

12. MTT is highly mutagenic. Treat all solutions and plates containing MTT with sodium hypochlorite (available chlorine 10–13%) to inactivate the MTT. The tetrazolium salt MTT is reduced by the mitochondrial dehydrogenase of viable cells to form a blue formazan product. It should also be noted that bacteria and mycoplasma could convert MTT. Only mycoplasma-free cells should be used. It is strongly advised that the viability of the cells be assessed visually with an inverted microscope before adding MTT.
13. International standards of murine TNF and human TNF can be obtained from the National Institute for Biological Standards and Control, Hertfordshire, UK. These can be used to standardize the L929s cytotoxicity assay. By definition 1 IU of murine TNF corresponds to 5 pg protein and 1 IU of human TNF to 25 pg protein.
14. Because the formazan crystals formed in these cells are difficult to solubilize, the treatment with SDS/HCl is much longer. Check under an inverted microscope that all crystals have been dissolved before measuring the absorbance.
15. Although similar results with the CT6 assay have been obtained in various laboratories, the actual protocol seems to be particularly sensitive to unknown, local environmental factors. When difficulties arise (high background, small window) the following changes can be tried: Using recombinant IL-2 instead of EL4-supernatant (or vice versa); testing various serum batches; and prolonging the duration of the last culture before the assay.

Acknowledgments

We thank M. Van Den Hemel for her expert assistance in the preparation of this manuscript. Research is supported by grants from the FWO-Vlaanderen, the IUAP program, and the GBOU program.

References

1. Loetscher, H., Stueber, D., Banner, D., Mackay, F., and Lesslauer, W. (1993) Human tumor necrosis factor alpha mutants with exclusive specificity for the 55-kDa or 75-kDa TNF receptors. *J. Biol. Chem.* **268,** 26,350–26,357.
2. Van Ostade, X., Vandenabeele, P., Everaerdt, B., Loetscher, H., Gentz, R., Brockhaus, M., et al. (1993) Human TNF mutants with selective activity on the p55 receptor. *Nature* **261,** 266–269.
3. Ameloot, P., Fiers, W., De Bleser, P., Ware, C. F., Vandenabeele, P., and Brouckaert, P. (2001) Identification of tumor necrosis factor (TNF) amino acids crucial for binding to the murine p75 TNF receptor and construction of receptor-selective mutants. *J. Biol. Chem.* **276,** 37,426–37,430.
4. Van Ostade, X., Vandenabeele, P., Tavernier, J., and Fiers, W. (1994) Human tumor necrosis factor mutants with preferential binding to and activity on either the R55 or R75 receptor. *Eur. J. Biochem.* **220,** 771–779.

5. Meager, A. (1991) A cytotoxicity assay for tumour necrosis factor using a human rhabdomyosarcoma cell line. *J. Immunol. Methods* **144,** 141–143.
6. Ranges, G. E., Bombara, M. P., Aiyer, R. A., Rice, G. G., and Palladino, M. A., Jr. (1989) Tumor necrosis factor-α as a proliferative signal for an IL-2-dependent T cell line: strict species specificity of action. *J. Immunol.* **142,** 1203–1208.
7. Sambrook, J., Fritsch, E. F., and Maniatis, T. *Molecular Cloning: A Laboratory Manual*, 2nd ed., Cold Spring Harbor Laboratory, Cold Spring Harbor, New York, 1989.
8. Sanger, F., Nicklen, S., and Coulson, A. R. (1977) DNA sequencing with chain-terminating inhibitors. *Proc. Natl. Acad. Sci. USA* **74,** 5463–5467.
9. Biggin, M. D., Gibson, T. J., and Hong, G. F. (1983) Buffer gradient gels and 35S label as an aid to rapid DNA sequence determination. *Proc. Natl. Acad. Sci. USA* **80,** 3963–3965.
10. Stanssens, P., Opsomer, C., McKeown, Y. M., Kramer, W., Zabeau, M., and Fritz, H. J. (1989) Efficient oligonucleotide-directed construction of mutations in expression vectors by the gapped duplex DNA method using alternating selectable markers. *Nucleic Acids Res.* **17,** 4441–4454.
11. Leemans, R., Remaut, E., and Fiers, W. (1989) Correlation between temperature-dependent cytoplasmic solubility and periplasmic export of a heterologous protein in *Escherichia coli*. *Gene* **85,** 99–108.

5

TNFα Promoter Polymorphisms

Silvia Fargion, Luca Valenti, Paola Dongiovanni, and Anna Ludovica Fracanzani

Summary

Polymorphisms in the promoter of the tumor necrosis factor alpha (TNFα) gene have been reported to affect the transcription rate and the release of this cytokine. Among the best studied, the –238 and –308 polymorphisms have been associated with an increased transcriptional activity and TNFα release, whereas the –863 polymorphism have been associated with a reduced transcriptional activity. A growing body of evidence indicates that these polymorphisms may affect susceptibility to different diseases.

Here we describe a method to detect the –238, –308, and –863 TNFα polymorphisms by the polymerase chain reaction (PCR) and restriction fragment length polymorphism (RFLP) analysis. Briefly, DNA is amplified by PCR using mutagenic primers containing a single base-pair mismatch adjacent to the polymorphic site to introduce a restriction site into the wild-type nucleotide sequences after amplification. The PCR products are then digested with specific restriction enzymes and analyzed by agarose gel electrophoresis.

Key Words: TNFα; promoter; polymorphism; restriction analysis; PCR; TNFα –308 polymorphism; TNFα –238 polymorphism; TNFα –863 polymorphism; genetic susceptibility.

1. Introduction

Investigators have become increasingly interested in the possible role of genetic polymorphisms in human diseases. Some polymorphisms have functional effects on the gene product and thus are the most useful type of polymorphism in disease-association studies, while others with no evidence of functional effects are simply useful markers. Functional effects are most likely to occur (1) when the polymorphisms are associated with an amino acid substitution in the gene product, (2) when a deletion or insertion results in a frameshift in the coding region, or (3) when the polymorphism directly affects gene transcription, RNA splicing, mRNA stability, or mRNA translation.

From: *Methods in Molecular Medicine, Vol. 98: Tumor Necrosis Factor*
Edited by: A. Corti and P. Ghezzi © Humana Press Inc., Totowa, NJ

Many common polygenic diseases have an autoimmune and/or inflammatory component involved in their pathogenesis. Individual variation in genes that encode proteins with an involvement in the immune and inflammatory responses is therefore a potentially important susceptibility factor. Thus far, one of the cytokine genes that has received much attention is tumor necrosis factor alpha (TNFα), possibly because it is located within the MHC gene cluster, raising the possibility that some reported MHC associations might be due to linkage to particular TNFα alleles ***(1,2)***. In fact, several studies showed that individual differences in TNFα production are inherited and could be linked to the MHC ancestral aplotype HLA A1-B8-DR3-DQ2-TNF308A, which is overrepresented in several autoimmune and inflammatory diseases ***(3)***.

A number of different polymorphisms exist in the promoter region of TNFα, of which the most frequent and best studied are those at position –238 and –308 ***(4,5)***. Though associations of these polymorphisms with susceptibility to a variety of diseases have been reported, consistent results have not been obtained, possibly due to the lack of a clear-cut functional significance. There have been a number of studies on the functional significance of both polymorphisms ***(6,7)***: Some reported increased transcriptional activity for the variant alleles ***(8–13)***, and others no difference compared to the wild type ***(14–16)***. Another polymorphism, at the position –863 in the promoter region, has been studied less extensively. Although the molecular mechanisms by which possibly functional single-nucleotide polymorphism (SNP) influences TNFα expression are poorly understood, it seems that interactions between nuclear proteins and the SNP sites provide information for the understanding of the allele specific modulation of TNFα expression ***(17)***. However, in the absence of reliable and consistent functional data, it is possible that many of the reported associations between TNFα alleles and disease susceptibility are either chance associations or reflect linkage with MHC genes ***(2,18)***.

1.1. TNFα –308 Polymorphism

The –308 G→A polymorphism, termed TNF2, is strongly linked to HLA aplotype A1-B8-DR3 ***(3)***. This linkage is of interest because it has been reported that individuals with this aplotype produce high levels of TNFα and are more susceptible to a wide spectrum of autoimmune diseases. Studies with the TNFα promoter linked to a reporter gene have shown that the TNF2 allele leads to an increased tissue-specific constitutive and inducible expression, both in vitro and in vivo, compared to the wild-type TNF1 allele ***(7,8,10,12,13)***.

Because of the different functions played by TNFα, the role of the –308 polymorphism in determining the susceptibility and/or the prognosis of various diseases has extensively been studied. Even if data are controversial, the polymorphism has been associated ***(19)*** with different diseases including:

- The prognosis of infective diseases (e.g., malaria and *H. Pylori*) and septic shock ***(20)***.
- Autoimmune and rheumatic diseases, and organ rejection ***(21,22)***.
- Autoimmune liver diseases and alcoholic steatohepatitis ***(23)***.
- The prognosis of non-Hodgkin's lymphoma ***(24)***.
- Alzheimer's disease and schizophrenia ***(25)***.

The prevalence of this polymorphism in healthy subjects from northern Italy as well as in other Caucasian populations is 0.12 ***(26)***.

1.2. TNFα –238 Polymorphism

Even if evidence is controversial ***(16)***, the TNFα –238 G→A polymorphism ***(5)*** has been associated with increased TNFα release ***(8,9)***. The TNF –238A allele has been associated with:

1. The susceptibility to tuberculosis, hepatitis C viral infection, and rheumatic diseases ***(27)***.
2. The degree of hepatic iron overload in hereditary hemochromatosis ***(26)***.
3. Insulin resistance, nonalcoholic fatty liver disease, and coronary heart disease ***(28)***.
4. Susceptibility to cancer ***(29)***.

The prevalence of this polymorphism in healthy subjects from northern Italy as well as in other Caucasian populations is 0.08 ***(26)***.

1.3. TNFα –863 Polymorphism

The –863 TNFα polymorphism (C→A substitution) is one of the most common genetic variants so far identified in the promoter region. A different binding of nuclear transcription factors (OCT-1 and NFκB) to the –863C and –863A alleles has been demonstrated ***(16,31)***; moreover, in healthy subjects with the –863A allele, a reduced transcriptional activity of TNFα in hepatocytes, monocytes, and adipocytes, and reduced serum levels of TNFα have been shown ***(11)***.

The TNF –863A allele has been associated with:

- Inflammatory bowel disease ***(31)***.
- Vascular dementia ***(25)***.

The prevalence of this polymorphism in healthy subjects from northern Italy as well as in other Caucasian populations is 0.17 ***(31)***.

1.4. Methodological Approach

The TNFα promoter polymorphisms are detected via polymerase chain reaction (PCR) and restriction fragment length polymorphism (RFLP) analysis

using mutagenic primers containing a single base-pair mismatch adjacent to the polymorphic site to introduce a restriction site into the wild-type nucleotide sequences after amplification ***(4,11,31,32)***.

2. Materials

1. Double-distilled water (ddH_2O).
2. NH_4^+ reaction buffer (10X): 160 m*M* $(NH_4)_2SO_4$, 670 m*M* Tris-HCl, pH 8.8 at 25°C, 0.1% Tween-20. Store at –20°C.
3. Mg^{2+} stock solution: 50 m*M* $MgCl_2$. Store at –20°C.
4. dNTPs (deoxynucleotides) mix 100 m*M*. Store at –20°C.
5. Oligonucleotide primers at 10 pmol/μL. Store at –20°C.

Forward –308:	5'- GCA ATA GGT TTT GAG GG<u>C</u> CAT G -3'
Reverse –308:	5'- GGG ACA CAC AAG CAT CAA GGA T -3'
Forward –238:	5'- AGA AGA CCC CCC TCG GAA <u>C</u>C -3'
Reverse –238:	5'- ATC TGG AGG AAG CGG TAG TG -3'
Forward –863:	5'- GGC TCT GAG GAA TGG GTT AC -3'
Reverse –863:	5'- CTA CAT GGC CCT GTC TTC GTT A<u>C</u>G -3'

Mismatch position is underlined

6. *Taq* DNA polymerase*.
7. DNA templates at 200–400 ng/μL*.
8. Ethidium bromide: 1 g of ethidium bromide in 100 mL of water. (It is a powerful mutagen and is toxic. Use under chemical fume hood. Avoid breathing the dust. Wear appropriate glasses when working with solution that contains this dye.)
9. TBE 10X: 108 g of Tris-(hydroxymethyl)aminomethane, 55 g of boric acid, 9.3 g of Na_2–EDTA; deionized water to a final volume of 1 L; the pH value of this solution is 8.3 (usually no pH adjustment is needed). The Tris compound may be harmful if inhaled, ingested, or absorbed through the skin. Wear appropriate gloves and safety glasses.
10. Ficoll 5X: 10 mL of TBE 10X, 0.8 mL of bromophenol blue, 3 g of Ficoll 400; deionized water to a final volume of 20 mL. Bromophenol blue may be harmful if inhaled, ingested, or absorbed through skin. Wear appropriate gloves and safety glasses. Use in a chemical fume hood.
11. Ficoll 3X: 3 parts of Ficoll 5X and 2 parts of TBE 1X.
12. DNA molecular weight markers of appropriate size*.
13. Restriction enzymes: *Nco*I for the –308 polymorphism, *Msp*I for the –238 polymorphism, *Tai*I for the –863 polymorphism, provided with buffers and BSA. Store at –20°C.

* For a *Taq* concentration of 5 U/μL.

14. Agarose gel equipment.
15. Thermal cycler.
16. Transilluminator.

3. Methods

3.1. Polymerase Chain Reaction (PCR)

3.1.1. TNFα –308 Polymorphism

1. Prepare a reaction mixture containing for each sample to be analyzed:

a. NH_4^+ buffer 10X (1X final conc.).	5 µL
b. $MgCl_2$ 50 m*M* (1.5 m*M* final conc.).	1.5 µL
c. dNTPs 10 m*M* (200 m*M* each final conc.).	1 µL each
d. Forward primer 10 m*M* (0.2 m*M* final conc.).	1 µL
e. Reverse primer 10 m*M* (0.2 m*M* final conc.).	1 µL
f. *Taq* polymerase (2.5 U final conc.).	0.5 µL*
g. ddH_2O to a final volume of 50 µL.	

2. Put 47 µL of reaction mixture in 0.25-mL amplification tubes.
3. Add 3 µL of DNA (about 200 ng/µL) to each sample, 3 µL of ddH_2O in the negative control sample.
4. Amplify the nucleic acids using the denaturation, annealing, and polymerization times and temperatures listed below (*see* **Note 1**):

a. 93°C for 3 min (denaturation).	
b. 92°C for 1 min (denaturation).	} 35 cycles
c. 63°C for 1 min (annealing).	
d. 72°C for 1 min (polymerization).	
e. 72°C for 10 min (polymerization).	

3.1.2. TNFα –238 Polymorphism

1. Prepare a reaction mixture containing for each sample to be analyzed:

a. NH_4^+ buffer 10X (1X final conc.).	5 µL
b. $MgCl_2$ 50 m*M* (1.5 m*M* final conc.).	1.5 µL
c. dNTPs 10 m*M* (200 µM each final conc.).	1 µL
d. Forward primer 10 µ*M* (0.2 µ*M* final conc.).	1 µL
e. Reverse primer 10 µ*M* (0.2 µ*M* final conc.).	1 µL
f. *Taq* polymerase (2.5 U final conc.).	0.5 µL*
g. ddH_2O to a final volume of 50 µL.	

2. Put 47 µL of reaction mixture in 0.25-mL amplification tubes.
3. Add 3 µL of DNA (about 200 ng/µL) to each sample, 3 mL of H_2O in the negative control sample.
4. Amplify the nucleic acids using the denaturation, annealing, and polymerization times and temperatures listed below:

* For a *Taq* concentration of 5 U/µL.

a. 94°C for 4 min (denaturation).
b. 58°C for 1 min (annealing).
c. 72°C for 45 s (polymerization).
d. 38 cycles (94°C for 1 min [denaturation]; 58°C for 1 min [annealing]; 72°C for 45 s [polymerization]).
e. 72°C for 10 min (polymerization).

3.1.3. TNFα –863 Polymorphism

1. Prepare a reaction mixture containing for each sample to be analyzed:

a. NH_4^+ buffer 10X (1X final conc.).	5 μL
b. $MgCl_2$ 50 m*M* (1.5 m*M* final conc.).	1.5 μL
c. dNTPs 10 m*M* (400 μ*M* each final conc.).	2 μL
d. Forward primer 10 μ*M* (0.6 μ*M* final conc.).	3 μL
e. Reverse primer 10 μ*M* (0.6 μ*M* final conc.).	3 μL
f. *Taq* polymerase (2 U final conc.).	0.4 μL*
g. ddH_2O to a final volume of 50 μL.	

2. Put 47 μL of reaction mixture in 0.25-mL amplification tubes.
3. Add 3 μL of DNA (about 200 ng/μL) to each sample, 3 μL of ddH_2O in the negative control sample.
4. Amplify the nucleic acids using the denaturation, annealing, and polymerization times and temperatures listed below:

a. 94°C for 3 min (denaturation).
b. 35 cycles (94° for 30 s [denaturation]; 59°C for 1 min [annealing]; 72°C for 2 min [polymerization]).

3.2. Agarose Gel Electrophoresis

1. Seal the open ends of the plastic tray supplied with the electrophoresis apparatus with tape to form a mold. Put an appropriate comb for forming the sample slots in the gel, and set the mold in the chemical fume hood.
2. Prepare the electrophoresis buffer (TBE 1X) to fill the electrophoresis tank and to cast the gel (*see* **Note 2**).
3. Prepare a solution of agarose in TBE 1X at a concentration appropriate for separating the particular size fragments expected in the DNA samples (3% agarose solution); add the correct amount of powdered agarose to a measured quantity of TBE 1X in a glass flask.
4. Loosely plug the neck of the flask with aluminum foil. Heat the agarose solution on a heating plate or in a microwave oven until the agarose dissolves; check the volume of the solution and, if reduced, replenish with H_2O.
5. Add ethidium bromide to a final concentration of 0.5 μg/mL. Mix the gel solution by gentle swirling, and pour the warm agarose solution into the mold. Check that no air bubbles are present in the gel; air bubbles present in the gel can be removed easily by poking them with a tip.

6. Allow the gel to set completely (30 min at room temperature), then pour a small amount of TBE 1X on the top of the gel and carefully remove the comb. Pour off the electrophoresis buffer and remove the tape. Mount the gel in the electrophoresis apparatus. Add just enough electrophoresis buffer to cover the gel.
7. Withdraw a sample (10 μL) from each reaction tube (including the negative control); mix with 5 μL of Ficoll 3X. Slowly load the sample mixture into the slots of the gel using a pipet. Load a DNA molecular marker into a slot.
8. Close the lid of the gel tank and attach the electrical leads so that the DNA will migrate toward the positive anode (red lead). Apply a voltage of 1.5 V/cm (measured as the distance between the positive and negative electrodes); bubbles should be generated at the anode and cathode, and within a few minutes the Bromophenol blue should migrate from the wells into the gel.
9. Run the gel until the bromophenol blue has migrated to an appropriate distance through the gel.
10. Turn off the electric current, remove the gel, examine the gel under UV lights (*see* **Note 3**) and photograph it. If bands of appropriate size (**Figs. 1–3**) are visualized in the lanes corresponding to DNA samples and no bands are visualized in the negative control, proceed to RFLP analysis (*see* **Notes 4** and **5**).

3.3. Restriction Fragment Length Polymorphism (RFLP) Analysis

3.3.1. The –308 Polymorphism

The PCR products (*see* **Note 6**) are then digested at 37°C with the *Nco*I restriction enzyme for 2 h using the a reaction mixture containing 5 U of *Nco*I (*see* **Note 7**), BSA, and an enzyme buffer as specified by the enzyme data sheet.

1. Add 5 μL of the reaction mixture (*see* **Note 8**) to 15 μL of PCR product in a 0.5-mL tube.
2. Add one drop of mineral oil to each tube to avoid evaporation.
3. Hold the reaction tubes at 37°C for 2 h.
4. Withdraw a sample (16 μL) from each tube, add 4 μL of Ficoll 5X and analyze the sample by electrophoresis through a 4% agarose gel.
5. The band pattern shown in **Fig. 1** is observed (*see* **Note 9** and **Fig. 1**).

3.3.2. The –238 Polymorphism

The PCR products (*see* **Note 6**) are then digested at 37°C with the *Msp*I restriction enzyme for 2 h using a reaction mixture containing 5 U of *Msp*I (*see* **Note 7**), BSA, and an enzyme buffer as specified by the enzyme data sheet.

1. Add 5 μL of the reaction mixture (*see* **Note 8**) to 15 μL of PCR product in a 0.5-mL tube.
2. Add one drop of mineral oil to each tube to avoid evaporation.
3. Hold the reaction tubes at 37°C for 2 h.

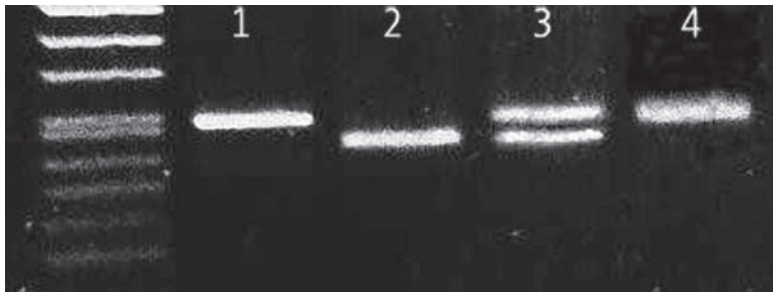

Fig. 1. The PCR yields a 144-base-pair (bp) product *(lane 1)*; the *Nco*I restriction enzyme cleaves the wild-type (TNF1) allele (restriction sequence: C'CATGG), giving rise to two different fragments of 126 and 18 bp. Thus, in subjects homozygous for the wild-type (TNF1) allele, a single band of 126 bp is observed *(lane 2)*; in heterozygous subjects (TNF1/TNF2), two bands of 144 and 126 bp *(lane 3)*; and in subjects homozygous for the mutated (TNF2) allele, a band of 144 bp *(lane 4)*.

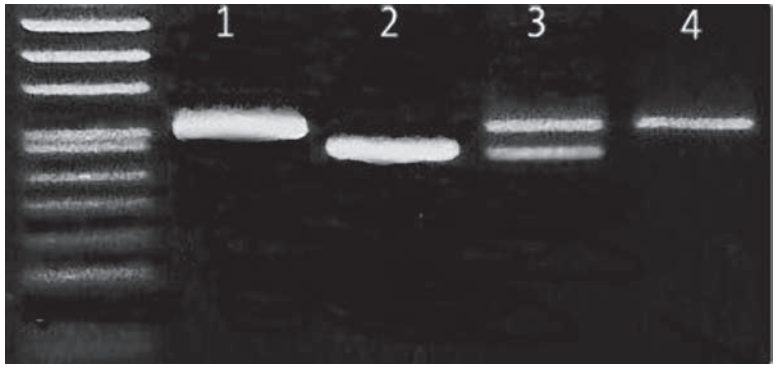

Fig. 2. The PCR yields a 151-base-pair product *(lane 1);* the *Msp*I restriction enzyme cleaves the wild-type (TNFG) allele (restriction sequence: C'CGG), giving rise to two different fragments of 132 and 19 bp. Thus, in subjects homozygous for the wild-type (TNFG) allele, a single band of 132 bp is observed *(lane 2)*; in heterozygous subjects (TNFG/TNFA), two bands of 151 and 132 bp *(lane 3)*; and in subjects homozygous for the mutated (TNFA) allele, a band of 151 bp *(lane 4)*.

4. Withdraw a sample (16 μL) from each tube, add 4 μL of Ficoll 5X and analyze the sample by electrophoresis through a 4% agarose gel.
5. The band pattern shown in **Fig. 2** is observed (*see* **Note 9** and **Fig. 2**).

3.3.3. The –863 Polymorphism

The PCR products (*see* **Note 6**) are then digested at 65°C with the *Tai*I restriction enzyme for 2 h using a reaction mixture containing 0.5 U of *Tai*I (*see* **Note 7**) and an enzyme buffer as specified by the enzyme data sheet.

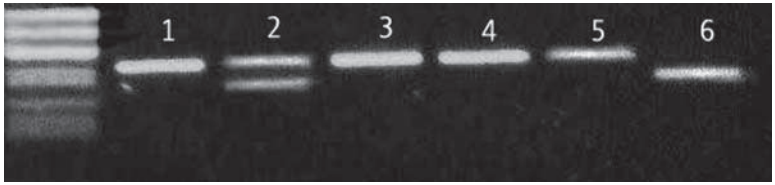

Fig. 3. The PCR yields a 125-base-pair product *(lane 1)*; the *Tai*I restriction enzyme cleaves the mutated (–863A) allele (restriction sequence: ACGT'), giving rise to two different fragments of 104 and 21 bp. Thus, in subjects homozygous for the wild-type (–863C) allele, a single band of 125 bp is observed *(lanes 3,4,5)*; in heterozygous subjects (–863C/A), two bands of 104 and 125 bp *(lane 2)*; and in subjects homozygous for the mutated (–863A) allele, a band of 104 bp *(lane 6)*.

1. Add 5 μL of the reaction mix (*see* **Note 8**) to 15 μL of PCR product in a 0.5-mL tube.
2. Add one drop of mineral oil to each tube to avoid evaporation.
3. Hold the reaction tubes for 2 h at 65°C.
4. Withdraw a sample (16 μL) from each tube, add 4 μL of Ficoll 5X and analyze the sample by electrophoresis through a 4% agarose gel.
5. The band pattern shown in **Fig. 3** is observed (*see* **Note 9** and **Fig. 3**).

4. Notes

1. Presence of bands in the negative controls that lack template DNA means that solutions or tubes have been contaminated with exogenous DNA sequences. This contamination is probably due to the presence of target sequences in solutions, reagents, and equipment used in PCR. To avoid this problem, it is better to carry out the PCR in a laminar flow hood equipped with ultraviolet light. Turn on the lights when the hood is not in use. Keep a set of pipets used only to handle PCR. Autoclave pipet tips and reaction tubes before use. Put on a fresh pair of gloves when beginning work and change them frequently. Prepare your own sets of reagents and store them in small aliquots. Add all components of the reaction to the tube before adding the DNA template. Whenever possible, include a positive control (a PCR tube that contains a small amount of the appropriate target sequence). Always include a control that contains all the components of the PCR except the template DNA (negative control); assemble this control before all of the other samples. If an amplification product appears in the negative control, no amplified products obtained in the reaction can be considered valid. It is then necessary to discard all solutions and reagents, to decontaminate instruments (contaminated pipets can be cleaned with alcohol and then irradiated with UV light), and to repeat the PCR reaction.
2. It is important to use the same batch of TBE 1X in both the electrophoresis tank and the gel. Small differences in ionic strength or pH create fronts in the gel that can affect the mobility of DNA fragments.

3. UV light is dangerous and can damage the retina. Never look at an unshielded UV light source with unprotected eyes. View only through a filter or safety glasses that absorb harmful wavelengths. UV radiation is also mutagenic and carcinogenic. Wear protective gloves when holding materials under the UV light source.
4. A generalized smear of amplified DNA that masks the desired product may occur. This may happen in case of amplification of primer dimers or when too much DNA template is used. Check the correct concentrations of each primer or reduce the amount of DNA.
5. Weak amplification (not readily detectable) implies defective reagents or a defective thermal cycler. Repeat the PCR reaction with fresh reagents and compare the pattern obtained using old and fresh reagents. If no differences are observed, use a different thermal cycler.
6. Always include a positive control to be sure that the enzyme has worked well.
7. Restriction enzymes are stable when they are stored at –20°C in a buffer containing glycerol. When carrying out restriction enzymes digestion, prepare the reaction mixture with all reagents except for the enzyme. Only at this point move the enzyme from the freezer to an ice container and dispense it in the reaction tube.
8. When digesting many DNA samples with the same enzyme, calculate the total amount of enzyme that is needed plus a small excess for the losses involved in transferring several aliquots.
9. A generalized smear can result when large quantities of DNA are cleaved if the digestion time or the amount of enzyme is increased. Pay attention to the digestion time, to the correct temperature of the reaction, and to the amount of enzyme used. Often, the amount of enzyme can be reduced if the digestion time is increased; in this case small aliquots can be removed during the course of the reaction and detected on an agarose gel to check the progression of the digestion.

References

1. Hajeer, A. H. and Hutchinson, I. V. (2001) Influence of TNFalpha gene polymorphisms on TNFalpha production and disease. *Hum. Immunol*. **62,** 1191–1199.
2. Daly, A. K. and Day, C. P. (2001) Candidate gene case-control association studies: advantages and potential pitfalls. *Br. J. Clin. Pharmacol.* **52,** 489–499.
3. Wilson, A. G., de Vries, N., Pociot, F., di Giovine, F. S., van de Putte, L. B. A., and Duff, G. W. (1993) An allelic polymorphism within the human tumour necrosis factor alpha promoter region is strongly associated with the HLA A1, B8 and DR3 alleles. *J. Exp. Med.* **177,** 577–560.
4. Wilson, A. G., di Giovine, F. S., Blakemore, A. I. F., and Duff G. W. (1992) Single base polymorphism in the human tumour necrosis factor alpha (TNFα) gene detectable by NcoI restriction of PCR product. *Hum. Mol. Genet.* **1,** 353.
5. D'Alfonso, S. and Richiardi, P. M. (1994) A polymorphic variation in a putative regulation box of the TNF alpha promoter region. *Immunogenetics* **39,** 150–154.
6. Wilson, A. G., Symon, J. A., McDowell, T. L., McDevitt, H. O., and Duff, G. W. (1997) Effects of a polymorphism in the human tumor necrosis factor alpha promoter on transcriptional activation. *Proc. Natl. Acad. Sci. USA* **94,** 3195–3199.

7. Abraham, L. J. and Koeger, K. M. (1999) Impact of the –308 TNF promoter polymorphism on the transcriptional regulation of the TNF gene: relevance to the disease. *J. Leuk. Biol*. **66,** 562–566.
8. Drouet, C., Shakov, A. N., and Jongeneel, C. V. (1991) Enhancers and transcription factors controlling the inducibility of the tumor necrosis factor-α in primary macrophages. *J. Immunol.* **147,** 1694–1700.
9. Ruwende, C., McGuire, W., Coleman, E., Kwiatkowski, D., Corrah, T., Whittle, H., et al. (1996) Association of a tumor necrosis factor promoter polymorphism with susceptibility to pulmonary tubercolosis. (Abstract) *Clin. Sci.* **90,** 3P.
10. Kroeger, K. M., Carville, K. S., and Abraham, I. J. (1997) The –308 tumor necrosis factor-α promoter polymorphism affects transcription. *Mol. Immmunol.* **34,** 391–399.
11. Skoog, T., van't Hooft, F. M., Kallin, B., Jovinge, S., Boquist, S., Nilsson, J., et al. (1999) A common functional polymorphism (C>A substitution at position –863) in the promoter region of the tumour necrosis factor-α (TNF-α) gene associated with reduced circulating levels of TNF-α. *Hum. Mol. Genet.* **8,** 1443–1449.
12. Kroeger, K. M., Steer, J. H., Joyce, D. A., and Abraham, L. J. (2000) Effects of stimulus and cell type on the expression of the –308 tumour necrosis factor promoter polymorphism. *Cytokine* **2,** 110–119.
13. Grimble, R. F., Howell, W. M., O'Reilly, G., Turner, S. J., Markovic, O., Hirrell, S., et al. (2002) The ability of fish oil to suppress tumor necrosis factor α production by peripheral blood mononuclear cells in healthy men is associated with polymorphisms in genes that influence tumor necrosis factor α production. *Am. J. Clin. Nutr.* **76**, 454–459.
14. Pociot, F., D'Alfonso, S., Compasso, S., Scorza, R., and Richiardi, P. M. (1995) Functional analysis of a new polymorphism in the human TNF α gene promoter. *Scand. J. Immunol.* **42,** 501–504.
15. Kaijzel, E. L., Bayley, J.-P., van Krugten, M. V., Smith, L., van de Linde, P., Bakker, A. M., et al. (2001) Allele-specific quantification of tumor necrosis factor alpha (TNF) transcription and the role of promoter polymorphisms in rheumatoid arthritis patients and healthy individuals. *Genes Immun*. **2,** 135–144.
16. De Jong, B. A., Westendorp, R. G. J., Bakker, A. M., and Huizinga, T. W. J. (2002) Polymorphisms in or near tumour necrosis factor (TNF)-gene do not determine levels of endotoxin-induced TNF production. *Genes Immun.* **3,** 25–29.
17. Hohjoh, H. and Tokunaga, K. (2001) Allele specific binding of the ubiquitous transcription factor OCT-1 to the functional single nucleotide polymorphism (SNP) sites in the tumor necrosis factor-alpha gene (TNFα) promoter. *Genes Immun.* **2**, 105–109.
18. Wilson, A. G. (1999) Genetics of tumour necrosis factor (TNF) in autoimmune liver diseases: red hot or red herring? *J. Hepatol.* **30,** 331–333.
19. Wilson, A. G., di Giovine, F. S., and Duff G. W. (1995) Genetics of tumour necrosis factor-α in autoimmune, infectious and neoplastic illnesses. *J. Inflamm*. **45,** 1–42.
20. McGuire, W., Hill, A. V. S., Allsopp, C. E. F., Greenwood, B. M., and

Kwiatkowski, D. (1994) Cerebral malaria is associated with a polymorphism in the promoter region of the human TNF-α gene. *Nature* **371,** 508–511.
21. Jacob, C. O., Fronek, Z., Lewis, G. D., Koo, M., Hansen, J. A., and McDevitt, H. O. (1990) Hereditable major histocompatibility complex class II-associated differences in production of tumour necrosis factor α: relevance to genetic predisposition to systemic lupus erythematosus. *Proc. Natl. Acad. Sci. USA* **87,** 1233–1237.
22. Field, M. (2001) Tumour necrosis factor polymorphisms in rheumatic diseases. *Q.J.M*. **94,** 237–246.
23. Donaldson, P. T. (1999) TNF gene polymorphisms in primary biliary cirrhosis: a critical appraisal. *J. Hepatol*. **31,** 366–368.
24. Juszczynski, J., Kalinka, E., Bienvenu, J., Woszczech, G., Borowiec, M., Robak, T., et al. (2002) Human leukocyte antigens class II and tumor necrosis factor genetic polymorphisms are independent predictors of non-Hodgkin lymphoma outcome. *Blood* **100,** 3037–3040.
25. McCusker, S. M., Curran, M. D., Dynan, K. B., McCullagh, C. D., Urquhart, D. D., Middleton, D., et al. (2001) Association between polymorphism in the regulatory gene encoding tumour necrosis factor alpha and the risk of Alzheimer's disease and vascular dementia: a case-control study. *Lancet* **357,** 436–439
26. Fargion, S., Valenti, L., Dongiovanni, P., Scaccabarozzi, A., Fracanzani, A. L., Taioli, E., et al. (2001) Tumor necrosis factor α promoter polymorphisms influence the phenotypic expression of hereditary hemochromatosis. *Blood* **97,** 3707–3712.
27. Hohler, T., Kruger, A., Gerken, G., Schneider, P. M., Meyer zum Buschenfelde, K. H., and Rittner, C. (1998) Tumor necrosis factor promoter polymorphism at position –238 is associated with chronic active hepatitis C infection. *J. Med. Virol*. **54,** 173–177.
28. Valenti, L., Fracanzani, A. L., Dongiovanni, P., Santorelli, G., Branchi, A., Taioli, E., et al. (2002) Tumor necrosis factor α promoter polymorphisms and insulin resistance in nonalcoholic fatty liver disease. *Gastroenterology* **122,** 274–280.
29. Jang, W. H., Yang, Y. I., Yea, S. S., Lee, Y. J., Chun, J. H., Kim, H. I., et al. The –238 tumor necrosis factor-alpha promoter polymorphism is associated with decreased susceptibility to cancers. *Cancer Lett*. **166,** 41–46.
30. Van Heel, D. A., Udalova, I. A., De Silva, A. P., McGovern, D. P., Kinouchi, Y., Hull, J., et al. (2002) Inflammatory bowel disease is associated with a TNF polymorphism that affects the interaction between the OCT1 and NF-κB transcription factors. *Hum. Mol. Genet*. **11,** 1281–1289.
31. Grove, J., Daly, A. K., Bassendine, M. F., and Day, C. P. (1997) Association of a tumor necrosis factor promoter polymorphism with susceptibility to alcoholic steatohepatitis. *Hepatology* **26,** 143–146.
32. Sambrook, J. and Russel, D. W., eds. *Molecular Cloning: A Laboratory Manual.* Cold Spring Harbor Laboratory, Cold Spring Harbor, New York, 2001.

6

Detection of TNF and TNF Receptor mRNA in Cells and Tissues

Roberto Furlan, Giuliana Salani, Alessandra Bergami, and Gianvito Martino

Summary

We describe a semiquantitative reverse transcriptase polymerase chain reaction (RT-PCR) technique for the quantification of the messenger RNA of human and murine tumor necrosis factor α (TNFα) and related receptors. This protocol can be adapted for blood, peripheral blood lymphocytes, or other tissues. We propose a dot-blot technique which, if properly set up, is fast and quantitatively reliable. We describe two different detection protocols employing either radioactive or, alternatively for laboratories that cannot or do not want to use radioactivity, fluorescent-labeled probes. We also describe our calculations for relative quantification, based on the use of a positive control sample that becomes the reference value used to compare experimental samples. These protocols have as their aim to provide a flexible tool that can be employed in several different human and murine experimental settings by laboratories with different equipment.

Key Words: RT-PCR; dot-blot; TNFα; TNF receptors; radioactive detection; fluorescent detection.

1. Introduction

Determination of cytokine production in vivo has been challenging in most experimental and clinical settings due to the nature of these molecules. In fact, their short half life and their autocrine/paracrine nature, leading to the formation of a so-called "local cytokine milieu" ***(1)***, creates the need to know their level at the site of production and makes the detection of their proteins often difficult, when not impossible, with current technologies. Furthermore, several cytokines are known to be biologically activated through proteolytic cleavage, through oligomerization, or both. The latter is the case for tumor necrosis factor alpha (TNFα), which is activated by the TNFα activating enzyme (TACE)

From: *Methods in Molecular Medicine, Vol. 98: Tumor Necrosis Factor*
Edited by: A. Corti and P. Ghezzi © Humana Press Inc., Totowa, NJ

and is able to engage its receptors only in trimeric form *(2)*. Thus, the relationship between TNFα mRNA levels and the biologically active protein is particularly indirect. Despite this caveat, in our experience the determination of the level of mRNA coding for TNFα and its receptors has been a useful tool in both experimental and clinical research *(3–5)* enabling, in general, the study of the involvement of this molecule in several biological processes.

From a technical point of view, mRNA levels can be determined by Northern blot, RNA protection assay (RPA), or reverse transcriptase polymerase chain reaction (RT-PCR). Quantification by Northern blot and RPA is more reliable in principle, but requires large amounts of starting material. This limitation is a considerable one, especially in clinical settings or in experimental animals where samples may be precious and of limited amount. In this respect RT-PCR represents a powerful tool, able to document gene transcription in very low amounts of starting material. Furthermore, concerning quantification, recent developments of RT-PCR—e.g., real-time RT-PCR—have considerably improved its performance and reproducibility. Real-time PCR, however, is not available everywhere, and conventional, semiquantitative RT-PCR has been successfully employed in a number of studies *(6)*.

To detect human and mouse TNFα and its receptors, we propose here an RT-PCR technique followed by dot-blot and radioactive or fluorescent detection of the amplicon. Quantification is normalized on the values of a housekeeping gene, namely glyceraldehyde 3-phosphate dehydrogenase (GAPDH). Although a number of genes have been proposed as housekeeping genes to normalize semiquantitative RT-PCR assays (e.g., β-actin, 18s RNA, and others), in our experience GAPDH is highly reliable.

We propose to calculate relative levels of expression of the targets for at least two reasons. First, it is technically easier and more flexible, depending on the available positive controls or reference samples. Second, it is easier to appreciate differences expressed as induction index than, for example, as femtomoles per cell. The disadvantage is that comparison of the results obtained in different groups, or in the same laboratory at distant time points, is difficult. In order to compare results obtained in different experiments in our laboratory, we prepare huge amounts of the positive controls that are included with each reaction, so that the same control can be used over the years. Alternatively, a precisely quantifiable plasmid may be used as positive control.

2. Materials

2.1. Tissues and RNA Extraction

1. Pelleted peripheral blood lymphocytes (approx 5×10^6 cells) or fresh/frozen tissue (approx 10–100 mg) (*see* **Note 1**).
2. RNAfast Isolation System (Molecular Systems) (*see* **Note 2**).

3. Chloroform.
4. Isopropanol.
5. Ethanol 100% and 75% (*see* **Note 3**).
6. DEPC water (*see* **Note 4**).

2.2. RT Reaction

1. Ready-to-Go You-Prime First-Strand Beads (Amersham Bioscience).
2. Primer pd$(N)_6$ (Amersham Bioscience).
3. 37°C and 65°C water baths or heat blocks.
4. RNase-free microfuge tube.

2.3. RT-PCR

1. Primers (*see* **Table 1**). All primers and probes should be aliquoted and stored at –20°C (*see* **Note 5**).
2. AmpliTaq DNA Polymerase 5 U/μL (Applied Biosystems).
3. GeneAmp 10X Buffer: 100 m*M* Tris-HCl, pH 8.3, 500 m*M* KCl (Applied Biosystems).
4. Mineral oil (Sigma).
5. Thermowell 96-well plate (Costar), Lid for Thermowell 96-well plate (Costar).
6. Thermal cycler.
7. Aerosol-resistant barrier tips.

2.4. Dot-Blot

1. Millipore Multiscreen Assay System or analog systems.
2. Vacuum flask trap.
3. Multichannel pipet.
4. Aerosol-resistance barrier tips.
5. 95°C water baths or heat blocks.
6. GeneScreen Plus, Hybridization Transfer Membrane (Life Science Products).
7. Whatman 3MM filter paper.
8. 0.8*M* NaOH, 20 m*M* EDTA.
9. 0.4*M* NaOH.
10. 2X SSC: 17.5 g sodium chloride, 8.8 g trisodium citrate, in 1 L of water. Store at room temperature.

2.5. Fluorescein Probe Labeling

1. Probes (*see* **Table 1**).
2. All probes should be stored at –20°C (*see* **Note 5**).
3. Gene Images 3'-Oligolabelling Module (Amerham Biosciences).
4. Eppendorf tubes, 1.5 mL.
5. Pipet tips.
6. Pipets.
7. 37°C water bath.

Table 1
Primers and Probes

Primer	Sequence	Temp
Mouse		
GAPDH 3'	CGCATCTTCTTGTGCAGTG	67.6°C
GAPDH 5'	GTTCAGCTCTGGGATGAC	66.8°C
GAPDH probe	CCCCCTGGCCAAGGTCATCCATGA	80.9°C
TNFα 5'	TTCTGTCTACTGAACTTCGGGGTGATCGGTCC	82.2°C
TNFα 3'	GTATGAGATAGCAAATCGGCTGACGGTGTGGG	82.2°C
TNFα probe	GCCGTTGGCCAGGAGGGCGTTGGCGCGCTG	90.4°C
TNFR-I 5'	CCATCCACCACAGCATACAG	53.1°C
TNFR-I 3'	GCCCCCTCCCCAGCCTTCAG	53.8°C
TNFR-I probe	CCCCAGCCTTCAGCCCCACCTCCGG	83.6°C
TNFR-II 5'	CAAATGGAAATGTGCTATGC	48.3°C
TNFR-II 3'	AACTGGGTGCTGTGGTCAAC	52.1°C
TNFR-II probe	CCAGGGCCCAGCCAAACTCC	75.0°C
Human		
GAPDH 5'	ACCACCATGGAGAAGGCTGG	72.3°C
GAPDH 3'	CTCAGTGTTAGCCCAGGATGC	72.8°C
GAPDH probe	GTGGAAGGACTCATGACCACAGTCCATGCC	82.2°C
TNFα 5'	GACCTCTCTCTAATCAGCCC	70.3°C
TNFα 3'	CAAAGTAGACCTGCCCAGAC	70.3°C
TNFα probe	CTCAGCGCTGAGATCAATCGGCCCGACTTA	82.2°C
TNFR-I 5'	CAAATGCCGAAAGGAAATGG	54.6°C
TNFR-I 3'	TGGAGGTGAAGGTGGAACTG	52.2°C
TNFR-I probe	AAGCCCCTGGCCCCAAACCC	76.4°C
TNFR-II 5'	GGCTGAGACTGCGGGATGGT	58.6°C
TNFR-II 3'	ATTTGGAGGCGGTGCTTTTT	55.3°C
TNFR-II probe	CGGGAAGCGGAGGTTGCAGGGAGC	82.4°C

2.6. Radioactive Probe Labeling

1. Probes (*see* **Table 1**).
2. [γ-^{32}P]-ATP.
3. T4-polynucleotide kinase (New England Biolabs) (*see* **Note 6**).
4. 10X kinase buffer.
5. Eppendorf tubes, 1.5 mL.
6. Pipet tips.
7. Pipets.
8. 37°C water bath.
9. 3*M* sodium acetate, pH 5.0.

10. Absolute ethanol precooled at –20°C.
11. Microcentrifuge capable of 13,000*g*.

2.7. Prehybridization and Hybridization With Fluorescent Probe

1. 20X SSC: 88 g trisodium citrate, 175 g sodium chloride. Make up to 1 L and filter. Store at room temperature.
2. 20% (w/v) sodium dodecyl sulphate (SDS).
3. 5% (w/v) dextran sulphate (molecular weight 500,000).
4. Hybridization bottles.
5. Hybridization oven.
6. Washing buffer I: 5X SSC, 0.1% (w/v) SDS.
7. Washing buffer II: 1X SSC, 0.1% (w/v) SDS prewarmed at 42°C.
8. Orbital shaker.

2.8. Prehybridization and Hybridization With Radioactive Probe

1. 20X SSC.
2. 100X Denhardt's solution: 2% (w/v) Ficoll (MW 400,000), 2% (w/v) polyvinylpyrrolidone (PVP, MW 40,000), 2% (w/v) bovine serum albumin (BSA). Make up to 1 L and filter.
3. 37% formamide (12.3*M*) (*see* **Note 7**).
4. 10% SDS.
5. 20 mg/mL sonicated salmon testes DNA (before addition, denature in a boiling water bath for 5 min and immediately place on ice).
6. Washing buffer I: 1X SSC, 0.1% SDS.
7. Washing buffer II: 0.1X SSC, 0.1% SDS prewarmed at 65°C.
8. Hybridization bottles.
9. Hybridization oven.

2.9. Indirect Detection of Fluorescein-Labeled Probe

1. ECF Signal Amplification Module (Amersham Pharmacia Biotech).
2. Buffer A: 17.5 g sodium chloride, 12.1 g Tris-HCl base. Adjust to pH 7.5 with concentrated HCl and make up to 1 L and filter. Store at room temperature.
3. Blocking buffer: 1:10 dilution of liquid block, from ECF Signal Amplification Module, in buffer A (1 mL/cm^2).
4. Antibody incubation buffer: antifluorescein AP conjugate diluted 5000-fold in buffer A containing 0.5% (w/v) bovine serum albumin fraction V (0.3 mL/cm^2).
5. Washing buffer: 0.3% (w/v) Tween-20 in buffer A (2 mL/cm^2).
6. Hybridization bottles.
7. Hybridization oven (*see* **Note 8**).

2.10. Signal Generation and Detection (see Note 9)

1. Detection buffer from ECF Signal Amplification Module (*see* **Note 10**).
2. Sheets of clear plastic.
3. Heat-sealer.

4. High performance laser scanning system, e.g., Typhoon 8600 (Amersham Pharmacia Biotech).

2.11. Autoradiography

1. Clear plastic wrap.
2. X-ray films (Kodak BioMax MS).
3. Autoradiography cassette.
4. Film developer.
5. Scanning densitometer.

3. Methods

3.1. Semiquantitative RT-PCR

3.1.1. Tissue and RNA Extraction

To extract and purify total RNA from tissues and cells, our method of choice is the use of commercially available reagents based on guanidinium thiocyanate and acid phenol (e.g., the RNAfast Isolation System, Molecular Systems).

This method includes the following steps:

1. Homogenization.
2. RNA Extraction.
3. RNA Precipitation.
4. RNA Wash.

3.1.1.1. Homogenization

1. Homogenize 10–100 mg of fresh/frozen tissue sample with 1 mL RNAfast reagent in a hand-held glass-teflon homogenizer.
2. Cells grown:
   a. In monolayer are lysed directly in a culture dish by adding RNAfast (1 mL per 3.5-cm Petri dish) and passing the lysate several times through a pipet. The cell lysate should be immediately transferred into a 1-mL Eppendorf tube.
   b. In suspension are spun down and lysed with RNAfast (1 mL per $5–10 \times 10^6$ cells). Washing the cells before addition of the RNAfast should be avoided, as this increases the possibility of mRNA degradation.
3. Use 5 volumes of RNAfast per volume of biological fluids

3.1.1.2. RNA Extraction

1. After homogenization store samples for 5 min at 4°C.
2. Add 0.2 mL of choloroform per 1 mL of RNAfast, shake vigorously for 15 s, and let samples stay on ice at 4°C for 15 min.

3.1.1.3. RNA Precipitation

1. Transfer the aqueous phase to a fresh tube (*see* **Note 11**), add an equal volume of isopropanol (*see* **Note 12**), and store samples for 10 min at 4°C.

2. Centrifuge samples at 12,000*g* (4°C) for 10 min (*see* **Notes 13** and **14**).

3.1.1.4. RNA Wash

1. Remove the supernatant and wash RNA pellet twice with 75% ethanol (1 mL RNAfast/1 mL 75% ethanol) by vortexing and centrifugation for 5 min at 7500*g* (4°C) (*see* **Note 13**).
2. At the end of the procedure briefly dry the pellet under vacuum for 5–10 min (*see* **Note 15**).
3. Dissolve the RNA pellet in 10 µL of DEPC-treated water (*see* **Note 4**).

3.1.2. RT Reaction

Reverse transcription (RT) of 5 µg total RNA is done with Ready-to-Go You-Prime First-Strand Beads with pd$(N)_6$ primer (0.2 µg).

1. Bring RNA sample to a volume of 32 µL in an RNA-free microfuge tube using DEPC-treated water (*see* **Note 4**).
2. Heat at 65°C for 10 min, then chill on ice for 2 min.
3. Transfer the RNA solution to the tube of Ready-to-Go You-Prime First-Strand Beads. Do not mix.
4. Add Primer pd$(N)_6$ 0.2 µg for sample; final volume must be 33 µL.
5. Mix the contents of the tube by vortexing. Centrifuge briefly to collect the contents at the bottom of the tube.
6. Incubate at 37°C for 60 min.
7. Store cDNA at –20°C.

3.1.3. RT-PCR

Each RT-PCR run includes one negative and two positive controls. Appropriate controls are as follows:

1. H_2O is used as negative control, to ensure that all reagents are free from contamination.
2. Two positive controls are included: cDNA obtained from RNA from mouse splenocytes or human peripheral blood lymphocytes (PBLs), unstimulated (1) and stimulated (2) with either concanavalin A (5 µg/mL for 24 h for mouse splenocytes; Sigma), or phytohemagglutinin (10 µg/mL for 24 h for human PBLs; Sigma) (*see* **Note 16**).

PCR is carried out in a final volume of 50 µL containing 2.5 U AmpliTaq DNA Polymerase, 100 µ*M* dNTPs, 20 pmol of each primer in a buffer containing 100 µ*M* Tris-HCl, pH 8.3, 500 m*M* KCl, 25 m*M* $MgCl_2$, and 5 µL of cDNA (*see* **Note 17**).

1. Assemble the PCR reaction, using aerosol-resistant barrier tips, preparing a master mix for all reactions, calculating the number of samples, including six controls (negative, unstimulated positive control, and stimulated positive control, in duplicate), and some excess, as in **Table 2**.

Table 2
Master Mix

Component	Amount[a]
GeneAmp 10X Buffer	n × 5 µL
$MgCl_2$	n × 3 µL
5' primer 10 pmol/µL	n × 2 µL
3' primer 10 pmol/µL	n × 2 µL
Nucleotides (100 m*M*)	n × 0.5 µL
Ampli Taq Polymerase	n × 0.5 µL
H_2O	n × 32 µL

[a]n = number of samples + controls + excess

2. Keep all reagents and samples on ice.
3. In a 96-well thermowell plate, add to each well 45 µL of master mix.
4. Add 5 µL of cDNA to each well.
5. Overlay every sample with two drops of mineral oil (when not using a thermocycler with heated lid).
6. Close lid and place in PCR Thermal Cycler.
7. Perform amplification on the thermal cycler as in **Table 3**.

3.1.4. Dot-Blot Protocol

1. Add to each well of the 96-well plate with the PCR products, 0.8 *M* NaOH and 20 m*M* EDTA, to obtain a final concentration of 0.4 *M* NaOH and 10 m*M* EDTA (1:2). Warm the samples at 95°C for 5 min to denature the PCR product, then immediately chill on ice.
2. Cut GenScreen Plus and two pieces of Whatman 3MM filter paper in the same size as a 96-well plate.
3. Wet the GenScreen Plus and only one Whatman 3MM filter paper in clean H_2O.
4. Assemble the dot-blot apparatus as shown in **Fig. 1**.
5. Add 500 µL of clean H_2O to each well.
6. Open vacuum and set it so that it takes approx 3 min to empty the well. Register and use this same setting for the next vacuum steps.
7. Close vacuum.
8. Load 50 µL of denatured PCR product in the wells.
9. Open vacuum (*see* above for settings). Keep it open for 5 min.
10. Add 200 µL of 0.4*M* NaOH to each well.
11. Open vacuum (*see* above for settings) and keep it open for 20 min.
12. Disassemble the dot-blot apparatus.
13. Briefly wash filter with 2X SSC.
14. Air-dry the filter on a piece of filter paper. No crosslinking is needed.

Table 3
PCR Reactions

	Denaturation	Annealing	Extension	Cycles
Mouse				
GAPDH	95°C × 1 min	66°C × 1 min	72°C × 1 min	2
	95°C × 1 min	64°C × 1 min	72°C × 1 min	2
	95°C × 1 min	62°C × 1 min	72°C × 1 min	2
	95°C × 1 min	66°C × 1 min	72°C × 1 min	24
TNFα	95°C × 3 min			
	95°C × 1 min	62°C × 1 min	72°C × 1 min	35
TNFR-I	95°C × 1 min	52°C × 1 min	72°C × 1 min	35
TNFR-II	95°C × 1 min	50°C × 1 min	72°C × 1 min	35
Human				
GAPDH	95°C × 1 min	50°C × 1 min	72°C × 1 min	30
TNFα	95°C × 3 min			
	95°C × 1 min	65°C × 1 min	72°C × 1 min	35
			72°C × 15 min	
TNFR-I	95°C × 1 min	53°C × 1 min	72°C × 1 min	35
TNFR-II	95°C × 1 min	55°C × 1 min	72°C × 1 min	35

3.2. Labeling, Hybridization, and Signal Detection With Fluorescein Probe

3.2.1. Fluorescein Probe Labeling

Oligonucleotide labeling reaction of 100 pmol of the probe is performed in 80 µL total volume according to the manufacturer's instructions (**Table 4**).

1. Thaw required tubes from the labeling components on ice, excluding the enzyme (*see* **Note 18**).
2. Add the labeling reaction components to a 1.5-mL Eppendorf tube, keeping it on ice (**Table 3**).
3. Mix gently by pipetting up and down.
4. Incubate the reaction mixture at 37°C for 60–90 min (*see* **Note 19**).
5. Store labeled probe on ice for immediate use (*see* **Note 20**).

3.2.2. Hybridization With Fluorescent Probe

Hybridization temperature is dependent on the particular probe sequence to be used. Ideally, stringency is controlled by the posthybridization washes.

1. Prepare the required volume (0.25 mL/cm^2) of prehybridization solution: 5X SSC, 0.1% (w/v) SDS, 0.5% (w/v) dextran sulphate, 1/20 final volume liquid block from the labeling kit.

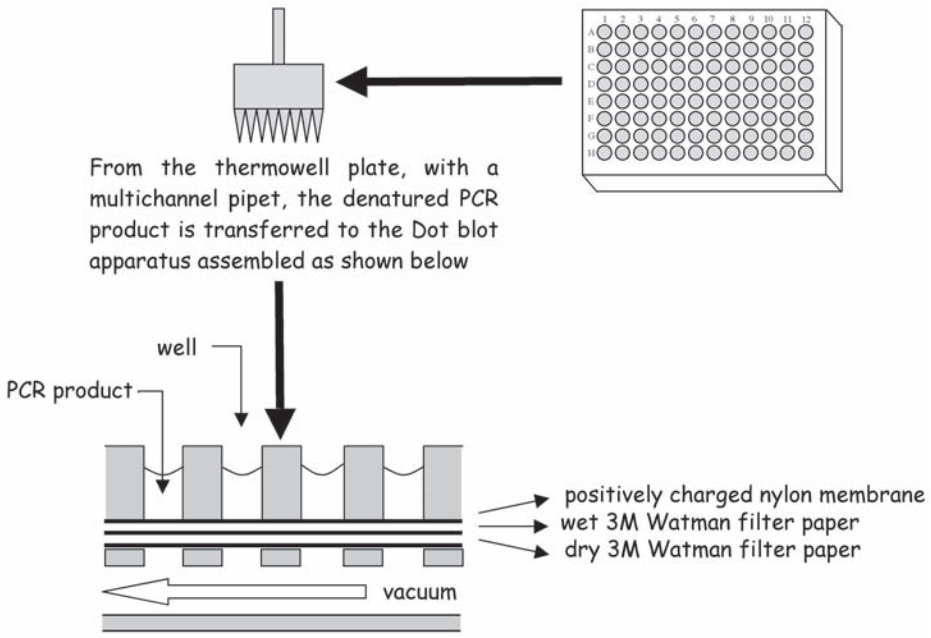

Fig. 1. Assembly of the dot-blot apparatus.

2. Place blot into the prehybridization solution and prehybridize at 60°C for a minimum of 30 min in a hybridization oven (*see* **Note 21**).
3. Add the labeled oligonucleotide probe to the buffer used for the prehybridization step (*see* **Note 22**). Typically, for the detection using ECF signal amplification module, use a probe concentration of 10 ng/mL.
4. Hybridize at 60°C overnight.
5. Remove the blot from the hybridization solution and place it in a new container. Cover with an excess (2 mL/cm^2 of membrane) of washing buffer I (*see* **Note 23**).
6. Incubate at room temperature for 5 min with constant agitation.
7. Repeat **step 6** with fresh buffer.
8. Discard the wash solution. Place blot in a new bottle and add an excess of appropriately prewarmed washing buffer II (2 mL/cm^2 of membrane).
9. Incubate at 42°C for 15 min in a hybridization oven.
10. Repeat **step 9** with fresh buffer (*see* **Note 24**).

3.2.3. Indirect Detection of Fluorescein-Labeled Probe

All the following steps are performed at room temperature, and all the incubations require constant agitation of the blot.

1. Briefly rinse the blot with an excess of buffer A (2 mL/cm^2 of membrane), at room temperature.

Table 4
Fluorescein-Labeling Reaction

Reagent	Amount per reaction
Fluorescein-11-dUTP	5 μL
Cacodylate buffer	8 μL
Terminal transferase	4 μL
Probe (100 pmol/μL)	1 μL
H_2O	62 μL

2. With gentle agitation, incubate blot for 1 h at room temperature in approximately 1.0 mL/cm^2 of block solution.
3. Repeat **step 1**.
4. Incubate the blot in the diluted conjugate (0.3 mL/cm^2 of membrane) with gentle agitation at room temperature for 1 h.
5. Remove unbound conjugate by washing for 3 × 10 min in the washing buffer (2 mL/cm^2 of membrane) at room temperature.

3.2.4. Fluorescent Signal Generation and Detection

1. Drain off any excess of wash buffer from the blot and place it in a bag of clear plastic.
2. Apply the detection reagent (25 μL/cm^2) to the blot using a pipet, and immediately spread the reagent evenly over the blot (*see* **Note 25**).
3. It is better to heat-seal the bag to prevent the blot from drying out (*see* **Note 26**).
4. When you are ready to scan, place the bag containing the blot face down over the sample holder for the Typhoon apparatus (*see* **Note 27**).
5. For more details regarding the use of the Typhoon apparatus, refer to the manual supplied with the machine.

3.3. Labeling, Hybridization, and Signal Detection With Radioactive Probe

3.3.1. Radioactive Probe Labeling

Oligonucleotide labeling of 3 pmol of the probe is performed in a total volume of 20 μL (**Table 5**).

1. To a 1.5-mL tube, on ice, add the labeling reaction components (**Table 5**).
2. Mix gently by pipetting up and down.
3. Incubate the reaction mixture at 37°C for 45 min.
4. Inactivate the enzyme by heating the reaction mixture at 65°C for 10 min.
5. Add to the mixture 2 μL of sodium acetate 3*M* and mix gently.
6. Add 40 μL of absolute ethanol at –20°C and keep the solution at –20°C for 1 h.

Table 5
Radiolabeling Reaction

Reagent	Amount per reaction
[γ-^{32}P]-ATP	1.5 μL
10X T4 kinase buffer	2 μL
T4 kinase (10 units/μL)	1 μL
Probe (1 pmol/μL)	3 μL
H_2O	12.5 μL

7. Centrifuge at maximum speed for 15 min.
8. Discard the supernatant and allow the pellet to dry.
9. Redissolve the pellet in 1 mL of water.

3.3.2. Hybridization With Radioactive Probe

1. Prepare the prehybridization solution: 5X SSC, 5X Denhardt's solution, 3.7 *M* formamide, 0.1% SDS, 0.15 mg/mL salmon testis DNA.
2. In a hybridization oven, prehybridize the blot in 10 mL of prehybridization solution, at least for 1 h at 42°C.
3. To the prehybridization solution, add the labeled probe and hybridize over night at 42°C.
4. Remove the blot from the hybridization solution and place it in a new container. Cover it with 30 mL of washing solution I.
5. Incubate at room temperature for 15 min with constant agitation.
6. Repeat **step 4** with fresh buffer.
7. Discard the wash solution. Place the blot in a clear bottle and cover with 30 mL of washing buffer II.
8. Incubate at the hybridization temperature for 15 min.
9. Repeat **step 7** with fresh buffer.

3.3.3. Autoradiography

Wrap the blot in a clear plastic wrap and subject it to autoradiography using X-ray film. Typically, 1–2 h of exposure to X-ray film will yield quantifiable results. It may be necessary to perform several autoradiography exposures for different time periods to distinguish between extremes of expression levels.

3.4. Calculation of Data

With both procedures described above, you will obtain a densitometric measure of the signal. Analysis softwares offer several parameters to evaluate the signal. The following suggested procedure allows relative quantification of your samples:

1. Calculate the volume of the signal of the samples.
2. Subtract the background volume calculated as the mean volume of at least three empty wells on the same filter.
3. For all targets and GAPDH, divide the obtained value by the mean value of the positive samples of your choice (either unstimulated or stimulated) present on the same filter.
4. Divide the values obtained for the targets by the value obtained for the GAPDH.

4. Notes

1. It is better to homogenize fresh tissue directly in RNAfast and keep it at –80°C until RNA extraction. In case of a frozen sample, add RNAfast directly to the frozen sample and homogenize immediately.
2. Start with 0.5 mL volume of RNAfast. Using 0.5 mL of RNAfast you can use 1.5-mL Eppendorf tubes throughout the extraction procedure.
3. Keep RNA in 100% ethanol at –80ºC if long-term storage is needed.
4. Instead of DEPC-treated water it is possible to use purchased ultrapure distilled water.
5. Commercially synthesized oligonucleotides are redissolved in sterile water as 100 pmol/μL stock solutions.
6. This enzyme catalyzes the transfer and exchange of Pi from the γ position of ATP to the 5'-hydroxyl terminus of oligonucleotides.
7. Toxic and/or mutagenic substance. Use appropriate safety measures.
8. Alternatively it is possible to use an orbital shaker.
9. From this step on wear powder-free gloves, or rinse gloved hands with water before working.
10. Avoid any skin contact with detection reagents.
11. Transfer in small aliquots to avoid transfer of the contaminating interface.
12. If you start with the same volume of RNAfast you can add the same volume of isopropanol to each sample.
13. You can centrifuge at room temperature.
14. The RNA pellet is often not visible. Orienting all the tubes in the centrifuge in the same way ensures that the pellet is on the same side in all tubes.
15. Alternatively, resuspend RNA in 100% ethanol, centrifuge, discard supernatant, and let the pellet dry in the open tubes for 20 min.
16. At the beginning of a study it is wise to prepare enough RNA from unstimulated and stimulated mouse splenocytes or human PBLs as positive controls for all PCR assays.
17. To avoid pipetting errors occurring with very small volumes, dilute cDNA in order to use at least 5 μL/reaction.
18. Place the enzyme on ice only immediately prior to use. Return the enzyme to a freezer (–30°C to –15°C) as soon as the required amount has been removed.
19. Purification of the probe after labeling is not necessary.
20. Place at –30°C to –15°C for long-term storage. Do not store in a frost-free freezer. Because the fluorescein molecule is light sensitive, it is advisable to store probes in the dark.

21. It is essential that the blots move freely within the buffer.
22. Avoid placing the probe directly on the blot; a small aliquot of the buffer may be removed and mixed with the probe before returning the mixture to the bulk of the hybridization buffer.
23. If the rinsing solution shows any precipitate it should be warmed slightly before use, until all material has dissolved.
24. If blots have to be stored at this stage, until ready to proceed with the detection, they must not be allowed to dry out.
25. This can be done by rolling a pipet over the blot surface.
26. Blots should not be exposed to bright light for long periods. It is advisable to store them in the dark.
27. The signal from the reagent will increase with time. Scanning 24 h after the addition of the reagent will provide a stronger signal.

References

1. Nicola, N. A., ed. *Guidebook to Cytokines and Their Receptors*. A Sambrook and Tooze Publication, Oxford University Press, Oxford, UK, 1994.
2. Black, R. A., Rauch, C. T., Kozlosky, C. J., Peschon, J. J., Slack, J. L., Wolfson, M. F., et al. (1997) A metalloproteinase disintegrin that releases tumour-necrosis factor-alpha from cells. *Nature* **385,** 729–733.
3. Martino, G., Consiglio, A., Franciotta, D. M., Corti, A., Filippi, M., Vandenbroeck, K., et al. (1997) Tumor necrosis factor alpha and its receptors in relapsing-remitting multiple sclerosis. *J. Neurol. Sci.* **152,** 51–61.
4. Furlan, R., Martino, G., Galbiati, F., Poliani, P. L., Smiroldo, S., Bergami, A., et al. (1999) Caspase-1 regulates the inflammatory process leading to autoimmune demyelination. *J. Immunol.* **163,** 2403–2409.
5. Furlan, R., Brambilla, E., Ruffini, F., Poliani, P. L., Bergami, A., Marconi, P. C., et al. (2001) Intrathecal delivery of IFN-gamma protects C57BL/6 mice from chronic-progressive experimental autoimmune encephalomyelitis by increasing apoptosis of central nervous system-infiltrating lymphocytes. *J. Immunol.* **167,** 1821–1829.
6. Platzer, C. and Blankenstein, T. Polymerase chain reaction to quantitate cytokine mRNA. In *Cytokines: A Practical Approach* (Balkwill, F. R., ed.), IRL Press at Oxford University Press, Oxford, UK, 1995.

7

Immunohistochemical Localization of TNFα and Its Receptors in the Rodent Central Nervous System

Paolo Bigini and Tiziana Mennini

Summary

The protocols for immunohistochemical localization of tumor necrosis factor α (TNFα), TNFRp55, and TNFRp75 in central nervous system (CNS) slices from laboratory animals are described. The procedure requires intracardiac perfusion of animals followed by fixation and cryostat sectioning in 30–40 μm slices. Free-floating sections are then incubated with the primary antibody followed by incubation with a secondary antibody species-specific for the type of animal in which the primary antibody was made. The secondary antibody is conjugated to biotin for the avidin-biotin complex (ABC) method. The horseradish peroxidase (linked to the ABC complex) allows, in the presence of H_2O_2, diaminobenzidine oxidation with chromogenic reaction and brown staining. Staining for both TNFα and its receptors is normally undetectable in CNS samples from control animals, but it is evident in neuroimmunological or neurodegenerative diseases. The technique is not quantitative, but allows qualitative comparison between samples with light-microscopic cellular resolution.

Key Words: TNFα; TNFRp55; TNFRp75; central nervous system; immunohistochemistry; motor neurons.

1. Introduction

In recent years, tumor necrosis factor alpha (TNFα) and its receptors received increasing interest, due to the key role of this cytokine in neurological diseases, such as ischemia ***(1)***, multiple sclerosis ***(2)***, and neurodegenerative disorders, including amyotrophic lateral sclerosis (*see* **ref. *3*** for review). Due to the complex cellular architecture of the CNS, it is important to detect the cellular population where cytokines changes occur. To this purpose immunohistochemical techniques for light microscopic resolution are required. This technique, however, is not quantitative, but allows only qualitative or semiquantitative comparison between samples. For this reason it is important

From: *Methods in Molecular Medicine, Vol. 98: Tumor Necrosis Factor*
Edited by: A. Corti and P. Ghezzi © Humana Press Inc., Totowa, NJ

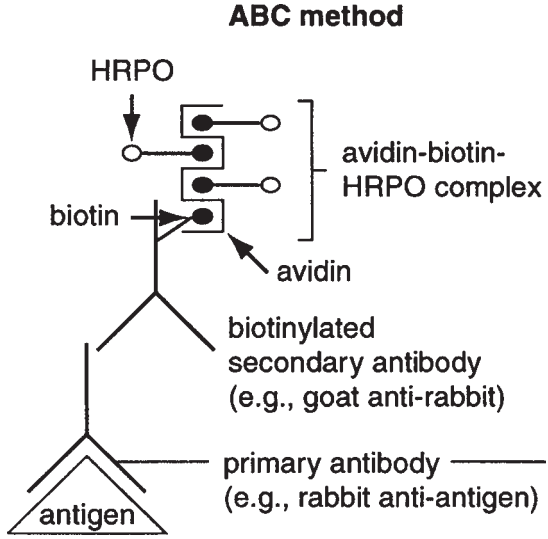

Fig. 1. Schematic representation of events characterizing the immunoperoxidase process of immunohistochemistry with ABC method. Abbreviations: ABC, avidin-biotin conjugate; HRPO, horseradish peroxidase (modified *from* **ref. *5***).

that the different samples to be compared are processed in the same experimental session. Here we summarize the most commonly used protocol for evaluating TNFα, TNFRp55, and TNFRp75 in CNS slices from laboratory animals. Before visualizing the cytokine of interest, tissues must be perfused, fixed and sectioned in 30–40 μm slices, and processed for immunohistochemical staining. Free-floating sections are incubated with the primary antibody to allow binding with the molecule of interest. Then incubation with a secondary antibody, species-specific for the type of animal in which the primary antibody was made, is carried out. The secondary antibody is generally conjugated to biotin for the avidin-biotin complex method (ABC, Vectastain kit), as summarized in **Fig. 1**. In such cases the horseradish peroxidase (linked to the ABC complex) allows, in the presence of H_2O_2, diaminobenzidine oxidation with chromogenic reaction and brown staining **(Fig. 1)**. **Figure 2** shows representative images of TNFα and TNFRp55, respectively, in a coronal section of cervical spinal cord from wobbler mice, a murine model of motor neuron degeneration ***(4)***. In control mice staining is absent (not shown), since TNFα and its receptors are normally not detectable in the CNS of healthy subjects.

2. Materials

1. Phosphate buffered saline (PBS).
2. Paraformaldehyde (PAF) (Sigma).

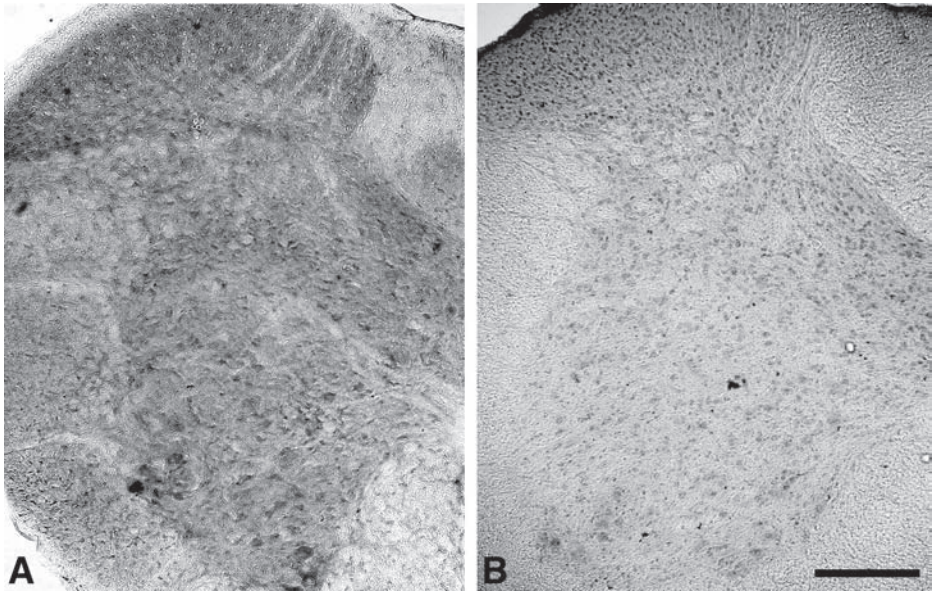

Fig. 2. Representative immunostaining for anti-TNFα antibody **(A)** and TNFR-I **(B)** in the cervical spinal cord sections of 12-wk-old wobbler mice. Scale bar: 250 μm.

3. Sucrose.
4. Isopentane.
5. Oct Compound Embedding Matrix Tissue Tek (Sakura-Nihombashi).
6. Tris-buffered saline (TBS).
7. Cryostat MICROM HM500OM (Carl Zeiss).
8. 48-well cell culture cluster.
9. Normal goat serum (NGS)(Vector).
10. Triton X-100 (Sigma).
11. 61E71: mouse monoclonal anti-human TNFα (HyCult Biotechnology).
12. HM104: rat polyclonal antimouse TNFRp55 (HyCult Biotechnology).
13. HM 101: rat polyclonal antimouse TNFRp75 (HyCult Biotechnology).
14. Antimouse secondary antibody (Vector).
15. Antirat secondary antibody (Vector).
16. Vectastain ABC-Kit (Vector).
17. 3,3'-Diaminobenzidine (DAB)(Sigma).
18. Precleaned microscope slides.
19. Micro glass cover slips.
20. DPX mountant for microscopy (DBH Laboratories).

3. Methods

In order to obtain an adequate sample of tissue for immunohistochemical experiments, the animals need perfusion as previously reported (*see* chapter

12), and, after perfusion, the spinal cord and the brain must be rapidly removed from vertebral column and skull, respectively, and processed following the protocol described below.

3.1. Preparation of Slices

1. Postfixation: The tissues are postfixed for 3 h at 4°C in PBS containing PAF 4%.
2. Cryopreservation: Postfixed samples are cryoprotected by three serial incubation at 4°C, 2 h each, in a solution of PBS containing increasing concentration of sucrose (10%, 20%, and 30%). This process allows removal of particles of water from tissues and prevents freezing artifacts.
3. Freezing: After cryopreservation the samples are roughly dried and dipped in cooled isopentane (–35°C to –45°C). The time of immersion varies between the different types of tissues and it depends on the size and the shape of sample. However, it must be long enough to result in complete freezing, but not so long as to cause shrinkage or cracking of tissue.
4. Tissues conservation: After freezing, the tissues could be stored at –70°C for months before sectioning (*see* **Note 1**).
5. Cryostat sectioning: the micrometric slices from 20 to 40 μm of thickness are obtained by sectioning the tissues using a microtome housed in a freezing chamber placed at a temperature of –20°C. Brain tissues are directly placed on the iced metal platform. To paste the sample on the platform, OCT compound is squeezed onto the platform surface. As the OCT begins to freeze the sample can be placed; when the OCT is completely frozen it is possible to connect the platform to the motor of the cryostat. To avoid the breaking of tissues during sectioning, spinal cord samples must be previously embebbed in a small cylinder of OCT following the same procedures described above.

3.2. Free-Floating Immunohistochemistry

1. Transfer micrometric slices into the wells containing TBS at room temperature, using the tip of a brush (*see* **Note 2**).
2. Place the wells on a shaking plate during the whole duration of the experiment.
3. Remove the remaining OCT, and rinse the slices three times, each time for 10 min, in TBS.
4. Preincubate the slices for 1 h at room temperature in a solution of TBS containing 10% NGS to reduce the nonspecific staining mainly due to crossreaction of secondary antibodies.
5. Staining:

    a. TNFα immunostaining: Incubate the slices overnight at room temperature in the following solution: TBS containing 1% NGS, 0.1% Triton X-100, and 0.2% primary antibody (61E71: mouse monoclonal antihuman TNFα, a kind gift from Dr. Wim Buurman, Maastricht, Netherlands; available from HyCult Biotechnology, www.hbt.nl).
    b. TNFRp55 and the TNFRp75 immunostaining: Incubate the slices overnight

at room temperature in the following solution: TBS containing 1% NGS, 0.2% Triton X-100 and 1% primary antibody (HM104: rat polyclonal antimouse TNFRp55, or HM 101: rat polyclonal antimouse TNFRp75, obtained from Dr. Wim Buurman). Triton X-100 is used to make the cell membrane permeable and allow the antibody to better penetrate inside the cell.

3.3. Visualization of Antibodies (ABC Method)

1. Rinse the slices three times, each time for 10 min, in TBS.
2. Preincubate the slices in the following solution: TBS pH 7.4 containing 3% NGS for 1 h at room temperature. This procedure is used in the anti-TNFα immunostaining exclusively, to avoid a nonspecific crossbridging between the secondary antimouse and the native tissue.
3. Immunostaining:
   a. TNFα immunostaining: Incubate the slices in TBS containing 1% NGS and 0.5% antimouse secondary antibody for 1 h at room temperature.
   b. TNFRp55 and TNFRp75 immunostaining: Incubate the slices in TBS containing 2% NGS and 0.5% antirat secondary antibody (Vector laboratories) for 1 h at room temperature.
4. Rinse the slices three times, each time for 10 min, in TBS.
5. 30 min prior to the following incubation, mix reagent A (avidin) and reagent B (biotinylated horseradish peroxidase) (Vector laboratories) with TBS to a final concentration of 1% (do not use Triton X-100 in this step).
6. Incubate for 1 h at room temperature in the solution reported above.
7. Rinse the slices once in TBS and twice in the same solution but adjusted to a pH from 7.8 to 8.3 (10 min each time).
8. Transfer the slices in TBS adjusted to pH 7.8–8.3 containing 0.5% DAB (w/v) and H_2O_2 (0.6 μL in 1 mL of solution; H_2O_2 is added just before application). As DAB is a photosensitive molecule, the DAB must be dissolved and stored in a dark vial until the incubation (*see* **Note 3**).
9. Maintain the slices in this solution from 30 s to 1–2 min. After this step, transfer the slices into the wells containing 0.9% NaCl and hold them in this solution (at 4°C) until the mounting on slides (*see* **Note 4**).

3.4. Mounting Sections on Slides

1. Transfer slices into a large Petri dish containing a solution of 0.9% NaCl to facilitate movement.
2. Remove the slices using the tip of a thin brush and place them on a gelatin-coated glass slide.

3.5. Slides Dehydration

1. Store the slides in a dust-free place to reduce excess saline solution around the sections, before the dehydration.
2. Immerse the slides in the following solutions for 3 min each solution:

a. H_2O.
b. 70% ethanol.
c. 95% ethanol.
d. 95% ethanol.
e. 100% ethanol.
f. 100% ethanol.

3. After dehydration the slides are transferred to xylene for at least 5 min to avoid drying out of the tissues.

3.6. Coverslip Application

1. After dehydration, apply a gel solution of xylene (DPX mountant for microscopy). This step is fundamental to avoid rehydration and irreversible damage of samples.
2. Gently apply a glass cover slip on the upper side of the slide.
3. The slides are dried overnight at room temperature and are then suitable for light microscopy observation (*see* **Note 5**).

4. Notes

1. Spinal cord tissues are particularly thin and are very sensitive to temperature changes. Sometimes just moving the Eppendorf tube containing the tissues away from the dry ice for a few seconds is enough to cause an immediate deterioration of sample. This risk is more frequent using newborn spinal cord tissues.
2. To obtain a homogeneous staining of samples, place only a few sections in each well and perform the incubation with shaking at a low speed. These precautions help to avoid the superimposition of slices and allow a constant flux of solution over the surface of the sections.
3. When the slices are transferred into a different well after incubation with DAB, it is important to rinse the tip of the brush with TBS after each dip (immersion) in the solution containing DAB. This method helps to stop the cholorimetric reaction reducing the risk of a DAB overexposure.
4. If, after incubation in DAB solution, the slices are weakly stained or completely unstained, it is possible to try an enhancement of signal by adding nickel-ammonium salt in the DAB solution. However, this method of enhancement is often a source of several side-effects, such as increasing the nonspecific staining, producing artifacts, and generating an intense background.
5. It is important to press uniformly on a side of the coverslip above the DPX applied on the slide. This procedure is important to avoid the formation of bubbles.

References

1. Meistrell, M. E., III, Botchkina, G. I., Wang, H., Di Santo, E., Cockroft, K. M., Bloom, O., et al. (1997) Tumor necrosis factor is a brain damaging cytokine in cerebral ischemia. *Shock* **8,** 341–348.
2. Ruddle, N. H., Bergman, C. M., McGrath, K. M., Lingenheld, E. G., Grunnet, M.

L., Padula, S. J., et al. (1990) An antibody to lymphotoxin and tumor necrosis factor prevents transfer of experimental allergic encephalomyelitis. *J. Exp. Med.* **172,** 1193–1200.

3. Ghezzi, P. and Mennini, T. (2001) Tumor necrosis factor and motoneuronal degeneration: an open problem. *Neuroimmunomodulation* **9**, 178–182.
4. Duchen, L. W. and Strich, S. J. (1968) An hereditary motor neurone disease with progressive denervation of muscle in the mouse: the mutant "wobbler." *J. Neurol. Neurosurg. Psychiatry* **31,** 535–542.
5. Ince, E. and Levey, A. Immunohistochemical localization of neurochemicals, in *Current Protocols in Neuroscience* (Crawley, J., et al., eds.) Wiley, Hoboken, NJ, 1997.

8

TNF Signaling

Key Protocols

Marta Muzio and Simona Saccani

Summary

Tumor necrosis factor (TNF) is a pleiotropic cytokine that signals inflammation as well as cell death. We focus herein on the inflammatory pathway, giving particular emphasis to the in vitro methods used to study intracellular signaling mediators. The signal transduction cascade that TNF triggers after binding to the TNF receptors (TNFRs), flows throughout a series of protein–protein interactions as well as kinase activations, and finally leads to the translocation of distinct transcription factors within the nucleus, eventually inducing the transcription of specific inflammatory genes. In this chapter, we describe the analysis of the TNF receptor signaling complex by immunoprecipitation (IP), the activation of different MAP kinases by Western blot, the analysis of transcription factor activation by either electrophoretic mobility-shift assay (EMSA) or reporter assay, and the analysis of TNF-induced genes by chromatin IP (ChIP).

Key Words: Inflammation; nuclear factor-κB (NF-κB); MAP kinases; immunoprecipitation; Western blot; EMSA; ChIP.

1. Introduction

Tumor necrosis factor α (TNFα) plays a crucial role in regulating apoptosis and inflammation as well as immunity and proliferation. To signal activation inside the cell, a TNF trimer binds to a cognate TNF receptor (TNFR) trimer, either of type I (p55-TNFR) or type II (p75-TNFR), on the cell surface ***(1–3)***. After binding to the receptors, a cascade of signaling events is triggered, and eventually leads to activation of distinct transcription factors in the nucleus.

First of all, a TNFR signaling complex is assembled proximal to the interior of the cell surface (*see* **Fig. 1**). Inhibitory molecules such as SODD are dis-

From: *Methods in Molecular Medicine, Vol. 98: Tumor Necrosis Factor*
Edited by: A. Corti and P. Ghezzi © Humana Press Inc., Totowa, NJ

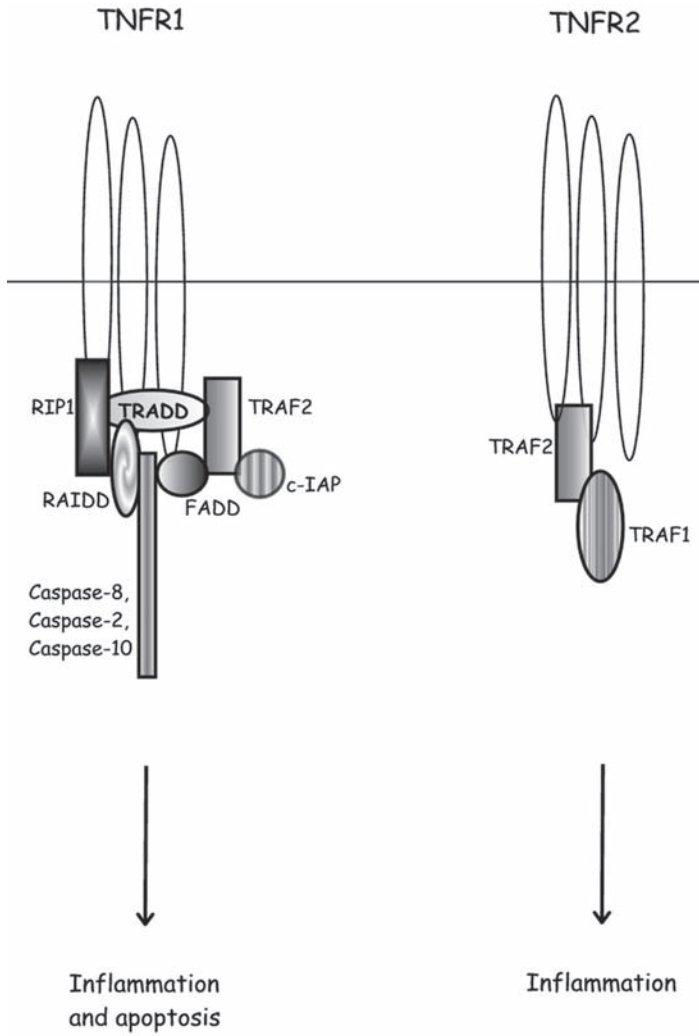

Fig. 1. Schematic representation of TNF receptor signaling complexes.

placed by TNF binding ***(4)***, and several adapters are now bound to the complex, namely FADD ***(5–7)***, TRADD ***(8–10)***, TRAF2 ***(11–13)***, c-IAP ***(14,15)***, RAIDD ***(16),*** and TRIP ***(17),*** together with a kinase (RIP1) ***(18–21)*** and distinct caspases ***(16,22–24)***. Immunoprecipitation can be used to study the formation of a TNFR signaling complex (*see* Chapter 3).

The activation of TNFR triggers two main kinase pathways: MAPK activation and IKK activation ***(1–3)***. In parallel to this, an apoptotic pathway flows throughout caspases cleavage ***(22–24)***, and a sphingomyelinase pathway pro-

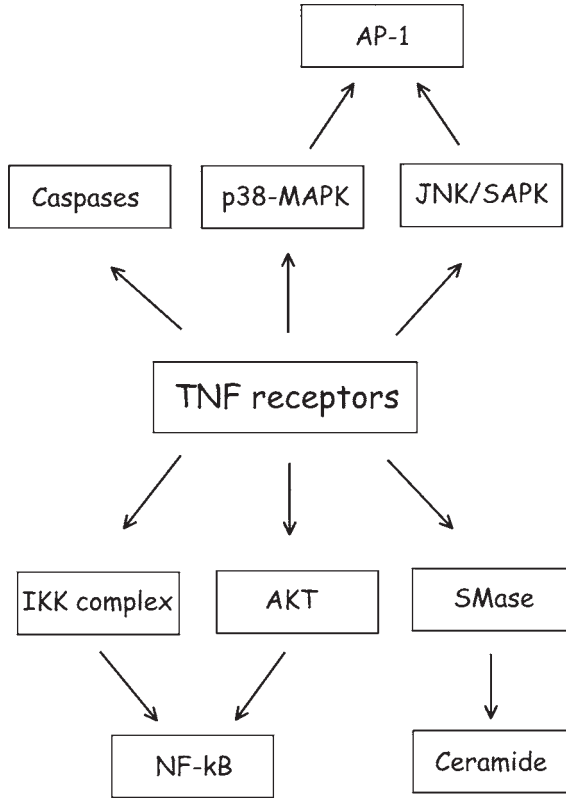

Fig. 2. Schematic representation of TNF receptor signaling pathways.

duces ceramide ***(3,25)*** (*see* **Fig. 2**). We focus herein on the MAPK and IKK pathways; apoptosis is the topic of the following chapter. The MAPK pathway leads to phosphorylation and activation of p38 MAPK and JNK/SAPK ***(3,26–28)***; this process can be followed by Western blot analysis (*see* Chapter 3). MAPKs contribute to the activation of the AP-1 transcription factor that participates in induction of TNF target genes ***(29)***.

The IKK complex includes the kinases IKK-α and IKK-β, and the scaffold protein IKK-γ ***(30–36)***; note that knockout studies suggest that IKK-α is not required for IKK activation by TNF ***(37)***. The IKK complex directly phosphorylates the IκB inhibitor and targets it for degradation; this allows for nuclear factor kappa B (NF-κB) to translocate into the nucleus and to activate additional TNF target genes ***(38)***. In addition to this, AKT activation by TNF also contributes to the induction of NF-κB transcriptional activity ***(39)*** (*see* **Fig. 2**). NF-κB activation can be monitored by either reporter assay or EMSA (*see* Chapter 3).

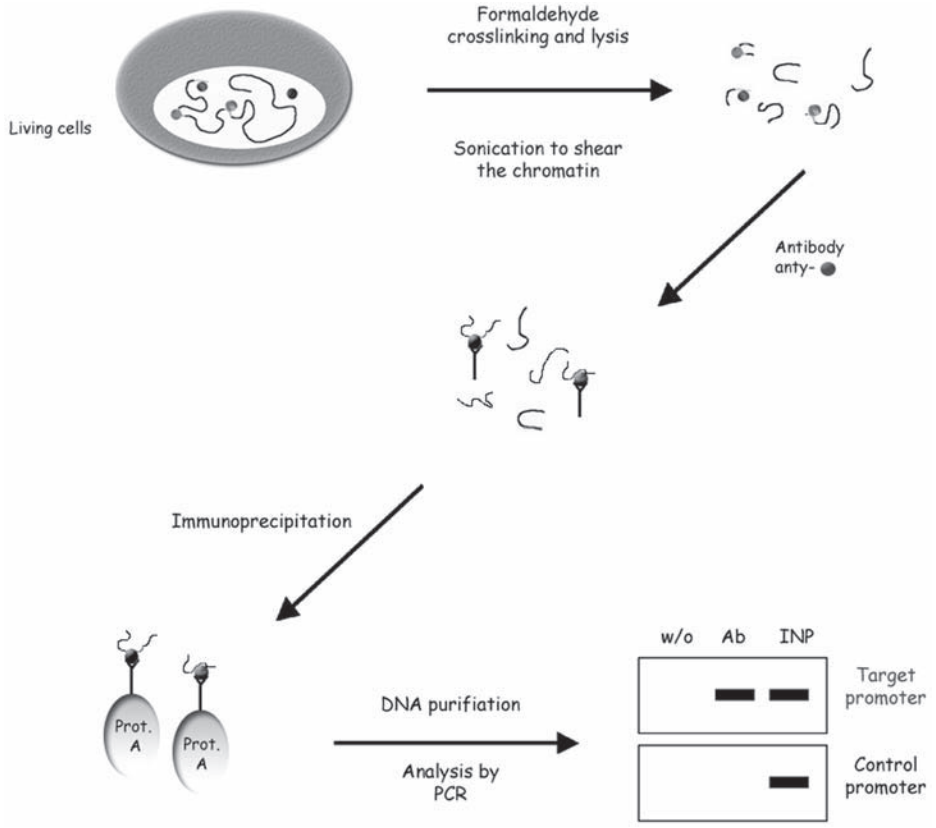

Fig. 3. Schematic representation of chromatin immunoprecipitation.

Finally, after TNF signaling several transcriptional complexes assemble onto specific promoters, and this allows for strict regulation of TNF-induced genes *(38)*. This particular event can be studied by using Chromatin IP methods as explained in Chapter 3 (*see* **Fig. 3**).

2. Materials

1. Cell lysis buffer for IP: 1% NP40, 50 m*M* Tris-HCl, pH 7.4, 1 m*M* EDTA, 150 m*M* NaCl, protease inhibitors cocktail, phosphatase inhibitors (*see* **Note 1**).
2. Cell lysis buffer for Western blot: 0.2% NP40, 50 m*M* Tris-HCl, pH 7.4, 1 m*M* EDTA, 150 m*M* NaCl, protease inhibitors cocktail, phosphatase inhibitors (*see* **Note 1**).
3. Binding buffer: 1% NP40, 50 m*M* Tris-HCl, pH 7.4, 1 m*M* EDTA, 500–1000 m*M* NaCl (*see* **Note 2**).
4. Protein A or G agarose beads (50% beads slurry in PBS) (*see* **Note 3**).

5. Phospho-p38-MAPK antibody.
6. p38-MAPK antibody.
7. Phospho-SAPK/JNK antibody.
8. SAPK/JNK antibody.
9. Custom 3X sample buffer: 150 m*M* Tris-HCl, pH 6.8, 6% SDS, 0.3% Bromophenol blue, 30% glycerol, add fresh β-mercaptoethanol 1 μL/100 μL, or commercially available premixed LaemmLi sample buffer or 4X SDS sample buffer (*see* **Note 4**).
10. Peroxidase-linked antimouse or antirabbit antibody.
11. Phosphate buffered saline (PBS).
12. Tris buffered saline (TBS).
13. PBST or TBST: 0.05–0.1 % Tween-20 into PBS or TBS, respectively.
14. SDS-PAGE precast or custom minigels, and running apparatus.
15. Custom or commercially available transfer buffer.
16. Nitrocellulose membrane.
17. Nonfat dry milk.
18. Chemiluminescent detection system.
19. Custom or commercially available nuclear factor-κB (NF-κB) reporter plasmid.
20. Custom or commercially available activator protein-1 (AP-1) reporter plasmid.
21. Custom or commercially available β-galactosidase plasmid.
22. Luciferase assay kit (luciferase assay substrate and luciferase cell lysis buffer).
23. 2X HBS: 280 m*M* NaCl, 50 m*M* HEPES, 1.5 m*M* $Na_2HPO_4 \cdot 2H_2O$, pH 7.1.
24. 80 m*M* CPRG.
25. β-Galactosidase reaction buffer: 80 m*M* Na_2HPO_4, 9 m*M* $MgCl_2$, 10 4m*M* β-mercaptoethanol.
26. Lysis buffer for EMSA: 250 m*M* NaCl, 50 m*M* Tris-HCl, pH 8.0, 1 m*M* EDTA, 0.1% NP40, 10% glycerol.
27. PMSF 0.1 *M* (100X).
28. Dithiothreitol (DTT) 1 *M*.
29. Poly-dI-dC 1 mg/mL.
30. 10X binding buffer for EMSA: 20 m*M* Tris-HCl, pH 7.5, 0.1 m*M* EDTA, pH 8, 2 m*M* DTT, 4 m*M* $MgCl_2$.
31. 50% glycerol.
32. Loading buffer for EMSA: 200 m*M* Tris-HCl, pH 7.5, 25% glycerol, 0.2% (w/v) bromophenol blue.
33. TEMED (*N*,*N*,*N*',*N*'-tetramethylenediamine).
34. 10% (w/v) ammonium persulfate (APS).
35. Acrylamide: bisacrylamide premix solution 29:1.
36. 10X TBE: 108 g Tris base, 55 g boric acid, 40 mL 0.5*M* EDTA, pH 8.0 in 1000 mL H_2O.
37. T4 polynucleotide kinase (PNK).
38. Mobility-shift probe: Annealed complementary oligonucleotides (**Subheading 3.4.1.**) carrying NF-κB DNA binding site).
39. Radio-labeled [γ-^{32}P]-ATP 3000 Ci/mmole.

40. 0.8-mL Sephadex G-50 column (custom made or preassembled).
41. Antibodies for super-shift.
42. Custom 20 × 20-cm glass plates for EMSA gels, and electrophoresis running apparatus.
43. Gel dryer.
44. Formaldehyde 37% (molecular biology grade).
45. L1 lysis buffer for ChIP: 50 m*M* Tris-HCl, pH 8.0, 2 m*M* EDTA, pH 8.0, 0.1% NP40, 10% glycerol.
46. L2 nuclear resuspension buffer: 1% SDS, 5 m*M* EDTA, pH 8.0, 50 m*M* Tris-HCl, pH 8.0.
47. Dilution buffer (DB): 0.5% NP40, 200 m*M* NaCl, 5 m*M* EDTA, 50 m*M* Tris-HCl, pH 8.0.
48. NF-κB antibodies.
49. Protein A or G agarose beads for Chromatin IP: 50% beads slurry in NaCl washing buffer.
50. Salmon sperm DNA 10 mg/mL (sonicated).
51. NaCl washing buffer: 0.1% SDS, 1% NP40, 2 m*M* EDTA, 500 m*M* NaCl, 20 m*M* Tris-HCl, pH 8.0.
52. LiCl washing buffer: 0.1% SDS, 1% NP40, 2 m*M* EDTA, 500 m*M* LiCl, 20 m*M* Tris-HCl, pH 8.0.
53. Elution buffer (EB): 1X TE, pH 8.0, 2% SDS).
54. GlycoBlue-glycogen 10 mg/mL (Abcam).
55. Absolute ethanol 100%.
56. 3 *M* NaCl.
57. 1X TE, pH 8.0.
58. RNase A 1 mg/mL.
59. Primers, sense and antisense, for promoter of TNFα-inducible gene under analysis (e.g., IκBα, IL-1β, MIP-1α).
60. 10 m*M* dNTP mix.
61. *Taq* polymerase and 10X amplification PCR buffer (commercially available).
62. Ponceau red
63. Ethidium bromide
64. Proteinase-κ

3. Methods

The protocols described below outline the most common methods used for in vitro study of TNF signaling, namely, the analysis of the TNF receptor signaling complex by immunoprecipitation (IP) (**Subheading 3.1.**), the analysis of different MAP kinases by Western blot (**Subheading 3.2.**), the analysis of transcription factors activation by either reporter assay (**Subheading 3.3.**) or electrophoretic mobility shift assay (EMSA) (**Subheading 3.4.**), and the analysis of TNF-induced genes by chromatin IP (ChIP) (**Subheading 3.5.**) (*see* **ref. *40*** for basic molecular biology protocols).

3.1. Analysis of the TNF Receptor Signaling Complex by Immunoprecipitation (IP)

TNF trimer binds to and activates a trimeric TNF receptor complex. The TNF receptor signaling complex includes several cytoplasmic mediators, namely FADD, TRADD, TRAF2, RAIDD, Caspase-8, -2, and -10, RIP1 (for TNFR-1) or TRAF1 and TRAF2 (for TNFR-2) (**Fig. 1**). To analyze the formation of a signaling complex within activated cells, the receptor can be immunoprecipitated by using a specific antibody, and associated molecules can be detected by Western blot. Alternatively, a specific signaling molecule can be immunoprecipitated, and binding receptor and/or additional signaling mediators can be found in the immunocomplexes.

3.1.1. Lysis of Cells for Immunoprecipitation

1. Wash the cells with PBS (1–10 million cells, depending on their size and available amount).
2. Resuspend pelleted cells with 500 μL of lysis buffer for IP.
3. Keep on ice for 10–20 min.
4. Spin 10–20 min with a minifuge at 4°C (18,000 *g*).
5. Recover supernatant and keep on ice (discard pelleted cell debris).

3.1.2. Immunoprecipitation

1. Adjust lysate to 500–1000 m*M* NaCl in a final volume of 1 mL of binding buffer (the higher salt concentration, the more specificity of protein binding).
2. Add specific antibody (1 μg of purified antibody, or 10 μL of serum or ascite as a starting point).
3. Gently rock for 1–4 h at 4°C.
4. Add protein A or G agarose beads (10 μL of 50% slurry).
5. Gently rock the tube for 30–60 min at 4°C.
6. Wash the beads twice with binding buffer (*see* **Note 5**).
7. Transfer into a new tube, and wash once with PBS.
8. Resuspend the beads in 1X sample buffer.
9. Freeze or load the sample onto SDS-PAGE.

3.1.3. Western Blot Analysis of Immunocomplexes

1. Boil the samples for 5 min (18,000 *g*).
2. Spin down to pellet the agarose beads (30 s in minifuge) (18,000 *g*).
3. Load supernatant onto SDS-PAGE minigel (10 × 10 cm) (8–15% depending on the molecular weight of the protein of interest; the bigger the protein, the lower percentage of acrylamide).
4. Run the gel by electrophoresis according to the manufacturer's instructions.
5. Electrotransfer to nitrocellulose membrane.
6. Stain with Ponceau red and wash with water (*see* **Note 6**).

7. Take a picture or photocopy of it if you like (as a gross loading control).
8. Wash the membrane with 20 mL of PBST or TBST (shake for 5–10 min).
9. Incubate the membrane with 20 mL of 5% nonfat milk in PBST or TBST.
10. Shake for 30 min at room temperature or overnight at 4°C.
11. Wash membrane with 20 mL of PBST or TBST (shake for 5–10 min).
12. Incubate with <10 mL of primary antibody diluted into 5% nonfat milk in PBST or TBST according to manufacturer's instructions. The correct antibody concentration can only be determined experimentally; serial dilutions of a new antibody are encouraged. (As a starting point, dilute your serum or ascite 1:1000.)
13. Shake 1–2 h at room temperature or overnight at 4°C.
14. Wash three times with 20 mL of PBST or TBST (shake for 5–10 min).
15. Incubate with secondary peroxidase-linked antibody (use antimouse if the primary antibody was a mouse antibody, and so on).
16. Wash four times with 20 mL of PBST or TBST (shake for 5–10 min).
17. Detect by using a chemiluminescent system.

3.2. Analysis of MAP Kinase Activation by Western Blot

After activation of the cells with TNF, a cascade of kinase activations occurs, and eventually leads to phosphorylation and activation of both JNK/SAPK and p38-MAPK (**Fig. 2**). Because phosphorylation determines activation of these kinases, they can be monitored by analyzing their phosphorylation status. To this aim, cell lysates can be analyzed by Western blot using a phospho-specific antibody directed against either JNK/SAPK or p38.

3.2.1. Lysis of Cells for Western Blot Analysis

1. Wash the cells with PBS (1–10 million cells, depending on their size and available amount).
2. Resuspend pelleted cells with 100 μL of lysis buffer for Western blot.
3. Keep on ice for 10–20 min.
4. Spin 10–20 min with a minifuge (18,000 *g*).
5. Recover supernatant (discard pelleted debris).
6. Put on ice.
7. Take an aliquot of each sample and determine protein concentration by the Bradford method.
8. Freeze at –80°C or load the sample onto SDS-PAGE.

3.2.2. Western Blot of Cell Lysates

1. Aliquot 30 μg of protein of each sample on ice.
2. Add lysis buffer to a final volume equal in all the samples.
3. Boil 5 min.
4. Spin briefly to recover the sample.
5. Load onto SDS-PAGE minigel (10 × 10 cm) (8–15% depending on the molecular weight of the protein of interest; the bigger the protein, the lower percentage of acrylamide).

6. Run the gel by electrophoresis according to the manufacturer's instructions.
7. Electrotransfer to nitrocellulose membrane.
8. Several antibodies that recognize human or mouse phospho-JNK or phospho-p38 are now commercially available. Use them to detect phosphorylated forms of JNK or p38 by Western blot as described in **Subheading 3.1.3., steps 6–17**. Always use anti-JNK or anti-p38 antibody as an internal control.

3.3. Analysis of Transcription Factors Activation by Reporter Assay

After activation of the cells with TNF, the TNFR signaling complex activates both the MAPK signaling cascade and the IKK complex. MAPK signaling ends with the activation of the transcription factor AP-1. On the other hand, IKK directly phosphorylates IκB and targets it for degradation; the transcription factor NF-κB is thus activated and translocated into the nucleus (**Fig. 2**). To study AP-1 or NF-κB activation, cell lines can be transfected with a specific reporter plasmid. Cotransfection with a signaling molecule, or dominant negative versions of it, can be performed to analyze its involvement into TNF signaling pathway. In addition, different stimuli can be used on transfected cells to determine synergism or antagonism with TNF into a specific cell line (*see* **Subheading 3.3.1.**).

An inducible reporter vector that contains the luciferase gene driven by a basic promoter element (TATA box) plus a specific inducible *cis*-enhancer element, such as NF-κB specific or AP-1 specific, can be used to analyze TNF signaling within human cell lines (**Subheading 3.3.2.**).

A β-galactosidase plasmid can be used as an internal control for monitoring transfection efficiency; a constitutive promoter drives transcription of the *lac*Z gene, that encodes the β-galactosidase enzyme. β-galactosidase is a convenient reporter enzyme that can be assayed directly in cell extracts by using a spectrophotometric assay (**Subheading 3.3.3.**).

3.3.1. Transfection of Cells

Two different methods can be used to transfect cell lines: lipid-mediated transfection (**Subheading 3.3.1.1.**), and calcium phosphate precipitation (**Subheading 3.3.1.2.**). It is important that the cells are maintained in a healthy state prior to plating for transfection, and during proliferation when transfected. Do not let the cells grow to confluence.

3.3.1.1. Lipid-Mediated Transfections

Lipids can be used to transfect both cell suspensions and adherent cells with high efficiency and low toxicity; several commercially available reagents are on the market, and have been tested on different cell lines. Please refer to the manufacturer's instructions for using specific reagents.

3.3.1.2. Calcium Phosphate Precipitation

This method can be used on adherent cells to obtain both high efficiency of transfection and low toxicity.

1. Divide the cells 1–2 d before transfection, and use them for calcium phosphate precipitation when they have reached 60% confluency. The steps below refer to a 10-cm dish; arrange doses as required.
2. Replace medium with 10 mL of transfection medium (**Note 7**).
3. Prepare DNA mix by adding 50 µL of 2.5 *M* $CaCl_2$ and <20 µL of DNA plasmids to 440 µL of double-distilled H_2O (*see* **Note 8** for DNA concentration).
4. Add DNA mix to 500 µL of 2X HBS. This critical step forms the calcium phosphate crystals (*see* **Note 9**).
5. Leave at room temperature for 5–30 min.
6. Disperse the calcium phosphate precipitate onto the cells, drop by drop.
7. Incubate at 37°C for 8–16 h.
8. Discard transfection medium, wash cells twice with saline, and incubate the cells with fresh medium for 24–48 h before luciferase assay.

3.3.2. Luciferase Assay

Lyse the cells and assay for luciferase according to the manufacturer's instructions. Briefly, dilute the lyophilized luciferase assay substrate and aliquot at –70°C to avoid multiple freeze–thaw cycles. Equilibrate luciferase assay substrate to room temperature before use. Mix substrate with cell lysate (which can also be aliquoted at –70°C) and immediately read with a manual luminometer. Alternately, a luminometer with injector can be used to mix and read.

3.3.3. β-Galactosidase Assay

The assay is done in triplicate by using 50–100 µg of the cell lysate (80 µL), in 96-well plates.

1. Mix cell lysate with 100 µL of β-galactosidase reaction buffer and 20 µL of CPRG (80 m*M*).
2. Incubate at room temperature in the dark.
3. Monitor until the color switches from yellow to red (it usually takes between 30 and 120 min).
4. Read at 570 nm.

β-galactosidase values are obtained by subtracting a blank. To normalize the luciferase data with transfection efficiency, divide luciferase values with β-galactosidase values for each sample (when β-galactosidase values are within a linear range) (*see* **Note 10**).

3.4. Analysis of Transcription Factor Activation by Electrophoretic Mobility-Shift Assay (EMSA)

The electrophoretic mobility-shift assay (EMSA) is a simple and rapid technique for the detection of sequence-specific DNA binding factors. In this assay, a crude protein extract or purified proteins can be used to test their binding activity to a specific DNA sequence. The reaction is then loaded onto a nondenaturing polyacrylamide gel. Proteins that specifically bind to the radiolabeled DNA fragment result in a discrete band having a retarded mobility with respect to the free DNA probe. This assay permits quantitative analysis of the affinity, the association/dissociation rate constant, the abundance, and the binding specificity of a DNA binding factor to a specific DNA binding site. Moreover, by using antibodies for different proteins (e.g., different NF-κBs) it is possible to get information on the different protein in the complexes bound to the DNA probe (the so-called super-shift). Please note that all manipulations of radiolabeled materials require appropriate safety procedures.

3.4.1. Preparation of the DNA Probe for EMSA

DNA fragments from 20–300 bp may be used as probe.

1. Mix 500 ng of oligo sense primer with 500 ng of oligo antisense primer in 100 µL of annealing buffer. Heat at 95°C for 5 min, switch off the heater, allow the mixture to slowly cool to 25°C, and finally put on ice. The dsDNA so prepared can be stored at –20°C.
2. Set up the radiolabeling reaction using 10 ng of dsDNA, 1 µL of 10X T4 PNK buffer, 1 µL of 1X T4 PNK, 2–5 µL of [γ-^{32}P]-ATP, and water to 10 µL. Incubate at 37°C for 60 min.
3. Stop the reaction by adding 0.5 µL EDTA, 0.5 *M*. Heat at 60°C for 5–7 min.
4. Add 1X TE to a final volume of 50 µL, and purify the radiolabeled probe on a Sephadex-50 column (free ATP will rest on the column). Keep on ice.
5. Count 2 µL in a scintillation counter to determine the specific activity (counts/min/µL). Usually it ranges from 50×10^5 to 1×10^6 counts/min/µL. The radiolabeled probe can be stored at –20°C for 4–6 wk.

3.4.2. Preparation of a Nondenaturing Polyacrylamide Gel

1. Assemble glass plates with 1.5 mm spacers (*see* **Note 11**).
2. Seal the bottom of the assembled glass plates with 2 mL of gel mix with 50 µL of 10% APS and 5 µL of TEMED (this gel polymerizes rapidly, about 1 min).
3. Add 450 µL of 10% APS and 70 µL TEMED to 60 mL nondenaturing gel mix (4–6% acrylamide in TE 1X). Swirl gently, and pour the gel mix between the glass plates; avoid bubble formation. Insert the comb, and let polymerize for at least 20 min at room temperature.
4. Remove the comb and attach the plates to the electrophoresis tank. Fill the upper and lower reservoirs with TE 1X.

5. Remove the bubbles from the wells with the help of a syringe.
6. Prerun the gel for 30 min at 20 mA constant (*see* **Note 12**).

3.4.3. Lysis of Cells and Binding Reaction

1. Transfer the cells to an ice bath. Collect and spin the cells at 1200 rpm in a centrifuge for 10 min at 4°C (300 *g*).
2. Aspirate completely the PBS and wash twice with ice-cold PBS.
3. After the last spin, aspirate carefully all the supernatant and lyse the pelleted cells with 100 μL of EMSA-lysis buffer with protease and phosphatase inhibitors. (Adjust the volume depending on the cell number and cell type.)
4. Leave on ice for 10–20 min.
5. Spin for 10 min at 4°C using a minifuge (18,000 *g*).
6. Transfer the supernatant into a new 1.5-mL tube.
7. Determine protein concentration of each sample using the Bradford method.
8. Proceed to binding reaction, or freeze the sample at –80°C.
9. Assemble the binding reaction at room temperature by using 10–20 μg of total cell extract (*see* **Note 13)**; adjust the volume to 6 μL with EMSA-lysis buffer, and add 2 μL of poly-dI-dC (to reduce the nonspecific protein–DNA binding), 2 μL of 10X binding buffer, 6 μL of 50% glycerol, 4 μL of ^{32}P radiolabeled probe (total count 10–30 × 10^3 counts/min), water to a final volume of 20 μL.
10. Incubate 20 min at room temperature (*see* **Notes 14** and **15**).
11. Add 2 μL of loading buffer, vortex, and spin quickly to collect the drops.

3.4.4. EMSA

1. Load the reactions onto a prerun gel and run at 20–30 mA for 1 h. (Prerun at 25mA for 30–60 min.)
2. Carefully open the glass plates with the help of a spatula allowing air to enter between the plates and the gel. The gel normally remains attached to only one plate.
3. Overlay 2 sheets of Whatman 3MM paper; the gel will stick to the papers.
4. Let gel dry for 1 h at 80°C.
5. Expose the dried gel to X-ray film, and leave it at –80°C overnight; alternatively, expose directly to the phospho-imager.

3.5. Analysis of TNF-Induced Genes by Chromatin IP (ChIP)

Nuclear factor kappa B is a family of five related transcription factors, namely RelA/p65, RelB, c-Rel, p100, and p105, where p100 and p105 are respectively the precursor of p52 and p50. NF-κBs are expressed as hetero- and/or homodimers in most vertebrate cells ***(38)***.

NF-κBs are sequestered, as inactive forms, in the cytoplasm via interaction with the inhibitory κB proteins (IκBs, p100, and p105). Upon proinflammatory stimulation, e.g., TNFα, the IK kinase (IKK) pathway is activated, and IκB is phosphorylated and targeted for proteosomal degradation. After IκB degrada-

tion, NF-κB is free to translocate into the nuclei and to bind to the decanucleotide DNA binding sites in the promoters and/or enhancers of several genes, e.g., chemokines and cytokines ***(38)***.

Using formaldehyde fixation of the cells and chromatin immunoprecipitation, it is possible to follow the in vivo spatial and temporal recruitment of transcription factors, as well as histone tail modifications, or components of transcriptional machinery at a single promoter level ***(41)***. For example, by using antibodies specific to NF-κB proteins, it is possible to monitor their recruitment to the promoters of TNF-induced genes ***(42,43)***.

3.5.1. Advance Preparation

1. Test the capability of the antibody to immunoprecipitate the target protein from formaldehyde-fixed nuclear extract. Polyclonal antibodies usually work under these conditions.
2. Set up DNA-sonication conditions on a formaldehyde-fixed extract, to break the chromatin into the desired fragment size (average 500–1000 bp). Sonicate in 1.5-mL tubes, and with volumes greater than 400 μL, to avoid foaming formation. After each pulse remove 50 μL of the sample, and analyze it on 1% agarose gel after DNA purification (*see* **Subheading 3.5.3.**).
3. Set up PCR conditions on sonicated genomic DNA. Test at least two sets of primers for each TNF-induced gene of interest (two sense and two antisense) in the four different combinations. To ensure a good final result, it is very important to find a strong, single-band PCR product now.

3.5.2. Formaldehyde Cell-Fixation and Lysis of the Cells for ChIP

1. Add 37% formaldehyde directly to the cells (5×10^6 cells) in their culture media, to a final concentration of 1%. Mix quickly, and leave the mixture at room temperature for the appropriate time (usually between 5 and 10 min).
2. Quench formaldehyde with Tris-HCl, pH 7.5, at final concentration of 125 m*M*.
3. Transfer the cells onto ice.
4. For adherent cells, aspirate media and wash the cells 3 times for 10 min each time with ice-cold PBS. Collect the cells into a 50-mL tube by scraping with PBS.
5. For suspension cells, collect the cells carefully into a 50-mL tube, and wash 3 times in ice cold PBS for 10 min.
6. Spin the cells at 1200 rpm in a microfuge for 10 min at 4°C.
7. Lyse cells in 600 μL of ice-cold L1 lysis buffer with protease and phosphatase inhibitors and 2 m*M* DTT.
8. Transfer to a 1.5-mL tube and leave it on ice for 5 min.
9. Spin at 3000 rpm in a microfuge (960*g*) 5 min at 4°C.
10. Transfer supernatant (cytoplasmic fraction) to a 1.5-mL tube.
11. Resuspend nuclei in 600 μL L2 buffer with protease and phosphatase inhibitors and 2 m*M* DTT.
12. Proceed to **Subheading 3.5.3.** or store sample at –80°C.

3.5.3. Chromatin Fragmentation

1. Sonicate as in **Subheading 3.5.1**. Usually 6 pulses of 10 s each are enough to fragment the chromatin to the right average size. (Between each sonication, keep the sample on ice for at least 40 s to avoid overheating.)
2. Spin the sample at 18,000*g* in a microfuge for 10 min at 8°C. (Make sure not to have any SDS precipitated in the tube; if so, warm the tube in your hand to complete clearing.)
3. Transfer supernatant into a new tube (*see* **Note 16**).

3.5.4. Chromatin IP

1. Dilute 140–200 µL L2 extracts 1:10 with DB buffer plus PMSF.
2. Preclear extract with 80 µL of protein A presaturated with salmon sperm DNA (*see* **Note 17**) for 1–3 h at 4°C in rotation.
3. Spin at maximum speed for 1 min at 4°C and carefully transfer into a new tube; avoid taking any protein A.
4. Add 1–2 µg of antibody.
5. Rotate overnight at 4°C.
6. Add 15–30 µL of presaturated protein A to each tube.
7. Rotate for 30 min at 4°C.
8. Spin at maximum speed for 1 min at 4°C (18,000 *g*).
9. Keep an aliquot (150–300 mL) of supernatant (genomic-DNA) to be used to normalize the PCR reaction (*see* **Subheading 3.5.5.**). (At this point, it is very important to handle the supernatants very carefully to avoid any contamination.)
10. Add 800 µL of NaCl washing buffer plus fresh 1X PMSF to the beads, and immediately spin at 13,000 rpm in a microfuge for 1 min at 4°C (18,000 *g*).
11. Aspirate the supernatants carefully making sure not to touch the beads (stop 1 mm from the interface).
12. Wash with 800 µL NaCl washing buffer plus fresh 1X PMSF for 5 min on ice.
13. Spin at 13,000 rpm in a microfuge for 1 min at 4°C.
14. Repeat **steps 12** and **13** two more times.
15. Wash with 800 µL of LiCl washing buffer plus fresh 1X PMSF for 5 min on ice.
16. Spin at 13,000 rpm in a microfuge for 1 min at 4°C.
17. Repeat **steps 15** and **16** two more times.
18. Wash with 1X TE for 5 min on ice.
19. Spin at 13,000 rpm in a microfuge for 1 min at 4°C.
20. Repeat **steps 18** and **19** two times to remove salts.
21. After the last spin, gently aspirate the supernatant; leave as little liquid as possible, without removing the beads.
22. Add 100 µL of EB at room temperature, and leave for 5 min, keeping the beads in suspension by flicking the tube wall.
23. Spin for 1 min at 13,000 rpm in a microfuge at room temperature, and transfer into a new tube.
24. Repeat **steps 22** and **23** two more times, and pool the supernatants.

3.5.5. Reversion of Crosslinking and DNA Purification

1. Revert crosslinking for 6 h to overnight at 65°C. Genomic-DNA from **Subheading 3.5.4. Step 9** must be processed as the "IP" DNA from this step forward.
2. Add 100 μg proteinase-K to each sample, and incubate for at least 1 h at 50°C.
3. Add 300 μL phenol/cloroform and vortex for 1 min at room temperature.
4. Centrifuge at 13,000 rpm in a microfuge for 10 min room temperature.
5. Transfer the aqueous phase into a new tube.
6. Add 10 μg of glycogen, 2 volumes of Ethanol and 1/10 of volume of 3 *M* NaCl.
7. Mix by inverting the tube several times and store overnight at –20°C to allow maximum DNA recovery.
8. Spin at 18,000*g* in a microfuge for 30 min at 4°C.
9. Aspirate the supernatants and let the pellet air-dry (do not dry under vacuum).
10. Resuspend "IP" samples into 30 μL of 1X TE, and "genomic DNA" samples into 150 μL of 1X TE by careful pipetting up and down several times.
11. Add 2 μL of 1 mg/mL RNase A.
12. Incubate at 37°C for 30 min.

3.5.6. Analysis of DNA by PCR

1. Assemble a PCR reaction in a total volume of 25 μL by using 1.5 μL of either purified "IP" DNA or genomic DNA as internal control (*see* **Note 18**).
2. Run 35–42 cycles of PCR. There are no absolute rules on the number of cycles to be run; it will vary from cell to cell, and from antibody to antibody.
3. Run 10 μL of amplified product on ethidium bromide-agarose gel.

4. Notes

1. Cell lysis buffer for IP and for Western blot can be prepared without protease and phosphatase inhibitors, and stored at room temperature for 1 mo. When needed, take an aliquot and add fresh protease and phosphatase inhibitors.
2. Binding buffer can be stored at room temperature for 1 mo.
3. Protein A or G agarose beads (50% bead slurry in PBS) can be stored at 4°C for 2 wk.
4. Custom 3X sample buffer without β-mercaptoethanol can be stored at room temperature for a few months. When needed, take an aliquot and add fresh β-mercaptoethanol.
5. To wash the agarose beads, spin down briefly (30–60 s in minifuge). The blank pellet that appears contains the beads and immunocomplexes; discard supernatant by gentle aspiration, add binding buffer, and mix by pipetting.
6. Use a small plastic container for Western blot incubations and washes; the more similar to the membrane size, the less amount of antibody can be used.
7. RPMI should not be used for transfection; DMEM or other specific transfection mediums are suitable for the formation of calcium phosphate precipitate.
8. 1 μg/μL is a good concentration for plasmids to be used for transfection. Use 1–10 μg of DNA for each 10-cm dish.

9. The calcium phosphate precipitation step requires the DNA mix to be added drop by drop to the 2X HBS solution. Vortexing the tube a couple of times should facilitate this critical step. To confirm that a high-quality calcium phosphate precipitate was formed, the mix can be analyzed under the microscope; crystals should be visible, but smaller then a single cell.
10. To calculate the linear range, incubate serial dilutions of commercially available β-galactosidase using the same assay. After 20–40 min of incubation, values over 1.8–2 are usually not in a linear range.
11. It is very important to remove any detergent traces from the glass because this disrupts protein–DNA interaction.
12. Prerun the gel before starting the EMSA binding reaction.
13. To improve the assay, in some cases it may be useful to use a nuclear protein extract instead of total extract.
14. It is possible using a different concentration of unlabeled competitor probe to get information on the binding specificity of the DNA–protein interaction under investigation.
15. A variation of the EMSA is to use an antibody to identify the proteins in the protein–DNA complexes (super-shift). Briefly, add either a specific antibody or an irrelevant antibody to the reaction; if the protein of interest is in the complex, the result will be a retardation of the complex mobility or a binding competition (varying from antibody to antibody).
16. It is better to use low-adhesion 1.5-mL tubes from this step forward.
17. Presaturate protein A or G by incubating for 1 h with 1 mg/mL of salmon sperm DNA at 4°C in rotation. Wash 2 times with NaCl washing buffer. Store at 4°C for 1 wk.
18. Perform the PCR reaction on genomic DNA after the PCR reaction tubes on "IP" DNA are closed, to avoid any contamination.

Acknowledgments

We thank Gioacchino Natoli for helpful suggestions.

References

1. Baud, V. and Karin, M. Signal transduction by tumor necrosis factor and its relatives. *Trends Cell Biol.* **11,** 372–377.
2. Chen, G. and Goeddel, D. V. (2002) TNF-R1 signaling: a beautiful pathway. *Science* **296,** 1634–1635.
3. MacEwan, D. J. (2002) TNF receptor subtype signaling: differences and cellular consequences. *Cell Signal.* **14,** 477–492.
4. Jiang, Y., Woronicz, J. D., Liu, W., and Goeddel, D. V. (1999) Prevention of constitutive TNF receptor 1 signaling by silencer of death domains. *Science* **283,** 543–546.
5. Chinnaiyan, A. M., Tepper, C. G., Seldin, M. F., O'Rourke, K., Kischkel, F. C., Hellbardt, S., et al. (1996) FADD/MORT1 is a common mediator of CD95 (Fas/

APO-1) and tumor necrosis factor receptor-induced apoptosis. *J. Biol. Chem.* **271,** 4961–4965.
6. Chinnaiyan, A. M., O'Rourke, K., Tewari, M., and Dixit, V. M. (1995) FADD, a novel death domain-containing protein, interacts with the death domain of Fas and initiates apoptosis. *Cell* **81,** 505–512.
7. Boldin, M. P., Varfolomeev, E. E., Pancer, Z., Mett, I. L., Camonis, J. H., and Wallach, D. (1995) A novel protein that interacts with the death domain of Fas/APO1 contains a sequence motif related to the death domain. *J. Biol. Chem.* **270,** 7795–7798.
8. Hsu, H., Xiong, J., and Goeddel, D. V. (1995) The TNF receptor 1-associated protein TRADD signals cell death and NF-kappa B activation. *Cell* **81,** 495–504.
9. Park, Y. C., Ye, H., Hsia, C., Segal, D., Rich, R. L., Liou, H. C., et al. (2000) A novel mechanism of TRAF signaling revealed by structural and functional analyses of the TRADD-TRAF2 interaction. *Cell* **101,** 777–787.
10. Hsu, H., Shu, H. B., Pan, M. G., and Goeddel, D. V. (1996) TRADD-TRAF2 and TRADD-FADD interaction define two distinct TNF receptor 1 signal transduction pathways. *Cell* **84,** 299–308.
11. Rothe, M., Wong, S. C., Henzel, W. J., and Goeddel, D. V. (1994) A novel family of putative signal transducers associated with the cytoplasmic domain of the 75 kDa tumor necrosis factor receptor. *Cell* **78,** 681–692.
12. Rothe, M., Sarma, V., Dixit, V. M., Goeddel, D. V., et al. (1995) TRAF2-mediated activation of NF-κB by TNF receptor 2 and CD40. *Science* **269,** 1424–1427.
13. Hu, H. M., O'Rourke, K., Boguski, M. S., and Dixit, V. M. (1994) A novel RING finger protein interacts with the cytoplasmic domain of CD40. *J. Biol. Chem.* **269,** 30,069–30,072.
14. Shu, H. B., Takeuchi, M., and Goeddel, D. V. (1996) The tumor necrosis factor receptor 2 signal transducers TRAF2 and c-IAP1 are components of the tumor necrosis factor receptor 1 signaling complex. *Proc. Natl. Acad. Sci. USA* **93,** 13,973–13,978.
15. Rothe, M., Pan, M. G., Henzel, W. J., Ayres, T. M., and Goeddel, D. V. (1995) The TNFR2-TRAF signaling complex contains two novel proteins related to baculoviral inhibitor of apoptosis proteins. *Cell* **83,** 1243–1252.
16. Duan, H. and Dixit, V. M. (1997) RAIDD is a new "death" adaptor molecule. *Nature* **385,** 86–89.
17. Lee, S. Y., Lee, S. Y., and Choi, Y. (1997) TRAF-interacting protein (TRIP): a novel component of the tumor necrosis factor receptor (TNFR)- and CD30-TRAF signaling complexes that inhibits TRAF2-mediated NF-kappaB activation. *J. Exp. Med.* **185,** 1275–1285.
18. Stanger, B. Z., Leder, P., Lee, T. H., Kim, E., and Seed, B. (1995) RIP: a novel protein containing a death domain that interacts with Fas/APO1 (CD95) in yeast and causes cell death. *Cell* **81,** 513–523.
19. Hsu, H., Huang, J., Shu, H. B., Baichwal, V., and Goeddel, D. V. (1996) TNF-dependent recruitment of the protein kinase RIP to the TNF receptor-1 signaling complex. *Immunity* **4,** 387–396.

20. Kelliher, M. A., Grimm, S., Ishida, Y., Kuo, F., Stanger, B. Z., and Leder, P. (1998) The death domain kinase RIP mediates the TNF-induced NF-kappaB signal. *Immunity* **8,** 297–303.
21. Devin, A., Cook, A., Lin, Y., Rodriguez, Y., Kelliher, M., and Liu, Z. (2000) The distinct roles of TRAF2 and RIP in IKK activation by TNF-R1: TRAF2 recruits IKK to TNF-R1 while RIP mediates IKK activation. *Immunity* **12,** 419–429.
22. Muzio, M., Chinnaiyan, A. M., Kischkel, F. C., O'Rourke, K., Shevchenko, A., Ni, J., et al. (1996) FLICE, a novel FADD-homologous ICE/CED-3-like protease, is recruited to the CD95 (Fas/APO-1) death—inducing signaling complex. *Cell* **85,** 817–827.
23. Boldin, M. P., Goncharov, T. M., Goltsev, Y. V., and Wallach, D. (1996) Involvement of MACH, a novel MORT1/FADD-interacting protease, in Fas/APO-1- and TNF receptor-induced cell death. *Cell* **85,** 803–815.
24. Vincenz, C. and Dixit, V. M. (1997) Fas-associated death domain protein interleukin-1beta-converting enzyme 2 (FLICE2), an ICE/Ced-3 homologue, is proximally involved in CD95- and p55-mediated death signaling. *J. Biol. Chem.* **272,** 6578–6583.
25. Schwandner, R., Wiegmann, K., Bernardo, K., Kreder, D., and Kronke, M. (1998) TNF receptor death domain-associated proteins TRADD and FADD signal activation of acid sphingomyelinase. *J. Biol. Chem.* **273,** 5916–5922.
26. Natoli, G., Costanzo, A., Ianni, A., Templeton, D. J., Woodgett, J. R., Balsano, C., et al. (1997) Activation of SAPK/JNK by TNF receptor 1 through a noncytotoxic TRAF2-dependent pathway. *Science* **275,** 200–203.
27. Song, H. Y., Regnier, C. H., Kirschning, C. J., Goeddel, D. V., and Rothe, M. (1997) Tumor necrosis factor (TNF)-mediated kinase cascades: bifurcation of nuclear factor-kappaB and c-jun N-terminal kinase (JNK/SAPK) pathways at TNF receptor-associated factor 2. *Proc. Natl. Acad. Sci. USA* **94,** 9792–9796.
28. Lee, S. Y., Reichlin, A., Santana, A., Sokol, K. A., Nussenzweig, M. C., and Choi, Y. (1997) TRAF2 is essential for JNK but not NF-kappaB activation and regulates lymphocyte proliferation and survival. *Immunity* **7,** 703–713.
29. Karin, M., Liu, Z., and Zandi, E. (1997) AP-1 function and regulation. *Curr. Opin. Cell. Biol.* **9,** 240–246.
30. Woronicz, J. D., Gao, X., Cao, Z., Rothe, M., and Goeddel, D. V. (1997) IkappaB kinase-beta: NF-kappaB activation and complex formation with IkappaB kinase-alpha and NIK. *Science* **278,** 866–869.
31. Regnier, C. H., Song, H. Y., Gao, X., Goeddel, D. V., Cao, Z., and Rothe, M. (1997). Identification and characterization of an IkappaB kinase. *Cell* **90**, 373–383.
32. Zandi, E., Rothwarf, D. M., Delhase, M., Hayakawa, M., and Karin, M. (1997). The IkappaB kinase complex (IKK) contains two kinase subunits, IKKalpha and IKKbeta, necessary for IkappaB phosphorylation and NF-kappaB activation. *Cell* **91,** 243–252.
33. Rothwarf, D. M., Zandi, E., Natoli, G., and Karin, M. (1998) IKK-gamma is an essential regulatory subunit of the IkappaB kinase complex. *Nature* **395,** 297–300.

34. Cohen, L., Henzel, W. J., and Baeuerle, P. A. (1998) IKAP is a scaffold protein of the IkappaB kinase complex. *Nature* **395,** 292–296.
35. Zhang, S. Q., Kovalenko, A., Cantarella, G., and Wallach, D. (2000) Recruitment of the IKK signalosome to the p55 TNF receptor: RIP and A20 bind to NEMO (IKKgamma) upon receptor stimulation. *Immunity* **12,** 301–311.
36. Chen, G., Cao, P., and Goeddel, D. V. (2002) TNF-induced recruitment and activation of the IKK complex require Cdc37 and Hsp90. *Mol. Cell.* **9,** 401–410.
37. Hu, Y., Baud, V., Delhase, M., Zhang, P., Deerinck, T., Ellisman, M., et al. (1999) Abnormal morphogenesis but intact IKK activation in mice lacking the IKKalpha subunit of IkappaB kinase. *Science* **284,** 316–320.
38. Karin, M. and Ben Neriah, Y. (2000) Phosphorylation and ubiquitination: the control of NF-κB activity. *Annu. Rev. Immunol*. **18,** 621–663.
39. Ozes, O. N., Mayo, L. D., Gustin, J. A., Pfeffer, S. R., Pfeffer, L. M., and Donner, D. B. (1999) NF-kappaB activation by tumour necrosis factor requires the Akt serine-threonine kinase. *Nature* **401,** 82–85.
40. Sambrook, J., Fritsch, E. F., and Maniatis, T. *Molecular Cloning: A Laboratory Manual*, Cold Spring Harbor Laboratory, Cold Spring Harbor, New York, 1989.
41. Hecth, A. and Grunstein, M. (1999) Mapping DNA interaction sites of chromosomal proteins using immunoprecipitation and polymerase chain reaction. *Methods Enzymol.* **304,** 399–314.
42. Saccani, S., Pantano, S., and Natoli, G. (2001) Two waves of nuclear factor kB recruitment to target promoters. *J. Exp. Med.* **193,** 1351–1359.
43. Saccani, S., Pantano, S., and Natoli, G. (2002) p38-Dependent marking of inflammatory genes for increased NF-kappa B recruitment. *Nat. Immunol.* **3,** 69–75.

9

More Than One Way to Die

Methods to Determine TNF-Induced Apoptosis and Necrosis

Tom Vanden Berghe, Geertrui Denecker, Greet Brouckaert, Dmitri Vadimovisch Krysko, Katharina D'Herde, and Peter Vandenabeele

Summary

In most cellular systems tumor necrosis factor (TNF) induces apoptotic cell death. However, in some particular cell lines, such as the L929sA fibrosarcoma, TNF induces necrotic cell death. This effect is not the result of an inability to die apoptotically, because triggering of Fas in L929sAhFas cells leads to apoptosis. Moreover, TNFR-1-induced necrosis can be reverted to apoptosis when cells are pretreated with geldanamycin, an Hsp90 inhibitor. In contrast, addition of caspase-inhibitors (zVAD-fmk) prevents Fas-induced apoptosis and switches it to necrosis. These results demonstrate that depending on the cellular context, the same stimulus can induce either apoptosis or necrosis. Apoptosis and necrosis are clearly distinguished by their morphology, although in the absence of phagocytosis, the late stage of apoptosis is associated with secondary necrotic cell death, which is hard to distinguish from necrotic cell death. Necrosis is described mostly in negative terms as cell death that is characterized by the absence of apoptotic parameters, such as caspase activation, cytochrome c release, and DNA fragmentation. Here we describe a selection of techniques used to distinguish both modes of TNFR-1-induced cell death, namely apoptotic or necrotic cell death.

Key Words: Tumor necrosis factor; Fas; apoptosis; necrosis; caspases.

1. Introduction

In contrast to the overflow of reports on the molecular mechanisms of apoptotic (type I) programmed cell death (PCD), reports on the molecular mechanisms of autophagic (type II) and necrotic (type III) PCD are sparse. All three distinct types of cell death have been observed in the developing embryo ***(1)***. In brief, these morphological changes include cell shrinkage and extensive chromatin condensation in type I PCD; formation of autophagic vacuoles inside

From: *Methods in Molecular Medicine, Vol. 98: Tumor Necrosis Factor*
Edited by: A. Corti and P. Ghezzi © Humana Press Inc., Totowa, NJ

the dying cell in type II PCD; and rapid loss of plasma membrane integrity and spillage of the intracellular content in type III PCD *(2)*. Depending on the stimulus and the cellular context, one distinct cell-death program will become apparent, most probably because every cell-death program is a result of self-propagating signals and of signals that suppress the other cell death programs *(3)*.

Apoptosis is morphologically characterized by membrane blebbing, shrinking of the cell and its organelles, internucleosomal degradation of DNA, and disintegration of the cell, after which the fragments are phagocytized by neighboring cells *(4,5)*. Necrosis is characterized by swelling of the cell and the organelles, and results in disruption of the cell membrane and lysis *(6,7)*. One of the cell lines intensively studied in our laboratory is the L929 fibrosarcoma cell line. In these cells, apoptotic as well as necrotic cell death can be induced. Stimulation of TNFR-1 in L929sA cells leads to necrotic cell death. This process is strongly enhanced by pretreatment with the pancaspase inhibitor zVAD-fmk or overexpression of CrmA *(8)*. In L929sAhFas cells transfected with human Fas, the apoptotic cell-death pathway can be induced by clustering of Fas with agonistic anti-Fas antibodies. This apoptotic cell-death process can be reverted to necrosis by inhibiting caspase activity *(9)*.

The signal transduction pathways of TNFR-1- and Fas-mediated apoptosis have been extensively studied *(10)*. Triggering of TNFR-1 and Fas leads to a FADD-mediated recruitment and activation of caspase-8. The downstream executioner caspase-3 is activated directly by caspase-8, which results in so-called type I apoptotic cell death *(11)*. In the case of type II apoptotic cell death, caspase-3 activation is propagated by a mitochondrial loop. In this latter case the mitochondrial cytochrome c contributes to the activation of caspase-3 through the formation of the apoptosome complex leading to the activation of caspase-9 and caspase-3 *(12)*. In both type I and type II apoptotic cell-death pathways there is release of cytochrome c, but in the former pathway it is not required for the activation of caspase-3, while in the latter pathway it is. Type I apoptotic cell death is not sensitive to Bcl-2 overexpression, while type II is *(11)*. A molecular link connecting the death-receptor-mediated activation of caspase-8 with the release of mitochondrial factors is provided by the caspase-8-mediated cleavage of Bid *(13)*. The C-terminal part of Bid translocates to the mitochondria, where it induces release of cytochrome c *(14)* and other mitochondrial factors, such as endonuclease G, Smac/DIABLO, and the serine protease Omi/HtrA2 *(15)*. These mitochondrial factors contribute in different ways to the activation of the downstream executioner caspases *(16)*, eventually leading to the cleavage of different substrates and causing the typical morphological and biochemical features of apoptotic cell death *(17)*.

As mentioned above, one way to induce caspase-independent necrotic cell death is to treat cells with an apoptotic stimulus in the presence of caspase

inhibitors ***(9)***. A. Kawahara and collaborators ***(18)*** showed that enforced dimerization of FADD in Jurkat cells treated with zVAD-fmk or in Jurkat cells deficient for caspase-8 resulted in a necrotic cell death, indicating that FADD may also function as an adapter to necrotic cell death. N. Holler and colleagues ***(19)*** demonstrated that necrotic cell death induced by FasL in the presence of caspase inhibitors is absent in Jurkat cells deficient for RIP, suggesting a role for the latter as adapter in necrotic cell death. Moreover, pretreatment of wild-type Jurkat cells with geldanamycin (GA), an inhibitor of Hsp90, protects these cells from FasL-mediated caspase-independent necrotic cell death in the presence of zVAD-fmk ***(19)***. Pretreatment of cells with GA results in the down modulation of RIP, confirming its possible role in necrotic cell death. We demonstrated that in L929 cells TNFR-1-induced necrosis switches to apoptosis by pretreatment with Hsp90 inhibitors ***(20)***. We conclude that necrotic cell death is also governed by defined signal transduction pathways leading to mitochondrial production of reactive oxygen radicals ***(6)*** and the release of lysosomal cathepsins (Festjens, N., et al., in preparation). Remarkably, both types of cell death are interchangeable depending on the cellular constellation of the L929sA cells: Anti-Fas-induced apoptosis is reverted to necrosis in the presence of caspase inhibitors ***(9)***, while TNFR-1-induced necrosis is reverted to apoptosis in the presence of Hsp90 inhibitors ***(20)***.

The problem with the detection of necrotic cell death is that other than the distinct morphology, no distinct biochemical parameter has been identified that unambiguously and positively differentiates necrotic from apoptotic death. Even the morphological evaluation of dying cells can be misleading, because apoptotic cells in the absence of phagocytosis proceed to a stage called secondary necrosis. Secondary necrotic cells resemble the necrotic ones, but they have gone through an apoptotic stage; therefore, it is generally advisable in cell-death research to perform time-kinetics experiments of the cell-death parameters. Necrotic cell death is described mostly in negative terms as cell death that is characterized by the absence of apoptotic parameters, such as caspase activation, cytochrome c release, and DNA fragmentation. Here we describe a selection of techniques used to distinguish both modes of TNFR-1-induced cell death, namely apoptotic or necrotic cell death.

2. Materials

1. Recombinant human TNF: produced in *Escherichia coli* and purified to at least 99% homogeneity. Specific biological activity 2.3×10^7 IU/mg as determined in a standardized cytotoxicity assay on L929sA cells.
2. Agonistic anti-Fas antibody (BioCheck GmbH): prepared as a 500-μg/mL stock solution; use at 250 ng/mL.
3. Geldanamycin (Sigma): prepared as a 1 m*M* stock solution in DMSO; use at 1 μ*M*.
4. Propidium iodide (Sigma): prepared as a 3 m*M* stock solution in PBS; use at 30 μ*M*.

5. Annexin V-binding buffer: 10 m*M* HEPES NaOH, pH 7.4, 150 m*M* NaCl, 5 m*M* KCl, 1 m*M* $MgCl_2$, 1.8 m*M* $CaCl_2$.
6. Annexin V-fluorescein isothiocyanate (FITC, Molecular Probes): use at 1 μg/mL.
7. Acridine orange (Sigma): prepared as a 10 mg/mL stock solution; use at 5 μg/mL.
8. PBS: 8 g/L NaCl, 0.2 g/L KCl, 2.89 g/L $Na_2HPO_4 \cdot 12H_2O$, 0.2 g/L KH_2PO_4.
9. Caspase lysis buffer: 1% NP40, 10 m*M* Tris-HCl, pH 7.4, 200 m*M* NaCl, 5 m*M* EDTA, 10% glycerol, 1 m*M* PMSF, 0.3 m*M* aprotinin, 1 m*M* leupeptin.
10. Cell-free system buffer (CFS-buffer): 10 m*M* HEPES NaOH, pH 7.4, 220 m*M* mannitol, 68 m*M* sucrose, 2 m*M* $MgCl_2$, 2 m*M* NaCl, 2.5 m*M* KH_2PO_4, 0.5 m*M* EGTA, 0.5 m*M* sodium pyruvate, 0.5 m*M* L-glutamine.
11. Antibodies: anti-cytochrome oxidase subunit IV (COX) (Molecular Probes), anti-cytochrome c (Pharmingen), anti-Bid (R&D Systems), anti-caspase-2 (gift from Dr. Sharad Kumar, Adelaide, Australia), anti-human caspase-3 (BioSource), anti-human caspase-6, -7, and -9 (StressGen Biotechnologies Corp.), antihuman caspase-8 (clone 12F5, BioSource), antimouse caspase-8 (Santa Cruz), antimouse caspase-9 (Cell Signaling Technology). Rabbit polyclonal antibodies raised against recombinant murine caspase-3, -6, and -7 were prepared at the Centre d'Economie Rurale (Laboratoire d'Hormonologie Animale, Marloie, Belgium). HRP-coupled secondary antibodies were obtained from Amersham Life Science (Amersham).
12. 5X LaemmLi buffer: 312.5 m*M* Tris-HCl, pH 6.8, 10% SDS, 50% glycerol, 20% β-mercaptoethanol.
13. Cathepsin and calpain extraction buffer: 20 m*M* HEPES NaOH, pH 7.5, 0.02% digitonin, 250 m*M* sucrose, 10 m*M* KCl, 1.5 m*M* $MgCl_2$, 1 m*M* EDTA, 1 m*M* EGTA, 1 m*M* pefablock (Boehringer-Mannheim).
14. Cathepsin reaction buffer: 50 m*M* sodium acetate, pH 6.0, 4 m*M* EDTA, 8 m*M* DTT, 1 m*M* pefablock (Boehringer-Mannheim).
15. Cathepsin L reaction buffer: 4*M* urea, 20 m*M* sodium acetate, pH 5.0, 4 m*M* EDTA, 8 m*M* DTT, 1 m*M* pefablock.
16. Calpain reaction buffer: 50 m*M* Tris-HCl, pH 7.5, 8 m*M* DTT.
17. Caspase fluorogenic substrates: Ac-DEVD-AMC, Ac-LEHD-AMC, Ac-YVAD-AMC, Ac-IETD-AMC, and Ac-WEHD-AMC (Peptide Institute, Osaka, Japan) prepared as 100 m*M* stock solution in DMSO; use at 50 μ*M*.
18. Cathepsin and calpain fluorogenic substrates: zRR-AMC (Calbiochem), zFR-AFC (Enzyme Systems Products) and succinyl-LLVY-AMC (Bachem) prepared as 10 m*M* stock solutions in DMSO; use at 50 μ*M*.
19. Transmission electron microscopic fixation buffer (TEM fixation buffer): 0.1 *M* sodium cacodylate, pH 7.4, 2% glutaraldehyde, 1 m*M* $CaCl_2$.
20. 3-(4,5-dimethylthiazol-2-yl)-2,5-diphenyltetrazolium bromide (MTT): prepared as a 5 mg/mL stock solution in PBS; use at 500 μg/mL.
21. SDS-HCl buffer: 10% SDS, 0.01 *N* HCl.

3. Methods

The methods described below outline a variety of techniques that have been used to distinguish between apoptotic and necrotic cell death in the same cellu-

lar context. These techniques rely on specific morphological and biochemical changes associated with these two processes. As an example, we will use the L929sA fibrosarcoma cell line. In these cells, apoptotic as well as necrotic cell death can be induced. Stimulation of TNFR-1 in L929sA cells leads to necrotic cell death. When the cells are pretreated with geldanamycin (GA) prior to exposure to TNF, the cells die in an apoptotic way ***(20)***. In L929sA cells transfected with human Fas (L929sAhFas), the apoptotic cell-death pathway is induced by clustering of Fas with agonistic anti-Fas antibodies ***(21)***. This apoptotic cell-death process is reverted to necrosis by inhibiting caspase activity ***(9)***. Thus, both death receptors TNFR-1 and Fas can induce apoptotic and necrotic cell death, depending on the cellular constitution.

3.1. The Use of Transmission Electron Microscopy to Study Apoptotic and Necrotic Cells

Transmission electron microscopic (TEM) analysis has been considered a "golden standard" in the field of cell-death research. Using Fourier methods, it provides a two- and three-dimensional image of the inner cell and thereby allows the understanding of biological structure–function relationships at (sub)cellular and molecular levels ***(22,23)***. Compared to light microscopy, TEM is time consuming and requires more expensive equipment, but it offers much higher resolving power (0.1–0.4 nm). For that reason, TEM provides much more detailed information about cellular morphology and is therefore the most accurate method for distinguishing apoptosis and necrosis in cell cultures. Preparation of dying cells for electron microscopy may be difficult because dying cells typically detach from their substrate, and spinning down these floating cells may cause damage to their original morphology. We have circumvented this problem by using macrophages to capture dying apoptotic and necrotic cells and in this way attaching them to the bottom of the tissue culture plate while they are being phagocytized.

1. Seed macrophages in adherent 6-well plates at 5×10^5 cells per well and target cells in uncoated 6-well suspension plates at 5×10^5 cells per well (*see* **Note 1**).
2. Induce target cells (e.g., L929sAhFas) to undergo apoptosis with, for example, agonistic anti-Fas antibody (250 ng/mL, for at least 1 h), or necrosis with, for example, hTNF (10,000 IU/mL, for at least 7 h) and collect them for co-incubation with the macrophages. The chosen time points depend on the kinetics of cell death.
3. Coculture macrophages and target cells (in a 1:1 ratio) at 37°C, 5% CO_2, for at least 1 h.
4. Fix cocultures of macrophages and target cells in the 6-well plate by immersion in TEM fixation buffer overnight at 4°C.
5. Rinse 3X for 5 min in 0.1*M* sodium cacodylate containing 7.5% w/v sucrose.

6. Postfix in 1% w/v OsO_4 in the same buffer (without sucrose) overnight at 4°C.
7. Rinse 3X for 5 min in 100 m*M* sodium cacodylate containing 7.5% w/v sucrose.
8. Dehydrate in a graded series of ethanol: 50% for 15 min, 70% for 20 min, 90% for 30 min, and 100% for 90 min.
9. Infiltrate with 100% ethanol: LX-112 resin (Ladd, Burlington, VT) (1:1 for 30 min, 1:2 for 30 min, and 100% LX-112 resin for 120 min).
10. Polymerize for at least 48 h at 60°C.
11. Break off the plastic of the polymerized block and saw into pieces to fit the ultramicrotome holders. Remove any remaining plastic bits from the cutting surface.
12. Make ultrathin sections of 60 nm with a diamond knife and mount on 100-mesh formvar-coated copper grids.
13. Stain with uranyl acetate (7.5% in double-distilled water, 1 drop per grid for 20 min) and Reynold's lead citrate (1 drop per grid for 10 min).
14. Examine the sections by TEM.

The earliest classic ultrastructural changes detectable in apoptosis are the condensation of chromatin to form uniformly dense masses that lay against the nuclear envelope ***(24)*** and the persistence of nucleolar structure until the very late stages ***(25)***. Further features displayed by most apoptotic cells include loss of specialized surface structures, such as microvilli and cell–cell contacts. The cell volume decreases and the cell density increases due to the marked condensation of cytoplasm. Membrane-bound apoptotic bodies of varying size are formed that contain well-preserved but compacted cytoplasmic organelles and/or nuclear fragments ***(24,26)*** (**Fig. 1B**). In contrast, no cell fragmentation appears in the course of necrosis, but a general cell hydration occurs, causing swelling of the organelles (endoplasmic reticulum, mitochondria). The cytoplasm becomes increasingly translucent and contains a mottled-looking nucleus due to condensation of nuclear chromatin in ill-defined masses. Finally, there is loss of plasma membrane integrity, and cell contents starts to leak out provoking inflammation (**Fig. 1C**).

3.2. The Use of Flow Fluorocytometry (FACS) to Study Apoptotic or Necrotic Cell Death

In this section, we will describe the use of flow fluorocytometry to distinguish between apoptotic and necrotic cell death by analyzing cell membrane permeability, cell morphology, phosphatidylserine (PS) exposure, DNA fragmentation, and lysosomal destabilization (*see* **Note 2**). For the different protocols described below, we first describe incubation and stimulation conditions.

1. Seed cells at 1.5×10^5 cells/mL per well the day before analysis in *uncoated* 24-well suspension plates, to avoid attachment of the cells to the bottom (*see* **Note 3**).
2. The next day, stimulate the cells with TNF (10,000 IU/mL), geldanamycin (1 μ*M*,

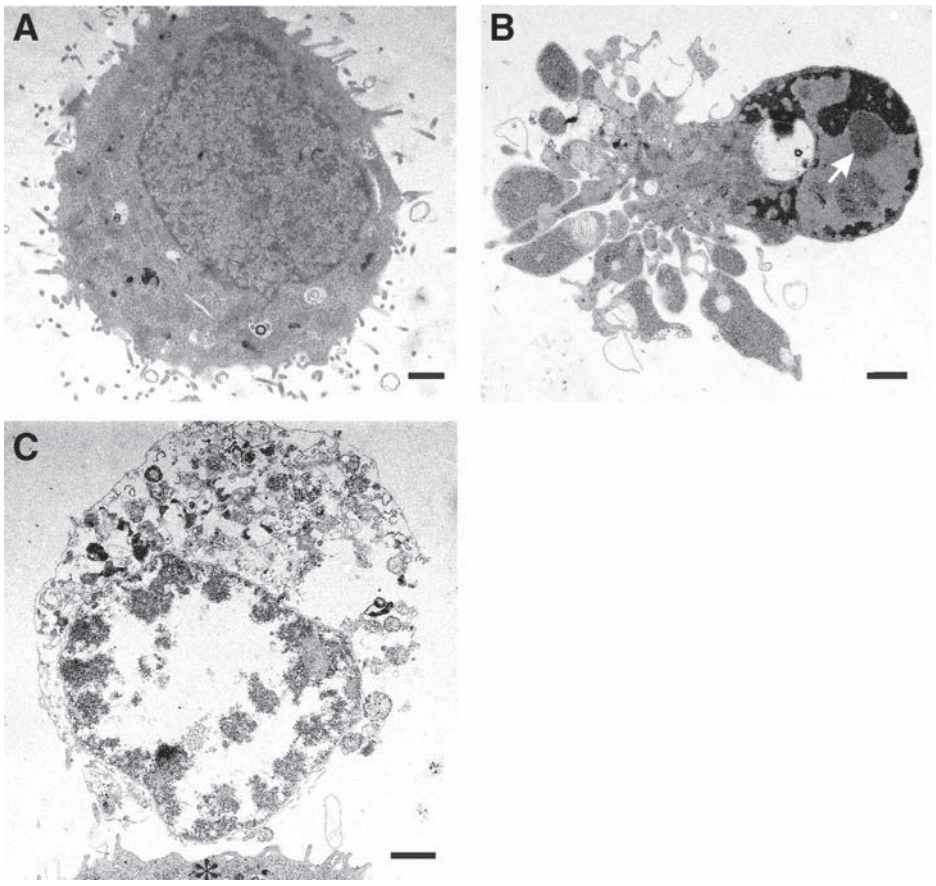

Fig. 1. Ultrastructural features of apoptotic and necrotic mouse L929sAhFas fibrosarcoma cells. Unstimulated cells **(A)** and cells exposed either to agonistic anti-Fas for 1 h **(B)** or to hTNF for 18 h **(C)**. **(A)** The cell shows microvilli protruding from the entire surface, a smoothly outlined nucleus with chromatin in the form of heterochromatin, and well-preserved cytoplasmic organelles. **(B)** Apoptotic cell with sharply delineated masses of condensed chromatin, convolution of the cellular surface, and formation of apoptotic bodies. Note the nucleolus (arrow) present near a cup-shaped chromatin margination. **(C)** Necrotic cell in close vicinity to a macrophage (asterisk), showing ill-defined edges of the clumps of compacted chromatin, swollen mitochondria with matrix densities, dissolution of membranes, and loss of plasma membrane integrity. Scale, bars: 1 μm.

18 h pretreatment) plus TNF (10,000 IU/mL), or anti-Fas (250 ng/mL), and analyze the cell samples from the suspension cultures at regular time intervals on a flow fluorocytometer (*see* **Note 4**).

3.2.1. Analysis of Cell Morphology vs Cell Permeability

Many studies report that apoptotic dying cells are smaller and denser than their living counterparts ***(4,27)***. Initially, the membrane of the cell starts to form blebs, which become separated from the main cell body. This phenomenon is followed by the shrinkage of the entire nucleus or, in other cases, budding outward of chromatin into smaller apoptotic bodies ***(28)***. These changes are accurately detected in the majority of cells by their light-scattering properties as measured by flow fluorocytometry. The forward-scatter reflects cell size, while the sideward-scatter reveals the degree of granularity of the cell. The protocol described below uses flow fluorocytometry to access changes in cell size and granularity as well as the loss of cell membrane integrity measured by propidium iodide (PI) uptake (*see* **Note 5**).

1. Transfer 300 µL of cells in suspension from the 24-well suspension plate to a 5-mL polypropylene round-bottom tube, and add 3 µL PI from a 3-m*M* stock solution. Keep cells on ice for 3–10 min (*see* **Note 6**).
2. Set up the flow fluorocytometer for forward-scatter and sideward-scatter both at linear scale on a dot plot to determine cell size and granularity (**Fig. 1**). Create a histogram in FL3 to detect PI uptake at 610 nm, e.g., on a FACS Calibur flow fluorocytometer (Becton Dickinson) equipped with a water-cooled argon-ion laser at 488 nm (*see* **Note 7**). To clearly see the dead cells on the dot plot, one can gate PI positive cells in red, for example, in the FL3 histogram.
3. After measurement, the tubes with the remaining suspension cells (at least 150 µL) or freshly prepared tubes (300 µL, *see* **step 1**) can be used to determine the percentage of cells with hypoploid DNA (*see* **Subheading 3.2.2.**).
4. The region of analysis is gated (R1) (*see* **Note 8**). At time point zero, the viable cell population is detected within the region of analysis; these cells are PI negative. In the case of TNFR-1-induced apoptosis in L929 cells (GA/TNF, **Fig. 2A-D**), the membrane of the cells starts to bleb at 2 h, causing increased diffraction of the laser beam, revealed by spreading of the dots (**Fig. 2B**). The release of apoptotic particles is detected by the occurrence of a population of small-sized PI-negative dots (negative because of the absence of DNA) in the lower-left corner of the dot plot (**Fig. 2B**). The condensation of the nucleus, shrinkage of the cells, and formation of DNA-containing apoptotic bodies is visualized by the population of PI-positive gray dots, appearing in the lower-left corner on the dot plot (**Fig. 2C**). The population in **Fig. 2D** illustrates the end stage of the apoptotic process, namely secondary necrosis. This population clearly colocalizes with the necrotic cell death population induced by TNF (**Fig. 2H**).

3.2.2. Analysis of DNA Fragmentation

DNA fragmentation is a hallmark of apoptosis and involves the formation of high molecular weight (>50 kbp) and nucleosome-sized (200 bp) DNA fragments ***(29,30)***. An easy and quantitative way to analyze DNA fragmentation is

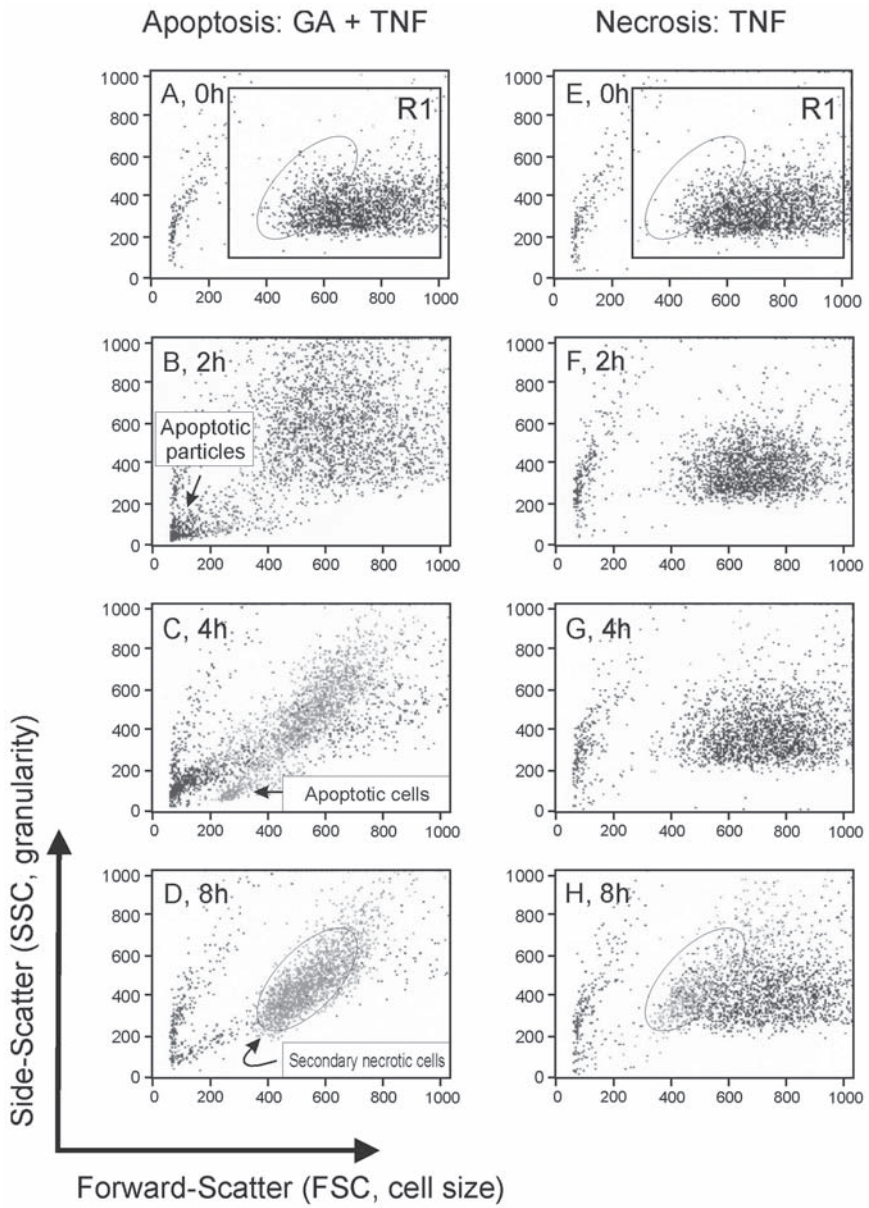

Fig. 2. Analysis of cell morphology versus cell permeability by flow fluorocytometry. Cells were analyzed by flow fluorocytometry for changes in cell size (side-scatter) and granularity (forward-scatter) as well as the loss of membrane integrity by propidium iodide uptake (FL3). L929 fibrosarcoma cells were pretreated for 18 h with or without geldanamycine (GA), followed by treatment with human TNF, as indicated. The differential changes in morphology between apoptotic and necrotic cells can be followed in time on the dot plots (side- vs forward-scatter). The appearance of PI-positive cells in time is indicated in gray on the dot plots.

by adding PI to the dying cell population and applying one freeze–thaw cycle to permeabilize cells and cell fragments. PI intercalates in the DNA, and the size of DNA fragments appears as a hypoploid DNA histogram.

1. Transfer 300 µL of cells in suspension from the 24-well suspension plate to a 5-mL polypropylene round-bottom tube, and add 3 µL PI from a 3 m*M* stock solution.
2. Subject the tubes to one freeze–thaw cycle by putting them shortly on liquid nitrogen. As a result of the freeze–thaw cycle, cells are permeabilized and become PI positive. Alternatively, use the remaining suspension cells (at least 150 µL) that were used for measurement of PI uptake in **Subheading 3.2.1**.
3. Analyze samples after thawing (*see* **Note 9**). Use the same experimental set up as described in **Subheading 3.2.1**.

Viable nondividing cells exhibit a clear diploid DNA peak (2n, G1), whereas dividing cells give rise to a tetraploid peak (4n, G2). A nonsynchronized population of cells shows a typical biphasic peak of 2n (G1) and 4n (G2) cells. During apoptosis, the DNA is fragmented and is partially lost as a result of the formation of apoptotic bodies. Therefore, apoptotic cells typically show a lower DNA fluorescence pattern as compared to necrotic cells that maintain their entire DNA content in the nucleus. Hence apoptotic cells with fragmented DNA appear as cells with a hypoploid DNA content and are represented as a hypoploid "sub-G1" peak. An example of a hypoploid DNA pattern as a result of TNFR-1-induced apoptosis in the presence of GA is shown in **Fig. 3B**. In TNFR-1-induced necrosis, this typically apoptotic event is absent, as illustrated in **Fig. 3D**.

3.2.3. Analysis of PS Exposure vs Cell Permeability

Plasma membranes of viable cells exhibit significant phospholipid asymmetry, with most of the phosphatidylserine (PS) residing on the inner, cytoplasmic membrane leaflet. PS is kept in the inner membrane by the rapid inward-moving action of an ATP-dependent phospholipid transporter, the aminophospholipid translocase. Early in the apoptotic process, this translocase is inhibited, while another, bidirectional aminophospholipid transporter, called scramblase, becomes activated ***(31)***. As a result, phospholipid asymmetry is lost, and cells increasingly expose PS on their outer membrane leaflet ***(32)***. Annexin V, a Ca^{2+}-dependent phospholipid-binding protein, preferentially binds to negatively charged phospholipids like phosphatidylserine and therefore is a useful tool to detect cells at the early stages of the apoptotic process ***(33)***. Using FITC-conjugated Annexin V in combination with PI uptake, the differential appearance between PS exposure and the loss of membrane integrity allows one to distinguish between apoptotic and necrotic cell death ***(6)*** (*see* **Note 10**). Apoptotic cells are characterized by a lag period between PS positivity and PI positivity. In necrotic cell death, both events coincide.

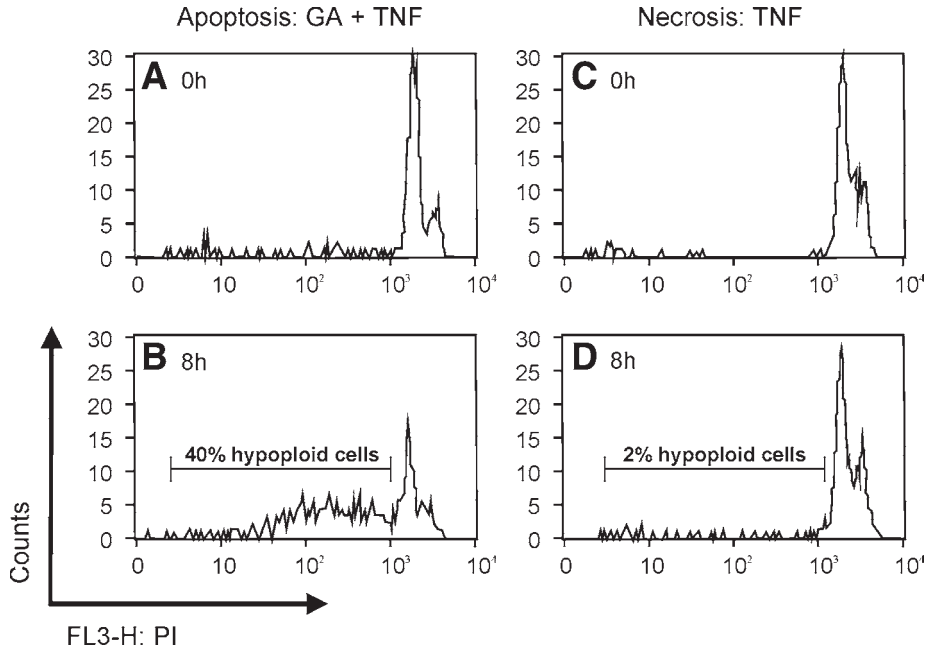

Fig. 3. Analysis of DNA fragmentation by flow fluorocytometry. Cells were analyzed by flow fluorocytometry for the detection of DNA hypoploidy. L929 fibrosarcoma cells were pretreated for 18 h with or without geldanamycin (GA), followed by treatment with human TNF, as indicated. The percentage of cells containing hypoploid DNA is the population of cells with lower fluorescence than the G1, 2n peak.

1. Transfer 1.5–3 × 10^5 cells to an Eppendorf tube, centrifuge the cells for 5 min at 250*g* at 4°C, and resuspend in 1 mL ice-cold Annexin V-binding buffer (*see* **Notes 6** and **11**).
2. Centrifuge the cells for 5 min at 250*g* at 4°C and resuspend in 300 µL of Annexin V-binding buffer containing 1 µg/mL of Annexin V-FITC. Incubate for 5 min on ice and protect from light.
3. Add 3 µL from a 3-m*M* PI stock solution to the same 300-µL cell suspension for 3–10 min for analysis.
4. Analyze samples by setting up the flow cytometer in the same way as described in **Subheading 3.2.1**. Create an extra dot plot showing Annexin V-FITC (FL1) versus PI (FL3), and set up quadrants dividing Annexin V-positive, Annexin V-negative, PI-positive, and PI-negative populations (*see* **Note 12**).

Membrane changes leading to PS exposure occur rapidly in TNFR-1-induced apoptotic cell death. In the presence of GA, the cell population shifts from the lower-left quadrant (PI-negative and Annexin V-negative cells, **Fig. 4A**) to the lower-right quadrant (PI-negative and Annexin V-positive cells, **Fig. 4B**). After PS exposure to the outer leaflet of the cell membrane, cells start

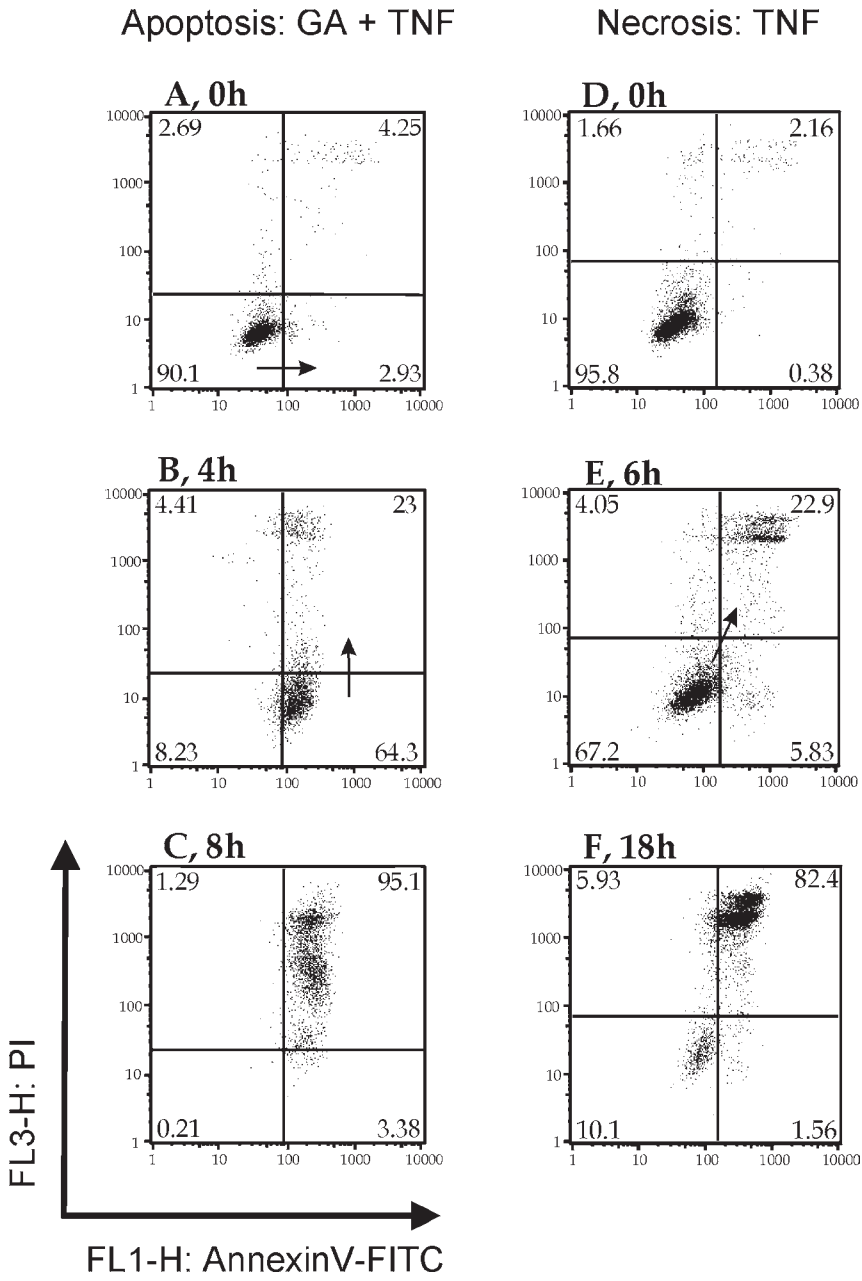

Fig. 4. Analysis of PS exposure versus cell permeability by flow fluorocytometry. Cells were analyzed by flow fluorocytometry for loss of membrane integrity by PI uptake and translocation of phophatidylserine to the outer leaflet of the plasma membrane by staining with Annexin V-FITC. L929 fibrosarcoma cells were pretreated for 18 h with or without geldanamycin (GA), followed by treatment with human TNF, as indicated.

losing their membrane integrity, and the population shifts to the upper-right quadrant (PI-positive and Annexin V-positive cells, **Fig. 4C**). During TNFR-1-induced necrotic cell death, PS exposure coincides with the permeabilization of the outer cell membrane. Consequently, cells immediately move from the lower-left quadrant (PI-negative and Annexin V-negative cells, **Fig. 4D**) to the upper-right quadrant of the dot plot (PI-positive and Annexin V-positive cells, **Fig. 4E,F**) without passing through the intermediate PI-negative and Annexin V-positive stage.

3.2.4. Analysis of Lysosomal Destabilization

During the last few years several reports have reprised the old concept that lysosomes might be involved in cell death, both by necrosis as well as by apoptosis ***(34,35)***. The role of lysosomes in cell death is a topic of increasing interest; therefore, we would like to describe a method to measure lysosomal stability. This observation is performed by following the uptake of the weak base acridine orange (AO) ***(36)***. Due to proton trapping, this vital dye mainly accumulates in the acidic vacuolar apparatus, preferentially in secondary lysosomes (*see* **Note 13**).

1. Stain the cells in the 24-well suspension plate by adding 5 µL of a 10-mg/mL stock solution of AO to 1.5–3 × 10^5 cells/mL, and incubate at 37°C for 15 min.
2. Wash with 1 mL PBS, centrifuge at 250*g* for 5 min and resuspend in PBS.
3. Set up the flow fluorocytometer as described in **Subheading 3.2.1**. Create a histogram in FL3 to detect impairment of AO uptake. To clearly see the cells with destabilized lysosomes on the dot plot, one can gate AO-negative cells in the FL3 histogram (*see* **Note 13**).

Exciting AO with green light results in red fluorescence at high (lysosomal) concentrations. This effect is revealed on a histogram by the peak of cells with still intact lysosomes (**Fig. 5A**). During TNFR-1-induced necrosis, the population of cells that have lost the capacity to accumulate AO in the lysosomes increases (**Fig. 5B–D**). The percentage of cells with low intensity of red fluorescence is used as a marker for the extent of lysosomal destabilization (impairment of AO uptake). At the end stage, the lysosomes of all cells have lost the capacity to retain AO (**Fig. 5D**).

3.3. Analysis of the Apoptotic Signal Transduction Cascade by Western Blot

In this section we will describe the use of Western blot to detect the activation of caspases (*see* **Note 14**), the cleavage of Bid to its truncated pro-apoptotic form (tBid), and finally by the release of cytochrome c from the mitochondria. These events are all absent in TNFR-1-induced necrotic cell death ***(6)***.

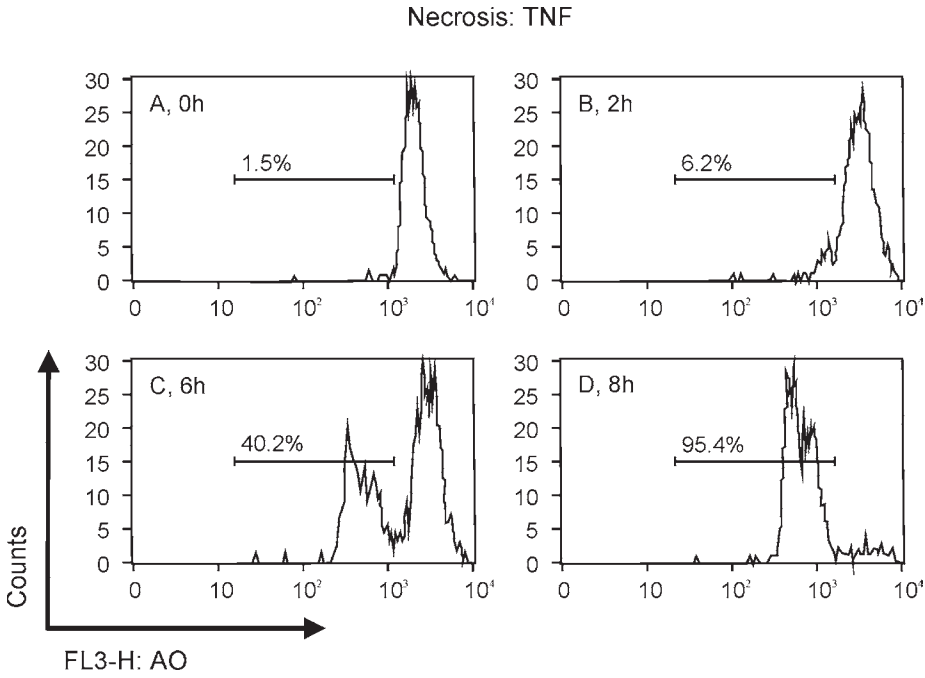

Fig. 5. Analysis of lysosomal destabilization by flow fluorocytometry. Cells were analyzed by flow fluorocytometry for the detection of lysosomal destabilization. L929 fibrosarcoma cells were treated with human TNF over time, as indicated. The percentage of cells with impaired uptake of acridine orange (AO) is gated.

1. Day 0: seed 2×10^5 cells/mL per well in coated 6-well tissue culture plates.
2. Day 1: stimulate the cells and collect the cell samples at regular time intervals in a 1.5-mL Eppendorf tube by scraping them.
3. Centrifuge the cells with medium for 5 min at 250*g*, aspirate the medium, and wash cells with 1 mL of cold PBS.
4. For analysis of activation of caspases follow **Subheading 3.3.1**. For analysis of Bid-cleavage and cytochrome c release, follow **Subheading 3.3.2**. Caspase, cathepsin, and calpain activation can also be analyzed by use of fluorogenic substrates (*see* **Subheadings 3.4.1.** and **3.4.2.**).

3.3.1. Analysis of Activation of Caspases

Caspases are a family of cysteine aspartate-specific proteases. They are synthesized as zymogens consisting of a prodomain of variable length, followed by a p20 and a p10 unit that contain the residues essential for substrate recognition and catalytic activity. They are activated either (1) via proximity-induced auto-proteolysis by interacting with a platform of adaptor proteins through a protein interaction motif in the prodomain (DED, death effector domain; or

CARD, caspase recruitment domain), or (2) by cleavage via upstream proteases in an intracellular cascade. The net result of these proteolytic activities is the separation of the prodomain from the p20 and p10 subunits, which form an active heterotetramer ***(17)***.

1. Follow the steps of **Subheading 3.3**.
2. Centrifuge the cells for 5 min at 250*g*, aspirate PBS, and lyse the cells in 150 µL cold caspase lysis buffer (*see* **Note 6**).
3. Remove cell debris by centrifuging the lysate (10 min at 20,800*g* at 4°C) and transfer the remaining cytosol to another Eppendorf tube. Add 1:5 volume of 5X LaemmLi buffer to the cell lysate and boil for 5–10 min at 98°C.
4. Load equal volumes per lane on 12.5% SDS-polyacrylamide gels (*see* **Note 15**). After separation, transfer to a nitrocellulose membrane and detect the different caspases with the appropriate antibodies. Reveal with chemiluminescence reagent plus (Nycomed Amersham plc).

Proteolytic activation of procaspases leads to the appearance of a typical p20 and p10 subunit (*see* **Note 16**). **Figure 6A** illustrates the activation of caspase-3 and -7 by the appearance of the p20 subunit in Fas-induced apoptosis (procaspase-3, black arrow; p20 subunit, white arrow). In TNFR-1-induced necrosis, p30 caspase-3 and -7 are not activated, and thus there is no appearance of a p20 subunit (**Fig. 6B**).

3.3.2. Analysis of Bid Cleavage and Cytochrome c Release

During death receptor-mediated apoptosis, the mitochondria are induced to release cytochrome c through the proteolytic activation of Bid to truncated Bid (tBid), which translocates to the mitochondria. To establish the role of the mitochondrial apoptotic pathway, one can detect the engagement of the mitochondria at the different stages: Bid proteolytic activation, tBid translocation, and cytochrome c release. In order to detect the release of cytochrome c in the cytosol, the organelle and cytosolic fraction of the cell should be separated without the spontaneous release of cytochrome c from the mitochondria due to artifacts of the organelle preparation. Therefore, a mild detergent, digitonin, is used (*see* **Note 17**).

1. Follow the steps of **Subheading 3.3**.
2. Centrifuge the cells for 5 min at 250*g*, remove PBS, and lyse in 100 µL 0.02% digitonin dissolved in cell-free system buffer (CFS-buffer); leave on ice for 1 min (*see* **Note 6**).
3. Centrifuge the lysate (10 min at 20,800*g* at 4°C) and transfer the cytosol to a separate Eppendorf tube. Add 1:5 volume of 5X LaemmLi buffer to the cytosolic lysate and 100 µL 1X LaemmLi buffer to the remaining organelle fraction and boil for 5–10 min at 98°C.
4. Load equal volumes of the organelle fraction or cytosolic cell lysate per lane on

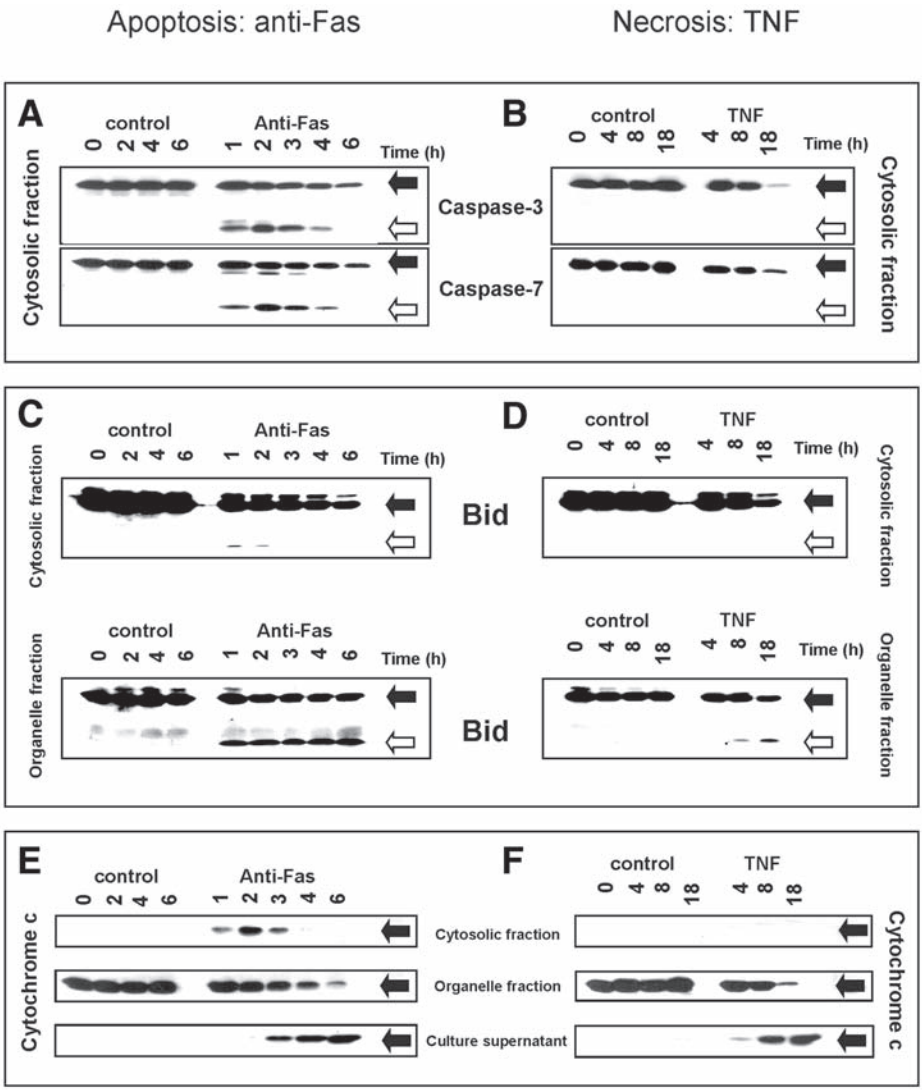

Fig. 6. Analysis of caspase activation, Bid cleavage, and cytochrome c release by Western blot. **(A)** and **(B)** Time kinetic analysis of caspase-3 and -7 activation during anti-Fas-induced apoptosis and TNFR-1-induced necrosis. Cytosolic fractions were prepared and analyzed by PAGE and Western blot. Open and solid arrows indicate processed p20 subunit and precursor procaspase, respectively. **(C)** and **(D)** Time kinetic analysis of the proteolytic activation and delocalization of Bid from the cytosol to the organelle fraction during anti-Fas-induced apoptosis and TNFR-1-induced necrosis. **(E)** and **(F)** Cellular distribution of cytochrome c in the cytosol and in the organelle fraction. Cytosolic and organelle fractions were prepared as described and were analyzed by Western blot. Solid and open arrows indicate full-length Bid and tBid, respectively.

12.5% SDS-polyacrylamide gels (*see* **Note 15**). After separation, transfer to a nitrocellulose membrane by electroblotting, and detect Bid cleavage and cytochrome c release with the appropriate antibodies or antisera. Reveal with chemiluminescence reagent plus (Nycomed Amersham plc).

Anti-Fas treatment results in an early cleavage of full-length Bid to its pro-apoptotic truncated form (tBid). Only for a short period and to a minor extent is tBid detectable in the cytosolic fraction. The vast majority of tBid becomes rapidly associated with the organelle fraction (**Fig. 6C**). Therefore, the safest way to detect the engagement of Bid one should look both at the disappearance of Bid from the cytosol and the appearance of tBid in the organelle fraction. In necrotic cells, no cleavage of p22 Bid is detectable either in the cytosol or in the organelle fraction (**Fig. 6D**). Only late in the necrotic process does Bid disappear from the cytosol due to cytosolic leakage. In addition, a small amount of tBid becomes detectable in the organelle fraction, probably because of alternative Bid cleavage by lysosomal proteases ***(37)***. The appearance of tBid in the organelle fraction during anti-Fas induced apoptosis coincides with the release of cytochrome c to the cytosol (**Fig. 6C,E**). We found that during secondary necrosis of anti-Fas-stimulated cells, cytochrome c also accumulates in the culture supernatant (**Fig. 6E**). TNFR-1-induced necrosis does not result in a detectable release of cytochrome c in the cytosol. However, in the late necrotic phase of TNF-stimulated cells, cytochrome c accumulates in the culture supernatant from the moment that cells lose their plasma membrane integrity (**Fig. 6F**).

3.4. Use of Fluorogenic Substrates to Distinguish Apoptotic or Necrotic Cell Death

To measure the actual activity of caspases instead of their proteolytic activation state, one can use fluorogenic substrates for caspases, cathepsins, or calpains. In the case of caspases, these substrates contain the minimal amino acid composition corresponding with the cleavage site of a typical substrate, coupled to 7-amino-4-methylcoumarin (AMC) or 7-amino-4-trifluoromethylcoumarin (AFC). Hydrolysis of the peptide substrate results in the release of free AMC or AFC, which are fluorescent and can be measured in a fluorometer.

3.4.1. Analysis of Caspase Activity Using Fluorogenic Substrates

The first synthetic substrates designed and used to measure and analyze caspase activities were based on the cleavage sites of the initially identified cellular protein substrates ***(17,38)***. These synthetic substrates were usually a tetrapeptide with aspartate at the position P1 (XXXD) conjugated to a fluorogenic AMC or AFC (*see* **Note 18**); for example, Ac-DEVD-AMC is derived from the caspase-3 cleavage site in poly-ADP ribosyl polymerase (PARP) and Ac-YVAD-AMC is derived from the caspase-1 cleavage site in prol-IL-1β.

1. Follow the steps of **Subheading 3.3**.
2. Centrifuge the cells for 5 min at 250*g*, aspirate PBS, and lyse the cells in 150 µL cold caspase lysis buffer (*see* **Note 19**). Add glutathione at a final concentration of 1 m*M* (*see* **Notes 6** and **20**).
3. Remove cell debris by centrifuging the lysate (10 min at 20,800*g* at 4°C) and transfer the cytosol to another Eppendorf tube ("cytosolic cell lysate").
4. Measure caspase activity by incubating 25 µg cytosolic cell lysate with 50 µ*M* of the fluorogenic substrate (e.g., Ac-DEVD-AMC) in 150 µL CFS-buffer. Add dithiothreitol (DTT) at a final concentration of 10 m*M* (*see* **Note 20**).
5. Monitor the release of fluorescent AMC for 1 h at 37°C at 2-min time intervals in a fluorometer (e.g., CytoFluor, PerSeptive Biosystems) using a filter with an excitation wavelength of 360 nm and a filter with an emission wavelength of 460 nm. Express data as the increase in fluorescence as a function of time (Δfluorescence/min) ***(6,20)***.
6. Caspase activity is only detected in apoptotic conditions.

3.4.2. Analysis of Cytosolic Cathepsin or Calpain Activity Using Fluorogenic Substrates

Several reports show an involvement of calpain activity in necrotic or caspase-independent cell death, for example, increased µ-calpain auto-proteolysis in necrotic fibers; a high Ca^{2+} requirement for necrotic cell death in *C. elegans*; and the activation of calpain I converting excitotoxic neuron death into caspase-independent cell death ***(39–41)***. Other reports show release of cathepsin B in cytosol during TNFR-1-induced apoptosis, and during necrosis or under conditions in which caspases are blocked ***(34,42)***, or show the involvement of lysosomal cathepsins in an alternative cleavage of PARP ***(43)*** and Bid ***(37)***.

1. Follow the steps of **Subheading 3.3**.
2. Centrifuge the cells for 5 min at 250*g*, aspirate PBS, and lyse the cells in 150 µL cathepsin and calpain extraction buffer; incubate cells for 5 min on ice (*see* **Note 6**).
3. Analyze the enzyme activities by adding 50 µ*M* zRR-AMC or zFR-AFC for cathepsin B and L, respectively, or 50 µ*M* succinyl-LLVY-AMC plus 2 m*M* Ca^{2+} for calpain measurements in appropriate reaction buffers: cathepsin reaction buffer, cathepsin L reaction buffer, and calpain reaction buffer, respectively.
4. Monitor the release of AFC (excitation 409 nm, emission 505 nm) or AMC (excitation 360 nm, emission 460 nm) for 1 h at 30°C at 2 min time intervals in a fluorometer (e.g., CytoFluor, PerSeptive Biosystems). Express data as the increase in fluorescence as a function of time (Δfluorescence/min).

3.5. Analysis of Cell Death on a Large Scale

In this part we describe two general and easy methods for determining the extent of cell death irrespective of the type of cell death. These methods allow

large screenings of conditions in 96-well plates, or optimization of concentrations of inhibitors or sensitizing reagents.

1. Seed cells the day before at 2×10^4 cells in 100 μL per well in 96-well plates.
2. Expose the cells to a serial dilution of TNF (horizontal dilution added to the cells in a 50 μL volume) in the absence or presence of different concentrations of inhibitor or sensitizing agent (vertical dilution added to the cells in a 50 μL volume) (*see* **Note 21**).

3.5.1. Lactate Dehydrogenase (LDH) Assay

Lactate dehydrogenase (LDH) is a cytosolic enzyme present within all mammalian cells. The intact plasma membrane is impermeable to LDH, and loss of its integrity is detectable by the release of LDH into the supernatant ***(44)***, where its enzymatic activity is measured. In vitro release of LDH from cells provides an accurate measure of cell membrane integrity and cell viability.

1. Remove 50 μL supernatant of cells under study to a 96-well plate.
2. Add 50 μL reconstituted substrate mixture (CytoTox 96™ Assay, Promega) (*see* **Note 22**).
3. Incubate for 30 min at room temperature.
4. Add 50 μL Stop solution to each well and analyze by spectrophotometry at 492 nm.
5. Results may be expressed either as optical absorbance values or as international units of enzyme (calculated from a standard curve obtained with the positive LDH control, which is provided with the system).

3.5.2. 3-(4,5-Dimethylthiazol-2-yl)-2,5-Diphenyltetrazolium Bromide (MTT) Assay

MTT is a pale yellow substrate that is cleaved by living cells to yield a dark blue formazan product, which is precipitated out as crystals. This process is catalyzed by succinate dehydrogenase complex II of the inner mitochondrial membrane, an enzyme involved in oxidative phosphorylation. The assay reflects both the number of cells as well as the activity status of the mitochondria. Damaged mitochondria in dead cells are affected in their capacity to cleave significant amounts of MTT (*see* **Note 23**). The colorimetric assay described thus measures both cytostatic as well as cytotoxic effects.

1. 18 h after stimulation add 20 μL of MTT solution to each well containing cells.
2. Incubate the plate in a CO_2 incubator at 37ºC for 4–6 h.
3. Add 80 μL of SDS-HCl buffer to each well to dissolve the formazan crystals.
4. Put the plate into the 37ºC incubator for an additional 6–8 h in order to dissolve the crystals.
5. Transfer the plate to the plate reader and measure absorbance at 595 nm (put reference filter at 655 nm).
6. The percentage of cell death (P_{cd}) is calculated using Equation 1:

$$P_{cd} = \left[1 - \frac{\left[\frac{A_{595}}{A_{655}}\right]t - \left[\frac{A_{595}}{A_{655}}\right]m}{\left[\frac{A_{595}}{A_{655}}\right]u - \left[\frac{A_{595}}{A_{655}}\right]m}\right] \times 100$$

where *t* indicates the absorbance ratio of treated cells, *u* indicates the absorbance ratio of untreated cells, and *m* indicates the absorbance ratio of the medium.

4. Notes

1. The target cells are grown in suspension plates in order to easily transfer the population of dying cells to the well of attached macrophages.
2. We will not describe the use of mitochondrial membrane-potential-sensitive dyes such as tetramethylrhodamine methyl, rhodamine123, JC-1 (Molecular Probes) or the use of dihydrorhodamine123 for measurement of oxygen radical species (ROS), because these methods do not distinguish the mode of cell death ***(45,46)***. In both cell-death pathways the membrane potential of the mitochondria drops, and the cells start producing ROS ***(6,47)***. In case of TNFR-1-induced cell death in L929 cells, it was shown that although ROS production occurs in both cell death pathways, it is only a crucial event in necrotic cell death ***(8,48)***.
3. To perform FACS analysis it is advisable to grow adherent cells in suspension as commented in **Note 1**. In this way it is possible to work faster during kinetics and avoid interfering manipulations, such as trypsin/EDTA treatment, which could lead to damage or permeabilization of the cells. Therefore, adherent cells are seeded on special uncoated suspension tissue culture plates (Sarstedt). It is important to test in advance whether the adherent cells allow growing in suspension conditions.
4. As a general rule it is important to perform time kinetics when analyzing cell-death parameters. The end stage of apoptosis, the so-called secondary necrosis, displays the same features as necrosis, i.e., loss of membrane integrity and leakage of proteins into the supernatant ***(6)***. Therefore, it is advisable to take samples at regular time intervals in order to detect the differential appearance of apoptotic or necrotic features.
5. Propidium iodide (PI) is a membrane-impermeable dye that stains fluorescent by intercalating into nucleic acid molecules. In this way PI can be used to measure the loss of cell-membrane integrity, as it enters the cell only if the cell membrane becomes permeable. When bound to nucleic acids, the absorption maximum for PI is 535 nm and the fluorescence emission maximum is 617 nm. PI can be excited with a xenon or mercury-arc lamp, or with the 488 line of an argon-ion laser. In practical terms, PI fluorescence is detected in the FL2 or FL3 channel of flow fluorocytometers. The broad emission spectrum of PI is a problem when combining it with other fluorochromes. Only fluorochromes with a clearly distinct emission spectrum or with a small emission-spectrum overlap can be used. The small overlap can be compensated for during FACS measurements.

6. Cells are kept on ice to stop further biochemical activity of the cell.
7. A typical FACS Calibur flow fluorocytometer can analyze five different parameters. Two detectors detect the light scatter: (1) forward scattered light (FSC, indicates cell size) and (2) side scattered light (SSC, indicates granularity). Three remaining photomultiplier tubes (PMTs) detect the fluorescent signals: (1) FL1 (green fluorescence; used for FITC, R123, GFP), (2) FL2 (red fluorescence; used for PI, CMTMros, PE), and (3) FL3 (far red fluorescence, used for PI, Cy-Chrome).
8. The region of analysis (R1) must be large enough that the dying cell population can also be measured. This population shifts to the left on the dot plot as compared to the living cells.
9. After the freezing procedure in liquid nitrogen, the samples can be stored indefinitely at –20°C, until analyzed.
10. With the methods presented, it is not possible to distinguish whether a positive Annexin V result during necrosis is due to extracellular PS exposure or to intracellular detection of PS, because Annexin V can also enter the cell as a consequence of loss of cell membrane integrity ***(32)***. This problem can only be solved using immunogold staining methods and transmission electron microscopy analysis. However, the PS-dependent recognition of necrotic cells by phagocytic cells strongly argues for the occurrence of PS at the surface of necrotic dying cells (Brouckaert G, et al., in press).
11. The staining protocol absolutely must be carried out in Annexin V-binding buffer because the binding of this protein to the phosphatidylserine is calcium dependent.
12. Include also single-stained cells in your experiment, i.e., cells stained only with Annexin V-FITC (no PI added) and cells stained only with PI (no Annexin V-FITC added), to set up compensation and quadrant markers. The absorption maximum for FITC is 494 nm and the fluorescence emission maximum is 518 nm.
13. The absorption maximum for AO is 489 nm and the fluorescence emission maximum is 520 nm. AO is also a metachromatic fluorophore. When excited by blue light (440–470 nm) it shows red fluorescence at high (lysosomal) concentrations and green fluorescence at low (nuclear and cytosolic) concentrations. If, however, green excitation light (515–560 nm) is used, only concentrated (lysosomal) AO is observed by its red or orange fluorescence. Qualitative analysis is done by fluorescence or confocal microscopy. For this purpose cells need to be seeded on glass coverslips.
14. In addition to the activation pattern of different caspases, the cleavage pattern of a variety of substrates can be detected, such as PARP and ICAD ***(17)***. Alternatively, caspase activation can be measured using fluorogenic caspase substrates (see **Subheading 3.4.1.**).
15. Different cell samples are lysed and processed in a standardized way with equal volumes, which should reflect the identical input of the cells at the beginning of the experimental setup. One should not correct for protein content because at later time points during the cell death process cells start to leak cytosolic proteins into the supernatant ***(6)***.

16. Depending on the antibody used, all proteolytic fragments or only one of them can be detected. Antibodies are also available that specifically recognize the activated form of caspases (PharMingen). These antibodies can also be used in FACS analysis to detect caspase activity in cells; alternatively, cell-permeable fluorogenic substrates can be used ***(49)***. These antibodies also allow immunodetection of active caspase in immunohistochemistry ***(50)***.
17. In L929 cells, 0.02% digitonin is capable of permeabilizing the plasma membrane, but it leaves the mitochondria and lysosomes intact. The concentration of digitonin used as well as the required lysis period is cell-type dependent. Therefore, a series of different concentrations of digitonin should be tested, to select the condition in which the outer membrane is permeabilized (by detection of cytosolic proteins such as actin), while the mitochondrial or lysosomal membranes remain intact (no detection of mitochondrial proteins such as COX, or lysosomal proteins such as hexosaminidase).
18. Acetyl(Ac)-DEVD-AMC is a substrate for caspase-3 and caspase-7 and is most commonly used. Other available substrates are Ac-LEHD-AMC for caspase-5, Ac-YVAD-AMC for caspase-1 and -4, Ac-IETD-AMC for caspase-8 and -6, and Ac-WEHD-AMC for caspase-1, -4, and -5 ***(17)***. The specificity of the substrates is not always restricted to the ones mentioned by the companies ***(51)***. The specificity problem is due to the fact that depending on the concentration of the caspase, the substrate specificity is lost. High concentrations of caspase-3 will also cleave Ac-IETD-AMC, the caspase-8 and -6 substrate. Therefore it is appropriate to combine enzymatic measurements of caspase activities with Western blot analysis to identify the actual presence and activation status of the caspase (**Subheading 3.3.1.**).
19. For analysis of caspase activity: Do not use pefablock protease inhibitors of other total protease inhibitor mixes as these interfere with caspase activity.
20. Caspases have a reactive cysteine in their catalytic site. To block enzymatic activity during the lysis, 1 m*M* oxidized gluthathion is added, which blocks caspase activity and avoids further auto-activation or proteolytic caspase cascades during lysis. When caspase activity is measured in CSF buffer, 10 m*M* dithiotreitol is added to neutralize GSH and liberate the catalytic cysteine.
21. It is often advisable to add the inhibitors or modulators of TNF responsivity 2 h before the administration of the TNF serial dilution to allow the inhibitors or modulators to penetrate the cell and to interfere with their intracellular molecular targets. In the case of geldanamycin, an Hsp90 inhibitor, a 16–18 h pretreatment is required to switch the cells from TNFR-1-induced necrosis to TNFR-1-induced apoptosis ***(20)***.
22. CytoTox 96 Assay is based on a coupled enzymatic assay involving the conversion of a tetrazolium salt, 2-*p*-(iodophenyl)-3-(*p*-nitrophenyl)-5-phenyltetrazolium chloride (INT), into a formazan product. The reaction is catalyzed by lactate dehydrogenase released from cells and by diaphorase present in the assay substrate mixture.

$$\text{Lactate} + NAD^+ \rightarrow \text{Pyruvate} + NADH$$
$$NADH + \text{INT} \rightarrow NAD^+ + \text{Formazan}$$

23. A problem with the MTT assay, especially at early stages of apoptotic cell death, is that these cells often have intact complex-II-activity MTT. Therefore, the modulatory effect of some compounds can be missed; moreover, some compounds may influence complex II activity without affecting cell death per se. One should watch carefully for these types of false negative or false positive effects in the MTT assay.

References

1. Schweichel, J. U. and Merker, H. J. (1973) The morphology of various types of cell death in prenatal tissues. *Teratology* **7,** 253–266.
2. Clarke, P. G. (1990) Developmental cell death: morphological diversity and multiple mechanisms. *Anat. Embryol. (Berl.)* **181,** 195–213.
3. Clarke, P. G. (2002) Apoptosis: from morphological types of cell death to interacting pathways. *Trends Pharmacol. Sci.* **23,** 308–309; author reply 310.
4. Kerr, J. F., Wyllie, A. H., and Currie, A. R. (1972) Apoptosis: a basic biological phenomenon with wide-ranging implications in tissue kinetics. *Br. J. Cancer* **26,** 239–257.
5. Wyllie, A. H., Kerr, J. F., and Currie, A. R. (1980) Cell death: the significance of apoptosis. *Int. Rev. Cytol.* **68,** 251–306.
6. Denecker, G., Vercammen, D., Steemans, M., Vanden Berghe, T., Brouckaert, G., Van Loo, G., et al. (2001) Death receptor-induced apoptotic and necrotic cell death: differential role of caspases and mitochondria. *Cell Death Differ.* **8,** 829–840.
7. Fiers, W., Beyaert, R., Declercq, W., and Vandenabeele, P. (1999) More than one way to die: apoptosis, necrosis and reactive oxygen damage. *Oncogene* **18,** 7719–7730.
8. Vercammen, D., Beyaert, R., Denecker, G., Goossens, V., Van Loo, G., Declercq, W., et al. (1998) Inhibition of caspases increases the sensitivity of L929 cells to necrosis mediated by tumor necrosis factor. *J. Exp. Med.* **187,** 1477–1485.
9. Vercammen, D., Brouckaert, G., Denecker, G., Van de Craen, M., Declercq, W., Fiers, W., et al. (1998) Dual signaling of the Fas receptor: initiation of both apoptotic and necrotic cell death pathways. *J. Exp. Med.* **188,** 919–930.
10. Beyaert, R., Van Loo, G., Heyninck, K., and Vandenabeele, P. (2002) Signaling to gene activation and cell death by tumor necrosis factor receptors and Fas. *Int. Rev. Cytol.* **214,** 225–272.
11. Scaffidi, C., Fulda, S., Srinivasan, A., Friesen, C., Li, F., Tomaselli, K. J., et al. (1998) Two CD95 (APO-1/Fas) signaling pathways. *EMBO J.* **17,** 1675–1687.
12. Li, P., Nijhawan, D., Budihardjo, I., Srinivasula, S. M., Ahmad, M., Alnemri, E. S., et al. (1997) Cytochrome c and dATP-dependent formation of Apaf-1/caspase-9 complex initiates an apoptotic protease cascade. *Cell* **91,** 479–489.
13. Kischkel, F. C., Hellbardt, S., Behrmann, I., Germer, M., Pawlita, M., Krammer, P. H., et al (1995) Cytotoxicity-dependent APO-1 (Fas/CD95)-associated proteins form a death-inducing signaling complex (DISC) with the receptor. *EMBO J.* **14,** 5579–5588.

14. Luo, X., Budihardjo, I., Zou, H., Slaughter, C., and Wang, X. (1998) Bid, a Bcl2 interacting protein, mediates cytochrome c release from mitochondria in response to activation of cell surface death receptors. *Cell* **94,** 481–490.
15. Van Loo, G., Demol, H., van Gurp, M., Hoorelbeke, B., Schotte, P., Beyaert, R., et al. (2002). A matrix-assisted laser desorption ionization post-source decay (MALDI-PSD) analysis of proteins released from isolated liver mitochondria treated with recombinant truncated Bid. *Cell Death Differ.* **9,** 301–308.
16. Van Loo, G., Saelens, X., van Gurp, M., MacFarlane, M., Martin, S. J., and Vandenabeele, P. (2002) The role of mitochondrial factors in apoptosis: a Russian roulette with more than one bullet. *Cell Death Differ.* **9,** 1031–1042.
17. Lamkanfi, M., Declercq, W., Depuydt, B., Kalai, M., Saelens, X., and Vandenabeele, P. The caspase family. In *Caspases: Their Role in Cell Death and Cell Survival* (Los, M. and Walczak, H., eds.). Landes Bioscience, Kluwer Academic, Georgetown, TX, 2003
18. Kawahara, A., Ohsawa, Y., Matsumura, H., Uchiyama, Y., and Nagata, S. (1998) Caspase-independent cell killing by Fas-associated protein with death domain. *J. Cell Biol.* **143,** 1353–1360.
19. Holler, N., Zaru, R., Micheau, O., Thome, M., Attinger, A., Valitutti, S., et al. (2000) Fas triggers an alternative, caspase-8-independent cell death pathway using the kinase RIP as effector molecule. *Nat. Immunol.* **1,** 489–495.
20. Vanden Berghe, T., Kalai, M., van Loo, G., Declercq, W., and Vandenabeele, P. (2003) disruption of HSP90 function reverts tumor necrosis factor-induced necrosis to apoptosis. *J. Biol. Chem.* **278,** 5622–5629.
21. Vercammen, D., Vandenabeele, P., Beyaert, R., Declercq, W., and Fiers, W. (1997) Tumour necrosis factor-induced necrosis versus anti-Fas-induced apoptosis in L929 cells. *Cytokine* **9,** 801–808.
22. Unwin, P. N. and Zampighi, G. (1980) Structure of the junction between communicating cells. *Nature* **283,** 545–549.
23. Unwin, P. N. and Ennis, P. D. (1984) Two configurations of a channel-forming membrane protein. *Nature* **307,** 609–613.
24. Cummings, M. C., Winterford, C. M., and Walker, N. I. (1997) Apoptosis. *Am. J. Surg. Pathol.* **21,** 88–101.
25. Falcieri, E., Gobbi, P., Cataldi, A., Zamai, L., Faenza, I., and Vitale, M. (1994) Nuclear pores in the apoptotic cell. *Histochem. J.* **26,** 754–763.
26. Kerr, J. F., Winterford, C. M., and Harmon, B. V. (1994) Apoptosis. Its significance in cancer and cancer therapy. *Cancer* **73,** 2013–2026.
27. Kitanaka, C. and Kuchino, Y. (1999). Caspase-independent programmed cell death with necrotic morphology. *Cell Death Differ.* **6,** 508–515.
28. Earnshaw, W. C. (1995) Nuclear changes in apoptosis. *Curr. Opin. Cell Biol.* **7,** 337–343.
29. Nagata, S. (2002) Breakdown of chromosomal DNA. *Cornea* **21,** S2–S6.
30. Nagata, S. (2000) Apoptotic DNA fragmentation. *Exp. Cell Res.* **256,** 12–18.
31. Bevers, E. M., Comfurius, P., Dekkers, D. W., Harmsma, M., and Zwaal, R. F. (1998) Regulatory mechanisms of transmembrane phospholipid distributions and

pathophysiological implications of transbilayer lipid scrambling. *Lupus* **7(Suppl 2),** S126–S131.

32. Martin, S. J., Reutelingsperger, C. P., McGahon, A. J., Rader, J. A., van Schie, R. C., LaFace, D. M., et al. (1995) Early redistribution of plasma membrane phosphatidylserine is a general feature of apoptosis regardless of the initiating stimulus: inhibition by overexpression of Bcl-2 and Abl. *J. Exp. Med.* **182,** 1545–1556.
33. Denecker, G., Dooms, H., Van Loo, G., Vercammen, D., Grooten, J., Fiers, W., et al. (2000) Phosphatidyl serine exposure during apoptosis precedes release of cytochrome c and decrease in mitochondrial transmembrane potential. *FEBS Lett.* **465,** 47–52.
34. Foghsgaard, L., Wissing, D., Mauch, D., Lademann, U., Bastholm, L., Boes, M., et al. (2001) Cathepsin B acts as a dominant execution protease in tumor cell apoptosis induced by tumor necrosis factor. *J. Cell Biol.* **153,** 999–1010.
35. Brunk, U. T., Neuzil, J., and Eaton, J. W. (2001) Lysosomal involvement in apoptosis. *Redox. Rep.* **6,** 91–97.
36. Neuzil, J., Weber, T., Schroder, A., Lu, M., Ostermann, G., Gellert, N., et al. (2001) Induction of cancer cell apoptosis by alpha-tocopheryl succinate: molecular pathways and structural requirements. *FASEB J.* **15,** 403–415.
37. Stoka, V., Turk, B., Schendel, S. L., Kim, T. H., Cirman, T., Snipas, S. J., et al. (2001) Lysosomal protease pathways to apoptosis. Cleavage of bid, not procaspases, is the most likely route. *J. Biol. Chem.* **276,** 3149–3157.
38. Thornberry, N. A., Rano, T. A., Peterson, E. P., Rasper, D. M., Timkey, T., Garcia-Calvo, M., et al. (1997) A combinatorial approach defines specificities of members of the caspase family and granzyme B. Functional relationships established for key mediators of apoptosis. *J. Biol. Chem.* **272,** 17,907–17,911.
39. Spencer, M. J., Croall, D. E., and Tidball, J. G. (1995) Calpains are activated in necrotic fibers from mdx dystrophic mice. *J. Biol. Chem.* **270,** 10,909–10,914.
40. Xu, K., Tavernarakis, N., and Driscoll, M. (2001) Necrotic cell death in *C. elegans* requires the function of calreticulin and regulators of Ca(2+) release from the endoplasmic reticulum. *Neuron* **31,** 957–971.
41. Lankiewicz, S., Marc Luetjens, C., Truc Bui, N., Krohn, A. J., Poppe, M., Cole, G. M., et al. (2000) Activation of calpain I converts excitotoxic neuron death into a caspase-independent cell death. *J. Biol. Chem.* **275,** 17,064–17,071.
42. Nakayama, M., Ishidoh, K., Kayagaki, N., Kojima, Y., Yamaguchi, N., Nakano, H., et al. (2002) Multiple pathways of TWEAK-induced cell death. *J. Immunol.* **168,** 734–743.
43. Gobeil, S., Boucher, C. C., Nadeau, D., and Poirier, G. G. (2001) Characterization of the necrotic cleavage of poly(ADP-ribose) polymerase (PARP-1): implication of lysosomal proteases. *Cell Death Differ.* **8,** 588–594.
44. Rae, T. (1977) Tolerance of mouse macrophages in vitro to barium sulfate used in orthopedic bone cement. *J. Biomed. Mater. Res.* **11,** 839–846.
45. Metivier, D., Dallaporta, B., Zamzami, N., Larochette, N., Susin, S. A., Marzo, I., et al. (1998) Cytofluorometric detection of mitochondrial alterations in early

CD95/Fas/APO-1-triggered apoptosis of Jurkat T lymphoma cells. Comparison of seven mitochondrion-specific fluorochromes. *Immunol. Lett.* **61,** 157–163.
46. Kroemer, G., Dallaporta, B., and Resche-Rigon, M. (1998) The mitochondrial death/life regulator in apoptosis and necrosis. *Annu. Rev. Physiol.* **60,** 619–642.
47. Lemasters, J. J., Nieminen, A. L., Qian, T., Trost, L. C., Elmore, S. P., Nishimura, Y., et al. (1998). The mitochondrial permeability transition in cell death: a common mechanism in necrosis, apoptosis and autophagy. *Biochim. Biophys. Acta* **1366,** 177–196.
48. Goossens, V., Grooten, J., De Vos, K., and Fiers, W. (1995) Direct evidence for tumor necrosis factor-induced mitochondrial reactive oxygen intermediates and their involvement in cytotoxicity. *Proc. Natl. Acad. Sci. USA* **92,** 8115–8119.
49. Sanchez, I., Mahlke, C., and Yuan, J. (2003). Pivotal role of oligomerization in expanded polyglutamine neurodegenerative disorders. *Nature* **421,** 373–379.
50. Lippens, S., Kockx, M., Knaapen, M., Mortier, L., Polakowska, R., Verheyen, A., et al. (2000) Epidermal differentiation does not involve the pro-apoptotic executioner caspases, but is associated with caspase-14 induction and processing. *Cell Death Differ.* **7,** 1218–1224.
51. Talanian, R. V., Quinlan, C., Trautz, S., Hackett, M. C., Mankovich, J. A., Banach, D., et al. (1997) Substrate specificities of caspase family proteases. *J. Biol. Chem.* **272,** 9677–9682.

10

Assessment of TNFα-Induced Endothelial Damage Through the Loss of Its Barrier Function

Elisabetta Ferrero

Summary

Tumor necrosis factor α (TNFα) appears to be the main mediator causing the systemic manifestations of sepsis and septic shock associated with edema ***(1,2)***. In vitro it augments movement of permeability tracers across endothelial cell monolayers ***(3,4)***. Herein we describe a method which permits quantification and assessment of changes in the integrity of endothelial monolayers by measuring transendothelial flux (luminal to subluminal) of tracer macromolecules in the absence of hydrostatic and oncotic pressure gradients. The system consists of two compartments separated by a polycarbonate filter and permits highly controlled conditions.

Key Words: Endothelium; paracellular transport; permeability; HUVEC; transwell.

1. Introduction

Tumor necrosis factor α (TNFα) is an established mediator of the acute phase response ***(5,6)***. Human recombinant TNFα has been shown to induce a vascular leak syndrome in mice and sheep, accompanied by increased pulmonary extravasation of permeability tracers ***(7,8)***. Indeed, the endothelial lining serves as a selective dynamic barrier between the vascular compartment of blood vessels and the underlying tissues. The integrity of this barrier is essential to control the transport of plasma components and circulating cells from the blood into the subendothelial compartments ***(9)***.

In normal conditions endothelial permeability permits the transport of vital substrates (e.g., water, solutes, hormones, drugs) to tissues and/or the removal of waste products ***(9,10)***. A central feature of endothelium under physiopathological conditions, such as wound healing, angiogenesis, and acute or chronic inflammation, is an increased permeability or loss of barrier function, resulting

From: *Methods in Molecular Medicine, Vol. 98: Tumor Necrosis Factor*
Edited by: A. Corti and P. Ghezzi © Humana Press Inc., Totowa, NJ

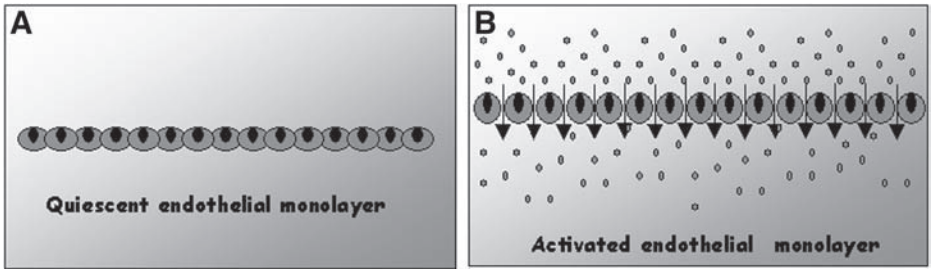

Fig. 1. Effect of permiabilizing agents on endothelial cells. **(A)** Quiescent endothelial monopermeabilizing layer under normal conditions. **(B)** Endothelial monolayer under the effect of permeabilizing agents (e.g., TNFα).

in tissue edema and changes in the physicochemical properties of interstitial compartments ***(11,12)***.

TNFα recognizes and binds two receptors on endothelial cell monolayers. Altered barrier function of endothelium in response to TNF or other inflammation mediators, such as interleukin (IL)-1, thrombin, and histamine, is accompanied by reversible cell rounding and interendothelial gap formation ***(13,14)***: this reversibility implies that the predominant transport pathway is a diffusive one (e.g., paracellular transport) (**Fig. 1**).

Regulation of paracellular transport is associated with modulation of actin-based systems that permit cell-to-cell and cell-to-matrix anchorage (**Fig. 2A**). However, endothelial cells (ECs) have also the attributes for transcellular transport. Indeed, ECs are endowed with caveolae and associated vesicles (the "large-pore" system), which compose a vesicular system involved in an active transcellular (nondiffusive) transport of molecules (**Fig. 2B**) ***(15–17).***

In this chapter, I describe a method for measuring, in vitro, the diffusion of molecules through confluent monolayers of ECs. This method allows assessment of the effect of the different stimuli on endothelial permeability, the latter being in direct relation to the molecular weight and to the size of the considered solute.

It should be kept in mind that:

1. different effectors act on different junctional components and with different kinetics, which may result in transient or prolonged increases in endothelial permeability ***(18)***. In particular, exposure to TNFα induces a significantly increased permeability that is time dependent (peaks at 6–8 h), reversible (returns to baseline after 16 h), and temperature dependent.
2. ECs obtained from different tissues/organs as well as EC lineages display different degrees of response, grading from sensitivity to resistance, also depending on donor and heterogeneity in the junctional architecture along the vasculature (intrinsic "leakiness"). In our hands, human umbilical vein endothelial cells

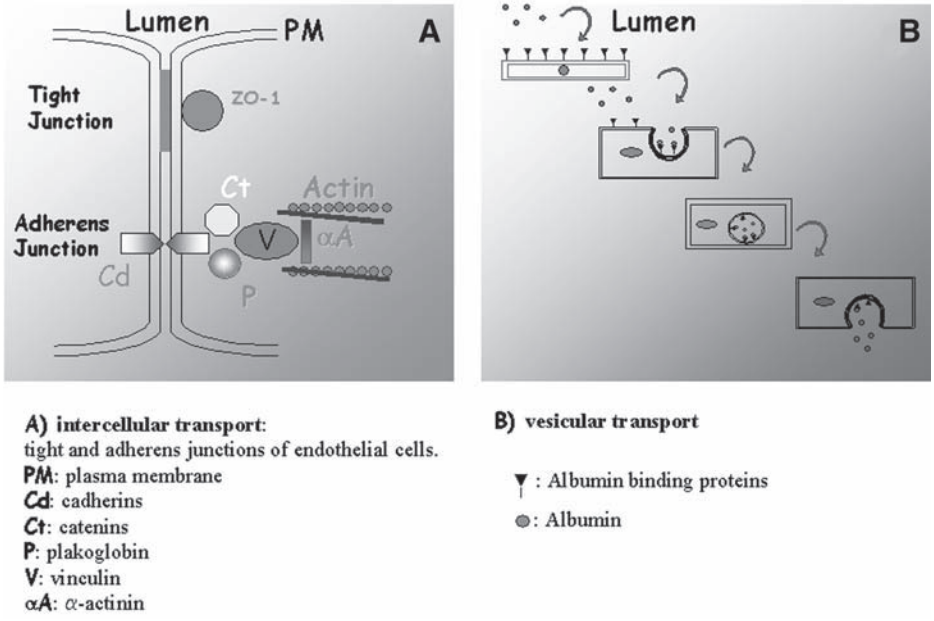

Fig. 2. Two possible pathways of transendothelial transport. **(A)** Diffusive paracellular transport. **(B)** Nondiffusive transport (vesicular transport).

(HUVECs) were better responders than EA hybrid 926, which in turn were better responders than ECV 304.

2. Materials

2.1. Cell Culture

1. Cells: HUVEC (obtained from umbilical cord by collagenase treatment), EA hybrid 926 (obtained from Dr. Cora Edgell, University of North Carolina), ECV 304 (obtained from American Type Culture Collection). The cells are cultured at 37°C and 5% CO_2 (*see* **Note 1**).
2. Complete Medium (CM) HUVEC: medium 199 (Bio Whittaker Europe), 20% FBS (HyClone), 5% penicillin-streptomycin solution (Sigma-Aldrich); ECGF 20 μg/mL (Roche), heparin 90 μg/mL (Parke-Davis). CM must be stored at –20°C and, when thawed, at 4°C.
3. Low serum medium: medium 199 with 1% FBS.
4. CM EA hybrid 926: DMEM (BioWhittaker Europe), 10% FBS (HyClone), 5% penicillin-streptomycin solution (Sigma): must be stored at 4°C.
5. CM ECV 304: Medium 199 (BioWhittaker Europe), 10% FBS (HyClone), 5% penicillin-streptomycin (Sigma): must be stored at 4°C.
6. Gelatin: gelatin type B obtained from bovine skin (Sigma). The gelatin is diluted in distilled water to a final concentration of 2%, sterilized using an autoclave, and then stored at 4°C.

2.2. Effectors and Reagents for the Assay (see Note 2)

1. Human albumin: Albutein 20% (Grigols).
2. ^{125}I-albumin (Molecular Wt 70,000D) (Amersham Pharmacia Biotech Limited): specific activity 10 MBq, (250 μCi). ^{125}I belongs to the second radiotoxicity group. Whoever handles ^{125}I-albumin must adopt the following precautions: use 2 pairs of gloves and plumb screens (thickness 0.02 mm). Because iodine accumulates in thyroid tissue and is volatile, it is important to avoid breathing it. Handling within a hood or glove box is recommended.
3. Fluorescein isothiocyanate (FITC)-dextran (Molecular Wt 40,000 D) (Sigma).
4. Transwell 6.5 mm diameter, 0.4 μm pore size (Costar).
5. Gamma-counter (Packard).
6. Fluorometer: Typhoon 8600 Variable Mode Imager (Molecular Dynamics).

3. Methods

The method we describe measures the luminal to subluminal flux of tracer macromolecules in the absence of hydrostatic and oncotic pressure gradients (both forces acting perpendicular to endothelial cells). The former is eliminated by maintaining equal fluid levels in both compartments. The latter is overcome by eliminating proteins in both compartments.

Premises: to appreciate differences in the interendothelial transit of molecules, the obvious prerequisite is that ECs form a confluent monolayer (*see* **Note 3**). In vitro, ECs reach confluence (**Fig. 3**) and build thin monolayers very similar to the lining which covers vessels in vivo.

Adjacent cells are in close contact, resembling "tiles," as assessed by transmission electron microscopy of a monolayer grown on a Transwell and stained immunogold by CD31 (**Fig. 4**). Therefore, cultured ECs mimic the vascular lining well.

We describe two methods based on the use of molecules with different weights and sizes, the effect of TNFα on endothelial permeability being not specific for albumin transfer ***(4)***.

The double-chamber system consists of two compartments, the inside (upper) and the outside (lower), separated by a polycarbonate microporous filter (**Fig. 5**).

3.1. How to Seed Cells

1. The upper side of the filter is coated with gelatin (2%).
2. HUVECs are seeded at 5×10^4 cells/filter (*see* **Note 1**); ECV and EA hybrid 926 cells at 2.5×10^4 cells/filter.
3. Cells are cultured in 200 μL of the appropriate CM and grown for 5 d to attain confluence (*see* **Note 3**); during this period the lower chamber is maintained empty.
4. 2 h before the experiment, cells are washed with medium 199 alone and then incubated with low serum medium, to favor quiescence without inducing apoptosis by starvation (*see* **Note 4**).

Fig. 3. Contrast-phase microscopy image of a HUVEC monolayer; the relief effect is obtained by computer elaboration of the original image (original magnification, ×200).

3.2. How to Start the Experiment

Two alternative methods are presented (*see* **Note 5**):

1. The putative inducer or inducers of permeability are added together with the chosen tracer (radioactive- or fluorescein-labeled): the addition of the tracer is considered time zero. If this method is adopted, the lower chamber must be filled with preheated 199 medium. Samples are collected from the lower compartment at fixed intervals.
2. The inducer or inducers are added before the tracer: in this case, the lower chamber is kept empty for the entire period of the treatment. After that, the tracer is added (and the time zero starts), the lower chamber is filled up with low serum medium, and the samples are collected from the lower wells at fixed intervals. In this setting, one plate per time interval must be considered.

Procedures in common with both methods are as follows:

1. When the tracer is added, fill up the lower chamber with 600 μL of 199 medium to equalize the levels in both chambers and avoid hydrostatic pressure.
2. Dilute tracers and effectors in medium 199 alone, to avoid colloidosmotic (oncotic) pressure.
3. Incubate Transwells under agitation (*see* **Note 6**).
4. Collect samples after 5 min equilibration.

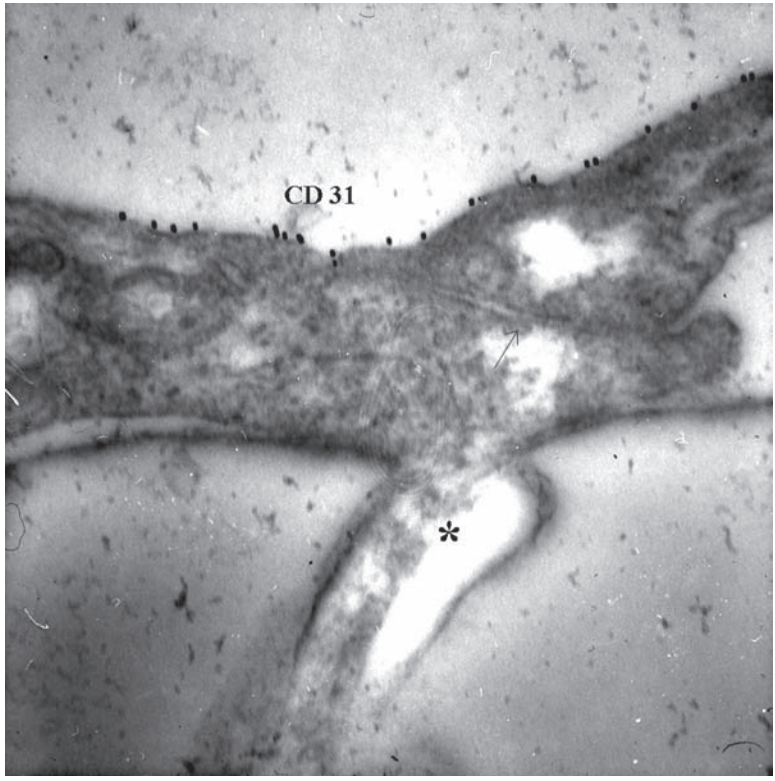

Fig. 4. Immunoelectron microscopy with anti-CD31 antibody (labeled with gold particles) of two endothelial cells seeded on a Transwell carbonate filter; arrow indicates the contact area between the cells; asterisk indicates the filter pore.

3.3. Transendothelial ^{125}I-Albumin Permeability

The endothelial cell surface expresses 60 kDa albumin receptors ***(19)***, which actively bind and transport albumin in a nondiffusive pathway (**Fig. 2B**). To exclude this process during the permeability assay, the receptors must be saturated. This can be achieved by incubating the EC layer for 30 min with 5 mg/mL of human unlabeled albumin before adding tracer solution. After washing, add the tracer solution and follow the passages described in **Subheading 3.2.**

At the end of the incubation period:

1. Collect 30 mL of culture medium from the lower chamber at fixed times after extensive washings (10 times).
2. Determine the transendothelial passage of ^{125}I-albumin using a gamma counter. Transendothelial albumin transport is monitored by sequential determination of

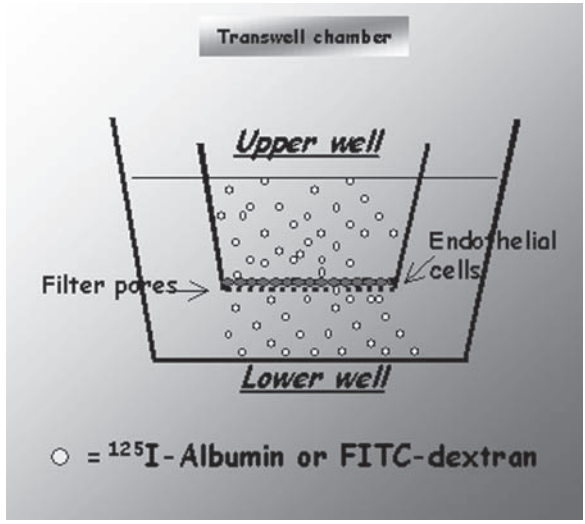

Fig. 5. Schematic illustration of the Transwell system.

mass flux, and by calculating the permeability coefficient or the percentage recovery ***(20)***.

a. Determination of permeability coefficient.
The Permeability Coefficient (PC) is derived from Fick's law of diffusion and is defined as show in Eq. 1:

$$\mathrm{PC} = \left(\frac{\text{mass flux of albumin, luminal chamber} \rightarrow \text{sublumimal chamber}}{[\text{albumin}]\ \text{luminal} - [\text{albumin}]\ \text{subluminal chamber}} \right) \qquad (1)$$

where [albumin] = albumin concentration.

This equation can be written in terms of known quantities, i.e., area of membrane (A), volume of luminal chamber (V_L), volume of subluminal chamber (V_S), sample time (t), albumin concentration in subluminal chamber at each sample time [$C_S(t)$] and total mass of protein (albumin) at each sample time [TP(t)]. Substitution of these quantities into the previous equation, integration, and rearrangement yield Equation 2:

$$PC = \left\{ \frac{\ln\left[\dfrac{1}{1 - \left(V_S + V_L\right)\left(\dfrac{[C_S(t)]}{[TP(t)]}\right)} \right]}{A\left[\dfrac{\left(V_S + V_L\right)t}{V_S V_L} \right]} \right\} \qquad (2)$$

b. Percent recovery calculation.
The TP(t) at the condition of each experiment and the final luminal [$C_S(t)$] and subluminal [$C_L(t)$] concentration are used to calculate the percent recovery of albumin as follow:

$$\% \text{ recovery} = \left\{ \frac{\left[C_S(t)\right]V_S + \left[C_L(t)\right]V_L}{\left[TP(t)\right]_{t\ \text{final}}} \right\} \times 100 \quad (3)$$

(*see* **Note 6**).

3.4. Transendothelial FITC-Dextran Permeability

1. Add FITC-dextran at 500 μg/mL in the luminal compartment.
2. Collect a 50 μL sample from the subluminal compartment.
3. Dilute sample 1:20 with PBS without Ca^{2+}/Mg^{2+}.
4. Determine the transendothelial passage of FITC-dextran using a spectrofluorometer. The fluorometric analysis gives the amount of FITC-dextran that passes from the luminal to the subluminal chamber.

4. Notes

1. Use primary HUVECs between the second and sixth passage; later they are leaky due to senescence.
2. TNFα itself could be toxic and may cause necrosis/detachment of ECs, resulting in a false detection of increased permeability. To check this, we suggest predetermination of the toxic activity of TNF e.g., through the acquisition of confocal images or by means of a conventional cytotoxicity test.
3. A major problem is how to assess confluence, since the polycarbonate filter inside the Transwell is optically impermeable. We overcome this problem by seeding the same number of cells in a flat 96-well plate, with a surface of 6.5 mm, like that of the inner chamber of the Transwell. Moreover, we randomly control the number of detached cells in the upper chamber during the entire period of culture. When we use ^{125}I-albumin as a tracer, we control that the spontaneous passage does not exceed 1% of the total radioactivity added after 5 min and exclude the positive ones.
4. When washings are required we suggest:
   a. Use preheated (37°C) buffer to maintain the endothelial continuity (cold may induce retraction of cells and increase the cell–cell interspace).
   b. Wash the chambers by turning them upside down, to avoid physical stress caused by pipetting.
5. Assays must be performed in triplicate to minimize variability.
6. This method, pioneered by Malik ***(9)***, suggested the use of a stirrer in the subluminal side. Given that the double-chamber system is static, it doesn't mimic the interstitial fluid dynamic operating in vivo, and suffers for the diffusional resistance offered by the lower fluid. Therefore, the Transwells should be incu-

bated with mild, continous agitation produced by an orbital mixer, or, at least, we suggest frequent mixing of the lower medium by pipetting.

7. The advantage of reporting data as PC is the ability to compare our data with other permeability models, since PC normalizes mass transfer with respect to the concentration gradient across the monolayer, area of the membrane, length of experiment, and chamber volumes.

Acknowledgments

The author thanks Silvia Scabini and Daniela Belloni for their helpful discussion and technical assistance; Chiara Foglieni for morphological acquisitions; and Biagio Eugenio Leone for electron microscopy.

References

1. Cannon J. G., Tompkins R. G., Gelfand J. A., et al. (1990) Circulating IL-1 and TNFα in septic shock and experimental endotoxic fever. *J. Infect. Dis.* **161,** 79–84.
2. Tracey K. J., Fong Y., Hesse D. G., et al. (1987) Anti-cachectin/TNF monoclonal antibodies prevent septic shock during lethal baceraemia. *Nature* **330,** 662–664.
3. Blikstad, I., Markey F., Carlsson, L., Persson, T., and Lindberg, U. (1978) Selective assay of monomeric and filamentous actin in cell extracts, using inhibition of deoxyribonuclease I. *Cell* **15,** 935–943.
4. Agarwal, S., Drysdale B. E., and Shin H. S. (1988) Tumor necrosis factor-mediated cytotoxicity involves ADP-ribosylation. *J. Immunol.* **140,** 4187–4192.
5. Goldblum, S. E. and Sun, W. L. (1990) Tumor necrosis factor-α augments pulmonary arterial transendothelial albumin flux in vitro. *Am. J. Physiol.* **258,** L57–L67.
6. Goldblum, S. E., Ding, X., and Campbell-Washington, J. (1993) TNFα induces endothelial cell F-actin depolymerization, new actin synthesis, and barrier dysfunction. *Am. J. Physiol.* **264,** C894–C905.
7. Lampugnani, M. G. and Dejana, E. (1997) Interendothelial junctions: structure**,** signaling and functional roles. *Curr. Opin. Cell. Biol.* **9,** 674–682.
8. Plante, G. E. (2002) Vascular response to stress in health and disease. *Metabolism* **51,** 25–30.
9. Malik, A. B., Lynch, J. J., and Cooper, J. A. (1989) Endothelial barrier function. *J. Invest. Dermatol*. **93,** 62S-67S.
10. Johnson, J., Meyrick, B., Jesmok, G., and Brigham K. L. (1989) Human recombinant tumor necrosis factor alpha infusion mimics endotoxemia in awake sheep. *J. Appl. Physiol.* **66,** 1448–1454.
11. Remick, D. G., Kunkel, R. G., Larrick, J. W., and Kunkel, S. L. (1987) Acute in vivo effects of human recombinant tumor necrosis factor. *Lab. Invest.* **56,** 583–590.
12. Lum, H. and Malik, A. B. (1994) Regulation of vascular endothelial barrier function. *Am. J. Physiol.* **267,** L223–L241.
13. Van Nieuw Amerongen, G., Draijer, R., Vermeer, M. A., and Van Hinsberg, V. W. M. (1998) Transient and prolonged increase in endothelial permeability induced by histamine and thrombin. *Circ. Res.* **83,** 1115–1122.

14. Rabiet, M. J., Plantier, J. L., Rival, Y., Genoux, R., Lampugnani, M. G., and Dejana, E. (1996) Thrombin-induced increase in endothelial permeability is associated with changes in cell-to-cell junction organization. *Arterioscler. Thromb. Vasc. Biol.* **16,** 488–496.
15. Simionescu, M., Gafencu, A., and Antohe, F. (2002) Transcytosis of plasma macromolecules in endothelial cells: a cell biological survey. *Microsc. Res. Tech.* **57,** 269–288.
16. Schnittler, H. J. (1998) Structural and functional aspects of intercellular junctions in vascular endothelium. *Basic Res. Cardiol.* **93,** s030–s039.
17. Stan, R. V. (2002) Structure and function of endothelial caveolae. *Microsc. Res. Tech.* **57,** 350–364.
18. Siflinger-Birnboim, A., Cooper, J. A., Del Vecchio, P. J., Malik, A. B. (1988) Selectivity of the endothelial monolayer: effects of increased permeability. *Microvasc. Res.* **36,** 216–227.
19. Tiruppathi, C., Finnegan, A., and Malik, A. B. (1996) Isolation and characterization of a cell surface albumin-binding protein from vascular endothelial cells. *Proc. Nat. Acad. Sci. USA* **93,** 250–255.
20. Casnocha, S. A., Eskin, S. G., Hall, E. R., and McIntire, L. V. (1989) Permeability of human endothelial monolayers: effect of vasoactive agonists and cAMP. *J. Appl. Phys.* **67,** 1997–2005.

11

Genetic Engineering in the Mouse

Tuning TNF/TNFR Expression

Eleni Douni, Maria Alexiou, and George Kollias

Summary

With the exponential increase in the number of genes identified by various genome projects, it has become imperative that efficient methods be developed for deciphering gene function. Genetically engineered strains of mice are now critical research tools for basic biomedical research and for genomic approaches for the development of new therapeutic treatments for human disease. Over the past ten years it has become possible to make essentially any mutation in the mouse by transgenesis and homologous recombination in embryonic stem cells. Current advances in the "genetic engineering of the mouse," including the tissue-specific activation or inactivation of gene expression combined with developing technologies for switching gene expression on and off at will, provide experimental settings unprecedented in their potential to offer answers to long-standing questions.

Key Words: TNF; TNFR; transgenic; knockout; conditional mice; models; human disease; gene targeting; homologous recombination; embryonic stem cells; Cre-loxP site-specific recombination system.

1. Introduction

Transgenic and knockout systems offer clear advantages over cellular systems as fine tools in the dissection and understanding of gene structure, expression, and function. In the tumor necrosis factor (TNF) field, much of the existing knowledge about TNF and TNF-receptor (TNFR) function is based, to a large extent, on what we have already learned by overexpressing these molecules in transgenic mice or by ablating their expression in knockout systems. Overexpression of TNF and its receptors in transgenic systems have led to the development and consequent characterization of specific disease models of

From: *Methods in Molecular Medicine, Vol. 98: Tumor Necrosis Factor*
Edited by: A. Corti and P. Ghezzi © Humana Press Inc., Totowa, NJ

human diseases ***(1)*** such as rheumatoid arthritis ***(2)***, systemic inflammation ***(3,4)*** and degenerative CNS diseases ***(5,6)***. In addition, a physiological role for TNF and its receptors in developmental or immunoregulatory processes has been unraveled in mice deficient in these molecules ***(7–10)***. More recently, conditional targeted mutagenesis systems have been developed ***(11,12)*** that allow control of both the tissue specificity and the onset (temporal control) of the mutation.

Even though detailed laboratory manuals on transgenic technologies may also be found elsewhere ***(13–15)***, we aim to provide a concise technical guide for the production of transgenic, knockout, and conditional mice in the field of TNF and its receptors.

2. Materials

1. TNF/TNFR genomic fragments.
2. pL2-neo, pNT, pEasy Flox, and Cre-expressing plasmids.
3. Restriction enzymes, β-agarase I (New England Biolabs), and tip-columns Elutip-D (Schleicher and Schuell) for DNA purification.
4. Electrophoresis equipment.
5. Borosilicate glass capillaries for needle construction (Harvard Apparatus; with inner filament for pronuclear injections, and without filament for holdings, transfer pipets and blastocyst injections).
6. Pipet construction equipment: pipet puller (David Kopf Instruments), microforge instrument (Narishige Co., Ltd.).
7. Animals: (CBA × C57BL/6) F_1 females both for the derivation of oocytes and as pseudopregnant foster mothers, (CBA × C57BL/6) F_1 fertile stud males, NMRI sterile stud males, and C57BL/6 stud males and females for derivation of blastocysts.
8. Stereomicroscope and a cold light source.
9. Surgical tools: watchmakers fine forceps, blunt forceps, scissors, wound clips.
10. Superovulation hormones: pregnant mare's serum gonadotropin, human chorionic gonadotropin (Intervet).
11, Mouth pipet assembly (Sigma).
12. M2 culture medium: 94.66 m*M* NaCl, 4.78 m*M* KCl, 1.71 m*M* $CaCl_2$, 1.19 m*M* KH_2PO_4, 1.19 m*M* $MgSO_4$, 4.15 m*M* $NaHCO_3$, 20.85 m*M* HEPES, 23.28 m*M* sodium lactate, 0.33 m*M* sodium pyruvate, 5.56 m*M* glucose, 0.4% BSA, 0.006% penicillin G potassium salt, 0.005% streptomycin sulfate, and 0.001% phenol red in double-distilled H_2O (ddH_2O).
13. M16 culture medium: 94.66 m*M* NaCl, 4.78 m*M* KCl, 1.71 m*M* $CaCl_2$, 1.19 m*M* KH_2PO_4, 1.19 m*M* $MgSO_4$, 25 m*M* $NaHCO_3$, 23.28 m*M* sodium lactate, 0.33 m*M* sodium pyruvate, 5.56 m*M* glucose, 0.4% BSA, 0.006% penicillin G potassium salt, 0.005% streptomycin sulfate, and 0.001% phenol red in ddH_2O.
14. Hyaluronidase (Sigma).
15. Paraffin oil.

16. Fluorinert FC-40 (Sigma).
17. Siliconized glass depression slide (BDH).
18. Microinjection equipment: inverted microscope with Hoffman optics (Nikon Ltd., Diaphot 200) and one pair of micromanipulators (Narishige Co., Ltd.).
19. Microinjection buffer: 7.5 m*M* Tris-HCl, pH 7.4, 0.2 m*M* EDTA in pyrogen-free sterilized water for injection.
20. Anaesthetic cocktail: 0.66 mg Xylazine, 0.1 mg Ketamin, and 0.033 mg Atropine per kg of body weight.
21. Adrenaline solution for surgery (1%).
22. Tail buffer: 50 m*M* Tris-HCl, pH 8.0, 0.1*M* EDTA, 0.1*M* NaCl, 1% SDS.
23. Proteinase K (Roche) 10 mg/mL in 50 m*M* Tris-HCl, pH 8.0.
24. Phenol/chloroform/isoamyl alcohol: 25:24:1, saturated in 100 m*M*, Tris-HCl, pH 8.0.
25. Pluripotent embryonic stem cell line.
26. FBS/FCS (ESC tested).
27. Trypsin/EDTA solution 0.25%.
28. PBS (Ca^{2+}/Mg^{2+} free).
29. Mitomycin C.
30. Electroporator (Gene Pulse Electroporator with capacity extender by Biorad).
31. Electroporation cuvets 0.4 cm (Biorad).
32. 20–200 μL multichannel pipet (8–12 channels) (Anachem).
33. Multichannel aspirator (Sigma).
34. Dimethylsulfoxide (DMSO).
35. Gelatin (powder or 2% solution, Sigma).
36. Lysis buffer for screening colonies in 96-well plates: 10 m*M* NaCl, 10 m*M* Tris-HCl, pH 7.5, 10 m*M* EDTA, 0.5% Sarcosyl.
37. ESC culture medium formulation: DMEM-high glucose (4.5 g/L, 1X, Invitrogen), 2 m*M* L-glutamine (from 100X, Invitrogen), nonessential amino acids (from 100X, Invitrogen), penicillin (100 units/mL) and streptomycin (100 μg/mL) (from 100X, Invitrogen), 0.1 m*M* 2-mercaptoethanol (from 50 m*M* stock, Invitrogen), 15% fetal calf serum, 10^3 units/mL LIF (ESGRO-Chemicon).
38. Restriction digestion mix: 1X appropriate restriction buffer, 1 m*M* spermidine, 100 μg/mL BSA, 50 μg/mL RNase A, 30 units/well restriction enzyme.

3. Methods

The methods described below outline the production of (1) transgenic mice, (2) knockout mice, and (3) conditional mice.

3.1. Production of Transgenic Mice by Pronuclear Injection of DNA

The gene transfer method most extensively and successfully employed is the microinjection of DNA directly into the pronuclei of fertilized mouse eggs ***(16)***. This method results in the stable chromosomal integration of the foreign DNA in 10–40% of the resulting mice ***(13)***.

Table 1
Genetic and Phenotypic Characteristics of Various Human TNF Transgenic Mouse Lines Generated in Our Laboratory

huTNF construct	Tg lines	Promoter	Phenotype	Reference
1. 	Tg 1278	wt	Normal	2
2. 	Tg 197, 3647	wt	Arthritis	2
3. 	Tg 211	CD2	Lymphoid lesions, systemic inflammation	3
	Tg K742	NF-L	Chronic CNS inflammation	6
	Tg K83	GFAP	Chronic CNS inflammation	6

Human TNF exons are represented as black boxes, the 3' untranslated region (UTR) as a white box. Striped boxes indicate the 3' UTR of the β-globin gene, whereas pA indicate the polyadenylation signal. Arrow indicates transcription initiation of the transgene. Tg: transgenic, wt: wild-type, NF-L: neurofilament, GFAP: glial fibrillary acidic protein, CNS: central nervous system.

3.1.1. Designing DNA Constructs for Transgenesis

Any cloned fragment of DNA, genomic or cDNA, can be used for microinjection. Because it has been shown that prokaryotic vector sequences can severely inhibit the expression of transgenes (***17***), they should be removed before microinjection. Therefore, the constructs should be designed in such a way that unique restriction sites on both sides of the insert should be considered. In addition, it has been experimentally deduced that the presence of introns facilitates transcription of the transgene, and therefore it is advisable to include them in cDNA-based constructs ***(18)*** (*see* **Note 1**).

As far as expression specificity is concerned, a variety of tissue-specific genes have been used to produce constructs expressed in transgenic mice (**Table 1**) (*see* **Note 2**). Concerning expression efficiency, it has been previously shown that deletion of the 3'-untranslated region (UTR) of TNF results in aberrant TNF expression ***(19)***. Therefore, replacement of the 3'-UTR of TNF by the relevant β-globin sequence allows overexpression of TNF in transgenic mice and leads to pathology ***(2)*** (**Table 1**).

The length of a DNA construct used for transgenesis has so far been limited only by cloning and handling considerations. In the past we have successfully used an 80-kb P1 bacteriophage insert containing the genomic locus of the human p75 TNFR for the production of transgenic mice ***(4)***.

3.1.2. Purification of DNA

One of the most important factors influencing the efficiency of pronuclear microinjections is the purity of DNA. DNA samples should be free of contaminants (e.g., agarose, organic solvents) that might decrease the viability of the zygotes. Several methods are available for isolating DNA fragments ***(20)***. The main steps involved are described below:

1. Grow bacteria containing the desired plasmid.
2. Isolate the plasmid (*see* **Note 3**).
3. Digest the plasmid with restriction enzymes.
4. Separate the fragment from the vector using preparative agarose gel electrophoresis.
5. Elute the DNA fragment by digestion with β-agarase I.
6. Purify the fragment with tip-columns Elutip-D.
7. Dissolve the fragment in the microinjection buffer.
8. Determine the concentration of DNA (*see* **Note 4**).
9. Dilute the fragment to the correct concentration for microinjection (usually adjusted to 4–6 μg/mL) and store at 4°C for less than 2 wk.
10. Stocks should be stored at –20 °C, and dilutions should be made fresh.

It is important to note that larger DNA molecules are especially at high risk of breakage if not handled very carefully. Therefore, for large DNA fragments (e.g., P1 or BAC inserts), sodium chloride gradients or preparative pulse-field gel electrophoresis should be used.

3.1.3. Recovery of Oocytes

The choice of the genetic background of zygotes is very important, because it has accounted for variations on the severity of phenotype in transgenic mice. In most cases, a cross between two F_1 mice (e.g., C57BL/6 × CBA) is used, because such combinations provide large numbers of good-quality embryos. To control the timing of ovulation, the animals are kept in a convenient light–dark cycle (e.g., 7 PM–5 AM). Because natural matings produce low numbers of zygotes, it is preferable that females be induced to superovulate as follows:

1. Inject 3- to 4-wk-old F_1 females intraperitoneally (IP) with 5 units of pregnant mare's serum gonadotropin (PMSG), at 2 PM of day 1.
2. Inject IP the female mice with 5 units of human chorionic gonadotropin (huCG), at 12 PM of day 3.
3. Place each female with an individually caged F_1 stud male.
4. On the same day prepare the culture dishes with M16 microdrop cultures under paraffin oil and leave in the CO_2 incubator to equilibrate overnight.
5. The following morning, check for vaginal plugs and sacrifice the females that have mated.
6. Collect the oviducts in a 35-mm Petri dish containing M2 medium.

7. Transfer one oviduct at a time into another 35-mm Petri dish containing 300 μg/mL hyaluronidase solution in M2 medium.
8. Tear the oviduct with forceps close to where the eggs are located (ampulla) and release the clutch of eggs.
9. Allow the eggs to incubate in the hyaluronidase solution no longer than 10–15 min to remove sticky cumulus cells.
10. Wash the eggs several times with M2 medium to remove the hyaluronidase and transfer them in CO_2–buffered M16 medium using transfer pipets.
11. Store eggs in the M16 microdrop cultures overlaid with paraffin oil, prepared the previous day.

3.1.4. Microinjection Procedure

We perform microinjections using an inverted microscope with Hoffman optics and a set of Narishige micromanipulators. The shape of the injection pipet is one of the most important factors for egg survival after injection. The injection pipets are made from glass capillaries (borosilicate glass capillaries, thin wall with inner filament) using a pipet puller ***(13)***. The holding pipet is a blunt, heat polished pipet, which holds the egg for microinjection. Its external diameter should be between 80 and 120 μm with an opening of 15–20 μm. Even though good pipets can be drawn and flame-polished by hand using a stereoscope and a microburner, it is easier to prepare optimal holding pipets using a microforge instrument ***(13)***. Pronuclear injections are carried out in a paraffin oil-covered drop of M2 medium, set on a siliconized glass depression slide.

1. Connect the left instrument tube, through a length of paraffin oil-filled Tygon tubing, to a micrometer syringe.
2. Fill the holding pipet with Fluorinert fluid FC-40 and connect it with the left instrument tube.
3. Connect the right instrument tube, through a length of air-filled Tygon tubing, to an air-filled 50-mL glass syringe.
4. Fill the injection pipet by dipping the blunt end into the DNA solution (approx 1 μL) and connect it to the right instrument tube (*see* **Note 5**).
5. Lower the holding and injection pipets into the drop of M2 medium.
6. Transfer a small number of eggs, usually 15–20, into the drop.
7. Break the tip of the injection pipet by letting it carefully touch the holding pipet.
8. At low magnification, use the holding pipet to pick a fertilized oocyte (2 pronuclei should be clearly visible), and focus the microscope at higher magnification to locate the pronuclei. It is usually safer for the egg to be held by the area of the zona pellucida next to the polar bodies. A pronucleus can be most easily injected if it is located as close as possible to the central axis of the holding pipet and close to the injection pipet. Select the most easily accessible pronucleus and, using the holding and injection pipets, bring the egg to the best position for microinjection (*see* **Note 6**).

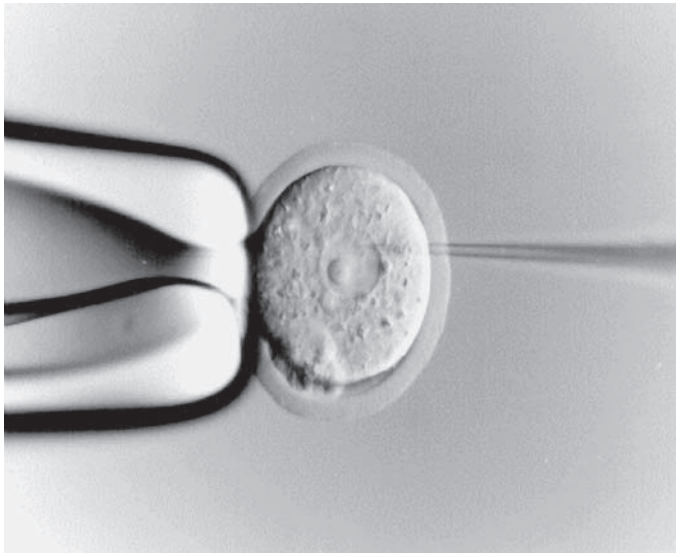

Fig. 1. Microinjection of DNA solution into one of the pronuclei of a mouse zygote.

9. Place the injection needle close to the egg and focus both the tip of the needle and the pronucleus at the same level.
10. Push the injection pipet through the zona pellucida and the egg membrane into the pronucleus. When the tip of the pipet appears to be inside the pronucleus, squeeze on the 50-mL air-filled syringe. Take care not to hit the nucleoli. If the pronucleus visibly swells, it has been successfully injected (**Fig. 1**). Then carefully withdraw the needle.
11. Place the injected oocyte to the one side of the optical field using low magnification, and proceed to the next one.
12. After having injected the first group of eggs, transfer them into M16 medium and store in the CO_2 incubator. Continue with the rest of the groups.

Microinjection is not a trivial process. A considerable learning time is needed before high efficiencies can be achieved. An experienced injector should expect that approx 75% of the eggs will survive injection. It is important to keep in mind that embryos are living material, which should be handled with care.

3.1.5. Transfer of Injected Eggs Into the Oviducts of Pseudopregnant Females

Mature F_1 female mice mated the previous night with vasectomized NMRI males are used as recipients for the injected eggs. Zygotes that have survived microinjection are usually transferred the same day (*see* **Note 7**) into the oviducts of pseudopregnant females as follows:

1. Anesthetize the pseudopregnant female by IP injection of anesthetic cocktail.
2. Swab the back of the mouse with ethanol and make a small midline incision in the skin at approximately the level of the last rib. The position of the ovary is indicated by a pink structure seen through the body wall.
3. Make a small incision and use blunt forceps to grasp and gently pull out the fat pad, which is attached to the ovary.
4. Place a clip on the fat pad to hold the oviduct in place and move the mouse under a stereo microscope. The use of a fiber optic illuminator is beneficial.
5. Expose the opening of the oviduct (infundibulum) by tearing the bursa with fine forceps (*see* **Note 8**).
6. Introduce the eggs into the oviduct using a mouth-driven, glass transfer pipet. Transfer approximately 10 eggs at the one-cell stage to each oviduct (*see* **Note 9**). Alternatively, transfer all 20 eggs in one oviduct. It will make no difference in the outcome.
7. Staple the edges of the skin together where the incision was made using one or two wound clips.
8. Return the mouse to its cage and leave it undisturbed in a warm, quiet place. Two or three recipient females are caged together in order to lower the possibility of losing some newborns due to small litter size. They usually give birth 19–20 d after the transfer.

Approximately 30% of microinjected zygotes transferred into the oviduct will develop to term.

3.1.6. Identification of the Transgenic Mice

Identification of transgenic mice is generally performed by standard Southern blot or dot/slot-blot hybridization techniques as well as by transgene-specific PCR amplification on genomic DNA prepared from mouse tail fragments.

3.1.7. Preparation of DNA From Tail Fragments of Mice

1. Cut off 1 cm of the tail into a 1.5-mL safe-lock polypropylene tube containing 0.5 mL of tail buffer.
2. Add 5 µL of 10 mg/mL proteinase K solution, mix, and incubate overnight at 55°C.
3. The next morning add 0.5 mL of the phenol/chloroform/isoamyl alchohol to each tube and vortex for 5–10 min.
4. Centrifuge for 10 min at 13,000*g* and collect the supernatant using pipet tips with cut ends to avoid any carryovers from the interface (*see* **Note 10**).
5. Precipitate DNA with 0.6 vol of isopropanol by inverting each tube several times until a white "cloud" containing DNA is visible.
6. Hook out the DNA using a sealed Pasteur pipet.
7. Immerse the DNA briefly in 70% ethanol, then in 100% ethanol, and let it dry for a few minutes.

8. Immerse the DNA in a tube containing 100 μL of sterile ddH_2O. Allow to stand for 15 min and discard the Pasteur pipet.
9. Store the DNA samples at –20°C (*see* **Note 11**).

3.1.8. Integration of Injected Genes and Establishment of Transgenic Lines

Transgenic mice that develop from injected eggs are termed "founders" and are bred with nontransgenic partners to establish transgenic lines. Recovery of two or more founders with similar phenotypes is usually considered sufficient verification that the phenotype is a result of the transgene expression. In general, it is accepted that integration occurs at a random site in the mouse genome, and that transgenes are usually inserted at a single chromosomal locus, either as single copies or more often as multiple copies in tandem head-to-tail arrays. More rarely, when exogenous DNA is integrated at two or more positions in the mouse genome, it is necessary to isolate and establish separate transgenic lines, each one having a unique integration site.

In addition, it has been observed that some of the transgenic founder mice may be mosaic for the transgene, where only a subset of cells carries the injected DNA. Mosaicism is not always a problem, since it can contribute to the survival of mice carrying an otherwise lethal or pathology-inducing transgene. For example, we have been able to analyze the pathology induced by human TNF in transgenic mice by studying the development of an early-lethal phenotype in the progeny of an unaffected mosaic transgenic founder ***(3)***.

3.2. Gene Targeting in Embryonic Stem Cells

Homologous recombination between the mammalian genome and homologous sequences placed in a targeting vector is known as gene targeting. This type of homologous recombination in mouse embryonic stem cells (ESCs) has made it possible to introduce directed specific mutations into the mouse germline and study the function of the mutated gene in the animal (**Fig. 2**). The most common application of this technology is the disruption of a target gene in the mouse germline (knockout mice). Interestingly, the more recently adopted combination of homologous and site-specific recombination in mammalian cells allows the introduction of subtle mutations in a targeted locus (*see* **Subheading 3.2.2.**).

3.2.1. Designing a Vector for Knocking Out a Gene

A targeting vector should contain two fragments of homologous sequences to a gene of interest that flank a functional region of the gene, e.g., exons. In order to isolate all of the clones that have stably integrated the vector DNA

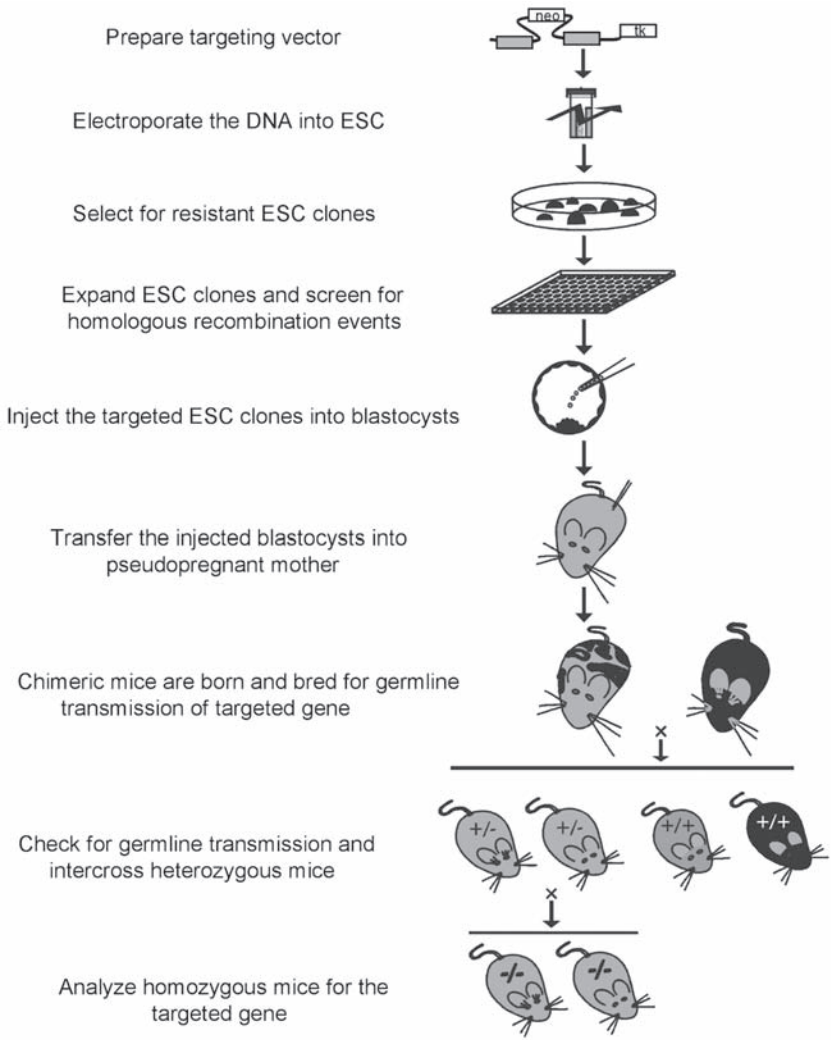

Fig. 2. Schematic representation of gene targeting in ESC.

(random or targeted), a positive selectable marker, e.g., the neomycin resistance gene (neo), is placed between the homology arms ***(21)***. Upon homologous recombination, the positive selectable marker will replace the functional region and create a "null" allele. Negative selection, usually imposed by the HSV thymidine kinase (tk) gene product when placed outside of one homology arm, is useful for the elimination of cells in which random integration has occurred.

In homologous recombination events, the tk gene is not introduced into the genome, and the cell will survive the negative selection. Thus, selection against

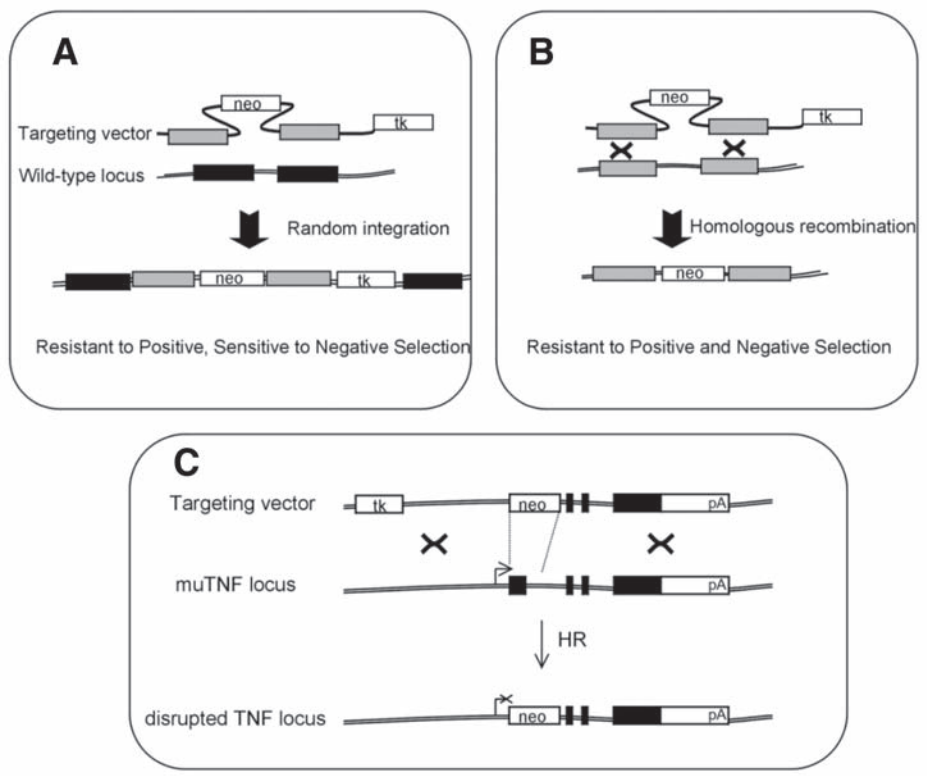

Fig. 3. Schematic representation of vector/target recombination events using the positive–negative selection approach. **(A)** Random vector insertion. **(B)** Gene targeting via homologous recombination (HR). **(C)** Gene-targeting vector used for the generation of TNF knockout mice *(7)*.

this cassette will kill cells that have integrated the vector at a random location (**Fig. 3A**), while targeted clones will survive (**Fig. 3B**). An example of the targeting vector used for the generation of TNF knockout mice by our research group in the past *(7)* is given in **Fig. 3C** (*see* **Note 12)**.

The length and the sequence of the homologous sequences in the vector affect the targeting frequency. The homologous sequences should be in the range of 5–8 kb and should be derived from genomic libraries isogenic with the ES cells used in the targeting experiment *(22–24)*. The targeting vector should be linearized before transfection into ES cells at a site outside the homologous sequences. It is also important to design a diagnostic Southern blot screening strategy for discriminating targeted ESC clones. Probes should be

tested and fragment sizes for both alleles (endogenous and targeted) with specific enzymes should be known before gene targeting.

3.2.2. Generating Subtle Mutations With Gene Targeting Techniques

In order to introduce subtle changes into a locus, a vector should be designed where the mutation is introduced in one of the homolgous arms, and the positive selectable marker can be removed from the recombinant locus. One of the most straightforward ways to remove the selectable marker after homologous recombination is to use site-specific recombination. Site-specific recombinase systems consist of two basic elements: the recombinase enzyme, and a DNA sequence that is specifically recognized by the particular recombinase. Currently, there are two such recombinase systems that have been applied in mouse gene targeting experiments: the Cre-loxP system from the bacteriophage P1 ***(25,26)*** and the Flp-FRT system from the budding yeast *Saccharomyces cerevisiae* ***(27)***. The site-specific recombinase Cre (**C**auses **re**combination) has been widely used with high recombination efficiencies in our murine systems. Cre protein catalyzes recombination between two 34–bp-long loxP (**lo**cus of **x**-ing-over of **P**1*)* recognition sites. Any DNA segment, flanked by two loxP sites ("floxed") of the same orientation, can be excised by Cre as a circular molecule (**Fig. 4A**), whereas it can be inverted when flanked by two loxP sites with opposite orientation. Recombination between two loxP sites is carried out in a precise way that leaves behind one fully functional loxP site.

To excise the positive selectable marker in mice, the targeted gene harbouring the floxed neo marker should first be transmitted through the germline via chimeras. Fertilized oocytes from mutant heterozygous mice are used for excision of the neo gene by transient expression of Cre as follows:

1. Microinject fertilized oocytes with a Cre expression plasmid (pMC-Cre-polyA) ***(28)*** at a concentration of 4–6 ng/μL.
2. Screen for deletion of neo marker in offspring heterozygous for the targeted gene, using PCR or Southern blot hybridization analysis.

Schematic representation of introducing mutations on the germline of mice using gene targeting and site-specific recombination approaches is shown in **Fig. 4B**. With this approach we have previously generated the $TNF^{\Delta ARE}$ mice, in which deletion of the 3' AU-rich elements (ARE) from the TNF mRNA led to TNF overexpression and development of chronic inflammatory poly-arthritis and Crohn's-like inflammatory bowel disease ***(19)***.

3.2.3. Embryonic Stem Cells

Embryonic stem cells (ESCs) are derived directly from the inner cell mass (ICM) of mouse blastocysts. When cultured in vitro they remain diploid and pluripotent even after a significant number of passages ***(22,29)*** maintaining

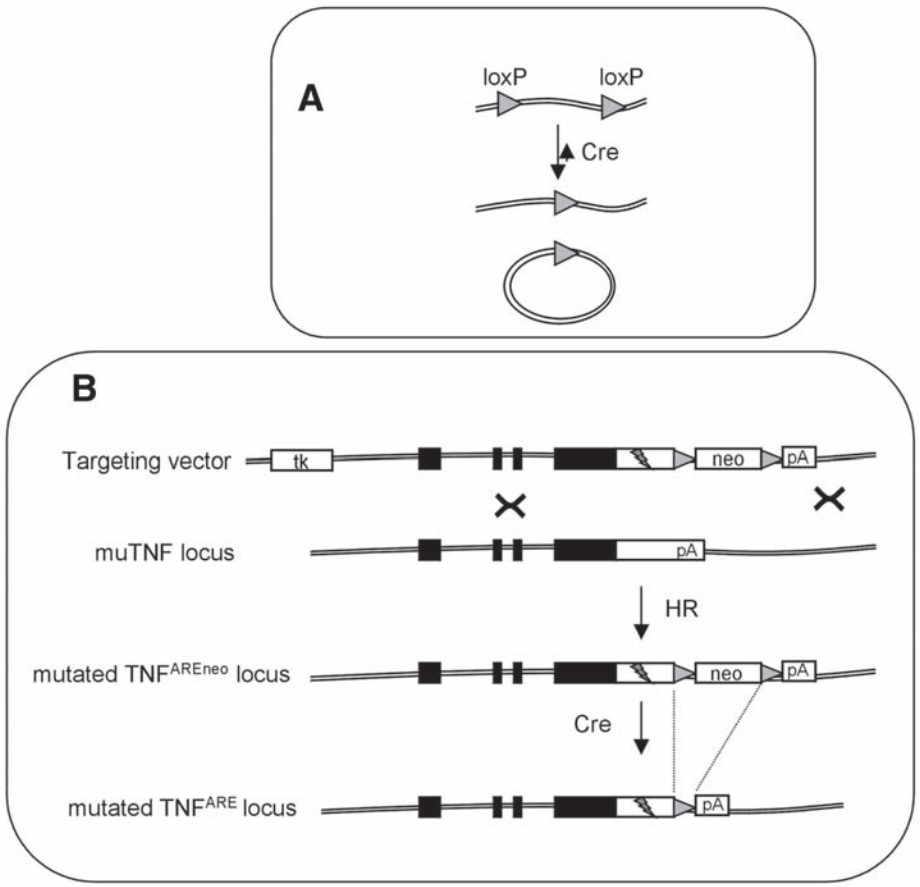

Fig. 4. Generating subtle mutations with gene targeting. **(A)** Cre mediated recombination. Recombination between two loxP sites (triangles) with the same orientation causes excision of the intervening segment as a circular molecule. **(B)** The gene targeting approach followed for the generation of the $TNF^{\Delta ARE}$ mice ***(19)*** is illustrated here. In an initial step the mutated $TNF^{\Delta AREneo}$ mice are produced by homologous recombination (HR) in ESC. Subsequently, the neo marker is excised (depicted by dotted lines) by transient expression of Cre in $TNF^{\Delta AREneo}$ zygotes producing the $TNF^{\Delta ARE}$ mice. Deletion of 69 bp containing the 3'ARE from the TNF locus is illustrated here as a lightning bolt (✎).

their ability, like ICM, to form chimeras. These properties enable ESCs to form among other cell types fully functional germ cells in chimeras ***(30)***. This feature makes it possible to generate mice derived exclusively from a single cell that has been cultured and manipulated in vitro. ESC lines have been derived from both inbred and outbred strains of mice. However, most existing ESC

lines are derived mainly from the 129 strains, although the C57BL/6 mouse strain is also used. Extensive description of the methods for isolating and culturing ESCs can be found in detailed laboratory manuals ***(13,31)***.

3.2.3.1. ESC Cultures

ESCs can be maintained in an undifferentiated state by optimal culture conditions. The quality of the culture medium and of fetal calf serum (FCS) is very important for the in vitro maintenance of ESC lines. Because only a limited number of sera are found to be of appropriate quality for ESCs, FCS should be routinely batch-tested. The ability of ESCs to remain pluripotent in culture is shown to be dependent on the presence in the culture medium of the cytokine leukemia inhibitory factor (LIF) ***(32,33)***. Usually recombinant LIF can be supplemented in the ESC medium. Another approach, more economical, for maintaining pluripotential ESCs is to culture them on layers of mitotically inactivated feeder cells that produce and secrete LIF, as well as other factors, into the medium.

3.2.3.2. Feeder-Cell Layers

Both permanently growing cell lines (e.g., STO fibroblasts) and primary mouse embryonic fibroblasts (PMEFs) have been successfully used as feeders. We use inactivated SNL fibroblasts (STO cells which are neo resistant) as feeders for some ESC lines such as CCE, and PMEFs for others such as R1(129/svJ), 129/3(129/ola), and Bruce 4 (C57Bl/6). Either of the feeder-cell types can grow happily in medium DMEM supplemented with 10% FBS/FCS.

3.2.3.3. Preparation of PMEFs*

1. Set up females with males (any mouse strain can be used for the preparation of PMEFs but a neo-resistant strain would be more useful). The following day check for copulation plugs (day 0.5 of pregnancy). Remove the mated females to a separate cage.
2. On day 13.5 of pregnancy, sacrifice the females, open the peritoneal cavity and remove the uteri carrying the embryos. Wash the uteri a couple of times in PBS and using sterilized dissection instruments dissect the embryos from the uteri in PBS. Remove the yolk sac, amnion, and placenta, and wash the embryos twice in fresh PBS to remove any blood.
3. Using a pair of fine forceps remove the head, the heart, the liver, and other viscera.
4. Wash the carcasses twice with PBS, put them—per litter—in a 60-mm dish, and mince finely with a sterile razor blade.
5. Remove the embryo carcasses into a sterile 15-mL conical tube containing 5–8 mL trypsin/EDTA solution.
6. Place the tube on a rotator in an incubator at 37°C for 10 min.

*Adapted from **refs. *13*** and ***34***.

7. Allow big pieces to settle out for 1–2 min, remove half of the trypsin/EDTA volume containing the loose cells into another tube, and neutralize with twice the volume of DMEM plus 10% FCS.
8. In the tube with the embryo pieces, replenish with half volume trypsin/EDTA, and repeat **steps 6** and **7** twice.
9. Mix the three tubes with neutralized trypsin—dissociated/single cell suspension—into a 50-mL conical tube and centrifuge.
10. Discard the supernatant and resuspend cells in DMEM plus 10% FCS. Plate out the suspension into three to four 100-mm tissue culture dishes, and incubate.
11. The following day change the medium to remove the cellular debris.
12. When the plates are confluent, split them 1:4 to 1:5 and allow them to grow to confluency. When confluent, freeze most cells into aliquots to have in stock. Process a small amount for your needs until the cell growth rate slows considerably and the cells change morphology. In this case, thaw a vial from your frozen stock and start expansion (*see* **Note 13**).

3.2.3.4. Preparation of Feeder-Cell Layers

1. In a confluent 100 mm dish of STO fibroblasts or PMEFs, aspirate the medium and replace with 6 mL DMEM plus 10% FCS. Add mitomycin C at a final concentration of 10 μg/mL (light-sensitive; should be thawed and mixed well before use) and incubate at 37°C, 5% CO_2, for 2–3 h.
2. Gelatinize the tissue culture dishes you will use to plate the feeders by adding enough of a 0.1% gelatin solution to cover their surface. Leave them at room temperature for 1–2 min. Aspirate the gelatin solution before plating the feeder cells.
3. Aspirate the mitomycin C-containing medium from the cells and wash them twice with 8 mL of PBS. Trypsinize the cells with 1 mL of the trypsin-EDTA solution for 3 min incubation at 37°C, 5% CO_2. Collect the cells—in a single cell suspension—in 5–6 mL DMEM plus 10% FCS.
4. Count the cells and plate in gelatin-coated dishes at a concentration of 2–3.5 × 10^5 cells/mL (i.e., 2 mL for a 35-mm dish, 10 mL for a 100-mm dish, and so on) (*see* **Note 14**).
5. Change the medium to ESC medium before adding ESCs.

3.2.4. Transfection of ESC

Several methods are available for the introduction of DNA into mammalian cells ***(35)***. Among them electroporation is the most widely used for gene targeting in ESCs. The protocol we use for electroporation is as follows:

1. Prepare the targeting vector DNA on a CsCl gradient and linearize it by digestion with the appropriate restriction enzyme (*see* **Note 15**). Check by gel electrophoresis that digestion is complete and extract the DNA by treatment with phenol/chloroform and chloroform. Precipitate with ethanol, wash with 70% ethanol, and resuspend in sterile double-distilled H_2O to 1 μg/μL.

2. On the day of electroporation, change the medium on your subconfluent cultures 2–4 h before harvesting to ensure that the cells are actively growing.
3. Wash the plates twice with 10 mL PBS, add 1.5 mL of the trypsin-EDTA solution, and place them back into the incubator for 4–5 min. Add 6 mL of medium to each plate and pipet vigorously to achieve single-cell suspension.
4. Centrifuge cells at 270*g* for 5 min and resuspend them in PBS. Count cell numbers.
5. Recentrifuge the cells and resuspend them in PBS at a final concentration of $1.25–2 \times 10^7$ cells/mL; the concentration depends on type of ESCs used.
6. Mix 0.8 mL of cell suspension with 20–40 μg of linearized vector in a sterile 1.5-mL tube.
7. Set up the electroporator for 240 V and 500 μF.
8. Transfer the suspension into an electroporation cuvet, place the cuvet in the electroporation chamber, and apply a single pulse. Make a note of the time constant.
9. Remove the cuvet and place it on ice for 15–20 min.
10. Resuspend the contents of each cuvet into a total of 30–40 mL ESC medium, and transfer into 3–4 100-mm plates containing feeder cells. Make sure cells are dispersed evenly—by rocking not swirling—when plated.
11. Change the medium the next morning and then once every day.
12, Two days (36–48 h) after electroporation begin drug treatment for positive selection (e.g., G418 for neo resistance) (*see* **Note 16**). Negative selection can be initiated 24 h later. In the case of gancyclovir, the concentration to be used is 2 μ*M*.
13. Feed the cells with fresh medium every day. Resistant colonies should appear 5–8 d after electroporation, and are ready to be picked within 3 d.

3.2.5. Picking and Expanding ESC Colonies

Single colonies are picked and transferred into single wells of a U-shaped 96-well plate containing trypsin-EDTA solution.

1. Add 25 μL of trypsin-EDTA solution in each well of a U-shaped 96-well plate.
2. Wash the plate containing the ESC colonies with 10 mL of PBS, and fill it with 10 mL of PBS.
3. Use a 20-μL micropipet, and sterile disposable pipet tips under a stereoscope to pick up individual colonies in a small volume of PBS (5–10 μL). Transfer individual colonies to the plate prepared in **step 1**.
4. After having finished one 96-well plate, place it in the incubator for 20 min.
5. Take a flat-bottomed 96-well plate containing feeder cells, aspirate the medium, and add 70 μL of ESC medium to each well.
6. Remove the plate with trypsinized colonies from the incubator and add 150 μL of ESC medium to each well. Use a multichannel pipet (8–12 channel) and sterile, disposable pipet tips to dissociate the ESC colonies by vigorously pipetting them up and down.
7. Transfer the contents of each well to the respective well of the plate prepared in **step 5**. Change the medium every day.

8. When cells are approaching confluency, split them 1:3. For this procedure, wash each well twice with 100 µL of PBS, add 30 µL of trypsin-EDTA solution and place them in the incubator for 3–5 min. Add 200 µL of ESC medium into each well, dissociate the colonies by vigorous pipetting, and split the contents in two feeder-cell-containing 96-well plates and one 96-well plate treated with gelatin only, without feeders. Take special care to change tips for each set of wells in order to avoid cross-contamination between colonies.

Two days later, the two plates with growing clones on feeders will be frozen, and the third plate will be split into two to three gelatinized 96-well plates without feeders, which will be used to prepare DNA.

3.2.6. Storage and Recovery of ESC Clones

Screening large numbers of ESC clones may be a time-consuming process. To minimize the time that ESCs are kept in culture, it is preferable to freeze them until screening is completed. ESCs may be frozen directly in the 96-well plate, making it possible to simultaneously freeze a large number of clones.

3.2.6.1. Freezing ESC Clones in 96-Well Plates

Cells are frozen in FCS with 10% DMSO, which is used in general to freeze ESCs (*see* **Note 17**)

1. Grow ESC clones close to confluency in feeder-cell-containing 96-well plates.
2. Feed the cells with fresh medium 2 h before freezing.
3. Aspirate the medium and wash the wells twice with 100 µL of PBS.
4. Add 25 µL of trypsin/EDTA solution per well and place the plates back into the incubator for 3–5 min.
5. Remove the plate from the incubator and add 100 µL of FBS/FCS in each well. Pipet up and down using the multichannel pipet until the ESCs are in single-cell suspension.
6. Transfer 110 µL from each well into a new 96-well plate and add dropwise an equal volume of 20% DMSO in FCS to obtain the correct 10% final concentration. Work as fast as possible.
7. Cover-seal the wells, under the lid, with SealPlate (press-apply adhesive sealing film for microplates) to prevent evaporation during storage at –70°C, and to prevent water from getting in during thawing (*see* **Note 18**).
8. Wrap the plates with insulating material—to ensure gradual freezing—such as bubble-wrap or cotton, place them in a styrofoam box, and freeze in a –70°C freezer until analysis of DNA is completed.

3.2.6.2. Thawing ESC Clones From 96-Well Plates

1. Prepare in advance 96-well plates containing feeder cells. Before use, feed with 100 µL of fresh ESC medium.

2. Warm sterile distilled water to 37°C and pour into a sterile 500 cm^2 tissue-culture or Pyrex dish. Place it in the incubator to remain equilibrated at 37°C.
3. Remove one frozen 96-well plate from the –70°C freezer, unwrap the insulating material, and place the plate directly on the surface of the water. Take care to prevent water entering the wells, by not having too much water.
4. Monitor the plate until its contents are thawed (approx 15 min).
5. Transfer each of the selected clones into a sterile 1.5-mL Eppendorf tube containing 1 mL of ESC medium. Wash the well with 200 μL of ESC medium to make sure that all ESCs are transferred into the tube.
6. Spin at 270*g* for 5 min and discard the supernatant. Resuspend the cells in 200 μL of ESC medium and transfer the thawed clones into individual wells of the plate prepared in **step 1**.
7. Feed the cells every day and divide when they become subconfluent.

3.2.7. Extraction and Restriction Enzyme Digestion of DNA in 96-Well Plates

1. Grow ESC clones in gelatinized 96-well plates until fully confluent.
2. Wash each well twice with 100 μL of PBS and add 50 μL of lysis buffer containing 400 μg/mL of proteinase K.
3. Seal the plate with SealTape and transfer it into a prewarmed box containing wet paper towels to create a humidified atmosphere; incubate in a 60°C oven overnight.
4. The next day move the plate to the bench and allow it to equilibrate to room temperature.
5. Add 2 vol of 100% ethanol to each well and let the plate stand on the bench for 30 min. Precipitate can be seen in the form of strings attached to the bottom of the dish. Spin at 270*g* for a couple of minutes if you want.
6. Dump off the ethanol by inverting the plates. Most of the DNA should remain attached to the bottom of the wells.
7. Wash the wells three times with 100 μL of 70% ethanol; each time remove the wash by inversion. At this stage the plates can be stored by leaving the final ethanol wash on, covering the plate with film, and leaving at –20°C.
8. After the last wash, air-dry the DNA-containing plate on the bench. Do not let the DNA dry too much as it will be then difficult to dissolve. However, be careful not to leave alcohol traces because it may interfere with some enzyme activity.
9. Prepare the restriction digestion mix.
10. Add 35 μL of the digestion mix into each well and incubate overnight at the appropriate temperature in a humidified atmosphere.
11. The next day load the digested DNA samples on agarose gels and prepare for Southern blot hybridization analysis.

3.2.8. Identification of Targeted ESC Clones

Screening for targeted ESC clones can be performed either by PCR or by Southern blot hybridization. PCR is often used for screening pooled clones,

and the individual clones of the positive pools are further analyzed by Southern blot. To minimize the risk of false-negative clones, we prefer to directly analyze clones by Southern blot and hybridization.

3.2.9. Generation of Chimeric Mice

Chimeric mice can be generated by one of several methods, including the injection of ESCs into blastocysts, aggregation or co-culture of 8-cell-stage embryos with ESC, and injection of ESC into 8-cell-stage embryos. Methods for the aggregation ***(36)*** and co-culture ***(37)*** of 8-cell-stage embryos with ESCs are relatively simple, and they do not require the sophisticated equipment used in the microinjection procedures. Morula injection has been developed relatively recently ***(38)*** as an alternative to the blastocyst injection method. However, blastocyst injection is currently the most widely used method for the production of germline chimeras using targeted ESC clones.

3.2.9.1. Production of Germline Chimeras by Injection of ESCs Into Mouse Blastocysts

We mostly use 129-derived ESCs to introduce our mutations. The choice of strain as blastocyst host for 129 cells found its match early on in C57BL/6 mice ***(39)***. This strain has been proved to be a compatible host with very efficient germline transmission. In addition, the differences in its coat color and other genetic loci provide very useful markers ***(40)***.

3.2.9.2. Setting Up Matings

1. Day 0: Set up matings between C57BL/6 males and females. Females in estrus (at least 6 wk old) are selected by examining for the appearance of a pink and swollen vagina.
2. Day 1: Identify females that have mated by checking for copulation plugs and place them in a separate cage for later collection of 3.5-d blastocysts (day 4). Set up additional matings between F_1 (C57BL/6 × CBA) females and vasectomized males for the production of pseudopregnant females.
3. Day 2: Check the F_1 females for plugs and place those that have mated in a separate cage. They will be used on day 4 (at 2.5 d of pseudopregnancy) as recipients for the injected blastocysts (*see* **Note 19**).

3.2.9.3. Recovery of Blastocysts

1. On the afternoon of day 3 prepare microdrop culture of M16 medium, in a 35-mm dish, under light mineral oil. Let culture dishes equilibrate overnight in a 5% CO_2, 37°C incubator.
2. On day 4, kill the C57BL/6 females (with a plug on day 1) and dissect out both uterine horns using two incisions: one next to the oviduct and the second at the distal end junction of the two uterine horns.

3. Use a 1-mL syringe (27-G needle) filled with medium M2 to flush the blastocysts out of the uteri into a 35-mm tissue culture dish containing 1 mL M2.
4. Collect the blastocysts under a stereoscope using a mouth-controlled, heat-drawn transfer pipet (with diameter slightly bigger than that of an expanded blastocyst). Wash in M2 medium and transfer into microdrop cultures of M16 medium overlaid with light mineral oil. Store in a 5% CO_2, 37°C incubator. At this stage, some blastocysts may not be fully expanded; they will become so later during the day.

3.2.9.4. Preparation of the Holding and Injection Pipets

The holding pipet is essentially the same as the one used for pronuclear injections (*see* **Subheading 3.1.4.**), except that a bend of approx 30° is introduced 2–3 mm from its end, using a microforge. The injection needle is used to collect individual ESCs and introduce them into the blastocoel cavity. It is prepared as follows:

1. Use thin-walled borosillicate capillaries like the ones used for pronuclear injections, but without an inner filament. For our needles we use the Kopf puller as well, but with a wider filament and different settings for Heat and Solenoid. The aim is to produce needles that have a relatively long section at the appropriate internal diameter, which should be slightly larger than an ESC (12–15 μm), allowing single cells to move freely without being deformed.
2. Place the pulled needle on a transparent silicone rubber sheet under a stereomicroscope, and using a sharp scalpel blade, snap it at the region of the appropriate diameter to create a sharp beveled point.
3. Use the microforge to make a bend of approx 30° close to the end of the injection needle. Make sure that the bevel is facing to the side.

3.2.9.5. Setting Up the Injection Chamber

The microscopes and micromanipulators described for pronuclear injections (*see* **Subheading 3.1.4.**) are also suitable for blastocyst injections. We again use Hoffman optics performing the injections at ×20 setting. The injections are done in the lid of a 35-mm tissue-culture dish because it is conveniently shallow and allows free movement of the holding and injection pipets. The medium used is DMEM supplemented with 10% FBS and 10 m*M* HEPES.

1. Spread evenly 1 mL of medium on 3/4 of the lid and overlay with light mineral or paraffin oil.
2. Set up the holding pipet as for pronuclear injections (*see* **Subheading 3.1.4.**). Fill the injection needle with light mineral oil and connect through a length of Tygon tubing to a glass syringe controlled by a sensitive micrometer head.
3. Lower the holding and injection pipets into the injection dish, and make appropriate adjustments to position their ends parallel to the bottom of the dish.

3.2.9.6. Preparation of ESCs for Blastocyst Injections

1. Two hours before harvesting, feed a subconfluent ESC-containing dish with fresh ESC medium.
2. Wash the plate twice with PBS, add trypsin-EDTA solution (approx 300–500 μL for a 35-mm dish) and leave it in the incubator for 3–5 min (*see* **Note 20**).
3. Add 2 mL of ESC medium and pipet vigorously to dissociate colonies into a single-cell suspension. A third to a half of the dish content will give you a sufficient amount of cells to use for injections. Plate the corresponding suspension on a gelatinized 35-mm dish.
4. Transfer the dish into the incubator for 35–45 min (*see* **Note 20**). During this period, feeder cells attach strongly to the surface of the gelatinized dish, while most of the viable ESCs only begin to adhere.
5. Carefully remove the medium containing the nonadherent cells. Add 2 mL of ESC medium to the dish and suspend the loosely adhering ESCs by pipetting gently so that you avoid removing the attached feeders with extensive mechanical action.
6. Centrifuge the suspension at 270*g* for 4 min at room temperature, resuspend the cell pellet in 0.5 mL ESC medium, and keep on ice.

3.2.9.7. Blastocyst Injection

1. Transfer 10 blastocysts into the injection dish.
2. Collect 12–18 ESCs in the injection needle (*see* **Note 21**). Select the smaller round cells with smooth, uniform appearance, as these are the healthy viable ones.
3. Use the holding pipet to pick up a blastocyst and focus in an appropriate point for injection. (These are usually points of intercellular junctions between adjacent trophectoderm cells.)
4. Bring the point of entry and the point of injection needle into the same focal plane (**Fig. 5**). Push the needle into the blastocoel cavity with a steady and smooth movement. A very slow movement may result in the blastocyst collapsing, making further penetration of the needle and injection impossible.
5. Release the ESC by carefully applying positive pressure. Shortly after injection the blastocyst collapses.
6. After having injected all the blastocysts, place them back into the incubator, where they are kept until they are transferred into foster mothers. Most commonly they start to re-expand by the time you are ready to transfer them.

3.2.9.8. Transferring Blastocysts Into the Uteri of Pseudopregnant Females

1. Anaesthetize the recipient female (see **Subheading 3.2.9.2.**) by an intraperitoneal injection of 0.1 mL of anaesthetic.
2. Swab the back of the mouse with ethanol and make a small midline incision in the skin at approximately the level of the last rib. Locate the position of the ovary, indicated by a pink structure seen through the body wall.

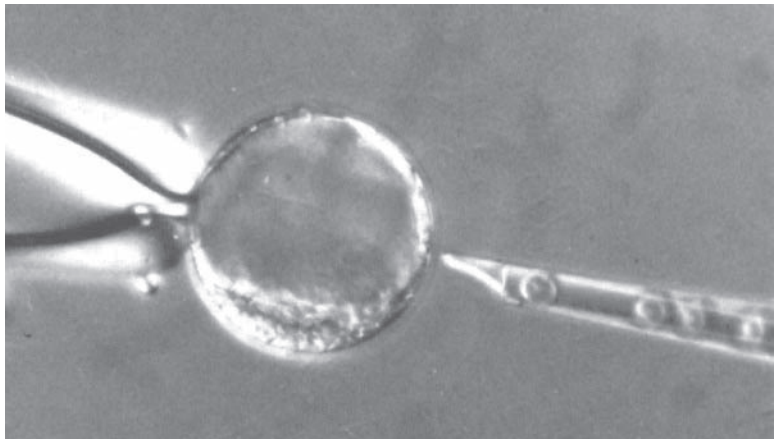

Fig. 5. Injection of ESC into the blastocoel cavity of a mouse blastocyst.

3. Make a small incision with Iris scissors through the body wall, and use blunt forceps to grasp and gently pull out the fat pad, which is attached to the ovary, thereby exposing the uterus. Clip fat pad to keep system in place.
4. Use a 27-gage needle to make a hole in the uterus close to the oviduct end.
5. Use a finely drawn transfer/Pasteur pipet to transfer eight blastocysts and a couple of air bubbles—indicators that embryos are in—into the uterus through the hole created by the needle. Uterian transfer is done unilaterally. The maximum number of blastocysts transferred per foster mother is 12 (*see* **Note 22**).
6. Gently push the uterus back into the peritoneal cavity.
7. When the operation is completed, staple together the edges of the skin where the incision was made using one or two small wound clips.
8. Keep the females warm until they have recovered from the anaesthetic. They should give birth 17 d later.

3.2.9.9. Detection of Chimerism, Test Breeding

1. Identification of chimeric newborns can be made at around 7 d after birth by the presence of the agouti coat color (derived from the ESC) on the black (C57BL/6) background. Since ESC lines with a male karyotype are more often used, expect a distortion of the sex ratio (towards males) in chimeric mice.
2. Cross male chimeras with C57BL/6 females to obtain ESC-derived progeny (agouti coat color).
3. Confirm germline transmission of the targeted allele, which is expected in 50% of the agouti progeny, by DNA analysis of mouse tail fragments.
4. Cross mice heterozygous for the targeted allele to obtain homozygous knockout mice.

3.3. Conditional Gene Targeting

As presented in **Subheading 3.2.**, conventional gene targeting generates a modified allele in all cells of the mouse. Conditional gene targeting refers to a gene modification in the mouse that is restricted to certain cell types (tissue-specific), to a particular stage within development (temporal-specific), or both ***(11)***. This methodology is particularly useful for elucidating a complete picture of gene function in cases where: (1) the conventional knockout leads to an early lethal phenotype, and/or (2) genes may exert their function at several stages of ontogeny and in different cell types.

For a conditional gene-targeting experiment, two separate mouse strains are typically generated and intercrossed; one carrying the conditional allele, a gene segment (or the entire gene) flanked by two loxP sites, and another expressing Cre recombinase (*see* **Subheading 3.2.2.**) in certain tissues or cell types, either constitutively or following induction by exogenous stimuli (**Fig. 6A**). In offspring, only cells expressing the Cre delete the target gene segment. This binary design offers great versatility to the system, as different Cre transgenics can be crossed to the same conditional allele to study gene function in a variety of cells.

3.3.1. Engineering Conditionally Targeted Alleles

Gene constructs that can be modified by Cre are usually introduced into the mouse genome by gene targeting (*see* **Subheading 3.2.**). Therefore, the rules of conventional gene targeting also apply in this case. The aim of gene targeting for the production of Cre-modifiable lines is to introduce loxP sites at specific and predefined places into the gene of interest, so that Cre-mediated recombination between these loxP sites will usually result in reactivation, inactivation, or replacement of a gene. All three types of conditional gene modifications have been successfully applied in mice ***(41–44)***.

Currently, the most popular use of conditional genetics is conditional gene inactivation using the "three-loxP" strategy developed by H. Gu and colleagues ***(41)***. The targeting vector should contain three loxP sites all in the same orientation, two flanking the selectable marker and the third one placed at such a distance from the loxP-flanked selectable marker so that the part of the gene to be modified is included between them (**Fig. 6B**) (*see* **Note 23**). After targeting of the 3-loxP vector into the genomic locus, the selectable marker can be removed by transient expression of Cre in fertilized oocytes as described in **Subheading 3.2.2.** As all three loxP sites are in the same orientation in the targeted allele, there will be three possible recombination products due to partial excision by Cre. After selection of the desired conditional allele among the

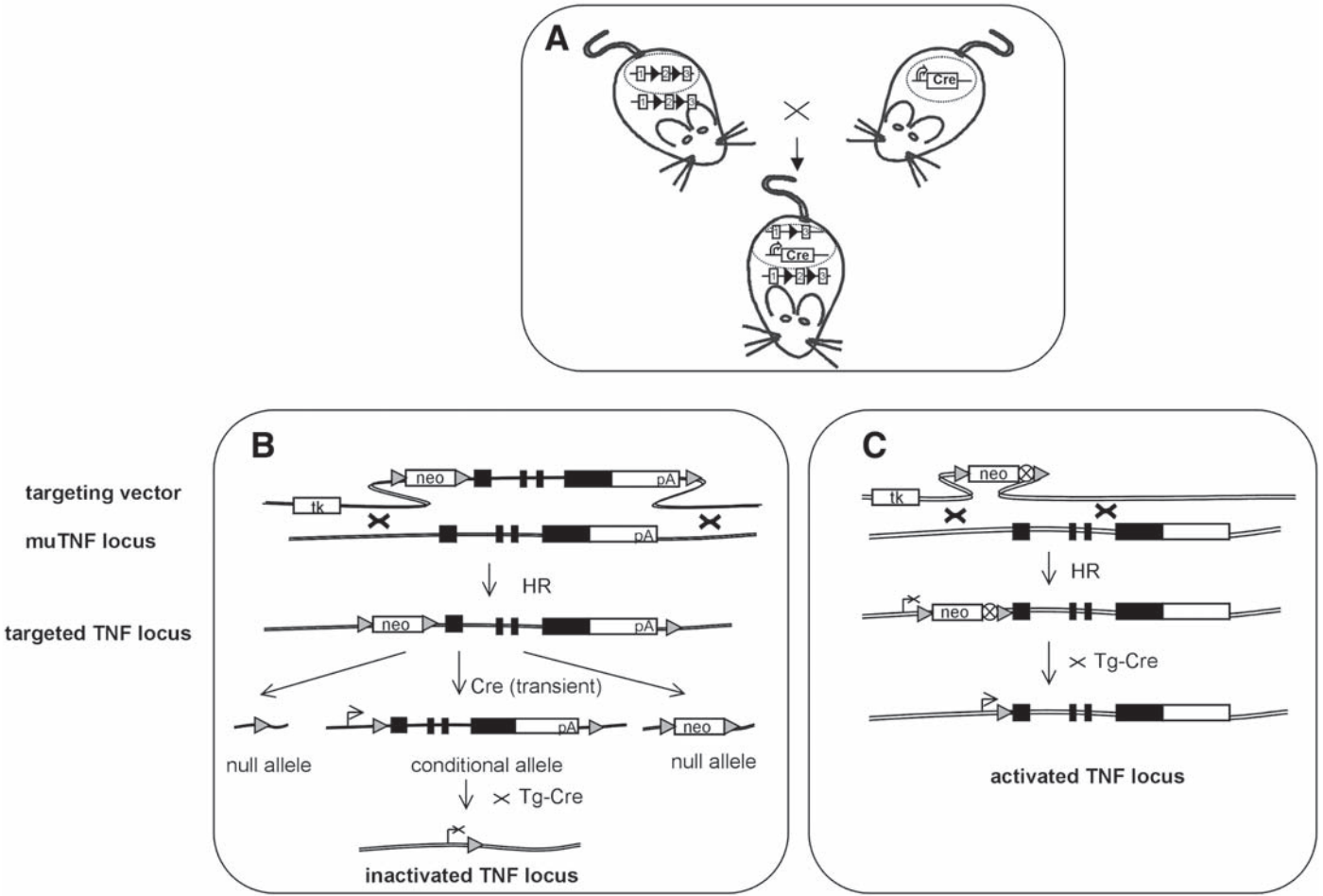

Fig. 6. Conditional gene targeting requires crossing between two separate mouse strains, one carrying the conditional allele and another expressing tissue-specific Cre recombinase **(A)**. In the double mutant mouse, if Cre is expressed in a cell it removes the loxP-flanked region rendering an allele either inactive **(B)** or active **(C)**. Examples of such applications are illustrated for the TNF locus.

null recombination products, and generation of the conditional mice, a further crossing to various strains expressing Cre recombinase in a cell-type-specific or inducible manner is required for conditional inactivation of the gene. The target gene becomes inactivated only in cells expressing Cre, but remains active in all other cells of the body.

For conditional gene reactivation, the gene is initially inactivated by the introduction of loxP-flanked inhibitory sequences into an area important for gene expression. Such areas may be a specific intron or a site between the transcription initiation and the ATG starting codon of the gene of interest. Removal of the inhibitory sequences by Cre-mediated recombination should result in a fully functional gene. By crossing to a Cre-expressing line, the inhibitory sequences are removed only in those tissues, or only after those developmental stages, in which Cre is expressed, allowing the conditional expression (reactivation) of the gene (**Fig. 6C**).

3.3.2. Cre-Expressing Transgenic Lines

The extent to which conditional gene targeting can be applied in biomedical studies depends at a technical level on the availability of Cre transgenic lines expressing Cre at sufficiently high levels under strict cell-type-specific and/or inducible control. At present, a wide number of Cre transgenic animals is available worldwide (*see* **Note 24**).

3.3.2.1. Generating Cell-Type-Specific Cre-Expressing Transgenic Mice

Both conventional transgenesis (*see* **Subheading 3.1.**) and targeted transgenesis (***15***) have been used for generating Cre-expressing transgenic lines. Cell-specific expression of Cre can be achieved by certain promoter/enhancer combinations. The choice of promoter/enhancer combination should also be based on developmental timing of expression, because even transient Cre-expression during development or in progenitor-cell types would result in generalized excision in the adult. In our lab, we have generated and characterized a collection of various Cre-expressing mice, which allows gene targeting in T cells, myeloid cells, hepatocytes, follicular dendritic cells and B cells, synovial cells, oligodendroglia, or oligodendrocytes (*see* **Note 24**).

3.3.2.2. Inducible Genetic Modifications

Inducible Cre expression is extremely useful in the analysis of the role of certain genes in adult animals, because it offers the opportunity of gene modification after the completion of the normal development of the organism or of its adaptive cell systems, such as the neuronal and the immune system. Although constitutive cell-specific Cre expression can be achieved with the

appropriate combination of promoters and enhancers, temporal control of Cre-mediated recombination can be exercised by regulating either the transcriptional or the posttranslational level of Cre expression. The most widely used binary transcription transactivation systems are the tetracycline-dependent regulatory systems. The tetracycline-inducible gene-expression system uses the DNA-binding domain of the tetracycline repressor (TetR) protein and the VP16 transcriptional activator domain, which are fused together. There are two versions of this system ***(45)***. In the original system, the transactivator (tTA) cannot bind DNA when tetracycline is present ("tet-off"), whereas in the modified version, the "reverse tTA" (rtTA) binds DNA only when the tetracycline is present ("tet-on"). A precise control on Cre expression can be accomplished by tissue-specific expression of the transactivator and administration of the inducer. Both tetracycline and ecdysone have been successfully used in transgenic mice ***(46,47)***.

Posttranslational control can be achieved by fusing Cre with a mutated ligand-binding domain (LBD) of steroid hormones that only bind synthetically produced steroid-hormone analogues. The fusion protein can be expressed under the control of a constitutive cell-specific promoter, but it remains in the cytoplasm. Administration of the synthetic analogue, such as Tamoxifen or RU-486, causes the translocation of the fusion protein to the nucleus where Cre gains access to loxP-flanked DNA targets ***(48–50)***.

3.3.2.3. Functional Characterization of Cre-Expressing Transgenic Lines

The efficiency and specificity of Cre-mediated recombination need to be tested at the cellular level using a transgenic reporter mouse line. Cre-expressing mice should be crossed to a reporter line carrying a reporter gene such as β-galactosidase (β-gal), green fluorescent protein (GFP), or placental alkaline phosphatase (PLAP), in an inactive form, which, however, can be reactivated by Cre-mediated recombination. This recombination is usually achieved by the insertion of loxP-flanked inhibitory sequences between a ubiquitously expressed promoter and the reporter gene. By crossing the reporter line with a Cre line, the inhibitory sequences are removed only in Cre-expressing cells, thus allowing their identification. We have routinely used a Z/EG double reporter (lacZ/EGFP) mouse line ***(51)*** and a knockin *lacZ* into the ROSA26 locus as reporter lines ***(52)***. The activity of *lacZ* and GFP can be assessed both in tissue sections ***(12,13)*** or by flow cytometry ***(12,53)*** (*see* **Note 25**). Analysis at the DNA level (detection of recombined alleles by PCR or Southern blot analysis) is very informative about the percentage of cells that have undergone recombination (efficiency), but for the identification of such cells (specificity), especially in solid tissues, direct visualization is preferred.

4. Notes

1. Most transgenic mice are produced for two general purposes: (1) to study the control of gene expression, and (2) to study the effects of transgene expression in the intact animal. In the former experiments, transgenic mice should contain the entire gene of interest, as well as several kilobases each of 5'- and 3'-flanking DNA, i.e., using P1- or BAC-cloned large genomic fragments. In the latter experiments, tissue-specific promoters as well as regulatory sequences should be used to drive the expression of a transgene in a specific pattern in the mouse. However, the transcriptional efficiency of transgenes is almost always influenced by the activation status of the neighboring chromatin at the insertion site. At present, position-independent expression of transgenes can only be obtained using specific *cis*-acting DNA elements called locus control regions (LCRs) ***(54,55)***.
2. When designing a tissue-specific transgene, the TBASE database for transgenic mice can be searched at http://tbase.jax.org.
3. The classic preparation of plasmid DNA is a time-consuming approach and includes the use of CsCl gradient centrifugation. Lately, several commercial kits have appeared on the market allowing easy and fast isolation of plasmid DNA using disposable chromatography columns. We recommend starting with a commercial kit and using the CsCl gradient method as an alternative.
4. The concentration is adjusted on an agarose gel by comparison to an older fragment of similar size that has been used successfully in previous experiments.
5. Avoid touching the blunt end of the injection pipet with fingers when preparing them, since it could contaminate the DNA solution and lead to egg damage.
6. If the pronuclei are small, it may help to bring the embryos back to the incubator for an hour and start the injection process later. If the embryos are left for too long at 37°C the two pronuclei will have fused and injection will be impossible.
7. It is also possible to culture the injected eggs overnight in vitro to the two-cell stage and then transfer them following the same procedure. However, in vitro culture may decrease embryo viability.
8. Rupture of the bursa often causes bleeding, which can obscure vision. To avoid this, apply a drop of a 0.1% solution of adrenaline directly on the bursa just before tearing it. This approach has no apparent adverse effects and prevents all bleeding from the ruptured bursa.
9. The narrow part of the transfer pipet should be 2–3 cm in length and 120–180 μm in external diameter, i.e., just larger than one egg and smaller than two. The presence of few bubbles after the eggs in the transfer pipet allows monitoring of the transfer procedure and ensures that all of the embryos have been successfully injected.
10. The quality of the DNA preparation at this stage is appropriate for slot-blot hybridization analysis, which provides a quantitative estimation for the copy number of the transgene.
11. The dissolved DNA can be directly used for PCR analysis. However, if the DNA is to be used for Southern hybridization analysis, a few more steps are included: after **step 2**, the samples should be digested with 1 μL of 10 mg/mL RNase A for

1 h at 37°C. **Steps 3** and **4** are repeated once more and are followed by an extra step of purification using 0.5 mL of chloroform/isoamyl alcohol.

12. We use the "pL2-neo" plasmid as a source of PMC-neo-poly(A) neomycin resistance cassette (kindly provided by Dr. Vasso Episkopou) as well as the "pNT" plasmid ***(56)*** bearing a herpes simplex virus thymidine kinase expression cassette.
13. We tend not to split PMEFs in high-dilution ratio, because in lower dilution they grow better for a longer period of time. Although it is hard to say how many passages they can sustain before they become senescent, their life span in culture is definitely smaller compared to stable lines used for feeders such as STO cells.
14. Inactivated feeders can be kept in frozen stocks as their active form. These stocks can prove very handy in case of emergency.
15. There are various methods for the DNA preparation used for gene targeting (e.g., kits using columns, and so forth). In our lab the CsCl preparation has worked the best since it delivers high-quality DNA without breaks, something very critical for the success of the targeting.
16. Use the minimum concentration of G418 that can kill all untransfected cells within 5–6 d. This concentration should be determined in advance by titration for each specific ESC line; usually it corresponds to 150–250 μg/mL active concentration.
17. Another cryoprotectant medium for freezing, which is considered the economic way, consists of 25% FCS and 10% DMSO in ESC culture medium.
18. We find SealPlate the most efficient treatment. However, there are alternatives, such as Parafilm, small caps per well, or addition of 100 μL of sterile, light paraffin oil to each well.
19. Alternatively, another method can be used to produce larger numbers of available synchronized blastocysts. In this protocol, superovulated immature females are used in the place of adult females. The females are again C57BL/6, 4–6 wk old, and they are mated with adult C57BL/6 males following the superovulation protocol in **Subheading 3.1.3.**
20. The time needed for the cell trypsinization, and for adherance in the preplating just before injection, varies among lines of ESC used. If not familiar, monitor cell detachment/attachment to the substrate following incubation for 3 min or 30 min, respectively.
21. The number of cells injected per blastocyst depends partly on how advanced developmentally the blastocyst is (early to fully expanded); it also depends on the condition of the cells to be injected. If more cells are expected to die, then the number increases.
22. Although we do the transfer to the uterus unilaterally, it is not prohibitive to transfer embryos into both uteri horns. Some laboratories practice this type of transfer, but to our experience the unilateral mode saves time without affecting the pregnancy outcome.
23. We use the "pEasy Flox" vector containing positive and negative selectable markers as well as 3-loxP sites (kindly provided by the group of Dr. Klaus Rajewsky) for the construction of conditional gene inactivation vectors.

24. Lists of currently available Cre-lines can be found at the following World Wide Web sites:

    - http://www.rnshri.on.ca/nagy/Cre.htm
      This web site is maintained by Nagy's lab, and it contains an excellent list of almost all Cre lines that have been made.
    - http://www.fleming.gr/molgen/animal_resources.htm
      This is our web site containing a detailed description of all the Cre-transgenic lines as well as TNF/TNFR transgenic lines and targeted mutant mice that have been generated and characterized by our lab.
    - gttp://jaxmice.jax.org/jaxmicedb/htmL/transgene.shtml
      This is the official web site of The Jackson Laboratory, listing all the Cre lines that can be purchased.

25. Although there is no direct evidence from our laboratory for intraline variability of Cre-expression and recombination efficiency, this is a parameter that should always be examined in each Cre-line. Furthermore, the recombination efficiency of a certain Cre-line should not be considered invariable for different loxP-flanked target-genes and should be assessed for each target gene separately.

Acknowledgments

The authors would like to thank all past and present members of our lab who contribute(d) work and ideas. The authors would also like to thank Dr. Daniel Grof for his help on the artwork. Work in the author's laboratory is currently supported by grants from the European Commission (QLG1-CT-1999-00202, QLK6-1999-02203).

References

1. Douni, E., Akassoglou, K., Alexopoulou, L., Georgopoulos, S., Haralambous, S., Hill, S., et al. (1996) Transgenic and knockout analyses of the role of TNF in immune regulation and disease pathogenesis. *J. Inflamm.* **47,** 27–38.
2. Keffer, J., Probert, L., Cazlaris, H., Georgopoulos, S., Kaslaris, E., Kioussis, D., et al. (1991) Transgenic mice expressing human tumour necrosis factor: a predictive genetic model of arthritis. *EMBO J.* **10,** 4025–4031.
3. Probert, L., Keffer, J., Corbella, P., Cazlaris, H., Patsavoudi, E., Stephens, S., et al. (1993) Wasting, ischemia, and lymphoid abnormalities in mice expressing T cell-targeted human tumor necrosis factor transgenes. *J. Immunol.* **151,** 1894–1906.
4. Douni, E. and Kollias, G. (1998) A critical role of the p75 tumor necrosis factor receptor (p75TNFR) in organ inflammation independent of TNF, lymphotoxin alpha, or the p55TNFR. *J. Exp. Med.* **188,** 1343–1352.
5. Probert, L., Akassoglou, K., Pasparakis, M., Kontogeorgos, G., and Kollias, G. (1995) Spontaneous inflammatory demyelinating disease in transgenic mice showing central nervous system-specific expression of tumor necrosis factor alpha. *Proc. Natl. Acad. Sci. USA* **92,** 11,294–11,298.

6. Akassoglou, K., Probert, L., Kontogeorgos, G., and Kollias, G. (1997) Astrocyte-specific but not neuron-specific transmembrane TNF triggers inflammation and degeneration in the central nervous system of transgenic mice. *J. Immunol.* **158,** 438–445.
7. Pasparakis, M., Alexopoulou, L., Episkopou, V., and Kollias, G. (1996) Immune and inflammatory responses in TNF alpha-deficient mice: a critical requirement for TNF alpha in the formation of primary B cell follicles, follicular dendritic cell networks and germinal centers, and in the maturation of the humoral immune response. *J. Exp. Med.* **184,** 1397–1411.
8. Pfeffer, K., Matsuyama, T., Kundig, T. M., Wakeham, A., Kishihara, K., Shahinian, A., et al. (1993) Mice deficient for the 55 kd tumor necrosis factor receptor are resistant to endotoxic shock, yet succumb to L. monocytogenes infection. *Cell* **73,** 457–467.
9. Rothe, J., Lesslauer, W., Lotscher, H., Lang, Y., Koebel, P., Kontgen, F., et al. (1993) Mice lacking the tumour necrosis factor receptor 1 are resistant to TNF-mediated toxicity but highly susceptible to infection by Listeria monocytogenes. *Nature* **364,** 798–802.
10. Erickson, S. L., de Sauvage, F. J., Kikly, K., Carver-Moore, K., Pitts-Meek, S., Gillett, N., et al. (1994) Decreased sensitivity to tumour-necrosis factor but normal T-cell development in TNF receptor-2-deficient mice. *Nature* **372,** 560–563.
11. Torres, R. M. and Kuhn, R., eds. *Laboratory Protocols for Conditional Gene Targeting.* Oxford University Press, New York, 1997.
12. Kassiotis, G., Pasparakis, M., and Kollias, G. Conditional and fixed cytokine gene modifications in transgenic and mutant mice. In *Cytokine Molecular Biology* (Blackwill, F., ed.), Oxford University Press, New York, 2000, pp. 155–188.
13. Nagy, A., Gertsenstein, M., Vintersten, K., and Behringer R. *Manipulating the Mouse Embryo: A Laboratory Manual.* (3rd ed.). Cold Spring Harbor Laboratory, Cold Spring Harbor, NY, 2003.
14. Wasserman, P. M. and DePamphilis, M. I., eds. *Methods in Enzymology: Guide to Techniques in Mouse Development.* vol. 225, Academic, San Diego, CA, 1993.
15. Joyner, A. L., ed. *Gene Targeting: A Practical Approach.* Oxford University Press, New York, 2001.
16. Gordon, J. W., Scangos, G. A., Plotkin, D. J., Barbosa, J. A., and Ruddle, F. H. (1980) Genetic transformation of mouse embryos by microinjection of purified DNA. *Proc. Natl. Acad. Sci. USA* **77,** 7380–7384.
17. Towens, T. M., Lingrel, J. B., Chen, H. Y., Brinster, R. L., and Palmiter, R. D. (1985) Erythroid-specific expression of human beta-globin genes in transgenic mice. *EMBO J.* **4,** 1715–1723.
18. Brinster, R. L., Allen, J. M., Behringer, R. R., Gelinas, R. E., and Palmiter, R. D. (1988) Introns increase transcriptional efficiency in transgenic mice. *Proc. Natl. Acad. Sci. USA* **85,** 836–840.
19. Kontoyiannis, D., Pasparakis, M., Pizarro, T. T., Cominelli, F., and Kollias, G. (1999) Impaired on/off regulation of TNF biosynthesis in mice lacking TNF AU-rich elements: implications for joint and gut-associated immunopathologies. *Immunity* **10,** 387–398.

20. Sambrook., J., Fritch, E. F., and Maniatis. T., eds. *Molecular Cloning: A Laboratory Manual.* Cold Spring Harbor Laboratory, Cold Spring Harbor, NY, 1989.
21. Mansour, S. L., Thomas, K. R., and Capecchi, M. R. (1988) Disruption of the proto-oncogene int-2 in mouse embryo-derived stem cells: a general strategy for targeting mutations to non-selectable genes. *Nature* **336,** 348–352.
22. Evans, M. J. and Kaufman, M. H. (1981) Establishment in culture of pluripotential cells from mouse embryos. *Nature* **292,** 154–156.
23. Te Riele, H., Maandag, E. R., and Berns, A. (1992) Highly efficient gene targeting in embryonic stem cells through homologous recombination with isogenic DNA constructs. *Proc. Natl. Acad. Sci. USA* **89,** 5128–5132.
24. Simpson, E. M., Linder, C. C., Sargent, E. E., Davidson, M. T., Morbaaten, L. E., and Sharp, J. J. (1997) Genetic variation among 129 substrains and its importance for targeted mutagenesis. *Nat. Genet.* **16,** 19–27.
25. Lasko, M., Sauer, B., Mosinger, B., Jr., Lee, E. J., Manning, R. W., Yu, S. H., et al. (1992) Targeted oncogene activation by site-specific recombination in transgenic mice. *Proc. Natl. Acad. Sci. USA* **89,** 6232–6236.
26. Nagy, A. (2000) Cre recombinase: the universal reagent for genome tailoring. *Genesis* **26,** 99–109.
27. Dymechi, S. M. (1996) Flp recombinase promotes site-specific DNA recombination in embryonic stem cells and transgenic mice. *Proc. Natl. Acad. Sci. USA* **93,** 6191–6196.
28. Araki, K., Araki, M., Miyazaki, J., and Vassalli, P. (1995) Site-specific recombination of a transgene in fertilized eggs by transient expression of Cre recombinase. *Proc. Natl. Acad. Sci. USA* **92,** 160–164.
29. Martin, G. R. (1981) Establishment of pluripotential cell lines from embryos cultured in medium conditioned by teratocarcinoma stem cells. *Proc. Natl. Acad. Sci. USA* **78,** 7634–7638.
30. Bradley, A., Evans, M., Kaufman, M. H., and Robertson, E. (1984) Formation of germ-line chimaeras from embryo-derived teratocarcinoma cell lines. *Nature* **23,** 255–256.
31. Turksen, K., ed. *Methods in Molecular Biology: Embryonic Stem Cells*, vol. 185. Humana, Totowa, NJ, 2002.
32. Williams, R. L., Hilton, D. J., Pease, S., Willson, T. A., Stewart, C. L., Gearing, D. P., et al. (1988) Myeloid leukaemia inhibitory factor maintains the developmental potential of embryonic stem cells. *Nature* **336,** 684–687.
33. Smith, A. G., Heath, J. K., Donaldson, D. D., Wong, G. G., Moreau, J., Stahl, M., et al. (1988) Inhibition of pluripotential embryonic stem cell differentiation by purified polypeptides. *Nature* **336,** 688–690.
34. Robertson, E. J. Embryo-derived stem cell lines. In *Teratocarnicomas and Embryonic Stem Cells: A Practical Approach* (Robertson, E. J., ed.). Oxford University Press, New York, 1987, pp. 71–112.
35. Lovell-Badge, R. H. Introduction of DNA into embryonic stem cells. In *Teratocarcinomas and Embryonic Stem Cells: A Practical Approach* (Robertson, E., ed.). Oxford University Press, New York, 1987, pp. 153–182.
36. Nagy, A. and Rossant, J. Production and analysis of ES cell aggregation chime-

ras. In *Gene Targeting. A Practical Approach* (Joyner, A. L., ed.). The Practical Approach Series. Oxford University Press, New York, 2000, pp. 177–206.
37. Wood, S. A., Pascoe, W. S., Schmidt, C., KemLer, R., Evans, M. J., and Allen, N. D. (1993) Simple and efficient production of embryonic stem cell-embryo chimeras by coculture. *Proc. Natl. Acad. Sci. USA* **90,** 4582–4585.
38. Stewart, C. I. Production of chimeras between embryonic stem cells and embryos. In *Methods in Enzymology: Guide to Techniques in Mouse Development* (Wasserman, P. M. and DePamphilis, M., eds.). Academic, San Diego, CA, 1993, pp. 843–848.
39. Schwartzberg, P. L., Goff, S. P., and Robertson, E. J. (1989) Germ-line transmission of a c-abl mutation produced by targeted gene disruption in ES cells. *Science* **246,** 799–803.
40. Papaioannou, V. and Johnson, R. Production of chimeras by blastocyst and morula injection of targeted ES cells. In *Gene Targeting: A Practical Approach* (Joyner, A. L., ed.). The Practical Approach Series. Oxford University Press, New York, 2000, pp. 133–175.
41. Gu, H., Marth, J. D., Orban, P. C., Mossmann, H., and Rajewsky, K. (1994) Deletion of a DNA polymerase beta gene segment in T cells using cell type-specific gene targeting. *Science* **265,** 103–106.
42. Tsien, J. Z., Chen, D. F., Gerber, D., Tom, C., Mercer, E. H., Anderson, D. J., et al. (1996) Subregion- and cell type-restricted gene knockout in mouse brain. *Cell* **87,** 1317–1326.
43. Akagi, K., Sandig, V., Vooijs, M., Van der Valk, M., Giovannini, M., Strauss, M., et al. (1997) Cre-mediated somatic site-specific recombination in mice. *Nucleic Acids Res.* **25,** 1766–1773.
44. Lam, K. P. and Rajewsky, K. (1998) Rapid elimination of mature autoreactive B cells demonstrated by Cre-induced change in B cell antigen receptor specificity in vivo. *Proc. Natl. Acad. Sci. USA* **95,** 13,171–13,175.
45. Lewandoski, M. (2001) Conditional control of gene expression in the mouse. *Nat. Rev. Genet.* **2,** 743–775.
46. Furth, P. A., St. Onge, L., Boger, H., Gruss, P., Gossen, M., Kistner, A., et al. (1994) Temporal control of gene expression in transgenic mice by a tetracycline-responsive promoter. *Proc. Natl. Acad. Sci. USA* **91,** 9302–9306.
47. No, D., Yao, T. P., and Evans, R. M. (1996) Ecdysone-inducible gene expression in mammalian cells and transgenic mice. *Proc. Natl. Acad. Sci. USA* **93,** 3346–3351.
48. Zhang, Y., Riesterer, C., Ayrall, A. M., Sablitzky, F., Littlewood, T. D., and Reth, M. (1996) Inducible site-directed recombination in mouse embryonic stem cells. *Nucleic Acids Res.* **24,** 543–548.
49. Feil, R., Brocard J., Mascrez, B., LeMeur, M., Metzger, D., and Chambon, P. (1996) Ligand-activated site-specific recombination in mice. *Proc. Natl. Acad. Sci. USA* **93**, 10,887–10,890.
50. Kellendonk, C., Tronche, F., Monaghan, A. P., Angrand, P. O., Stewart, F., and

Schutz, G. (1996) Regulation of Cre recombinase activity by the synthetic steroid RU 486. *Nucleic Acids Res.* **24,** 1404–1411.

51. Novak, A., Guo, C., Yang, W., Nagy, A., and Lobe, C. G. (2000) Z/EG, a double reporter mouse line that expresses enhanced green fluorescent protein upon Cre-mediated excision. *Genesis* **28,** 147–155.
52. Soriano, P. (1999) Generalized lacZ expression with the ROSA26 Cre reporter strain. *Nat. Genet.* **21,** 70–71.
53. Nolan, G. P., Fiering, S., Nicolas, J. F., and Herzenberg, L. A. (1988) Fluorescence-activated cell analysis and sorting of viable mammalian cells based on beta-D-galactosidase activity after transduction of Escherichia coli lacZ. *Proc. Natl. Acad. Sci. USA* **85,** 2603–2607.
54. Grosveld, F., van Assendelft, G. B., Greaves, D. R., and Kollias, G. (1987) Position-independent, high-level expression of the human beta-globin gene in transgenic mice. *Cell* **51,** 975–985.
55. Kollias, G. and Grosveld, F. The study of gene regulation in transgenic mice. In *Transgenic Animals* (Grosveld, F. and Kollias, G., eds.). Academic, London, 1991, pp. 79–98.
56. Tybulewicz, V. L., Crawford, C. E., Jackson, P. K., Bronson, R. T., and Mulligan, R. C. (1991) Neonatal lethality and lymphopenia in mice with a homozygous disruption of the c-abl proto-oncogene. *Cell* **65,** 1153–1163.

12

TNFα in Experimental Diseases of the CNS

Roberto Furlan, Pia Villa, Giorgio Senaldi, and Gianvito Martino

Summary

Tumor necrosis factor α (TNFα) is a crucial mediator involved in the communications between immune and nervous systems in physiological conditions, and its relevance is amplified during disease. Considered originally detrimental and a target for therapeutic intervention, recently it has also gained attention for its protective role, especially in central nervous system (CNS) confined diseases. Thus, TNFα has become the key molecule illustrating the peculiar and still not completely understood pathways by which inflammatory and immune reactions occur in the brain. Several human pathologies that lack an efficient therapy and that carry enormous social costs rely on these mechanisms. Thus, further research is needed to improve our knowledge and to allow the identification of therapeutic targets or strategies for immune-mediated inflammatory disease of the CNS in which TNFα is primarily involved. We describe here how to induce experimental autoimmune encephalomyelitis, cerebral malaria, and brain ischemia in rodents, and some protocols to analyze them. The application of innovative research strategies or original therapeutic approaches to these experimental models may be rewarding in terms of advancement in a field that is crucial for the management of many human patients.

Key Words: TNFα; central nervous system; EAE; cerebral malaria; cerebral ischemia.

1. Introduction

Tumor necrosis factor α (TNFα) is produced in the brain by all the main cellular components: neurons, microglia, and astrocytes ***(1–3)***, and it has been recently shown to contribute to regulation of synaptic strength in physiological conditions ***(4)***. TNFα is actively transported from the blood to the brain through the blood–brain barrier ***(5)***, probably signaling to the brain the existence of peripheral inflammatory processes. However, TNFα is a typical proinflammatory cytokine that promotes neuronal and oligodendroglial death in vitro as well as in vivo ***(6)***. By contrast, in apparently similar conditions, TNFα has also been reported to induce neuroprotection ***(7)***. Thus, these reports suggest a

From: *Methods in Molecular Medicine, Vol. 98: Tumor Necrosis Factor*
Edited by: A. Corti and P. Ghezzi © Humana Press Inc., Totowa, NJ

complex identity for TNFα, paradoxically promoting neurodegeneration and demyelination in some circumstances, and offering protection and fostering remylination in others. Here we describe the role of TNFα in experimental murine models of CNS disease, the protocol to induce such diseases, and some ancillary techniques useful for their analysis.

1.1. TNFα and the CNS

Several functions have been attributed to TNFα in the CNS, including generation of fever *(8)*, enhancement of slow-wave sleep *(9)*, stimulation of pituitary hormone secretion *(10)*, activation of microglia and astrocytes *(11–13)*, regulation of cellular traffic through the blood–brain barrier by acting on the endothelium *(14)*, influence on synaptic strength *(4)*, and in pathological conditions contribution to oligodendrocyte apoptosis *(15)* and demyelination on the one hand, and neuroprotection and myelin repair on the other *(7)*. But what are the cells producing TNFα in the CNS, and what cells in the CNS bear TNF receptors? TNFα immunoreactive neurons were identified in the hypothalamus, in the bed nucleus of the stria terminalis, in the caudal raphe nuclei, and along the ventral pontine and medullary surface *(1)*. TNFα-positive innervation was reported within areas involved in autonomic and endocrine regulation, including the hypothalamus, amygdala, bed nucleus of the stria terminalis, parabrachial nucleus, dorsal vagal complex, nucleus ambiguus, and thoracic sympathetic preganglionic cell column *(1)*. Astrocytes are able to release TNFα, and they certainly express both the p75 and the p55 TNF receptors. The engagement of TNFR on astrocytes leads to their activation and proliferation, to the expression of MHC class II molecules on their surface, and to the release of chemokines, PDGFα, and neurotrophins *(11,16)*. Astrocytes activated by TNFα induce apoptotic oligodendroglial death in vivo *(6)*, and activate, in turn, cerebral endothelium. Microglial cells are the major source of TNFα in the CNS and express both p75 and p55 receptors *(17)*. It is, in fact, believed that in these cells TNFα acts as an autocrine-paracrine growth factor. Brain endothelial cells do not produce TNFα but express both the p75 and p55 receptors *(18)*, which, when engaged, determine increased expression of adhesion molecules *(19)* or determine the release of soluble factors (e.g., prostaglandin E_2) active in the brain parenchyma *(10)*.

Since its primary action is as a proinflammatory cytokine, TNFα has been mainly studied in animal disease models. In mouse models of CNS inflammatory diseases, results have been, as illustrated below, contradictory.

1.2. TNFα in Experimental Autoimmune Encepahlomyelitis

The prototypical, chronic, immune-mediated demyelinating disease of the CNS is multiple sclerosis (MS). MS is of unknown etiology, and it is charac-

terized by the presence of perivascular inflammatory infiltrates in the CNS containing T and B cells and activated macrophages, thus suggesting that MS is a T-cell mediated, CNS-confined, chronic, inflammatory, demyelinating disease in which the ultimate effector cells are activated macrophages ***(20)***. The inflammatory process, leading to multifocal patchy demyelination and axonal loss, is mainly sustained by proinflammatory cytokines, that along with chemokines, adhesion molecules, and metalloproteinases, modulate at different levels the immunopathogenic process underlying MS ***(21)***. MS is modeled in animals by experimental autoimmune encephalomyelitis (EAE), which can be induced in rodents and nonhuman primates by active immunization with whole myelin, myelin proteins, myelin peptides, or nonmyelin CNS antigens (***22,23***; *see* **ref.** ***24*** for review). Despite being performed on a more accessible model than the human CNS, the immunological studies on EAE in rodents have not produced conclusive data on the role of the various immune mediators on the pathological process leading to lesion formation in the CNS (reviewed in **ref.** ***25***). TNFα, especially, has been shown to play both a destructive and a protective role in EAE pathogenesis. TNFα is probably the most studied cytokine in MS and EAE, and it is released at high levels during MS and EAE ***(26–30)***.

Several lines of transgenic mice have been generated that overexpress both soluble and membrane-bound TNFα in different CNS cells. Most of these mice display spontaneous demyelination with macrophage infiltration or, at least, increased susceptibility to EAE (reviewed in **refs.** ***31,32***). Deletion-mutant mice lacking the TNFα gene have been also generated, and they display delayed onset and decreased severity of EAE, possibly because of a reduced release of monocyte attractant chemokines (*see* **ref.** ***31*** for review). TNFR-I-deficient mice behave like $TNF\alpha^{-/-}$ mice, but TNFR-II-deficient mice develop more severe forms of myelin oligodendrocytic glycoprotein $(MOG)_{35–55}$-induced EAE ***(33)***. Along the line of this latter result, the generation of a $TNF\alpha^{-/-}$ mice backcrossed onto a C57BL/6 background revealed a powerful protective role of TNFα in EAE induced by immunization with the 35–55 peptide of the MOG ***(34)***. Furthermore, TNFα has been shown to promote proliferation of oligodendrocytes and remyelination in a cuprizone-induced model of demyelination ***(7)***.

Therapeutic approaches targeting TNFα in EAE and human MS have yielded contradictory results. In EAE, blockade of TNFα leads to reduced pathology ***(35–37)***, although systemic administration of TNFα alleviated EAE in TNFα deficient mice ***(34)***. In human MS trials, by contrast, therapies aimed at the blockage of TNFα have failed, showing even worsening of symptoms in some patients ***(38,39)***. Thus, TNFα emerges as playing a multifaceted role in the pathogenic and repair mechanisms of EAE and MS. The disease induced by immunization with $MOG_{35–55}$ in C57BL/6 mice seems the more appropriate

model for further investigations aimed at reconciling experimental and clinical data that may be only apparently discordant.

1.3. TNFα in Cerebral Malaria

At the global level, malaria still represents a major health problem. It is a leading cause of morbidity, and its consequences, in terms of disability and mortality, oppress the poorest nations with devastating socioeconomic effects ***(40–42)***. Malaria is a parasitic disease caused by protozoa of the genus *Plasmodium*. Cerebral malaria (CM) is a common clinical expression of *P. falciparum* infection, especially among children, and a primary cause of death. CM is lethal if untreated, and even when treated, it frequently results in mortality ***(43)***. CM pathogenesis remains largely unknown, but it has been clear for a while that it largely depends on the inflammatory host reaction to the parasite, encompassing TNF production ***(44)***. In simplified terms, sequestration of blood cells, including parasitized red blood cells (pRBC), in the brain capillaries, critically favored by proinflammatory cytokines, would result in CM via blood flow obstruction and ischemia ***(45)***.

The evidence for TNF involvement in human CM is abundant but circumstantial in nature. A number of studies have shown that high levels of circulating TNF are a hallmark of CM and correlate with manifestations of disease severity such as depth of coma, multiple organ dysfunction, and mortality ***(46–51)***. These studies, however, have not documented a causative role for TNF in CM, even if one of them ***(50)*** showed that pentoxifylline, an inhibitor of TNF production ***(51)***, exerts beneficial effects on the course of CM in children. This effect is associated to a decline of TNF serum levels. However, the evidence for TNF involvement in experimental CM is unequivocal.

A few animal models of CM have been developed ***(53)***, but the one established by G. E. Grau et al. ***(54)*** in mice using *P. berghei* ANKA has been instrumental in demonstrating the contribution of the immune system and TNF to CM pathogenesis. This model results from the parenteral injection of *P. berghei* ANKA-pRBR into mice of susceptible strains, such as the CBA/Ca or the C57Bl/6. It consists of an acute syndrome dominated by neurological signs (paralysis, ataxia, convulsions) that arises 6–9 d after infection and is invariably lethal 12–36 h after onset. The injection of *P. berghei* ANKA-pRBR into mice of resistant strains, such as the BALB/c, does not result in any acute syndrome or early mortality, but in a state of chronic anemia that is lethal during the fourth week of infection. The finding that athymic nude mice are protected against CM initially suggested that the immune response is responsible for the development of CM ***(55)***. This hypothesis was then largely confirmed and expanded by a number of other findings, such as that T-cell depletion ***(56,57)***, cyclosporin A treatment ***(58)***, and the lack of IRF-1 ***(59)*** protect against CM.

Passive immunization experiments first pointed to TNF as an essential mediator in the pathogenesis of CM ***(60)***. These experiments involved the use of polyclonal anti-mouse TNF Ab, similarly to those that proved the relevance of TNF to endotoxin-induced lethality ***(61)***. Later experiments, involving the use of transgenic mice expressing a TNFR-I construct as a decoy reagent, confirmed the role of TNF in CM pathogenesis ***(62)***. Subsequent experiments using mice lacking either TNFR-I or TNFR-II showed that TNFR-II, but not TNFR-I, plays a critical role in CM pathogenesis, possibly because ICAM-1 upregulation on brain endothelium may occur in absence of TNFR-I but not TNFR-II ***(63)***. In fact, endothelial ICAM-1 seems to contribute to cell sequestration in brain capillaries by interacting with LFA-1 expressed on blood cells ***(64).***

In conclusion, it is difficult to say how relevant the *P. berghei* ANKA model by Grau et al. is to human CM. *P. falciparum*-pRBCs show pathogenically important features that permit their binding to the endothelium. These features do not find counterparts in *P. berghei*-pRBCs ***(45)***. Thus, human CM is characterized by pRBC sequestration in brain capillaries, while experimental CM essentially by sequestration of leukocytes ***(54)***. Lesions of the brain capillary endothelium seem to occur similarly in the two conditions ***(54)***, however, making it reasonable to accept that at least to a certain extent, *P. berghei* ANKA infection of susceptible mice is a valid tool to deepen our knowledge of human CM.

1.4. TNFα in Ischemia

Brain ischemia is among the leading causes of mortality and disability in the Western world ***(65)***. Ischemic brain injury results from a complex sequence of pathophysiological events that evolve over time and space. The major pathogenic mechanisms of this cascade include energy failure and excitotoxicity, peri-infarct depolarizations, apoptosis, and inflammation ***(65,66)***. The inflammatory response has been shown in experimental animal models by the elevation in the ischemic cortex of mRNA levels of TNFα as early as 1 h after the onset of ischemia ***(67)*** followed by TNF protein expression, with a peak occurring at 6 h ***(68,69)*** or shortly thereafter ***(67)*** in ischemic neurons ***(67,69)***, astrocytes, microglia, and in infiltrating leukocytes ***(67–69)***. Also the two TNF receptors p55 and p75, which mediate the diverse activities of TNF, have been shown to be upregulated during cerebral ischemia, with p55 (which has been implicated in transducing cytotoxic signaling of TNFα) appearing within 6 h and p75 at 24 h after the onset of ischemia ***(69)***. Expression of cerebral TNFα has been recently found also during human ischemic stroke ***(70)***.

Cytotoxic activities of TNF might be mediated through both increased synthesis of the cytokine and upregulated expression of one or both receptors. A pathological role of TNF in mediating ischemic brain damage has been suggested by the protection provided by the administration of inhibitors of TNFα

synthesis *(71)*, anti-TNF antibodies *(71)*, soluble type 1 TNF receptors *(72,73)* or TNF binding protein *(74)*. Several activities could account for the proposed role of TNF in mediating brain damage during ischemia. TNFα potentially activates endothelial cells, increases vascular permeability and cerebral edema *(75)*, reduces cerebral blood flow *(76)*, and stimulates apoptosis *(77,78)*. Besides these direct effects, TNFα may mediate brain damage through the activities of secondary mediators, which have been directly implicated in the pathogenesis of ischemic brain injury, including IL-1 *(79)*, nitric oxide *(80)*, and ICAM *(81)*.

Evidence for a protective role of TNFα in cerebral ischemia was observed in TNFR knockout mice *(82)*. Considered together, these results indicate that in response to ischemia, low levels of TNFα may be beneficial, but excessive production of this cytokine within the early postinjury phase is deleterious *(83)*. At later time points, when the initial TNFα surge declines, a delayed response by which TNFα activates an "antideath" pathway may contribute to recovery of the injured tissue. At these later time points the effect of anti-TNF drugs, antibodies, or soluble receptors subsides, and, different from transgenic models, TNFα can be synthesized, activate its receptors, and stimulate protective mechanisms *(83)*. The exact timing and extent of TNFα activation are very important.

In this scenario the pharmacological inhibition of TNFα in the early postinjury phase seems a promising tool to provide protection from cerebral ischemia. To identify new TNFα inhibitors that are protective against cerebral ischemia, reliable experimental models are necessary. One of these is the rat model of permanent occlusion of the middle cerebral artery (MCA) *(84,85)*, the vessel most commonly affected in stroke syndromes. This model of focal cerebral ischemia, which is characterized by a core of densely and often irreversibly injured tissue surrounded by an "ischemic penumbra," containing potentially salvageable tissue *(85)*, has gained increasing acceptance owing to its relevance to the human clinical setting. Different approaches to MCA occlusion with varying difficulties have been described *(84,85)*. The approach by S. T. Chen et al. *(86)*, employing a surgically less demanding, more distal occlusion of the MCA above the rhinal fissure, coupled with permanent ipsilateral and temporary contralateral common carotid artery occlusions, has resulted in the development of a predictable large cortical infarct. This model has been used to study the protective role of anti-TNF strategies *(69,71)*.

2. Materials

2.1. EAE Induction

1. 10-mL glass syringes.
2. 30-mL glass tubes (corex).

3. 21-gage needles.
4. Incomplete Freund's Adjuvant (IFA) (Sigma).
5. Heat-inactivated, lyophilized *Mycobacterium tuberculosis* strain H37R (Beckton Dickinson, formerly DIFCO).
6. 1-mL syringes with removable 25-gage needle.
7. Myelin oligodendrocyte glycoprotein (MOG), residues 35–55 (MEVGWYRSPF-SRVVHLYRNGK), purity over 95% (*see* **Note 1**).
8. Pertussis toxin (pancreatic islet activating) from *Bordetella pertussis* (Sigma).
9. Female C57BL/6 mice, 18–20 g (6–8 wk old).

2.2. Perfusion

1. A piece of styrofoam and a large tray.
2. 1X PBS, 5 m*M* EDTA, 0.01% sodium nitrite.
3. Freshly prepared 4% paraformaldehyde in 1X PBS, pH 7.4.
4. Peristaltic pump, 10 mL/min.
5. 18- and 25-gage needles.
6. Surgical instruments for microdissection (e.g., scissors, forceps Klemmer, and so forth).
7. 8% chloral hydrate in saline.

2.3. CM Induction

1. 21-gage needles.
2. *P. berghei* ANKA-pRBC suspension in PBS containing 10% glycerol (10^7 cells/mL). The percentage of pRBC should be around 80%. This suspension should be stocked frozen at –80°C. *P. berghei* ANKA-pRBC are initially obtained from a fellow investigator or prepared in-house by bleeding mice of CM-resistant strains chronically infected with *P. berghei* ANKA.
3. Female CBA/Ca or C57BL/6 mice, 18–20 g (8–10 wk old).
4. Animals should be housed under a regimen of 12 h light/dark cycles and given ordinary food and water *ad libitum*.

2.4. Parasitemia Determination

1. Glasses for blood smears.
2. Blades for tail nicks.
3. Hematoxylin stain solution.

2.5. Ischemia Induction

1. Chloral hydrate: 400 mg/kg per 8 mL saline solution (154 m*M* NaCl).
2. Electric clippers.
3. Surgical instruments for microdissection (e.g., scissors, microforceps, microhooks), which must be immersed in disinfectants before surgery.
4. 4–0 silk and 3–0 polyester sutures, and absorbable gelatin sponge.
5. Heating blanket and monitor of body temperature with a rectal probe.

6. Dissecting microscope.
7. Dental drill.
8. Bipolar forceps connected to an electrosurgical unit.

2.6. Measurement of Infarct Volume

1. Brain slicer.
2. 4% (w/v) 2,3,5-triphenyltetrazolium chloride (TTC) in saline solution.
3. 4% paraformaldehyde in 50 m*M* phosphate buffer saline (PBS), pH 7.4.
4. Computerized image analysis system.

3. Methods

3.1. EAE Induction

1. Emulsion preparation. For the emulsion's final volume, calculate 300 μL/mouse and at least 2–3 mL excess. In a glass tube, resuspend the lyophilized $MOG_{35–55}$ peptide at 1.33 mg/mL in 1X PBS (*see* **Note 2**).
2. In a second glass tube, prepare a homogeneous suspension of 8 mg/mL *Mycobacterium tuberculosis* in IFA to obtain CFA. The lyophilized *M. tuberculosis* does not dissolve in IFA. A homogenous suspension can be obtained by careful stirring with a glass syringe, but *M. tuberculosis* will immediately reprecipitate at the bottom of the tube (*see* **Note 3**).
3. In a third glass tube, mix the $MOG_{35–55}$ peptide and the CFA in a 1:1 volume ratio. Mix the emulsion by aspirating and expelling with a glass syringe through a 21-gage needle until it becomes firm, dense, and very creamy (*see* **Note 4**). This usually takes at least 5–10 min of mixing.
4. When the emulsion is ready, fill the 1-mL syringes by aspirating the emulsion through the 21-gage needle you used to mix it, remove the needle, and replace the original 25-gage needle (*see* **Note 5**). Then, swing the syringe in order to have the emulsion toward the piston and push the latter until the dead (air) volume of the syringe is filled. If properly done, you will now have 900 μL emulsion in the syringe, exactly the amount needed for three mice.
5. Inject 100 μL of emulsion subcutaneously in three different sites of female C57BL/6 mice, 6–8 wk old (*see* **Note 6**). Two injections are performed under the rostral part of the flanks and one at the tail base (**Fig. 1**) (*see* **Note 7**).
6. Inject each mouse intravenously with 500 ng of PT resuspended in 100 μL PBS (*see* **Note 8**). This latter procedure must be repeated 48 h after injection of the emulsion.

3.2. EAE Clinical Evaluation

1. Clinical score and body weight is recorded daily.
2. Mice will usually have 1–2 g of weight loss in the days preceding clinical onset, which usually occurs, variably, between the day 9 and day 18 after immunization.
3. A nonparametric scale with five steps is used for clinical evaluation (**Fig. 2**). Mice are taken from the cage by the tail and observed from the abdominal side:

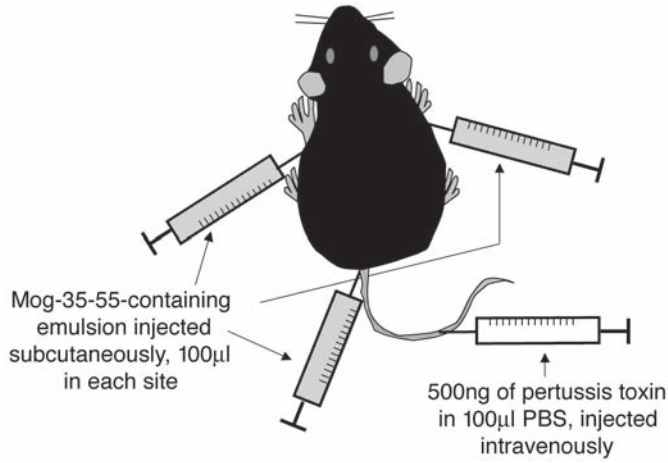

Fig. 1. EAE induction.

healthy mice extend their hind limbs very wide when held in this position. An asymmetric position, especially with one of the hind limbs retracted close to the abdomen, may represent an initial sign of disease. A weak tail and an unsteady gait are the signs at onset. To reveal an uncertain gait, it is useful to observe mice walking on a grid, like the cage cover. Healthy mice move quickly on a grid, almost as though on firm ground. Sick mice are unsure, move slowly, and often stumble. In the absence of other signs, we score the uncertain gait on the cage cover as 1.5. Another useful examination is that of the righting reflex. Trying to put a healthy mouse on its back results in such a quick flipping to the upright position that it is impossible to see the abdomen. A sick mouse may have a slow, very slow, to complete impairment in the righting reflex. In the absence of other signs, we score any grade of impairment of the righting reflex as 2. Paraparesis (score 3) and involvement of forelimbs (score 4) are easily identified (*see* **Note 9**).

3.3. Transcardial Perfusion of EAE Mice

At the time of sacrifice, transcardial perfusion ensures optimal quality of CNS tissues for any further histopathological examination.

1. Prepare a piece of Styrofoam in a tray under a chemical hood, and the peristaltic pump, with the final tubing connected to a 25-gage needle.
2. Induce deep surgical anesthesia in mice by injecting ip 0.6 g/kg of chloral hydrate in saline (approx 150 µL of an 8% solution for a 20-g mouse).
3. Test deep pain reflexes before starting (i.e., absence of limb retraction when firmly pinching the footpad with a forceps).
4. Fix the limbs of the mouse to a Styrofoam support in a tray using 18-gage needles (**Fig. 3**).
5. Using the scissors, open the thorax with diverging cuts starting from the lower

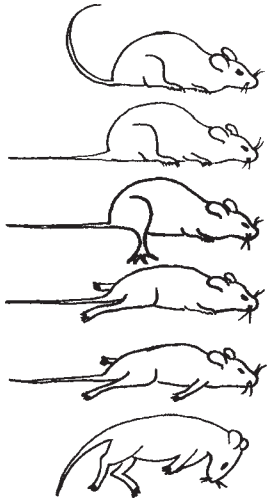

0	Healthy mouse
1	Weak or flaccid tail. (When the mouse, put on a grid like the cage cover, has gait problems = 1.5)
2	Unsteady gait (ataxia), hind limb paresis, or slow righting reflex
3	Paraparesis, complete hind limb paralysis
4	Paraparesis with fore limb involvement
5	Moribund or death

Fig. 2. EAE clinical evaluation.

edge of the sternum and directed to the back. Removing the diaphragm will reveal the beating heart (**Fig. 3**).

6. Connect the peristaltic pump to the bottle containing 1X PBS, 5 m*M* EDTA, and 0.01% sodium nitrite (*see* **Note 10**), and switch it on (10 mL/min), taking care that there are no bubbles in the tubing.
7. Insert the 25-gage needle in the left ventricle of the beating heart. In few seconds the auricola of the right atrium will swell due to the excessive fluid in the circulation. Using the scissors, make a cut in the auricola of the right atrium.
8. Allow the washing fluid to circulate for approx 5 min. If the needle and the cuts have been properly performed, viscera (e.g., the liver) will become rapidly pale. Stop the pump and change the connection to the paraformaldehyde. Switch the pump on again and let the fixative flow for approx 5–10 min (*see* **Note 11**). When the mouse is completely stiff, stop the pump and remove tissues (i.e., brain and spinal cord). A postfixation in 4% paraformaldehyde in 1X PBS, pH 7.4, for at least 2 h is required before processing.

3.4. CM Induction

1. Rapidly thaw pRBC suspension in a 37°C water bath.
2. Dilute 1:2 using PBS.
3. Immediately inject 10^6 pRBC per mouse ip in a volume of 200 µL (*see* **Note 12**).
4. Monitor mice daily for the appearance of CM signs and for survival.

3.5. Parasitemia Determination

1. Bleed mice by tail nick.
2. Prepare conventional blood smear for the examination of peripheral blood cellularity.
3. Let it air-dry.

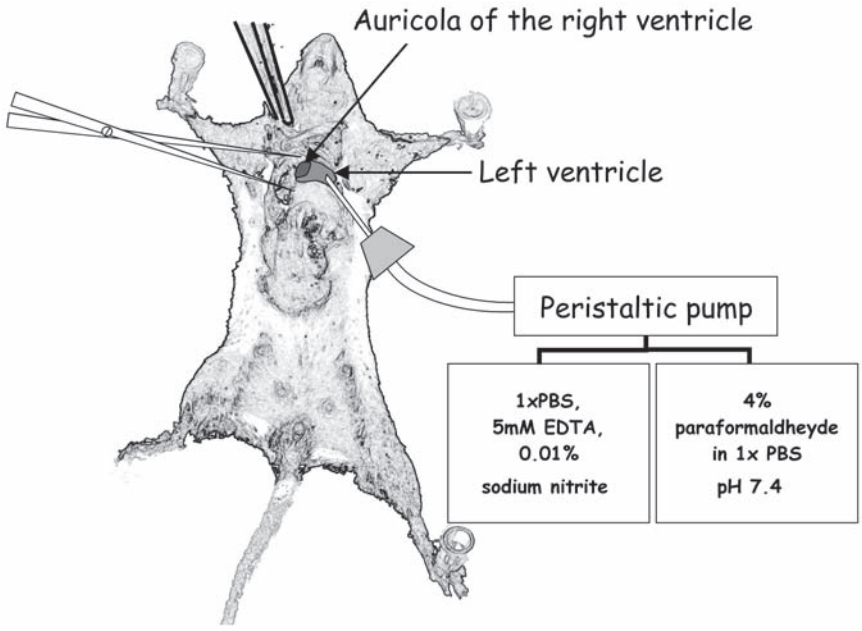

Fig. 3. Transcardial perfusion.

4. Stain it with hematoxylin for few minutes.
5. Determine percentage of pRBC by counting under the microscope the red blood cells (RBCs) harboring plasmodial life forms (trophozoites) vs total RBC count.

3.6. Ischemia Induction (86)

1. Anesthetize fed male Sprague-Dawley rats (250–280 g) (*see* **Notes 13** and **14**) by intraperitoneal injection of chloral hydrate (400 mg/kg) (*see* **Note 15**). For the duration of the anesthesia, monitor body temperature with a rectal probe and maintain it within physiological limits (37.0°C ± 0.5°C) using a heating pad (*see* **Note 16**).
2. Shave the ventral neck and the area between the right eye and ear, wipe this area with antiseptic, and expose the left common carotid (LCC) artery through a midline ventral cervical incision. Isolate the LCC preserving the vagus nerve, and place a loop of 4–0 silk around the artery for future manipulation. Expose the right common carotid artery and permanently occlude it by double ligation with 4–0 silk and a cut between the two ligatures.
3. Make a 1.5-cm scalp incision at the midpoint between the right eye and ear, cut and retract the temporalis muscle on the upper and lateral margins in order to expose the zygoma and squamosal bone. Using a dissecting microscope and a dental drill make a hole 2 mm in diameter, 2 mm rostral to the fusion of the zygoma with the squamosal bone. Perform the drilling under a continous drip of sterile saline to avoid transmission of heat to the underlying cortex until a thin

shell of bone is left. Remove this bone carefully with a microhook and microforceps to avoid injury to the underlying structures. Expose the right MCA by piercing the dura mater with a 30-gage needle in a location close to MCA and extending the dural opening with a microhook. Elevate the right MCA from the cortical surface by using a microhook, and thermocoagulate and sever the MCA by using bipolar forceps connected to an electrosurgical unit, distal to the rhinal artery, about midway between the MCA bifurcation and anterior cerebral artery without underlying cortical injury. Cover the area of MCA with a small piece of absorbable gelatin sponge, allow the temporalis muscle to fall back into place, and suture the overlying skin.

4. Temporarily occlude the LCC artery for 60 min by using traction provided by a fine forceps, and maintain anesthesia by supplemental doses as needed (about 40 mg/kg ip). Close the incision with a suture, keep the animal on a heating blanket until recovery from anesthesia, and then return it to its cage for 24 h with unlimited access to food and water. After surgery, animals are somewhat clumsy but are able to walk, eat and drink.
5. For the number of rats to use in each experimental group, *see* **Note 17**.

3.7. Measurement of Infarct Volume

1. Infarct volume is measured 24 h after MCA occlusion by using tetrazolium dye ***(87)***.
2. Kill the rat by decapitation, remove the brain quickly and carefully without perfusion, and keep it in ice-cooled saline.
3. Cut serial 1-mm-thick sections through the entire brain using a brain slicer.
4. Place individual sections in 6-well plates and incubate for 10 min in 2 mL of saline at 37°C.
5. Add 2 mL of 4% (w/v) TTC solution at 37°C and incubate for 30 min in the dark with gentle stirring to ensure even exposure for the staining.
6. Drain excess TTC and store slices at 4°C in 12-well plates with 1.5 mL of 4% paraformaldehyde in PBS. The sections can be stored in this manner for up to 7 d until tissues are scanned for image acquisition.
7. Quantification of the infarct size is done using a computerized image analysis system where a digital image of the two sides of each TTC-stained section is obtained. The area of injury is delineated by outlining the region in which the TTC is not reduced, i.e., nonviable tissue. For cases in which the necrosis is so severe that tissue is actually lost and the borders cannot be directly assessed, an outline of the contralateral side is used to evaluate the volume of injured brain.
8. The infarct size of each section is represented by the mean of the two sides.
9. Total volume of the infarct is calculated by reconstruction of the serial 1-mm-thick sections.

3.8. Characteristics of the Model

This model of focal and irreversible ischemia allowing only partial reperfusion, by employing a relatively noninvasive surgical procedure, produces a reproducible large cortical infarct, as shown in **Fig. 1**, with no impair-

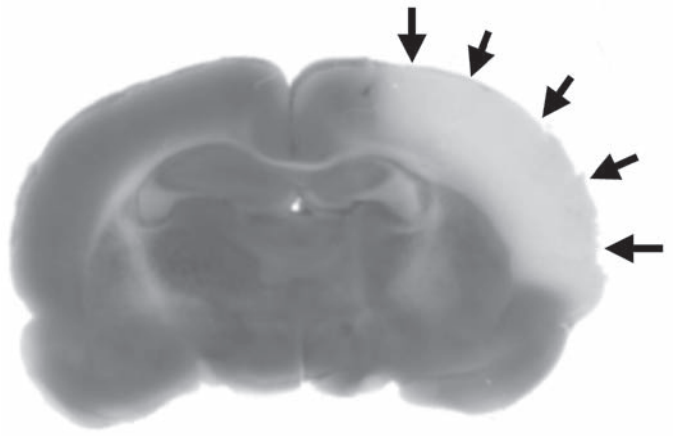

Fig. 4. Coronal brain section of an ischemic rat.

ment of motor function. The temporary occlusion of the contralateral (LCC) artery is necessary to reduce cerebral blood flow in the MCA territory into the ischemic range (18% of control). The mortality rate in this model is very low (7%), and in fact this ischemia model enables long-term survival, which allows study of the chronology of biochemical changes in cerebral infarction and offers a quantitative measure of the efficacy of pharmacological intervention. Moreover, the advantages of using the rat for stroke study include the similarity of its intracranial circulation to that of humans, the abundant neurochemical data derived from rat brain studies, and the relatively low animal cost.

4. Notes

1. Quality of the peptide is the most relevant issue to obtain a good disease. Incomplete incidence or very low severity of EAE are almost invariably related to peptide's quality.
2. In order to avoid waste of material due to weighing procedures, we usually dissolve the lyophilized $MOG_{35–55}$ peptide in 1X PBS at 2 mg/mL, sterilize by filtration via a 0.2-μm syringe filter (for in vitro immunological assays), and store it at –80°C in 1-mL aliquots for several months, up to 1 yr, without loss of encephalitogenicity.
3. To improve the suspension, *M. tuberculosis* can be further triturated in a mortar with a pestle to obtain a finer powder, before mixing with IFA.
4. To check the emulsion's quality, let a drop of it fall onto water: A good emulsion stays compact without dissolving and without blurred edges.
5. Since the emulsion is very dense, a great pressure has to be applied to push the needed amount out of the syringe. This pressure can lead to popping off of the needle, and sometimes the emulsion comes out with great pressure and can get

into the operator's eyes. Therefore, great care has to be taken to put the 25-gage needle back onto the 1-mL syringe, pressing it firmly. Additionally, the connection can be stabilized with a small piece of parafilm. The operator should wear eye protection.

6. Mice should be housed in an SPF animal facility, or at least in a clean conventional room, because viral, bacterial, and especially parasitic infections can alter the disease course (Furlan, R., personal observation).
7. Injections under the skin of the flanks is performed at the thoracic level to avoid the possibility of injecting the emulsion intraperitoneally: subsequent peritoneal inflammation leads to an altered gait, which is often confused with the clinical manifestation of EAE.
8. Pertussis toxin can be stored at –80°C in aliquots at the final concentration needed, for at least 6 mo, with only a minor loss of activity.
9. When we have mice with grade 3 or 4 EAE, we put wet food pellets in the cage to allow paraplegic mice to eat and survive.
10. This solution will (1) wash all the organs, removing the blood and preparing them for fixation; (2) avoid clotting in the small vessels (EDTA); and (3) relax vessel walls (sodium nitrite) facilitating the flux of the fixative. If solution are at 4°C and kept on ice during perfusion, tissue preservation will increase.
11. Muscle contractions are possible during fixative flow and indicate a good perfusion.
12. It is critical that the pRBS suspension is rapidly thawed and immediately injected upon thawing to avoid loss of parasite life in the suspension. It is also critical that this suspension be gently agitated at regular times while proceeding with the injections to prevent pRBC from precipitating.
13. Animals need to acclimate to the animal facility for at least 4–5 d before surgery.
14. The choice of the strain is important. In fact, it has been shown that among the normotensive strains, mean infarct volume was smallest and most variable in Wistar-Kyoto rats, and somewhat larger and more consistent in Sprague-Dawley rats ***(84)***.
15. The choice of anesthesia must be made carefully because various anesthetics produce direct central nervous system effects. For example, halothane or barbiturates are central nervous system depressants and act to decrease cerebral metabolism in a dose-dependent fashion. Others, such as ketamine and nitric oxide, have excitatory effects and may not result in a reduction in cerebral metabolism. Furthermore, different anesthetics have varying effects on the cerebral vasculature; some have shown to produce a degree of vasodilation (e.g., halothane), whereas others vasoconstrict (e.g., barbiturates). In Sprague-Dawley rats, chloral hydrate, which produces surgical anesthesia with excellent analgesia, is particularly useful when studying CNS function, as it may have less depressant effects on neuronal function.
16. It is important to maintain the body temperature of the rat at physiological levels for the duration of the anesthesia because even moderate hypothermia can confer marked protection.

17. In order to get a statistically significant result, 8–9 rats are suggested for each experimental group.

References

1. Breder, C. D., Tsujimoto, M., Terano, Y., Scott, D. W., and Saper, C. B. (1993) Distribution and characterization of tumor necrosis factor-alpha-like immunoreactivity in the murine central nervous system. *J. Comp. Neurol.* **337,** 543–567.
2. Lieberman, A. P., Pitha, P. M., Shin, H. S., and Shin, M. L. (1989) Production of tumor necrosis factor and other cytokines by astrocytes stimulated with lipopolysaccharide or a neurotropic virus. *Proc. Natl. Acad. Sci. USA* **86,** 6348–6352.
3. Frei, K., Siepl, C., Groscurth, P., Bodmer, S., Schwerdel, C., and Fontana, A. (1987) Antigen presentation and tumor cytotoxicity by interferon-gamma-treated microglial cells. *Eur. J. Immunol.* **17,** 1271–1278.
4. Beattie, E. C., Stellwagen, D., Morishita, W., Bresnahan, J. C., Ha, B. K., Von Zastrow, M., et al. (2002) Control of synaptic strength by glial TNFalpha. *Science* **295,** 2282–2285.
5. Gutierrez, E. G., Banks, W. A., andKastin, A. J. (1993) Murine tumor necrosis factor alpha is transported from blood to brain in the mouse. *J. Neuroimmunol.* **47,** 169–176.
6. Akassoglou, K., Bauer, J., Kassiotis, G., Pasparakis, M., Lassmann, H., Kollias, G., et al. (1998) Oligodendrocyte apoptosis and primary demyelination induced by local TNF/p55TNF receptor signaling in the central nervous system of transgenic mice: models for multiple sclerosis with primary oligodendrogliopathy. *Am. J. Pathol.* **153,** 801–813.
7. Arnett, H. A., Mason, J., Marino, M., Suzuki, K., Matsushima, G. K., and Ting, J. P. (2001) TNF alpha promotes proliferation of oligodendrocyte progenitors and remyelination. *Nat. Neurosci.* **4,** 1116–1122.
8. Leon, L. R. (2002) Invited review: cytokine regulation of fever: studies using gene knockout mice. *J. Appl. Physiol.* **92,** 2648–2655.
9. Deboer, T., Fontana, A., and Tobler, I. (2002) Tumor necrosis factor (TNF) ligand and TNF receptor deficiency affects sleep and the sleep EEG. *J. Neurophysiol.* **88,** 839–846.
10. Ek, M., Engblom, D., Saha, S., Blomqvist, A., Jakobsson, P. J., and Ericsson-Dahlstrand, A. (2001) Inflammatory response: pathway across the blood-brain barrier. *Nature* **410,** 430–431.
11. Selmaj, K. W., Farooq, M., Norton, W. T., Raine, C. S., and Brosnan, C. F. (1990) Proliferation of astrocytes in vitro in response to cytokines. A primary role for tumor necrosis factor. *J. Immunol.* **144,** 129–135.
12. Merrill, J. E. (1991) Effects of interleukin-1 and tumor necrosis factor-alpha on astrocytes, microglia, oligodendrocytes, and glial precursors in vitro. *Dev. Neurosci.* **13,** 130–137.
13. Merrill, J. E., Ignarro, L. J., Sherman, M. P., Melinek, J., and Lane, T. E. (1993) Microglial cell cytotoxicity of oligodendrocytes is mediated through nitric oxide. *J. Immunol.* **151,** 2132–2141.

14. Sedgwick, J. D., Riminton, D. S., Cyster, J. G., and Korner, H. (2000) Tumor necrosis factor: a master-regulator of leukocyte movement. *Immunol. Today* **21,** 110–113.
15. Selmaj, K. W. and Raine, C. S. (1988) Tumor necrosis factor mediates myelin and oligodendrocyte damage in vitro. *Ann. Neurol.* **23,** 339–346.
16. Murphy, C. A., Hoek, R. M., Wiekowski, M. T., Lira, S. A., and Sedgwick, J. D. (2002) Interactions between hemopoietically derived TNF and central nervous system-resident glial chemokines underlie initiation of autoimmune inflammation in the brain. *J. Immunol.* **169,** 7054–7062.
17. Sawada, M., Kondo, N., Suzumura, A., and Marunouchi, T. (1989) Production of tumor necrosis factor-alpha by microglia and astrocytes in culture. *Brain Res.* **491,** 394–397.
18. Osburg, B., Peiser, C., DomLing, D., Schomburg, L., Ko, Y. T., Voigt, K., et al. (2002) Effect of endotoxin on expression of TNF receptors and transport of TNFalpha at the blood-brain barrier of the rat. *Am. J. Physiol. Endocrinol. Metab.* **283,** E899–E908.
19. Omari, K. M. and Dorovini-Zis, K. (2003) CD40 expressed by human brain endothelial cells regulates CD4+ T cell adhesion to endothelium. *J. Neuroimmunol.* **134,** 166–178.
20. Martino, G. and Hartung, H. P. (1999) Immunopathogenesis of multiple sclerosis: the role of T cells. *Curr. Opin. Neurol.* **12,** 309–321.
21. Kieseier, B. C., Storch, M. K., Archelos, J. J., Martino, G., and Hartung, H. P. (1999) Effector pathways in immune mediated central nervous system demyelination. *Curr. Opin. Neurol.* **12,** 323–336.
22. Swanborg, R. H. (2001) Experimental autoimmune encephalomyelitis in the rat: lessons in T-cell immunology and autoreactivity. *Immunol. Rev.* **184,** 129–135.
23. Brok, H. P., Bauer, J., Jonker, M., Blezer, E., Amor, S., Bontrop, R. E., et al. (2001) Non-human primate models of multiple sclerosis. *Immunol. Rev.* **183,** 173–185.
24. Uccelli, A. Animal models of demyelination of the central nervous system. In *From Basic Immunology to Immune-Mediated Demyelination* (Martino, G. and Adorini, L., eds.). Springer-Verlag, Milan, Italy, 1999, pp. 233–245.
25. Lassmann, H. (2002) Mechanisms of demyelination and tissue destruction in multiple sclerosis. *Clin. Neurol. Neurosurg.* **104,** 168–171.
26. Hofman, F. M., Hinton, D. R., Johnson, K., and Merrill, J. E. (1991) Tumor necrosis factor identified in multiple sclerosis brain. *J. Exp. Med.* **170,** 607–612.
27. Selmaj, K., Raine, C. S., Cannella, B., and Brosnan, C. F. (1991) Identification of lymphotoxin and tumor necrosis factor in multiple sclerosis lesions. *J. Clin. Invest.* **87,** 949–954.
28. Issazadeh, S., Ljungdahl, A., Hojeberg, B., Mustafa, M., and Olsson, T. (1995) Cytokine production in the central nervous system of Lewis rats with experimental autoimmune encephalomyelitis: dynamics of mRNA expression for interleukin-10, interleukin-12, cytolysin, tumor necrosis factor alpha and tumor necrosis factor beta. *J. Neuroimmunol.* **61,** 205–212.
29. Furlan, R., Martino, G., Galbiati, F., Poliani, P. L., Smiroldo, S., Bergami, A., et

al. (1999) Caspase-1 regulates the inflammatory process leading to autoimmune demyelination. *J. Immunol.* **163,** 2403–2409.
30. Renno, T., Krakowski, M., Piccirillo, C., Lin, J. Y., and Owens, T. (1995) TNFalpha expression by resident microglia and infiltrating leukocytes in the central nervous system of mice with experimental allergic encephalomyelitis. Regulation by Th1 cytokines. *J. Immunol.* **154,** 944–953.
31. Probert, L., Eugster, H. P., Akassoglou, K., Bauer, J., Frei, K., Lassmann, H., et al. (2000) TNFR1 signalling is critical for the development of demyelination and the limitation of T-cell responses during immune-mediated CNS disease. *Brain* **123,** 2005–2019.
32. Ruuls, S. R., Hoek, R. M., Ngo, V. N., McNeil, T., Lucian, L. A., Janatpour, M. J., et al. (2001) Membrane-bound TNF supports secondary lymphoid organ structure but is subservient to secreted TNF in driving autoimmune inflammation. *Immunity* **15,** 533–543.
33. Eugster, H. P., Frei, K., Bachmann, R., Bluethmann, H., Lassmann, H., and Fontana, A. (1999) Severity of symptoms and demyelination in MOG-induced EAE depends on TNFR1. *Eur. J. Immunol.* **29,** 626–632.
34. Liu, J., Marino, M. W., Wong, G., Grail, D., Dunn, A., Bettadapura, J., et al. (1998) TNF is a potent anti-inflammatory cytokine in autoimmune-mediated demyelination. *Nat. Med.* **4,** 78–83.
35. Ruddle, N. H., Bergman, C. M., McGrath, K. M., Lingenheld, E. G., Grunnet, M. L., Padula, S. J., et al. (1990) An antibody to lymphotoxin and tumor necrosis factor prevents transfer of experimental allergic encephalomyelitis. *J. Exp. Med.* **172,** 1193–1200.
36. Selmaj, K., Raine, C. S., and Cross, A. H. (1991) Anti-tumor necrosis factor therapy abrogates autoimmune demyelination. *Ann. Neurol.* **30,** 694–700.
37. Croxford, J. L., Triantaphyllopoulos, K. A., Neve, R. M., Feldmann, M., Chernajovsky, Y., and Baker, D. (2000) Gene therapy for chronic relapsing experimental allergic encephalomyelitis using cells expressing a novel soluble p75 dimeric TNF receptor. *J. Immunol.* **164,** 2776–2781.
38. The Lenercept Group. (1999) TNF neutralization in MS: results of a randomized, placebo-controlled multicenter study. *Neurology* **53,** 457–465.
39. van Oosten, B. W., Barkhof, F., Truyen, L., Boringa, J. B., Bertelsmann, F. W., von Blomberg, B. M., et al. (1996) Increased MRI activity and immune activation in two multiple sclerosis patients treated with the monoclonal anti-tumor necrosis factor antibody cA2. *Neurology* **47,** 1531–1534.
40. Luhan, M. *Malaria*. WHO Press Office Fact Sheet 94. World Health Organization, Geneva, Switzerland, 1996, pp. 1–3.
41. Najera, J. A. and Hempel, J. *The Burden of Malaria*. WHO Press Office Publication CTD/MAL/96.10, World Health Organization, Geneva, Switzerland, 1996, pp. 1–58.
42. Sachs, J. and Malanay, P. (2002) The economic and social burden of malaria. *Nature* **415,** 680–685.

43. Greenwood, B. M., Bradley, A. K., Greenwood, A. M., Byass, P., Jammeh, K., Marsh, K., et al. (1987) Mortality and morbidity from malaria among children in a rural area of The Gambia, West Africa. *Trans. R. Soc. Trop. Med. Hyg.* **81,** 478–486.
44. Clark, I. A., Chaudhri, G., and Cowden, W. B. (1989) Roles of tumor necrosis factor in the illness and pathology of malaria. *Trans. R. Soc. Trop. Med. Hyg.* **83,** 436–440.
45. Miller, L. H., Baruch, D. I., Marsh, K., and Doumbo, O. K. (2002) The pathogenic basis of malaria. *Nature* **415,** 673–679.
46. Grau, G. E., Taylor, T. E., Molyneux, M. E., Wirima, J. J., Vassalli, P., Hommel, M., et al. (1989) Tumor necrosis factor and disease severity in children with *falciparum* malaria. *N. Engl. J. Med.* **320,** 1586–1591.
47. Kwiatkowski, D., Hill, A. V. S., Sambou, I., Twumasi, P., Castracane, J., Manogue, K. R., et al. (1990) TNF concentration in fatal cerebral, non-fatal cerebral, and uncomplicated *Plasmodium falciparum* malaria. *Lancet* **336,** 1201–1204.
48. Butcher, G. A., Garland, T., Ajdukiewicz, A. B., and Clark, I. A. (1990) Serum tumor necrosis factor associated with malaria in patients in the Solomon Islands. *Trans. R. Soc. Trop. Med. Hyg.* **84,** 658–661.
49. Shaffer, N., Grau, G. E., Hedberg, K., Davachi, F., Lyamba, B., Hightower, A. W., et al. (1991) Tumor necrosis factor and severe malaria. *J. Infect. Dis.* **163,** 96–101.
50. Di Perri, G., Di Perri, I. G., Monteiro, G. B., Bonora, S., Hennig, C., Cassatella, M., et al. (1995) Pentoxifylline as a supportive agent in the treatment of cerebral malaria in children. *J. Infect. Dis.* **171**, 1317–1322.
51. Manish, R., Tripathy, R., and Das, B.K. (2003) Plasma glucose and tumor necrosis factor-alpha in adult patients with severe *falciparum* malaria. *Trop. Med. Int. Health* **8,** 125–128.
52. Sinha, B., Semmler, J., Eisenhut, T., Eigler, A., and Endres, S. (1995) Enhanced tumor necrosis factor suppression and cyclic adenosine monophosphate accumulation by combination of phosphodiesterase inhibitors and prostanoids. *Eur. J. Immunol.* **25,** 147–153.
53. Lou, J., Lucas, R., and Grau, G. E. (2002) Pathogenesis of cerebral malaria: recent experimental data and possible applications in humans. *Clin. Microbiol. Rev.* **14,** 810–820.
54. Grau, G. E., Piguet, P. F., Vassalli, P., and Lambert, P. H. (1989) Tumor-necrosis factor and other cytokines in cerebral malaria: experimental and clinical data. *Immunol. Rev.* **112,** 49–70.
55. Finley, R. W., Mackey, L. J., and Lambert, P. H. (1982) Virulent *P. berghei* malaria: prolonged survival and decreased cerebral pathology in T cell-deficient nude mice. *J. Immunol.* **129,** 2213–2218.
56. Grau, G. E., Piguet, P. F., Engers, H. D., Louis, J. A., Vassalli, P., and Lambert, P. H. (1986) L3T4$^+$ T lymphocytes play a major role in the pathogensis of murine cerebral malaria. *J. Immunol.* **137,** 2348–2354.
57. Belnoue, E., Kayibanda, M., Vigario, A. M., Deschemin, J.C., van Rooijen, N., Viguier, M., et al. (2002) On the pathogenic role of brain-sequestered $\alpha\beta$CD8$^+$ T cells in experimental cerebral malaria. *J. Immunol.* **169,** 6369–6375.

58. Grau, G. E., Gretener, D., and Lambert, P. H. (1987) Prevention of murine cerebral malaria by low dose cyclosporin A. *Immunology* **61,** 521–525.
59. Senaldi, G., Shaklee, C. L., Guo, J., Martin, L., Boone, T., Mak, T. W., et al. (1999) Protection against the mortality associated with disease models mediated by TNF and IFN-gamma in mice lacking IFN regulatory factor-1. *J. Immunol.* **163,** 6820–6826.
60. Grau, G. E., Fajardo, L. F., Piguet, P. F., Allet, B., Lambert, P. H., and Vassalli, P. (1986) Tumor necrosis factor/cachectin as an essential mediator in murine cerebral malaria. *Science* **237,** 1210–1212.
61. Beutler, B., Milsark, I. W., and Cerami, A. (1986) Passive immunization against cachectin/tumor necrosis factor protects mice from lethal effects of endotoxin. *Science* **229,** 869–871.
62. Garcia, I., Araki, K., Miyazaki, Y., Araki, M., Juillard, P., Grau, G. E., et al. (1995) Transgenic mice expressing soluble TNFR1-IgG3 molecules are protected from lethal septic shock and cerebral malaria, and are highly sensitive to *Listeria monocytogenes* and *Leishmania major* infections. *Eur. J. Immunol.* **25,** 2401–2407.
63. Lucas, R., Lou, J. N., Juillard, P., Moore, M., Bluethmann, H., and Grau, G. E. (1997) Respective role of TNF receptors in the development of experimental cerebral malaria. *J. Neuroimmunol.* **72,** 143–148.
64. Grau, G. E., Pointaire, P., Piguet, P. F., Engers, H. D., Louis, J. A., Vassalli, P., et al. (1991) Late administration of monoclonal antibody to leukocyte function antigen 1 abrogates incipient murine cerebral malaria. *Eur. J. Immunol.* **21,** 2265–2267.
65. Dirnagl, U., Iadecola, C., and Moskowitz, M. A. (1999) Pathobiology of ischaemic stroke: an integrated view. *Trends Neurosci.* **22,** 391–397.
66. Lee, J. M., Grabb, M. C., Zipfel, G. J., and Choi, D. W. (2000) Brain tissue responses to ischemia. *J. Clin. Invest.* **106,** 723–731.
67. Liu, T., Clark, R. K., McDonnell, P. C., Young, P. R., White, R. F., Barone F. C., et al. (1994) Tumor necrosis factor-α expression in ischemic neurons. *Stroke* **25,** 1481–1488.
68. Buttini, M., Appel, K., Sauter, A., Gebicke-Haerter, P.-J., and Boddeke, H. W. (1996) Expression of tumor necrosis factor alpha after focal cerebral ischaemia in the rat. *Neuroscience* **71,** 1–16.
69. Botchkina, G. I., Meistrell, M. E., III, Botchkina, I. L., and Tracey, K. J. (1997) Expression of TNF and TNF receptors (p55 and p75) in the rat brain after focal cerebral ischemia. *Mol. Med.* **3,** 765–781.
70. Sairanen, T., Carpen, O., Karjalainen-Lindsberg, M. L., Paetau, A., Turpeinen, U., Kaste, M., et al. (2001) Evolution of cerebral tumor necrosis factor-alpha production during human ischemic stroke. *Stroke* **32,** 1750–1758.
71. Meistrell, M. E., III, Botchkina, G. I., Wang, H., Di Santo, E., Cockroft, K. M., Bloom, O., et al. (1997) Tumor necrosis factor is a brain damaging cytokine in cerebral ischemia. *Shock* **8,** 341–348.
72. Dawson, D. A., Martin, D., and Hallenbeck, J. M. (1996) Inhibition of tumor necrosis factor-alpha reduces focal cerebral ischemic injury in the spontaneously hypertensive rat. *Neurosci. Lett.* **218,** 41–44.

73. Navashiro, H., Martin, D., and Hallenbeck, J. M. (1997) Inhibition of tumor necrosis factor and amelioration of brain infarction in mice. *J. Cereb. Blood Flow Metab.* **17,** 229–232.
74. Nawashiro, H., Martin, D., and Hallenbeck, J. M. (1997) Neuroprotective effects of TNF binding protein in focal cerebral ischemia. *Brain Res.* **778,** 265–271.
75. Brett, J., Gerlach, H., Nawroth, P., Steinberg, S., Godman, G., and Stern, D. (1989) Tumor necrosis factor/cachectin increases permeability of endothelial cell monolayers by a mechanism involving regulatory G proteins. *J. Exp. Med.* **169,** 1977–1991.
76. Tureen, J. (1995) Effect of recombinant human tumor necrosis factor-alpha on cerebral oxygen uptake, cerebrospinal fluid lactate, and cerebral blood flow in the rabbit: role of nitric oxide. *J. Clin. Invest.* **95,** 1086–1091.
77. Decoster, E., Vanhaesebroeck, B., Vandenabeele, P., Grooten, J., and Fiers, W. (1995) Generation and biological characterization of membrane-bound, uncleavable murine tumor necrosis factor. *J. Biol. Chem.* **270,** 18,473–18,478.
78. Wong, G. H. and Goeddel, D. V. (1994) Fas antigen and p55 TNF receptor signal apoptosis through distinct pathways. *J. Immunol.* **152,** 1751–1755.
79. Relton, J. K. and Rothwell, N. J. (1992) Interleukin-1 receptor antagonist inhibits ischaemic and excitotoxic neuronal damage in the rat. *Brain Res. Bull.* **29,** 243–246.
80. Zhang, J., Dawson, V. L., Dawson, T. M., and Snyder, S. H. (1994) Nitric oxide activation of poly(ADP-ribose) synthetase in neurotoxicity. *Science* **263,** 687–689.
81. Wang, X., Yue, T. L., Barone, F. C., and Feuerstein, G. Z. (1995) Demonstration of increased endothelial-leukocyte adhesion molecule-1 mRNA expression in rat ischemic cortex. *Stroke* **26,** 1665–1669.
82. Bruce, A. J., Boling, W., Kindy, M. S., Peschon, J., Kraemer, P. J., Carpenter, M. K., et al. (1996) Altered neuronal and microglial responses to excitotoxic and ischemic brain injury in mice lacking TNF receptors. *Nat. Med.* **2,** 788–794.
83. Shohami, E., Ginis, I., and Hallenbeck J. M. (1999) Dual role of tumor necrosis factor alpha in brain injury. *Cytokine Growth Factor Rev.* **10,** 119–130.
84. Ginsberg, M. D. and Busto, R. (1989) Rodent models of cerebral ischemia. *Stroke* **20,** 1627–1642.
85. Luvisotto, T. L. and Sutherland, G. R. Animal models of stroke. In *Advances in Neurochemistry* (Bachelard, H., ed.), Plenum, New York, 1997, pp. 117–144.
86. Chen, S. T., Hsu, C. Y., Hogan, E. L., Maricq, H., and Balentine, J. D. (1986) A model of focal ischemic stroke in the rat: reproducible extensive cortical infarction. *Stroke* **17,** 738–743.
87. Bederson, J. B., Pitts, L. H., Germano, S. M., Nishimura, M. C., Davis, R. L., and Bartkowski, H. M. (1986) Evaluation of 2,3,5-triphenyltetrazolium chloride as a stain for detection and quantification of experimental cerebral infarction in rats. *Stroke* **17,** 1304–1308.

13

In Vivo Vascular Leakage Assay

Maria Elena Ferrero

Summary

This chapter describes the methods for measuring the increase in vascular permeability induced by tumor necrosis factor α (TNFα), or other mediators, in vivo in animal models. Mouse liver or kidney are perfused through the portal vein or the renal artery, respectively, by intravascular injection of a blue dye (trypan blue or Evans blue) combined with albumin. When endothelial permeability is increased, the dye extravasates and reaches the subendothelial spaces. Thus, subsequent washing of dye-perfused organs with saline cannot remove the dye. The perfusates are drawn from the suprahepatic inferior vena cava (for the liver) and from the renal vein (for the kidney). After perfusion, the livers and kidneys are removed, homogenized, and centrifuged. Spectrophotometric analysis of supernatants, at 540 nm, is then performed. The increase in optical density values is indicative of the increase in dye retention, hence of vascular leakage.

Key Words: Vascular permeability; dye perfusion; mouse; liver; kidney; TNFα.

1. Introduction

Septic shock and anaphylactic shock are systemic reactions characterized by many clinical manifestations; among them, the vascular collapse is caused by some mediators, such as tumor necrosis factor α (TNFα) and histamine, which are released by the immune system cells. These mediators determine the increase of vascular permeability, through the alteration of the endothelial cell junction integrity. Studies on TNFα induced increase of vascular leakage require the use of laboratory methods.

1.1. Basic Principle of the Method

The vascular leakage, expressed as loss of fluid, occurs in the vessels of microcirculation, i.e., capillaries and venules, which consist of endothelial cells

From: *Methods in Molecular Medicine, Vol. 98: Tumor Necrosis Factor*
Edited by: A. Corti and P. Ghezzi © Humana Press Inc., Totowa, NJ

and basement membrane, rather than pericytes. The permeability barrier is represented by the endothelium; the basement membrane is a mechanical support. If the endothelial layer is not interrupted, plasma does not leak out. In fact, the integrity of endothelial cell junctions prevents the passage of plasma into the extravascular space. When vascular leakage occurs, i.e., when endothelial cells contract and create a gap between them, plasma escapes through the gaps. If the gaps are increased, plasma proteins also escape through the endothelium, in relation with their molecular weight (first albumin, then globulins and fibrinogen), and may reach the subendothelial tissues.

The method described here, useful to demonstrate the modifications of vascular leakage in vivo, is based on intravenous injection of a soluble blue dye that combines with albumin. The method is a classic one and is named "bluing." At the level of leaky vessels, the albumin-dye complex leaks out into the extravascular space, but the vessel itself is not labeled. In fact, the complex crosses the basement membrane irreversibly, as compared with carbon black or other particles that are too large and cannot cross such a membrane. The bluing test is very sensitive because albumin, which carries the blue dye, is among the smallest plasma proteins. So albumin is also suitable for detecting small leaks.

The method is useful for measuring the vascular leakage induced by TNFα or other compounds after in vivo administration.

2. Materials

1. Surgical equipment.
2. Polytron (Kinematica GmbH).
3. Spectrophotometer.
4. NaCl (sodium chloride) (Sigma-Aldrich).
5. Wash solution: 0.9 g NaCl in 100 mL distilled water, at 37°C.
6. Trypan blue or Evans blue (Sigma-Aldrich).
7. Albumin from murine serum, prepared from fraction V albumin (Sigma-Aldrich).
8. Dye solution: 0.85 g NaCl, 0.5 g trypan blue or Evans blue, 0.4 g albumin from murine serum (Sigma-Aldrich) in 100 mL distilled water at 37°C.
9. Phosphate buffer: 0.2*M* K_2HPO_4, to which is added 0.2*M* KH_2PO_4 until the pH reaches 7.4, at 4°C.
10. Halothane (Hoechst).
11. Pentobarbital (Sigma-Aldrich).
12. Nylon monofilament (Ethicon).
13. Silk monofilament (Ethicon).
14. Polyethylene tube (Portex Ltd.).
15. Deoxycholic acid (Sigma-Aldrich).

3. Methods

The methods described below outline (1) the use of animals, (2) the surgical procedure, and (3) the dye extraction and measurement.

3.1. Animals and Solutions

During the experiments, principles of laboratory animal care are followed. Experiments and care of the mice are in accordance with standard ethical guidelines (NIH, 1985) ***(1)***. BALB/c male inbred mice weighing about 20 g (Charles River) are used (*see* **Note 1**). To demonstrate the leakage modifications of the microcirculation we use the liver or the kidney perfusion methods. In fact, both the organs present many capillaries (hepatic sinusoids or glomerular capillaries, respectively). Following the increase of vascular permeability, the dye-albumin complex (*see* **Subheading 2**) reaches the subendothelial spaces in the liver and in the kidney; the successive washing by organ perfusion with saline (*see* **Subheading 2**) doesn't remove the extravasated dye.

3.2. Surgical Procedures

Described below are the steps that can be utilized in the preparation of the mice for liver or kidney perfusion.

3.2.1. Operative Technique for the Perfusion of Mouse Liver

Anesthesia is induced by halothane exposure. Alternatively, mice are treated with pentobarbital (0.1 mL of 6% pentobarbital solution, in distilled water, per 100 g body weight).

1. Fix the mice to the operating table by means of nooses bound to the paws.
2. Perform a midline incision extending from the sternal xiphoid process to the caudal margin of the rib cage and along the abdomen to the pubis.
3. Perform two successive transversal incisions starting near the middle of the midline incision to increase the surgical area. Retract the bowel to the left of the mouse, and expose the liver, the portal vein, the hepatic artery, the right kidney, the inferior vena cava, and the bile duct.
4. Place two 7-0 circumferential silk nooses, separated by 2–3 mm, around the portal vein near the proximal hepatic level, under the bifurcation of the portal vein (**Fig. 1,** *no. 1*).
5. Cannulate the portal vein with a polyethylene tube (with external diameter of 0.94 mm and internal diameter of 0.75 mm) (**Fig. 1,** *no. 2*) and advance it past the previously placed ligatures; fix the latter around the cannula. It is important, during the placement of the nooses, to avoid the involvement of the hepatic artery (which is under the portal vein), because it is necessary to maintain blood perfusion of the liver.
6. Perform a thorax cut. This operation must be very rapid and last no more than 2.5

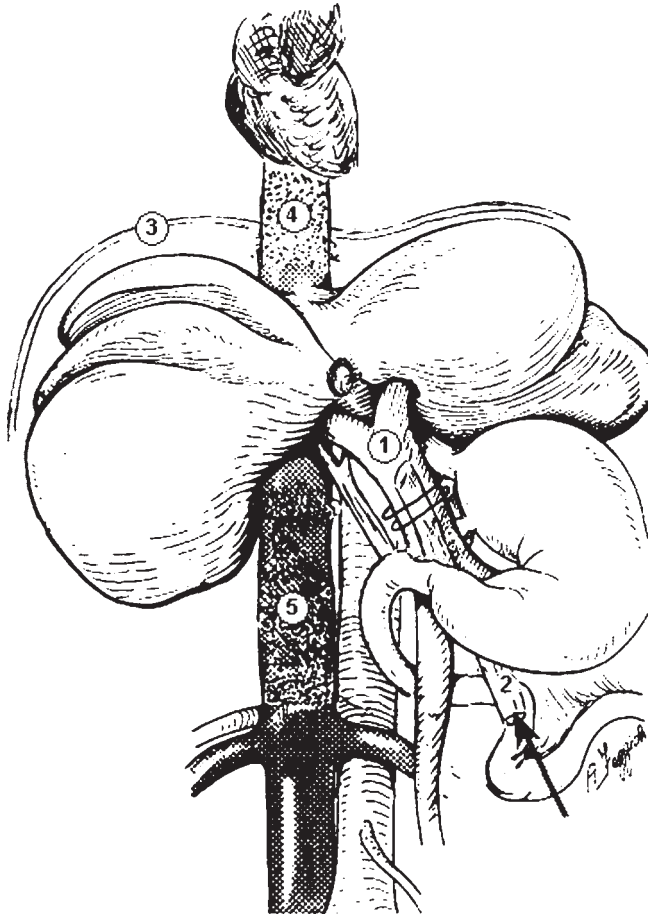

Fig. 1. Surgical area for mouse liver perfusion. Portal vein *(1)*, cannula *(2)*, diaphragm (*3*), inferior vena cava (*4* and *5*). *See* text for surgical procedure. Modified from Marni A., et al. (Reprinted with permission from **ref. *8***.)

min, to limit the anoxia of the hepatic tissue. In fact, when the thoracotomy occurs, breathing stops and the heartbeat becomes irregular.

7. Open the thorax by a transverse incision over and along the diaphragm insertion (**Fig. 1,** *no. 3*). Then, perform two longitudinal incisions starting at the ends of the transverse incision and moving toward the head. Reflect the resulting area to the cranial level (by means of a surgical clamp), then cut it. Sever the vagus and the diaphragmatic nerves to paralyze the diaphragm.
8. Start the perfusion with dye solution through the cannula. At the same time, cut the inferior vena cava (**Fig. 1,** *no. 4*), at the level of the juncture of suprahepatic veins, to permit to the perfusion medium to flow down.

9. Alternatively, place an 8-0 nylon noose around the inferior vena cava immediately under the heart (**Fig. 1,** *no. 4*) and place another ligature around the abdominal vena cava (**Fig. 1,** *no. 5*) (*see* **Note 2**).
10. Cannulate the inferior vena cava by directly inserting a polyethylene tube through the right atrium. Advance the cannula past the diaphragm and secure it with the previously placed circumferential nylon ligature. Then secure the ligature around the abdominal vena cava (**Fig. 1,** *no. 5*).
11. Start the perfusion through the cannula and cut the portal vein (**Fig. 1,** *no. 1*), as previously reported by Branster and Morton ***(2)***.
12. Perform continuous perfusion with approx 2 mL of dye solution. When the liver surface appears homogeneously blue, start perfusion with saline for about 2 min. The washing requires the use of 5–6 mL of saline solution. The whole operation lasts about 10 min.

3.2.2. Operative Technique for the Perfusion of Mouse Kidney

1. After anesthesia induction, make an abdominal incision in the midline, extend it laterally, and move the bowel to the mouse's left.
2. Use the right kidney for perfusion, because the mesenteric artery arises from the aorta at the same level as the right renal artery, and a cannula can be passed from one to the other without blood loss and without stopping the blood flow to the kidney.
3. To expose the major abdominal vessels and the right kidney, cut away fat and perivascular tissue by blunt dissection.
4. Tie the adrenal branch of the right renal artery (**Fig. 2,** *no. 8*) and expose the following blood vessels and the ureter (*see* **Fig. 2**):

   1 Inferior vena cava just below the liver.
   2 Aorta, above the mesenteric artery.
   3 Mesenteric artery, near the aorta.
   4 Mesenteric artery, more distant from the aorta than 3.
   5 Right renal artery, at its origin from the aorta.
   6 Abdominal inferior vena cava.
   7 Left renal vein.
   8 Adrenal branch of the right renal artery.
   9 Ureter.
   10 Right renal vein.

5. Insert the injecting cannula and tie it in position *3* and *5*. Start the perfusion with approx 2 mL of dye solution. It is followed by saline perfusion (3–4 mL). Flow down the perfused medium through a cut of the right renal vein (position *10*). The whole operation lasts about 12 min.

3.2.3. TNFα Administration

The injection of the substances for which leaking activity is to be tested is performed intraperitoneally or intravenously, approx 30 min before the begin-

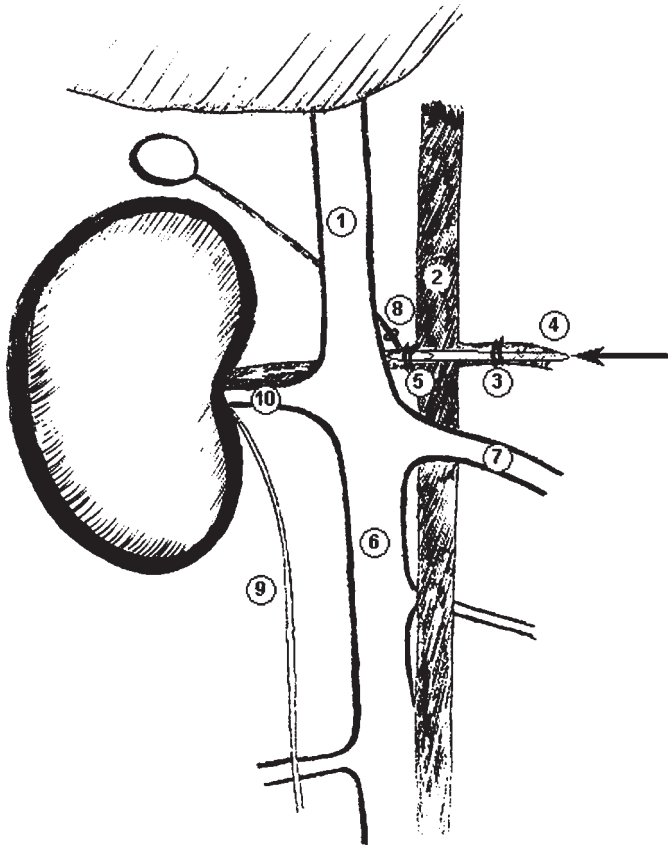

Fig. 2. Surgical area for mouse kidney perfusion. Inferior vena cava (*1* and *6*), aorta *(2)*, mesenteric artery (*3* and *4*), right renal artery *(5)*, left renal vein *(7)*, adrenal branch *(8)*, ureter *(9)*, right renal vein *(10)*. *See* text for surgical procedure.

ning of the surgical procedures ***(3–7)***. TNFα is responsible for most of the clinical features of septic shock or vascular leak syndrome. This cytokine is utilized in many experimental studies to test the capacity of some molecules to inhibit or prevent its known ability to increase endothelial permeability. TNFα is used in vivo at concentrations varying from 0.002 μg to 2 μg, intraperitoneally or intravenously injected, for each mouse weighing about 20 g. TNFα is administered from 15 to 30 min before the perfusion of mouse liver or kidney. The molecule being tested for potential capacity to inhibit or prevent the TNFα-induced vascular leakage can be administered together with TNFα, or immediately before or after TNFα injection.

3.3. Dye Extraction and Measurement

3.3.1. Preparation of Tissue Extracts

1. At the end of washing with saline, immediately remove the liver or the kidney and weigh it in a polycarbonate centrifuge tube. Then suspend the tissues in cooled buffered phosphate solution (pH 7.4), containing 0.2*M* K_2HPO_4 and 0.2*M* KH_2PO_4, in the ratio of 1 g tissue per 3 mL solution.
2. Homogenize the tissue suspensions by means of a Polytron (Kinematica GmbH).
3. Centrifuge the homogenates at 25,000*g* for 15 min and wash the pellets with buffered phosphate solution.
4. Recover the supernatants and, only if lipid interference occurs (i.e., when the supernatants are opaque), treat them with deoxycholic acid. The latter is used in the proportion of 10% (v/v), at the concentration of 10% in saline.

3.3.2. Spectrophotometric Assay

The presence of dye in the supernatants, clarified by the use of deoxycholic acid solution, is analyzed using a spectrophotometer (Py Unicam SP 650) at 540 nm. The presence of dye is indicated by the increase in optical density, compared to controls obtained from liver or kidney perfused with saline alone. Optical density values of the latter samples do not significantly differ from those obtained from mouse livers or kidneys dye-perfused and saline washed. Optical density values obtained from organ samples of mice treated with TNFα are significantly increased (*see* **Note 3**).

4. Notes

1. Results are more reproducible when using inbred strains of mice, to reduce biological differences between individuals. BALB/c mice are preferable.
2. The perfusion of mouse liver is more "physiological" if it is performed from the portal vein to the inferior suprahepatic vena cava.
3. Optical density values of samples run on a spectrophotometer at 540 wavelength, obtained from the organs of mice treated with TNFα, can vary in relation to the specific activity of TNFα and to its concentration. Murine TNFα instead of human TNFα is preferable. Optical density values for perfused livers derived from TNFα-treated mice can vary from 0.670 to 1.5 units, and those from perfused kidneys from 0.4 to 0.8 units. The values for livers or kidneys obtained from untreated mice can vary from 0.15 to 0.3 units.

Acknowledgments

The author thanks Alessandro Fulgenzi for technical assistance and Dr. Angelo Corti for providing murine TNFα.

References

1. Wall, P. D. (1993) Vigilance in defence of animal welfare. *Pain* **54,** 239.
2. Branster, M. V. and Morton, R. K. (1957) Isolation of intact liver cells. *Nature* **180,** 1283–1284.
3. Ferrero, E., Villa, A., Ferrero, M. E., Toninelli, E., Bender, J. R., Pardi, R., et al. (1996) Tumor necrosis factor α-induced vascular leakage involves PECAM 1 phosphorilation. *Cancer Res.* **56,** 3211–3215.
4. Fulgenzi, A., Bertelli, A. A., Magni, E., Ferrero, E., and Ferrero M. E. (2001) In vivo inhibition of TNF alpha-induced vascular permeability by resveratrol. *Transplant Proc.* **33,** 2341–2343.
5. Ferrero, E., Zocchi, M. R., Magni, E., Panzeri, M. C., Curnis, F., Rugarli, C., et al. (2001) Roles of tumor necrosis factor p55 and p75 receptors in TNF-alpha-induced permeability. *Am. J. Physiol. Cell Physiol.* **281,** C1173–C1179.
6. Bertelli, A. A. E., Baccalini, R., Battaglia, E., Falchi, M., and Ferrero M. E. (2001) Resveratrol inhibits TNFα-induced endothelial cell activation. *Therapie* **56,** 613–616.
7. Ferrero, E., Magni, E., Curnis, F., Villa, A., Ferrero, M. E., and Corti, A. (2002) Regulation of endothelial cell shape and barrier function by chromogranin A. *Ann. NY Acad. Sci*. **971,** 1–4.
8. Marni, A., Ferrero, M. E., and Gaja, G. (1988) Metabolic function of grafted liver in rats. *Transplantation* **46,** 830–835.

14

Animal Models of Endotoxic Shock

Pia Villa and Pietro Ghezzi

Summary

Endotoxin/lipopolysaccharide (LPS) is the major mediator that triggers the cellular and humoral responses of the shock induced by Gram-negative bacteria. The toxic responses of LPS are mediated by various factors and mainly by tumor necrosis factor α (TNFα). To study the role of TNF and to identify anti-TNF molecules in endotoxic/septic shock, numerous animal models have been utilized. The models described here are among the most widely used and are represented by LPS given at high dose, or at low dose in D-galactosamine-sensitized mice. The endpoints of these models are the survival, the organ toxicity, or the regulation of cytokines, and in particular of TNFα. An additional and more complex model of endotoxic/septic shock, the polymicrobial model of cecal ligation and puncture, where a synergistic interaction of several mediators occurs, is then described.

Key Words: TNF; LPS; endotoxic shock; polymicrobial sepsis; CLP.

1. Introduction

Activation of the immune system by Gram-negative bacteria, their products, or both can result in a cascade of events leading to endotoxic shock, a situation in which large amounts of cytokines, such as tumor necrosis factor α (TNFα), interleukin (IL)-1 and IL-6, as well as other inflammatory mediators, are produced. If unaltered, these events frequently lead to death. Endotoxin/lipopolysaccharide (LPS), a component of the cell wall of Gram-negative bacteria, was identified many years ago as a major mediator that triggers the massive cellular and humoral responses observed in shock induced by Gram-negative bacteria ***(1)***. The toxic effects of LPS are mediated by factors produced by host cells, mainly TNFα, as shown by the protective effects of TNF antibodies ***(2)***. There are two other points in favor of a role of TNFα in

From: *Methods in Molecular Medicine, Vol. 98: Tumor Necrosis Factor*
Edited by: A. Corti and P. Ghezzi © Humana Press Inc., Totowa, NJ

the pathogenesis of endotoxic shock: (1) endotoxin induces the production of TNFα, in vivo and in vitro, at an early time ***(3–5)***; (2) administration of TNFα to laboratory animals reproduces almost all the effects of LPS and in particular fever, hypertrigliceridemia, hypotension, and death ***(4)***. Furthermore, increased serum TNFα levels were measured in human volunteers treated with low doses of LPS, thus suggesting the relevance to man of the studies in animal models ***(6)***. TNFα has also been shown to be a mediator responsible for the initiation of the lethal toxicity of LPS in animals treated with a low dose of LPS and D-galactosamine, a liver-specific transcription inhibitor that increases the sensitivity to LPS itself ***(7,8)***. Unlike the response to high-dose LPS alone, death in this model is a direct result of hepatocyte apoptosis ***(9)***, which causes fulminant hepatitis, with TNFα and p55 TNF-receptor signaling playing an essential role.

Neutralizing monoclonal anti-TNF antibodies provided protection against shock during lethal bacteremia induced by *Escherichia coli* infusion in baboons, indicating that TNFα is also a mediator of fatal bacteremic shock ***(10)***. However, in other animal models of sepsis, such as the polymicrobial model of cecal ligation and puncture (CLP) or the intraperitoneal Gram-negative bacterial challenge, where the elevation of TNFα is only modest, inhibition of only TNFα failed to improve survival and even lessened it, suggesting that in these more complex models of sepsis a TNF requirement by the local defense mechanisms occurs ***(11–14)***. More recently it has been shown that a combination immunotherapy with soluble TNF receptors plus IL-1 receptor antagonist decreases sepsis mortality when provided for a sufficient amount of time ***(15)***. Moreover, drugs that inhibit the synthesis of multiple pro-inflammatory mediators, including TNFα, IL-6 and nitric oxide, were able to protect against death during polymicrobial sepsis, suggesting that the pathogenesis of this lethal syndrome is dependent upon the synergistic interaction of several mediators ***(16–18)***.

The models described here are among those most used to study anti-TNF molecules and TNF or TNFR knockout mice in sepsis, and include: (1) LPS at high dose, (2) LPS at low dose in D-galactosamine sensititized animals, and (3) polymicrobial sepsis induced by CLP. The endpoints of these models are either the survival or the immune regulation of cytokines and in particular of TNFα.

2. Materials

1. LPS (*see* **Note 1**) dissolved in saline at stock concentration of 5–10 mg/mL and sonicated for 5 min at room temperature in an immersion bath sonifier. This solution can be kept frozen for several months and has to be sonified each time after thawing and before use.
2. D-(+)-galactosamine hydrochloride.
3. Sterile, pyrogen-free saline.

4. Dexamethasone.
5. Tribromoethanol (Avertin) (375 mg/kg ip). Stock solution: 100 g in 100 mL of 2-methyl-2-butanol, which must be kept at 4°C in the dark. At the moment of the experiment dilute (1:40) this solution in saline (final concentration 2.5% w/v) and inject 15 μL/g. At this dosage surgical anesthesia is characterized by rapid induction and recovery, with 20–30 min duration of surgical anesthesia.
6. Sterile needles of different sizes (18-gage, 20-gage, 25 gage).
7. Surgical instruments for CLP: a scalpel, a pair of blunt dissecting forceps and scissors, and a fine needle holder, which are sterilized before surgery; sterile 4-0 catgut and polyester sutures.
8. Antibiotics for CLP: gentamycin and clindamycin.
9. Tryptic soy agar (Difco). Suspend 40 g of the powder in 1 L of purified water, mix thoroughly, heat with frequent agitation and boil for 1 min to completely dissolve the powder, then autoclave at 121°C for 15 min. For preparation of plates add 100 μL of samples (blood, peritoneal lavages, or tissue homogenates), serially diluted in saline, to 10 mL of the sterile agar that has been previously cooled to 50–55°C and incubate at 37°C for 24 h, after which the colonies are counted.

3. Methods

The methods described below refer to three experimental models of endotoxic/septic shock that are widely used to study immune regulations of cytokines, and in particular TNFα: (1) LPS at high dose, (2) LPS at low dose with D-galactosamine, and (3) CLP.

3.1. LPS at High Dose

1. Animals. Male or female BALB/c mice, weighing approx 20–24 g, fed standard rodent chow and water *ad libitum* (*see* **Note 2**).
2. Pilot experiment (*see* **Notes 1** and **2**):
   a. To find the optimal dose of LPS perform a pilot experiment with three groups of three mice each.
   b. Dilute the stock solution of LPS with saline and inject it into mice intraperitoneally in a total volume of 200 μL per animal.
   c. Check the mortality twice a day for the following 3 d, and then choose the dose of LPS that produces 80–100% lethality.
3. Lethality experiment (*see* **Notes 1** and **2**)
   a. Treat the experimental groups (about seven to eight mice/group) with the dose of LPS chosen in the pilot experiment.
   b. Check the mortality twice a day for up to 10 d after injection.
   c. We suggest introduction of a positive control in each series of experiments, i.e., a group treated with both LPS and a drug that protects from endotoxic shock (e.g., dexamethasone at the dose of 30 mg/kg ip, given 30 min before LPS) ***(19)*** (*see* **Note 3**).

4. Cytokine measurements

   a. To measure some pro-inflammatory cytokines (e.g., TNFα and IL-6) treat some mice (at least five mice/group) intraperitoneally with the lethal or a lower dose of LPS.
   b. Kill the mice 90 min later.

   These cytokines can be detected in serum and in some organs, mainly liver and lungs, which are important for organ failure.

3.2. LPS at Low Dose in D-Galactosamine-Sensitized Mice

1. Animals: BALB/c, C57BL/6, C3H/HeN, or CD1 mice of both sexes, weighing approx 20–27 g, fed standard rodent chow and water *ad libitum* (*see* **Note 2**).
2. Pilot experiment (*see* **Notes 1** and **2**):

   a. To find the optimal dose of LPS perform a pilot experiment with 3 groups of 3 mice each.
   b. Inject the mice intraperitoneally with galactosamine (700 mg/kg) together with LPS (5–50 μg/kg) in a total volume of 200 μL per animal.
   c. Check the mortality within 24 h.

3. Lethality experiment (*see* **Notes 1, 2,** and **3**):

   a. Inject the mice intraperitoneally with galactosamine (700 mg/kg) together with LPS at the dose chosen in the pilot experiment.
   b. Check the mortality within 24 h.
   c. Mice develop a fulminant hepatitis within 8 h after LPS/D-galactosamine challenge with release of serum aminotransferases, and by this time they begin to die, with most dying during the first 6–9 h.

4. Characteristics of the model:
   Leukocyte infiltration is observed after 1 h, and the final stage is characterized by complete destruction of the centrolobular and midzonal hepatocytes ***(8)***. The expression pattern of TNFα and a variety of cytokines has been recently shown in this model by G. Sass et al. ***(20)***.

3.3. Cecal Ligation and Puncture

1. Animals: Any variety of mouse strains of both sexes can be used for CLP. We and others have used male CD-1 mice, 5- to 6-wk-old, weighing approx 25–28 g, fed standard rodent chow and water *ad libitum* (*see* **Note 2**).
2. Surgical procedure ***(21)*** (*see* **Note 4**):

   a. Anesthetize the mouse with avertin ip (375 mg/kg) and place it supine and immobilized on a surgical platform (**Fig. 1**).
   b. Shave the anterior abdominal wall and clean the area with ethyl alcohol.
   c. Make a 7–10 mm vertical abdominal incision in the left lower quadrant using the scalpel. Open the muscular layer using a pair of blunt scissors to split it and bring the cecum out.

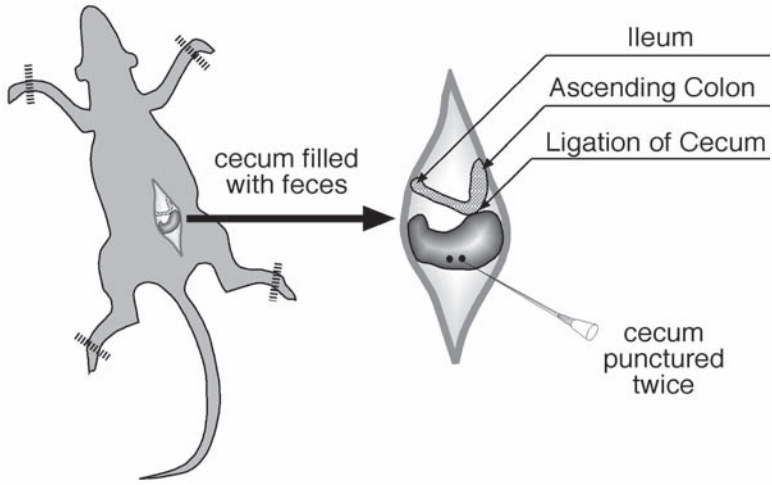

Fig. 1. Experimental design of cecal ligation and puncture model.

d. Isolate the cecum by placing a sterile 4-0 silk tie around it, immediately below the ileocecal valve, taking care not to obstruct the small or large intestine.
e. Puncture the cecum twice on the antimesenteric side with a needle and gently squeeze to ensure that the puncture sites have not closed off and that a small amount of feces is extruded on the surface of the bowel. The gage of the needle can vary from 18 gage to 25 gage, depending on the desired mortality to be induced (*see* **Note 5**).
f. Replace the cecum into the peritoneal cavity and close the incision in two running layers using 4-0 catgut absorbable suture for the muscle layer and 4-0 polyester for skin.
g. Inject the mice subcutaneously with 1 mL of saline to favor resuscitation.
h. Allow the animals to recover and provide food and water *ad libitum*. Use of antibiotics (gentamycin 3.2 mg/kg and clindamycin 40 mg/kg subcutaneously immediately after surgery and once a day for the following 3 d) is the rule, unless these agents alter the particular parameters to be studied.
i. Examine the mice twice a day for the first 5 d because the majority of animals die within 2–4 d. If animals exhibit undue stress or signs of imminent death, such as loss of righting reflex or panting, euthanize promptly.
j. Check the mortality for up to 10 d after surgery.

The model of CLP has close parallels to the clinical setting, including the polymicrobial nature of the peritonitis and the pattern of remote organ failure, mainly lung damage.

3. Parameters to evaluate:
The infection can be monitored by counting the bacterial colony-forming units in the blood, starting 3–6 h after surgery, in peritoneal lavage and in tissue

homogenates ***(21)***. The pattern of cytokines, including TNF, its soluble receptors, IL-1, IL-6, and/or chemokines is well documented ***(22,23)***.

4. Notes

1. LPS from various sources can be used, and the toxicity of the specific LPS must be checked in a pilot experiment. In our laboratory we currently use LPS from *Escherichia coli*—serotype 055:B5—at the concentrations of 4, 5, and 6 mg/mL of saline, corresponding to 40, 50, and 60 mg/kg, respectively, for the pilot experiments of LPS at high dose.
2 Reproducible reactions of animals to LPS require that any previous exposure of the animals to bacterial contact is minimized, that bacterial infection is strictly excluded, and that any solvent injected is pyrogen free. The first two points require animal housing facilities that meet good laboratory practice rules and provide for the bacteriological and virological control of the health state of the animal. Even if the animals are specific-pathogen free, the sensitivity of mice of either sex to LPS varies over a wide range and depends not only on the strain and the age of the animals, but also on the time of the day and the season of the year. Because these variables and their mutual interference are unpredictable, the sensitivity of the dose dependence of the animals against LPS must be checked in pilot experiments. Moreover, animals must be allowed to acclimate in the animal facility at 20°C on a 12-h light/dark cycle for at least 4–5 d before experiment.
3. Routinely pharmacologically active compounds are given 30 to 60 min before either LPS alone or galactosamine/LPS. If administered more than 60 min prior to the LPS challenge, care must be taken to the induction of LPS tolerance ***(24)*** by omnipresent endotoxin in chemicals and solvents. Unsuitable solvents in these models are dimethyl sulfoxide or ethanol.
4. Even though the technique is fairly simple, close attention and adherence to certain technical details like standard laparatomy, gentle handling of tissues, constant site of cecal ligation, standardization of the needle size and the number of punctures are very important in reproducing uniform results.
5 There is a relationship between mortality and the size of cecal puncture: with the small (25-gage) needle a sublethal model results; medium-sized (21- to 22-gage) needles lead to approx 50% mortality, and the larger (18-gage) needles cause 100% mortality by 48–72 h ***(17,21–23,25)***.

References

1. Hewett, J. A. and Roth, R. A. (1993) Hepatic and extrahepatic pathobiology of bacterial lipopolysaccharides. *Pharmacol. Rev.* **45,** 382–411.
2. Beutler, B., Milsark, I. W., and Cerami, A. (1985) Passive immunization against cachectin/tumor necrosis factor protects mice from lethal effect of endotoxin. *Science* **229,** 869–871.
3. Mahoney, J. R., Jr., Beutler, B. A., Le Trang, N., Vine, W., Ikeda, Y., Kawakami, M., et al. (1985) Lipopolysaccharide-treated RAW 264.7 cells produce a mediator that inhibits lipoprotein lipase in 3T3-L1 cells. *J. Immunol.* **134,** 1673–1675.

4. Beutler, B. and Cerami, A. (1986) Cachectin and tumor necrosis factor as two sides of the same biological coin. *Nature* **320,** 584–588.
5. Ulich, T. R., Guo, K., and del Castillo, J. (1989) Endotoxin-induced cytokine gene expression in vivo. I. Expression of tumor necrosis factor mRNA in visceral organs under physiologic conditions and during endotoxemia. *Am. J. Pathol.* **134,** 11–14.
6. Michie, H. R., Manogue, K. R., Spriggs, D. R., Revhaug, A., O'Dwyer, S., Dinarello, C. A., et al. (1988) Detection of circulating tumor necrosis factor after endotoxin administration. *N. Engl. J. Med.* **318,** 1481–1486.
7. Lehmann, V., Freudenberg, M. A., and Galanos, C. (1987) Lethal toxicity of lipopolysaccharide and tumor necrosis factor in normal and D-galactosamine-treated mice. *J. Exp. Med.* **165,** 657–663.
8. Wendel, A. (1990) Biochemical pharmacology of inflammatory liver injury in mice. *Methods Enzymol.* **186,** 675–680.
9. Zhao, Y., Li, S., Childs, E. E., Kuharsky, D. K., and Yin, X. M. (2001) Activation of pro-death Bcl-2 family proteins and mitochondria apoptosis pathway in tumor necrosis factor-alpha-induced liver injury. *J. Biol. Chem.* **276,** 27,432–27,440.
10. Tracey, K. J., Fong,Y., Hesse, D. G., Manogue, K. R., Lee, A. T., Kuo, G. C., et al. (1987) Anti-cachectin/TNF monoclonal antibodies prevent septic shock during lethal bacteraemia. *Nature* **330,** 662–664.
11. Echtenacher, B., Falk, W., Mannel, D. N., and Krammer, P. H. (1990) Requirement of endogenous tumor necrosis factor/cachectin for recovery from experimental peritonitis. *J. Immunol.* **145,** 3762–3766.
12. Bagby, G. J., Plessala, K. J., Wilson, L. A., Thompson, J. J., and Nelson, S. (1991) Divergent efficacy of antibody to tumor necrosis factor-alpha in intravascular and peritonitis models of sepsis. *J. Infect. Dis.* **163,** 83–88.
13. Zanetti, G., Heumann, D., Gerain, J., Kohler, J., Abbet, P., Barras, C., et al. (1992) Cytokine production after intravenous or peritoneal gram-negative bacterial challenge in mice. Comparative protective efficacy of antibodies to tumor necrosis factor-alpha and to lipopolysaccharide. *J. Immunol.* **148,** 1890–1897.
14. Remick, D., Manohar, P., Bolgos, G., Rodriguez, J., Moldawer, L., and Wollenberg, G. (1995) Blockade of tumor necrosis factor reduces lipopolysaccharide lethality, but not the lethality of cecal ligation and puncture. *Shock* **4,** 89–95.
15. Remick, D. G., Call, D. R., Ebong, S. J., Newcomb, D. E., Nybom, P., Nemzek, J. A., et al. (2001) Combination immunotherapy with soluble tumor necrosis factor receptors plus interleukin 1 receptor antagonist decreases sepsis mortality. *Crit. Care Med.* **29,** 473–481.
16. Villa, P., Demitri, M. T., Meazza, C., Sironi, M., Gnocchi, P., and Ghezzi, P. (1996) Effects of methyl palmitate on cytokine release, liver injury and survival in mice with sepsis. *Eur. Cytokine Netw.* **7,** 765–769.
17. Villa, P., Meazza, C., Sironi, M., Bianchi, M., Ulrich, P., Botchkina, G., et al. (1997) Protection against lethal poly-microbial sepsis by CNI-1493, an inhibitor of pro-inflammatory cytokine synthesis. *J. End. Res.* **4,** 197–204.

18. Ulloa, L., Ochani, M., Yang, H., Tanovic, M., Halperin, D., Yang, R., et al. (2002) Ethyl pyruvate prevents lethality in mice with established lethal sepsis and systemic inflammation. *Proc. Natl. Acad. Sci. USA* **99,** 12,351–12,356.
19. Bertini, R., Bianchi, M., and Ghezzi, P. (1988) Adrenalectomy sensitizes mice to the lethal effects of interleukin 1 and tumor necrosis factor. *J. Exp. Med.* **167,** 1708–1712.
20. Sass, G., Heinlein, S., Agli, A., Bang, R., Schumann, J., and Tiegs, G. (2002) Cytokine expression in three mouse models of experimental hepatitis. *Cytokine* **19,** 115–120.
21. Villa, P., Shaklee, C. L., Meazza, C., Agnello, D., Ghezzi, P., and Senaldi, G. (1998) Granulocyte colony-stimulating factor and antibiotics in the prophylaxis of a murine model of polymicrobial peritonitis and sepsis. *J. Infect. Dis.* **178,** 471–477.
22. Ebong, S., Call, D., Nemzek, J., Bolgos, G., Newcomb, D., and Remick, D. (1999) Immunopathologic alterations in murine models of sepsis of increasing severity. *Infect. Immun.* **67,** 6603–6610.
23. Villa, P., Sartor, G., Angelini, M., Sironi, M., Conni, M., Gnocchi, P., et al. (1995) Pattern of cytokines and pharmacomodulation in sepsis induced by cecal ligation and puncture compared with that induced by endotoxin. *Clin. Diagn. Lab. Immunol.* **2,** 549–553.
24. Freudenberg, M. A. and Galanos, C. (1988) Induction of tolerance to lipopolysaccharide (LPS)-D-galactosamine lethality by pretreatment with LPS is mediated by macrophages. *Infect. Immun.* **56,** 1352–1357.
25. Baker, C. C., Chaudry, I. H., Gaines, H. O., and Baue, A. E. (1983) Evaluation of factors affecting mortality rate after sepsis in a murine cecal ligation and puncture model. *Surgery* **94,** 331–335.

15

Collagen-Induced Arthritis as a Model for Rheumatoid Arthritis

Richard O. Williams

Summary

Collagen-induced arthritis (CIA) is an animal model of rheumatoid arthritis (RA) that is widely used to address questions of disease pathogenesis and to validate therapeutic targets. Arthritis is normally induced in mice or rats by immunization with autologous or heterologous type II collagen in adjuvant. Susceptibility to collagen-induced arthritis is strongly associated with major histocompatibility complex class II genes, and the development of arthritis is accompanied by a robust T- and B-cell response to type II collagen. The chief pathological features of CIA include a proliferative synovitis with infiltration of polymorphonuclear and mononuclear cells, pannus formation, cartilage degradation, erosion of bone, and fibrosis. As in RA, pro-inflammatory cytokines, such as tumor necrosis factor α (TNFα) and interleukin (IL)-1β, are abundantly expressed in the arthritic joints of mice with CIA, and blockade of these molecules results in a reduction of disease severity.

Key Words: Rheumatoid arthritis; autoimmunity; experimental animal models; adjuvant arthritis; collagen-induced arthritis; type II collagens mice.

1. Introduction

Rheumatoid arthritis (RA) is a chronic, disabling disease that affects some 1% of the population. In recent years, much has been learned about the mediators that contribute to the pathogenesis of RA, and a number of studies have pointed to a key role for tumor necrosis factor α (TNFα) in the disease process. Indeed, the success of infliximab, a chimeric anti-TNFα monoclonal antibody ***(2–4)***, and etanercept, a soluble p75-TNFR-Fc fusion protein ***(16,24)***, in the clinic is a testament to the pathological significance of this cytokine in RA. However, there is still a lack of knowledge of the underlying causes of the

From: *Methods in Molecular Medicine, Vol. 98: Tumor Necrosis Factor*
Edited by: A. Corti and P. Ghezzi © Humana Press Inc., Totowa, NJ

disease, and it is for this reason, together with the need for more effective and less toxic remedies, that animal models of arthritis are being studied.

Animal models are used in many different kinds of research, including the testing of new therapies, the identification of pro-inflammatory mediators, the analysis of genetic susceptibility factors, and in the search for markers of disease progression ***(25)***. Of the various animal models of arthritis, collagen-induced arthritis (CIA) has come to be the most widely used model for studies of therapeutic intervention. In general, these studies may be described as prophylactic (treatment administered before onset of arthritis) or therapeutic (treatment administered after onset of arthritis), and these two experimental approaches may not necessarily provide the same results. For example, when given prior to disease onset, a number of T-cell-targeted therapies (e.g., anti-CD4, anti-IL-12, CTLA4-Ig) have been shown to be effective in blocking the development of arthritis by inhibiting or altering the immune response that precedes the development of the disease. However, such treatments are usually found to be much less effective in halting the progression of disease once the inflammatory response is underway ***(9,11,18,23)***.

CIA occurs in rats, mice, and primates following immunization with type II collagen in adjuvant. Pathological changes include synovitis with infiltration of polymorphonuclear and mononuclear cells, pannus formation, erosion of bone and cartilage, and fibrosis. In mice, immunization with heterologous (usually bovine, chick, or rat) type II collagen usually leads to a relatively acute form of arthritis. In contrast, immunization with autologous (mouse) collagen results in a more protracted disease course ***(1,8,12)***, and the chief determinant of chronicity in CIA is likely to be the extent to which the immune response is targeted at self-collagen, as opposed to the collagen used for immunization. This supposition is supported by the observation that transgenic DBA/1 mice, which overexpress the TCR-β gene from a T-cell clone that recognizes mouse type II collagen, develop chronic arthritis, whereas their nontransgenic littermates develop a self-limiting form of the disease ***(14)***.

This chapter will focus on CIA in mice. This model has been widely studied as a model of RA, largely on the basis of the pathological similarities between the two diseases ***(7)***. Thus, both RA and CIA exhibit similar patterns of synovitis, pannus formation, erosion of cartilage and bone, fibrosis, and loss of joint mobility ***(21)***. Another key similarity between RA and CIA is that susceptibility to both diseases is strongly associated with genes encoding major histocompatibility (MHC) class II molecules, suggesting the involvement of $CD4^+$ T cells in the pathogenesis of both forms of arthritis. Thus, susceptibility to CIA is restricted to mouse strains bearing MHC types $I\text{-}A^q$ and $I\text{-}A^r$, and this is analogous to human RA, where certain subtypes of DR4 and DR1 are strongly associated with susceptibility to the disease. In addition to the cellular arm of

the immune response, it is also recognized that, as in human RA, humoral responses play a significant role in the pathogenesis of CIA *(7)*. However, it should be borne in mind that convincing data have not yet emerged pointing definitively to a role for type II collagen autoimmunity in the bulk of RA patients.

Another important feature of CIA that bears strong similarities with RA is the expression of pro-inflammatory cytokines, including TNFα and interleukin (IL)-1β, in the joints of mice with arthritis *(13)* and the fact that blockade of these molecules results in reductions in both the clinical and histological severity of disease *(5,10,17,20,22,26–28)*.

2. Materials

2.1. Purification of Type II Collagen

1. Powdered cartilage (*see* **Note 1**).
2. 4*M* guanidine-HCl, 0.05*M* Tris-HCl, pH 7.5.
3. 0.5*M* and 0.1*M* acetic acid.
4. Sodium chloride.
5. 70% (v/v) formic acid.
6. Pepsin from porcine gastric mucosa (3X crystalized; Sigma-Aldrich).
7. 0.02*M* Na_2HPO_4, pH 9.4.

2.2. Immunization of Mice

1. Male DBA/1 mice, 8–12 wk of age (Harlan-Olac).
2. Type II collagen.
3. 0.1 *M* acetic acid.
4. *Mycobacterium tuberculosis* H37 RA (Difco).
5. Incomplete Freund's adjuvant (IFA; Difco).
6. Fentanyl 0.2 mg/mL and fluanisol 10 mg/mL (Hypnorm®).

2.3. Measurement of Anti-Collagen IgG

1. Type II collagen.
2. 0.05*M* Tris-HCl, 0.2 *M* NaCl, pH 7.4.
3. Nunc-Immuno microtiter plates (Nalge-Nunc).
4. 0.05% (v/v) Tween-20 in phosphate buffered saline (PBS).
5. 2% (w/v) bovine serum albumin (BSA) in PBS.
6. Test sera.
7. Standard serum sample.
8. HRP-conjugated anti-IgG, anti-IgG1, and anti-IgG2a (BD Biosciences).
9. TMB microwell peroxidase substrate system (Kirkegaard and Perry).
10. 4.5*N* H_2SO_4.

2.4. Analysis of T-Cell Responses

1. Type II collagen-immunized DBA/1 mice.
2. Cell strainers (70 μ*M*; Falcon).
3. Hank's balanced salt solution (HBSS).

4. Complete medium: RPM1 1640 containing 10% (v/v) heat-inactivated fetal calf serum or 1% (v/v) mouse serum, 100 U/mL penicillin, 100 μg/mL streptomycin, $2 \times 10^{-5}M$ 2-mercaptoethanol and 20 m*M* L-glutamine.
5. 0.05% (v/v) Tween-20 in PBS.
6. 2% (w/v) BSA in PBS.
7. Recombinant IL-5, IL-10, and IFNγ (Peprotech).
8. The following capture/biotinylated detect antibody pairs: IL-5, TRFK5/TRFK4; IL-10, JES5-16E3/JES5–2A5; IFNγ, R4-6A2/XMG1.2 (Immunokontact).
9. Streptavidin-HRP (BD Biosciences).
10. TMB microwell peroxidase substrate system (Kirkegaard and Perry).
11. 4.5*N* H_2SO_4.
12. [^{3}H]-thymidine (Amersham).

3. Methods

3.1. Purification of Type II Collagen

The method of purification of type II collagen from cartilage is based on the studies of E. J. Miller ***(15)*** and D. Herbage et al. ***(6)***.

1. Powder cartilage in a liquid nitrogen freezer mill (Spex). If unavailable, the cartilage may be ground to a fine powder using a pestle and mortar placed in a bath of dry ice and liquid nitrogen.
2. To remove proteoglycans, suspend powdered cartilage in 5 volumes of 4*M* guanidine-HCl in 0.05*M* Tris-HCl, pH 7.5, for 24 h at 4°C. Centrifuge at 14,000*g* for 1 h at 4°C.
3. Discard supernatant and wash cartilage pellet with 0.5*M* acetic acid to remove guanidine-HCl. Centrifuge at 14,000*g* for 1 h at 4°C.
4. To solubilize collagens, resuspend cartilage pellet in 20 vol of 0.5*M* acetic acid. Adjust pH of the suspension to 2.8 using 70% formic acid. Add 1 g of pepsin for every 20 g of cartilage (wet weight). Leave stirring for 48 h at 4°C.
5. Centrifuge at 14,000*g* for 1 h at 4°C and discard pellet. To precipitate type II collagen from the supernatant, add NaCl gradually with stirring to give a final concentration of 0.89 *M*. Leave to equilibriate overnight at 4°C then centrifuge at 14,000*g* for 1 h at 4°C.
6. Dissolve pellet in 0.1*M* acetic acid. Then inactivate residual pepsin by dialyzing against 0.02*M* Na_2PO_4, pH 9.4. The collagen will form a precipitate.
7. Centrifuge at 14,000*g* for 1 h at 4°C, then redissolve pellet in 0.1*M* acetic acid.
8. Dialyze against 0.1*M* acetic acid and freeze-dry. Store at 4°C in a dessicator.
9. Purity of the collagen can be assessed on a 5% SDS-polyacrilamide gel. In addition, the presence of contaminating proteoglycans (which may not be detected by gel electrophoresis) can be assessed according to the method of A. Ratcliffe ***(19)***. In brief, 40 μL of sample is added to 250 μL of 1,9-dimethylmethylene blue in formate buffer (pH 3.5) in a 96-well microtiter plate. The absorbance is then read immediately at 600 nm using an ELISA plate reader. A standard curve is constructed by titrating a known concentration of chondroitin sulphate.

3.2. Induction and Assessment of Arthritis

1. Dissolve type II collagen at 4 mg/mL in 0.1 *M* acetic acid overnight at 4°C, with vigorous stirring. Collagen dissolved in this way may be stored at –20°C (*see* **Note 2**).
2. To produce complete Freund's adjuvant (CFA), grind *M. tuberculosis* with a pestle and mortar to produce a fine powder, then suspend in IFA (approx 3 mg *M. tuberculosis*/mL of IFA). This should be carried out in a fume hood and with a face mask to prevent inhalation of *M. tuberculosis* powder.
3. Emulsify dissolved type II collagen with an equal volume of CFA on ice, using a syringe (preferably glass) or an Ultra-Turrax (IKA) in short bursts to prevent heating. The emulsion should be thick enough not to drip out of the vessel when inverted.
4. Sedate mice by intraperitoneal injection of 100 µL of 10% (v/v) Hypnorm®, diluted in distilled water.
5. Shave rumps of mice using electric clippers to facilitate the injection.
6. Inject emulsion intradermally (as far as possible) at two or more sites at the base of the tail using a glass syringe or a latex-free syringe and a 23-gage needle. The needle becomes blunt easily and should be changed frequently. Each mouse should receive 0.1 mL of emulsion in total. The emulsion should be shallow enough to be visible under the skin (*see* **Note 3**).
7. Some workers boost the mice with a second intraperitoneal injection of 100 µg type II collagen in 100 µL of 0.1 *M* acetic acid, 21 d after primary immunization. However, we have not found this to be necessary.
8. Monitor mice for arthritis every day from day 14 after immunization, although the peak time of arthritis onset is around day 30 (*see* **Note 4**).
9. To compare the clinical severity of arthritis a scoring system may be used:

   0 = normal
   1 = slight swelling and/or erythema
   2 = pronounced swelling
   3 = ankylosis

   Each limb is graded in this way, giving a maximum score of 12 per mouse. In addition, paw-swelling can be monitored using calipers (Poco 2T, Kroeplin).
10. To compare histological severity, paws are removed at postmortem, fixed in buffered formalin (10% v/v), then decalcified in EDTA in buffered formalin (5.5% w/v). The tissues are then embedded in paraffin, sectioned, and stained with hematoxylin and eosin. The severity of arthritis may be graded as mild, moderate, or severe based on the following criteria:

    mild = minimal synovitis, cartilage loss and bone erosions limited to discrete foci
    moderate = synovitis and erosions present but normal joint architecture intact
    severe = synovitis, extensive erosions, joint architecture disrupted

    Alternatively, the proportion of joints with erosions (defined as demarcated defects in cartilage or bone filled with inflammatory tissue) can be determined.

3.3. Measurement of Anti-Collagen IgG

Serum levels of anti-collagen IgG provide a marker of the magnitude of the humoral anti-collagen response, whereas levels of IgG1 and IgG2a serve as extremely valuable in vivo markers of Th2 and Th1 responses, respectively.

1. Make up stock solution of type II collagen in 0.05 *M* Tris-HCl/0.2*M* NaCl, pH 7.4, at 1 mg/mL. Aliquot and store at –20°C (*see* **Note 2**).
2. Coat ELISA plate with type II collagen at 2–5 μg/mL in 0.05*M* Tris-HCl/0.2*M* NaCl, pH 7.4, overnight at 4°C.
3. Block for 1 h at room temperature with 2% BSA.
4. Incubate test sera (diluted in PBS/Tween-20) for 2 h at room temperature. Levels of anti-collagen IgG may vary enormously between mice, and it is important to serially dilute samples to ensure that comparisons are made based on the linear portion of the titration curve. A suggested starting dilution is 1/100, with seven three- to fivefold dilution steps. Include a standard serum sample on each plate. Pooled serum from collagen-immunized mice or affinity purified anti-collagen IgG can be used as a standard.
5. Wash 6 times with PBS/Tween-20, then detect bound IgG with HRP-conjugated anti-mouse IgG, IgG1, or IgG2a.
6. Develop with TMB substrate. Stop reaction with 4.5 *N* H_2SO_4 and read at 450 nm.

3.4. Analysis of T-Cell Responses

1. Proliferative responses may be measured by incorporation of [^{3}H]-thymidine in response to stimulation with type II collagen, and cytokines in culture supernatants can be measured by ELISA.
2. Make up stock solution of type II collagen in 0.05*M* Tris-HCl/0.2*M* NaCl, pH 7.4, at 1 mg/mL. Collagen in solution can be kept at 4°C for up to 3 mo (for stimulation of T cells only; *see* **Note 2**).
3. Remove draining (inguinal) lymph nodes from collagen-immunized mice.
4. Push nodes through cell strainer using syringe plunger, then wash three times in HBSS.
5. Resuspend at 5 × 10^6 cells/mL in complete medium and culture for 72 h (37°C; 5% CO_2) in the presence or absence of type II collagen (50 μg/mL).
6. Remove supernatant for measurement of IL-5, IL-10, and interferon (IFN)γ (*see* **Note 5**). Coat ELISA plates with respective capture monoclonal antibody (MAb) (overnight at 4°C), block with 2% BSA (1 h at room temperature), then incubate supernatants (overnight at 4°C). Generate standard curve using appropriate recombinant cytokine at a range of 10,000 pg/mL to 14 pg/mL for IL-5 and IL-10, and 100,000 pg/mL to 137 pg/mL for IFNγ. Wash six times with PBS/Tween-20, then incubate with biotinylated detect MAb. Wash six times with PBS/Tween-20, then add HRP-conjugated streptavidin (1 h at room temperature) and develop with TMB substrate. Stop the reaction with 4.5 *N* H_2SO_4 and read at 450 nm.
7. To determine the rate of T-cell proliferation, pulse cells with [^{3}H]-thymidine and culture for a further 16 h. Harvest cells and assess for incorporation of radioactivity.

4. Notes

1. Source of cartilage. For immunization of mice, type II collagen from bovine, porcine, or chick cartilage is normally used. Alternatively, mouse collagen (from sternums) may be used, which results in a more chronic relapsing form of arthritis. This form is reported to be more similar to human RA than conventional CIA induced with heterologous collagen ***(12)***. The yield and solubility of the type II collagen is greater when derived from young animals due to the reduced level of crosslinking. The sternum, nasal septum, or articular cartilage may be used. A good source is femoral head cartilage from a young calf. Peel off the cartilage from the surface of the bone using a scalpel, and wearing chain mail gloves and eye protection for safety. The cartilage is white. Avoid the underlying bone, which is pink. In the case of sternum or nasal septum, the cartilage should be chopped into small pieces. Type II collagen for immunization can also be purchased from Chondrex.
2. Storage of collagen. Once in solution, it is important for type II collagen to be maintained at a low temperature to prevent denaturation. Proper storage is crucial for successful immunization and for measurement of anti-collagen antibody levels, whereas T-cell activity is less sensitive to the conformational state of the collagen molecule.
3. Establishing the model. Two factors of importance in determining incidence of arthritis are the concentrations of *M. tuberculosis* in the adjuvant and collagen in the acetic acid. To establish the system, high concentrations can be used, e.g., 3 mg *Mycobacterium* per mL of IFA, and collagen at 4 mg/mL of acetic acid. These concentrations invariably induce high incidence, but the arthritis is severe and acute in nature, and therefore the amounts can subsequently be reduced once the system is known to be working.

   The most likely reasons for a failure to induce a high incidence of arthritis include the following: (1) The collagen preparation is of low purity or in a denatured form. (2) There is concurrent infection in the mouse colony, the mice are immature (less than 8 wk of age), or females rather than males are used. (3) The concentration of type II collagen or *M. tuberculosis* in the emulsion used for immunization is insufficient, the emulsion is not thick enough, or it is injected too deeply.
4. Ethical considerations and the use of humane endpoints. Following immunization, mice will develop arthritis of varying degrees of severity, and novel treatment regimes may produce unexpected adverse effects. Hence, mice should be monitored on a daily basis for signs of ill health or distress. Clearly defined humane endpoints should be strictly enforced. For example, any mouse showing severe and sustained paw swelling should be humanely killed. Any mouse which has lost 20% or more of its body weight should be humanely killed. Any mouse with severe lameness should be humanely killed. Any mouse with dyspnea, ruffled fur, weakness, dehydration, or a hunched appearance should be humanely killed. Any mouse showing blistering at the injection site should be humanely killed. In addition, the duration of experiments involving arthritic animals should be minimized, compatible with the aims of the study.

5. Measurement of T-cell cytokines. In general, IL-5, IL-10, and IFNγ can be measured in culture supernatants of collagen-stimulated T cells taken from mice with active disease, whereas IL-2 and IL-4 are difficult to detect, probably because of consumption of these cytokines by proliferating cells. An alternative is therefore to study cytokine expression by intracellular staining and FACS analysis. Another important factor is that Th2 cells are usually found in low abundance in DBA/1 mice immunized with CFA, although immunomodulatory treatments may influence the Th1:Th2 ratio.

References

1. Boissier, M. C., Feng, X. Z., Carlioz, A., Roudier, R., and Fournier, C. (1987) Experimental autoimmune arthritis in mice. I. Homologous type II collagen is responsible for self-perpetuating chronic polyarthritis. *Ann. Rheum. Dis.* **46,** 691–700.
2. Elliott, M. J., Maini, R. N., Feldmann, M., Kalden, J. R., Antoni, C., Smollen, J. S., et al. (1994a) Treatment with a chimaeric monoclonal antibody to tumour necrosis factor α suppresses disease activity in rheumatoid arthritis: results of a multi-centre, randomised, double blind trial. *Lancet* **344,** 1105–1110.
3. Elliott, M. J., Maini, R. N., Feldmann, M., Long-Fox, A., Charles, P., Bijl, H., et al. (1994b) Repeated therapy with a monoclonal antibody to tumour necrosis factor α in patients with rheumatoid arthritis. *Lancet* **344,** 1125–1127.
4. Elliott, M. J., Maini, R. N., Feldmann, M., Long-Fox, A., Charles, P., Katsikis, P., et al. (1993) Treatment of rheumatoid arthritis with chimeric monoclonal antibodies to tumour necrosis factor α. *Arthr. Rheum.* **36,** 1681–1690.
5. Geiger, T., Towbin, H., Cosenti-Vargas, A., Zingel, O., Arnold, J., Rordorf, C., et al. (1993) Neutralization of interleukin-1β activity in vivo with a monoclonal antibody alleviates collagen-induced arthritis in DBA/1 mice and prevents the associated acute-phase response. *Clin. Exp. Rheum.* **11,** 515–522.
6. Herbage, D., Bouillet, J., and Bernengo, J. C. (1977) Biochemical and physiochemical characterization of pepsin-solubilized type-II collagen from bovine articular cartilage. *Biochem. J.* **161,** 303–312.
7. Holmdahl, R., Andersson, M. E., Goldschmidt, T. J., Jansson, L., Karlsson, M., Malmström, V., et al. (1989) Collagen induced arthritis as an experimental model for rheumatoid arthritis. Immunogenetics, pathogenesis and autoimmunity. *APMIS* **97,** 575–584.
8. Holmdahl, R., Jansson, L., Larsson, E., Rubin, K., and Klareskog, L. (1986) Homologous type II collagen induces chronic and progressive arthritis in mice. *Arthr. Rheum.* **29,** 106–113.
9. Hom, J. T., Butler, L. D., Riedl, P. E., and Bendele, A. M. (1988) The progression of the inflammation in established collagen-induced arthritis can be altered by treatments with immunological or pharmacological agents which inhibit T cell activities. *Eur. J. Immunol.* **18,** 881–888.
10. Joosten, L. A. B., Helen, M. M. A., van de Loo, F. A. J., and Van den Berg, W. B. (1996) Anticytokine treatment of established type II collagen-induced arthritis in

DBA/1 mice: a comparative study using anti-TNFα, anti-IL-1α/β, and IL-1Ra. *Arthr. Rheum.* **39,** 797–809.
11. Malfait, A.-M., Butler, D. M., Presky, D. H., Maini, R. N., Brennan, F. M., and Feldmann, M. (1998) Blockade of IL-12 during the induction of collagen-induced arthritis (CIA) markedly attenuates the severity of the arthritis. *Clin. Exp. Immunol.* **111,** 377–383.
12. Malfait, A. M., Williams, R. O., Malik, A. S., Maini, R. N., and Feldmann, M. (2001) Chronic relapsing homologous collagen-induced arthritis in DBA/1 mice as a model for testing disease-modifying and remission-inducing therapies. *Arthr. Rheum.* **44,** 1215–1224.
13. Marinova-Mutafchieva, L., Williams, R. O., Mason, L. J., Mauri, C., Feldmann, M., and Maini, R. N. (1997) Dynamics of proinflammatory cytokine expression in the joints of mice with collagen-induced arthritis (CIA). *Clin. Exp. Immunol.* **107,** 507–512.
14. Mauri, C., Chu, C. Q., Woodrow, D., Mori, L., and Londei, M. (1997) Treatment of a newly established transgenic model of chronic arthritis with nondepleting anti-CD4 monoclonal antibody. *J. Immunol.* **159,** 5032–5041.
15. Miller, E. J. (1972) Structural studies on cartilage collagen employing limited cleavage and solubilization with pepsin. *Biochemistry* **11,** 4903–4909.
16. Moreland, L. W., Baumgartner, S. W., Schiff, M. H., Tindall, E. A., Fleischmann, R. M., Weaver, A. L., et al. (1997) Treatment of rheumatoid arthritis with a recombinant human tumor necrosis factor receptor (p75)-Fc fusion protein. *N. Engl. J. Med.* **337,** 141–147.
17. Piguet, P. F., Grau, G. E., Vesin, C., Loetscher, H., Gentz, R., and Lesslauer, W. (1992) Evolution of collagen arthritis in mice is arrested by treatment with anti-tumour necrosis factor (TNF) antibody or a recombinant soluble TNF receptor. *Immunology* **77,** 510–514.
18. Ranges, G. E., Sriram, S., and Cooper, S. M. (1985) Prevention of type II collagen-induced arthritis by in vivo treatment with anti-L3T4. *J. Exp. Med.* **162,** 1105–1110.
19. Ratcliffe, A., Doherty, M., Maini, R. N., and Hardingham, T. E. (1988) Increased concentrations of proteoglycan components in the synovial fluids of patients with acute but not chronic joint disease. *Ann. Rheum. Dis.* **47,** 826–832.
20. Thorbecke, G. J., Shah, R., Leu, C. H., Kuruvilla, A. P., Hardison, A. M., and Palladino, M. A. (1992) Involvement of endogenous tumor necrosis factor α and transforming growth factor β during induction of collagen type II arthritis in mice. *Proc. Natl. Acad. Sci. USA* **89,** 7375–7379.
21. Trentham, D. E. (1982) Collagen arthritis as a relevant model for rheumatoid arthritis: evidence pro and con. *Arthr. Rheum.* **25,** 911–916.
22. Van den Berg, W. B., Joosten, L. A., Helsen, M., and van de Loo, F. A. (1994) Amelioration of established murine collagen-induced arthritis with anti-IL-1 treatment. *Clin. Exp. Immunol.* **95,** 237–243.
23. Webb, L. M., Walmsley, M. J., and Feldmann, M. (1996) Prevention and amelioratrion of collagen-induced arthritis by blockade of the CD28 co-stimula-

tory pathway: requirement for both B7-1 and B7-2. *Eur. J. Immunol.* **26,** 2320–2328.
24. Weinblatt, M. E., Kremer, J. M., Bankhurst, A. D., Bulpitt, K. J., Fleischmann, R. M., Fox, R. I., et al. (1999) A trial of etanercept, a recombinant tumor necrosis factor receptor:Fc fusion protein, in patients with rheumatoid arthritis receiving methotrexate. *N. Engl. J. Med.* **340,** 253–259.
25. Williams, R. O. (1998) Rodent models of arthritis: relevance for human disease. *Clin. Exp. Immunol.* **114,** 330–332.
26. Williams, R. O., Feldmann, M., and Maini, R. N. (1992) Anti-tumor necrosis factor ameliorates joint disease in murine collagen-induced arthritis. *Proc. Natl. Acad. Sci. USA* **89,** 9784–9788.
27. Williams, R. O., Ghrayeb, J., Feldmann, M., and Maini, R. N. (1995) Successful therapy of collagen-induced arthritis with TNF receptor-IgG fusion protein and combination with anti-CD4. *Immunology* **84,** 433–439.
28. Wooley, P. H., Dutcher, J., Widmer, M. B., and Gillis, S. (1993) Influence of a recombinant human soluble tumour necrosis factor receptor Fc fusion protein on type II collagen-induced arthritis in mice. *J. Immunol.* **151,** 6602–6607.

16

Myocardial Infarction

Animal Models

Stefano Chimenti, Eleonora Carlo, Serge Masson, Antonio Bai, and Roberto Latini

Summary

Among the cardiovascular pathologies, ischemic heart disease is the leading cause of congestive heart failure as well as permanent premature disabilities. Reperfusion of a previously ischemic heart is a standard clinical procedure. Even if beneficial, reperfusion triggers an inflammatory response that contributes to the acute extension of ischemic injury and later participates in the reparative processes of the damaged myocardium. Occlusion of a major coronary artery in small rodents, followed or not followed by reperfusion, has proven to be a good model to assess the relevance of pathophysiological processes and drug effects in the setting of myocardial ischemia. Models involving reperfusion appear to be particularly suitable to study the inflammatory response, which is much more marked than with permanent ischemia. Ischemia/reperfusion of the myocardium in wild-type and transgenic animals (mostly mice) allows the possibility of testing the vast array of mediators that orchestrate the sequelae of inflammation, including tumor necrosis factor (TNF). Moreover, this model allows testing of the protective effects of anti-inflammatory drugs in experimental myocardial infarction.

Key Words: Myocardial infarction; heart; ischemia; ischemia/reperfusion; coronary artery ligation.

1. Introduction

The progressive increase in life expectancy at birth and the shift of major causes of death and disability in the more advanced societies from nutritional deficiencies and infectious diseases to chronic degenerative diseases have generated further expectations on the clinical management of these emerging pathologies. It is estimated that approx 31% of all deaths in the world in 1998 were attributable to atherothrombotic cardiovascular diseases, although this proportion is significantly more elevated in Western countries ***(1)***. Experimen-

From: *Methods in Molecular Medicine, Vol. 98: Tumor Necrosis Factor*
Edited by: A. Corti and P. Ghezzi © Humana Press Inc., Totowa, NJ

tal research with appropriate animal models of documented relevance for human cardiovascular pathologies should contribute to the vast effort to respond to this emergency.

Modern animal models of myocardial infarction use mainly small rodents (rats or mice) both for practical reasons (lower cost and requirements for facilities) and because molecular biology tools (reagents and generation of transgenic animals) are more easily available for those species. Though pharmacological models ***(2)*** or microembolization ***(3)*** have been proposed in the past to create diffuse cardiac microinfarctions, most techniques for producing myocardial infarction in small rodents are based on the surgical occlusion of a coronary artery and are derived from the procedures originally described by H. Selye and collaborators ***(4).*** The surgical model of permanent coronary artery occlusion has been subsequently characterized in terms of histological, anatomical, and functional variables by various investigators ***(5–8)*** and it is currently used for pathophysiological studies and drug evaluation for myocardial infarction, left ventricular dysfunction, and heart failure.

Anticoagulant/thrombolytic therapies and invasive procedures of revascularization are usually performed in the clinical setting after acute myocardial infarction to restore blood flow in the coronary vessels. Even if beneficial overall, reperfusion of a previously ischemic myocardium triggers inflammation that reflects cellular response to injury ***(9)*** but may also contribute to additional damage. In vivo small rodent models of cardiac ischemia (surgical occlusion of a coronary artery) followed by reperfusion have been developed to mimic more closely the human situation and also to study reperfusion-induced cardiac injury, in particular the inflammatory processes associated to ischemia-reperfusion ***(10)***. These models require sophisticated techniques and good operative skills, because acute surgical trauma may trigger potent inflammatory responses even in sham-operated animals and obscure the "true" pathophysiology of cardiac ischemia and reperfusion ***(11–12)***.

Acute myocardial infarction and reperfusion of previously ischemic cardiac tissue is associated with a strong inflammatory response that contributes to the acute extension of the initial injury, but that also participates in mechanisms of repair of the myocardium. In this complex sequence of pathophysiological events, tumor necrosis factor-α (TNFα) plays a multifaceted role. It exerts a specific hypertrophic effect on isolated cardiac myocytes (net synthesis of protein) ***(13)*** and promotes contractile dysfunction mediated by release of cardiac nitric oxide ***(14)***. Furthermore, short-term administration of exogenous TNFα to healthy rats induces a progressive but reversible depression of left ventricular function and its dilation ***(15)***, possibly through a control of the subtle balance between proteins that affect collagen turnover (metalloproteinases and their natural inhibitors) ***(16)***. TNFα protein production and gene transcription,

and the expression of one of its cellular receptors, TNFR-1, is consistently elevated acutely in the myocardium after myocardial infarction induced by permanent ligation of the left anterior descending coronary artery ***(17)***. In contrast, the endogenous TNF system seems to exert a protective effect in the infarcted myocardium. Indeed, infarct size and the extent of apoptosis are significantly larger in mice lacking both TNFα receptors and subjected to acute coronary artery occlusion than in wild-type mice ***(18)***. The apparently double-faceted role played by TNFα in myocardial infarction, reducing and/or increasing injury, is still the object of active experimental research.

2. Materials

2.1. Inhalant Anesthesia

1. Pre-anesthesia: ketamine (Sigma), acepromazine (Prequillan®, Fatro).
2. Anesthesia (isoflurane (Forane®, Abbott), oxygen, and nitrous oxide (Air Liquide),Vaporizer (Ohmeda), system for gases aspiration (Fluovac and Fluosorber, Harvard), ventilator for rodents (Ugo Basile), perspex induction chamber.

2.2. Injectable Anesthesia

1. Rat: Equithesin (9.7 mg/mL pentobarbital in saline, 42.6 mg/mL chloral hydrate in 1,2-propandiol, 21.2 mg/mL $MgSO_4$ in absolute ethanol).
2. Mouse: Avertin 2.5% (5 g 2,2,2-tribromoethanol, 5 mL tertiary amyl alcohol; add 0.1 mL of solution to 3.9 mL of saline).

2.3. Drugs and Solutions

1. Ampicillin (Amplital®, Pharmacia).
2. Polyvinylpyrrolidone (Betadine®, Viatris).
3. Benzoxonium chloride (Bialcol Med®, Novartis).
4. Evans blue (Sigma) 5% w/v.
5. Disinfectant for surgical instruments (Alcoholic Blue Citrosil®, Manetti Roberts).

2.4. Instruments

1. Endotracheal intubation: Small straight anatomical forceps, curved jewelers' forceps, large paperclip, 18-gage (23-gage for mouse) needle cannula.
2. Surgery: Curved scissors, straight scissors, curved jewelers' forceps, needle-holder, rib spreader, metal clips, hemostat.
3. Miscellaneous: Cotton, paper adhesive tape, board, 1-mL syringes with removable 25- or 26-gage needle, 7-0 suture (Ethicon).

3. Methods

The method for the rat is described in detail with the help of serial pictures, mainly for practical reasons: Being that the rat is 10-fold larger than the mouse,

pictures appear more clear and easier to understand. The procedure for the mouse is practically identical, but with few changes that are specified in the Notes section.

3.1. Myocardial Infarction

1. Use male or female rats or mice (*see* **Note 1**).
2. Apply anesthesia (*see* **Note 2**).
3. Implement mechanical ventilation through an endotracheal cannula (*see* **Note 3**) (**Fig. 1A**).
4. Open the chest at the left fourth intercostal space (use hemostats or round end scissors to open without cutting in order to reduce bleeding) (**Fig. 1B**).
5. Place rib spreader taking maximal care not to damage the lung; expose the left ventricle (**Fig. 1C**).
6. Open the pericardium; when possible leave the pericardium intact.
7. Ligate the left anterior coronary artery (LAD) without exteriorization of the heart (*see* **Note 4**).
8. Use 7-0 silk suture (Ethicon) for coronary ligation.
9. Tie a plain knot and a reverse knot (for ischemia/reperfusion, a single knot is tightened and can be released after a chosen time) (*see* **Note 5**) (**Fig. 1D–1E**).
10. Close the chest under negative pressure and close the wound with metal clips (*see* **Note 6**).
11. The rat is weaned from mechanical ventilation under ECG monitoring (*see* **Note 7**).
12. Postsurgical analgesia is achieved with buprenorphine 0.1–0.5 mg/kg subcutaneously at awakening followed by another dose 8–12 h later.
13. Antibiotic prophylaxis is achieved by a single injection of ampicillin, 150 mg/kg subcutaneously, right after surgery.
14. The estimate of the adequate number of animals in each group is discussed in **Note 8**.

3.2. Evaluation of Area at Risk (AAR) and Extent of the Scar (Ischemia/Reperfusion Model)

1. When sacrificing the animal at the end of an experiment follow the protocol in **Subheading 3.1., steps 1–5**.
2. Tie the previously loosened knot (at time of LAD ligation, remember to leave 1–2 cm of thread to ease this step).
3. Inject 1 mL (0.3 mL for mouse) 5% Evans blue into the femoral vein or the right ventricular chamber and wait 2 min (**Fig. 1F**).
4. Rapidly excise the heart, blot it, and embed it for optical coherence tomography (OCT); place the mold on dry ice.
5. Once the heart is hard (to allow a better cutting it usually takes 3–5 min) cut into 1-mm serial transverse sections to identify a perfused portion (blue) and the AAR (unstained, white), which is the portion of the myocardium that was supplied by the tied coronary artery (**Fig. 2A**) (*see* **Note 8**).

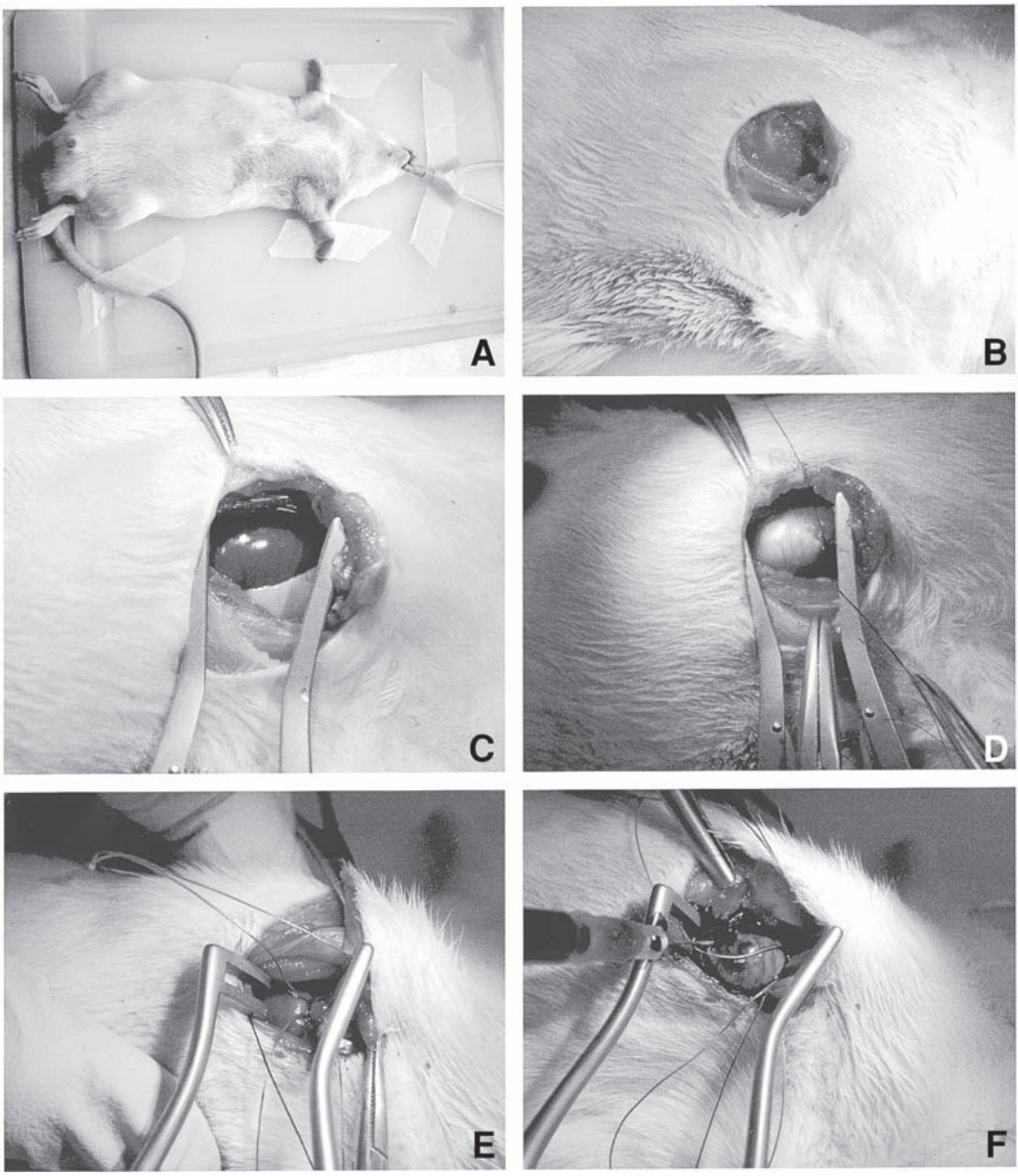

Fig. 1. Steps for coronary artery ligation in the rat. **(A)** Ventilation. **(B)** Opening of chest. **(C)** Placement of rib spreader. **(D)** Tightening of ligature. **(E)** Release of ligature in ischemic/reperfusion model. **(F)** Injection of Evans blue.

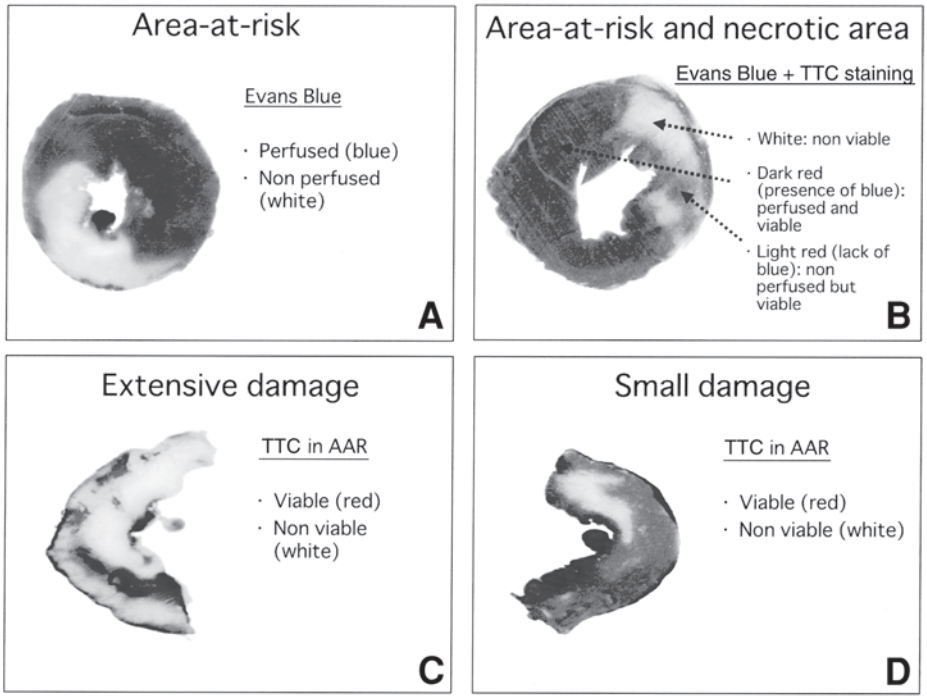

Fig. 2. Method for the assessment of area at risk (Evans blue) and cardiac damage (TTC negative) in heart sections. **(A)** Perfusion with Evans blue. **(B)** Myocardium staining. **(C)** Extensive damage. **(D)** Minor damage.

6. Sections are incubated at room temperature for 20 min in tetrazolium chloride (TTC), and then put in 4% formaldehyde to increase contrast between stains (blue and red). An adequate contrast for image analysis of the sections is obtained after incubation from 24 h to few days. **Fig. 2** shows the differences in color between different areas of myocardium: perfused, nonperfused but viable, and nonperfused and dead (**Fig. 2B**). By computing infarct area relative to that of the AAR isolated by cutting (**Fig. 2C, D**), one can correct for individual differences in infarct size; in this case, infarct size will be expressed as a percent of the AAR, not of the whole left ventricle.

4. Notes

1. Any body weight and age; caution should be taken with older animals in the anesthesia step (i.e., older animals require less anesthetic).
2. Many anesthetics can be used, each one with limitations (such as negative inotropic action, proarrhythmic effect, and so forth). Only long experience with a specific anesthetic will minimize the risks while obtaining satisfactory anesthesia and analgesia ***(19,20)***. The agents/procedures most frequently used by the authors are:

   a. Rat: Equithesin 3 mL/kg; ketamine 100 mg/kg ip and acepromazine 1 mg/kg ip; chloral hydrate 250 mg/kg ip.
   b. Mouse: ketamine 150 mg/kg ip and acepromazine 0.8 mg/kg ip; avertin 250 mg/kg ip.
   c. Premedication for inhalant anesthesia: ketamine 30 mg/kg ip and acepromazine 0.75 mg/kg ip.
   d. Volatile anesthetics, such as isoflurane, can be used for inhalation anesthesia; in this case, weaning from ventilator and complete awakening of the animal will occur within 5 to 10 min, much faster than with injectable anesthetics.

3. Mechanical ventilation:

   a. Rat: 60 breaths/min, tidal volume 1.2 mL/100 g BW.
   b. Mouse: 120 breaths/min, tidal volume 1.5 mL/100 g BW.

4. This procedure is less traumatic and more accurate than the one performed on the exteriorized heart; it is important in this model to avoid any manipulation, mechanical stress, and trauma of the heart that would amplify *per se* inflammatory responses. The ligature is usually located just below the left atrial appendix. Adequate illumination of the intramural arteries with fiberoptics (usually more than one can be visualized in rat and mouse) gives further accuracy to the surgeon. By placing the suture closer to the heart apex, smaller infarcts can be obtained. This technique does not allow 100% yield of infarcts of predictable size, mainly because of individual anatomical differences in the coronary tree; it is not infrequent to have one or two animals out of 20 without infarct (or with a very small one), unexpectedly. Echocardiography is the most reliable noninvasive method to select infarcted animals as early as a few days after CAO.
5. In case reperfusion will follow an ischemia period, only one plain knot will be tied. Then, several tricks are available to ease the loosening of the knot, without damaging the myocardium with risk of hemorrhage; the one preferred by the authors is to tighten the knot over two rings of suture (3–0), which can then be pulled to start reperfusion 30 to 45 min after coronary ligation (**Fig. 1E**). Leave the loosened suture around the LAD for the determination of AAR.
6. It is crucial to obtain optimal reduction of the pneumothorax. Two techniques can be used:

   a. A soft rubber tube connected to a 10-mL syringe (5-mL syringe for the mouse) is introduced into the open chest. The coat is sealed around the tube with two fingers and the air aspired.
   b. The air outflow of the ventilator is closed for three to four respiratory cycles in order to inflate the lungs and eliminate the air from the chest. Then the coat is sealed. This technique is less invasive and the consequent risk of lung damage reduced.

7. Ischemia is confirmed by the appearance of ventricular ectopies (discoloration of the heart surface), while reperfusion is verified by reddening of previously discolored areas. Sham-operated animals undergo the same surgical procedures,

without ligation of LAD. Sham-operated animals are essential, especially when studying inflammatory processes.

8. The number of animals required in each experimental group should be estimated, considering the individual variability of infarct size and mortality (15% to 50%, according to different groups, occurring mainly within the first 24 h after LAD ligation in rats, and the first 48 h after LAD ligation in mice), which has to be established by the individual investigator with a specific strain of animals. (Mortality can be different with different strains; this phenomenon is observed in particular when using transgenic mice.) On the average, 18 animals undergo the operation to obtain a final number of 10 animals suitable for the experiment.

References

1. Yusuf, S., Reddy, S., Ounpuu, S., and Anand, S. (2001) Global burden of cardiovascular diseases. Part I: general considerations, the epidemiological transition, risk factors, and impact of urbanization. *Circulation* **104,** 2746–2753.
2. Rona, G., Chappel, C. I., Balazs, T., and Gaudry, R. (1959) An infarct-like myocardial lesion and other toxic manifestations produced by isoproterenol in the rat. *AMA Arch. Pathol.* **67,** 443–455.
3. Medvedev, O. S. and Gorodetskaya, E. A. (1993) Systemic and hemodynamic effects of perindopril in experimental heart failure. *Am. Heart J.* **126,** 764–769.
4. Selye, H., Bajusz, E., Grasso, S., and Mendell, P. (1960) Simple techniques for the surgical occlusion of coronary vessels in the rat. *Angiology* **11,** 398–407.
5. Anversa, P., Beghi, C., Kikkawa, Y., and Olivetti, G. (1985) Myocardial response to infarction: morphometric measurement of infarct size and myocyte cellular hypertrophy. *Am. J. Pathol.* **118,** 484–492.
6. Anversa, P., Beghi, C., Kikkawa, Y., and Olivetti, G. (1986) Myocardial infarction in rats: infarct size, myocyte hypertrophy, and capillary growth. *Circ. Res.* **58,** 26–37.
7. Pfeffer, M. A., Pfeffer, J. M., Fishbein, M. C., Fletcher, P. J., Spadaro, J., Kloner, R. A., et al. (1979) Myocardial infarct size and ventricular function in rats. *Circ. Res.* **44,** 503–512.
8. Pfeffer, J. M., Pfeffer, M. A., Fletcher, P. J., and Braunwald, E. (1991) Progressive ventricular remodeling in rat with myocardial infarction. *Am. J. Physiol.* **260,** H1406–H1414.
9. Entman, M. L., Michael, L. H., Rossen, R. D., Dreyer, W. J., Anderson, D. C., Taylor, A. D., et al. (1991) Inflammation in the course of early myocardial ischemia. *FASEB J.* **5,** 2529–2537.
10. Himori, N. and Matsuura, A. (1989) A simple technique for occlusion and reperfusion of coronary artery in conscious rats. *Am. J. Physiol.* **256,** H1719–H1725.
11. Nossuli, T. O., Lakshminarayanan, V., Baumgarten, G., Taffet, G. E., Ballantyne, C. M., Michael, L. H., et al. (2000) A chronic model of myocardial ischemia-reperfusion: essential of cytokine studies. *Am. J. Physiol.* **278,** H1049–H1055.

12. Entman, M. L., Nossuli, T. O., Lakshminarayanan, V., and Michael, L. H. (2000) For want of a few good shams. *Am. J. Physiol.* **278,** H1017–H1018.
13. Yokoyama, T., Nakano, M., Bednarczyk, J. L., McIntyre, B. W., Entman, M., and Mann, D. L. (1997) Tumor necrosis factor-α provokes a hypertrophic growth response in adult cardiac myocytes. *Circulation* **95,** 1247–1252.
14. Finkel, M. S., Oddis, C. V., Jacob, T. D., Watkins, S. C., Hattler, B. G., and Simmons, R. L. (1992) Negative inotropic effects of cytokines on the heart mediated by nitric oxide. *Science* **257,** 387–389.
15. Bozkurt, B., Kribbs, S. B., Clubb, F. J., Michael, L. H., Didenko, V. V., Hornsby, P. J., et al. (1998) Pathophysiologically relevant concentrations of tumor necrosis factor-α promote progressive left ventricular dysfunction and remodeling in rats. *Circulation* **97,** 1382–1391.
16. Sivasubramanian, N., Coker, M. L., Kurrelmeyer, K. M., MacLellan, W. R., DeMayo, F. J., Spinale, F. G., et al. (2001) Left ventricular remodeling in transgenic mice with cardiac restricted overexpression of tumor necrosis factor. *Circulation* **104,** 826–831.
17. Irwin, M. W., Mak, S., Man, D. L., Qu, R., Penninger, J. M., Yan, A., et al. (1999) Tissue expression and immunolocalization of tumor necrosis factor-α in postinfarction dysfunctional myocardium. *Circulation* **99,** 1492–1498.
18. Kurrelmeyer, K. M., Michael, L. H., Baumgarten, G., Taffet, G. E., Peschon, J. J., Sivasubramaninan, N., et al. (2000). Endogenous tumor necrosis factor protects the adult cardiac myocyte against ischemic-induced apoptosis in a murine model of acute myocardial infarction. *Proc. Natl. Acad. Sci. USA* **97,** 5456–5461.
19. Gross, D. R. *Animal Models in Cardiovascular Research*, Kluwer Academic Publishers, Dordrecht, The Netherlands, 1994.
20. Wixson, S. K. and Smiller, K. L. Anesthesia and analgesia in rodents. In *Anesthesia and Analgesia in Laboratory Animals* (Kohn, D. F., Wixson, S. K., White, W. J., and Benson G. J., eds.), Academic, London, 1997, pp. 165–203.

17

Tumor Vascular Therapy With TNF

Critical Review on Animal Models

Timo L. M. ten Hagen and
Alexander M. M. Eggermont

Summary

To study tumor therapeutic treatment modalities, whether from a clinical, preclinical, or fundamental point of view, the use of clinically relevant animal models is indispensable. Particularly when the treatment comprises a multitargeted approach, (e.g., both tumor cells and endothelial cells are targeted), the in vitro data will be of very limited value. Well-chosen animal models will provide conclusive data on the activity of the drug in the complex in vivo setting. Moreover, when the treatment targets the stromal compartment of the tumor rather than the tumor cells directly, insight into the mechanism of action is only possible when studied in vivo. This approach is of great importance for studies on the use of tumor necrosis factor-α (TNFα) in solid tumor therapy. Although TNFα has shown activity toward tumor cells in vitro directly, we and others have demonstrated that an important activity of this cytokine is directed toward the tumor vasculature. To elucidate the working mechanism of TNFα and to test possible treatment modalities, the animal models described here are crucial. In this chapter we will describe the use of specific animal models for efficacy studies, such as isolated limb perfusion and isolated liver perfusion in the rat.

Key Words: Tumor necrosis factor; tumor animal models; sarcoma; melanoma; isolated limb perfusion; isolated hepatic perfusion; systemic treatment; long circulating liposomes; Doxil.

1. Introduction

Targeting the tumor vasculature in the treatment of cancer is a highly favorable approach. Not only is the vasculature the first target encountered by systemically injected drugs, it is also very important for the survival of the tumor. First, studies with antiangiogenic agents have demonstrated that inhibition of the tumor vascular growth can have a profound effect on tumor development

From: *Methods in Molecular Medicine, Vol. 98: Tumor Necrosis Factor*
Edited by: A. Corti and P. Ghezzi © Humana Press Inc., Totowa, NJ

(1,2). Moreover, destruction of the tumor-associated vasculature (TAV), or manipulation of the endothelial lining of the TAV, to facilitate, for instance, augmented extravazation of chemotherapeutic agents, was shown to improve greatly the concomitant chemotherapy ***(3)***. We have shown in an isolated limb perfusion (ILP) setting that tumor necrosis factor-α (TNFα) strongly enhances accumulation of a co-administered drug in tumor tissue, which is accompanied by a strongly enhanced tumor response. Comparable results were obtained in the isolated liver perfusion setting (isolated hepatic perfusion [IHP]). Also in the systemic treatment setting, TNFα at low dose acts on the tumor-associated vasculature, inflicting increased permeability. These changes in the pathophysiology of the tumor result in an augmented accumulation of the co-administered drug, which is accompanied by a dramatically improved tumor response. TNFα is an example of a drug that has rather specific activity on tumor endothelial cells, resulting in cell morphology changes, integrin expression alterations, and apoptosis. The endothelial lining provides a favorable target, as it appears that endothelial cells of the TAV do not develop resistance toward the drugs used, as tumor cells tend to do.

In this chapter we will describe the use of specific animal models for efficacy studies, such as isolated limb perfusion and isolated liver perfusion in the rat.

First, we will describe the isolated perfusion models in rats that we used for testing the efficacy of TNFα in combination with chemotherapy and to elucidate possible working mechanisms of TNFα. Second, studies with systemically applied TNFα will be discussed. One of the most important aspects of animal studies is the reproducibility of the experiments. Therefore, one should be certain that the animals are in good shape and are not suffering from any disease. It is important to perform health inspections and to demand animals with the same bacterial status with every new batch. For all animal models described in this chapter, the protocols were approved by the committee for animal research of Erasmus University, Rotterdam, the Netherlands. The experimental protocols adhered to the rules outlined in the Dutch Animal Experimentation Act of 1977.

2. Isolated Limb Perfusion

Drug delivery to solid tumors is one of the most challenging aspects in cancer therapy. Whereas agents seem promising in the test tube, clinical trials often fail due to unfavorable pharmacokinetics, poor delivery, low local concentrations, and limited accumulation in the target cell. Several of these barriers can be met by increasing local drug levels, while limiting exposure to sensitive sites. A straightforward approach in increasing local drug levels, while reducing systemic exposure and unwanted dilution, is the isolated perfusion. Here we will discuss in particular the ILP and the IHP settings. Especially in the ILP, dramatic results have been obtained.

2.1. The Clinical Setting

The technique of ILP was pioneered by O. J. Creech, E. T. Krementz, and their coworkers at Tulane University in New Orleans *(4)*. In ILP, regional concentrations of chemotherapeutic agents can be achieved that are 15 to 25 times higher than those reached after systemic administration, and without systemic side effects *(5)*. In the clinical setting, isolation of the blood circuit of a limb is achieved by clamping and cannulation of the major artery and vein, connection to an oxygenated extracorporeal circuit, ligation of collateral vessels, and application of a tourniquet. Once isolation is secured, drugs can be injected into the perfusion circuit. Because of its efficacy and low regional toxicity profile, melphalan is the standard drug, most commonly used at a dose of 10 mg/L perfused tissue for a leg and at 13 mg/L for an arm *(6)*. Tissue temperatures in the limbs are monitored, and radiolabeled albumin or erythrocytes are injected into the extracorporeal circuit so leakage into the systemic circulation can be detected *(7)*. Leakage monitoring is mandatory, especially now that high doses of TNFα are used in the treatment of soft-tissue sarcomas. After 1–1.5 h of perfusion, the limb is rinsed with an electrolyte solution, cannulas are removed, and the vessels are repaired. During the per-fusion, vasoconstriction in cutis and subcutis is prevented by using a warm-water mattress. In vivo drug uptake by in-transit metastases is two times higher at 39.5°C than at 37°C *(8)*. Moreover, tumor cells *per se* are sensitive to heat, and hyperthermia also improves uptake of drug by the tumor cells, especially at temperatures >41°C *(9,10)*. In rats we have demonstrated, however, that increasing the temperature above 38–39°C results in enhanced local toxicity when used in combination with TNFα *(11)*.

2.2. Rat Isolated Limb Perfusion Model

We developed a rat ILP model that closely mimics the clinical setting with respect to modality, tumor response, and tumor pathophysiology (**Fig. 1**). The perfusion technique was performed as described previously *(11–13)*. For the rat ILP, two different sarcoma tumor are used: the high-grade, rapidly growing and metastasizing BN-175 soft-tissue sarcoma (syngeneic in BN rat) *(12)*, and the intermediate-grade, rapidly growing and metastasizing ROS-1 osteosarcoma (syngeneic in WAG/Rij rat) *(13)*. For the described experiments, small fragments (3–5 mm) of the tumor, taken from a donor rat with an appropriate tumor with diameter of 12–14 mm, were implanted into the right hind limb of a recipient rat. Rat weight should be around 250 g. To increase reproducibility, we implant tumor fragments rather than injecting cells. The tumor fragments are derived from a donor rat that has been injected from a single batch of cells stored on liquid nitrogen. When the tumor is dissected from the donor rat, the

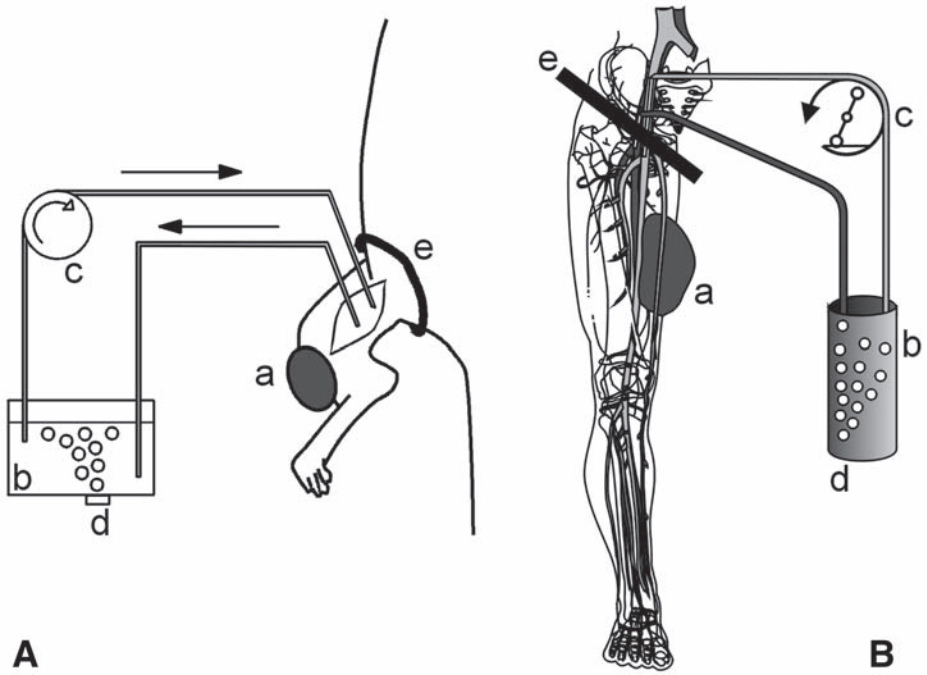

Fig. 1. Schematic representation of the isolated limb perfusion (ILP) in animal **(A)** and human **(B)** settings. In our laboratory the WAG/Rij and BN rats are used for the animal ILP. Basically the experimental ILP is the same as the clinical ILP. Above the tumor *(a)* an incision is made to expose the main veins and arteries, the a. femoralis and v. femoralis, which are cannulated and connected to an extracorporeal circuit. This circuit includes a reservoir *(b)* which is connected to a pump *(c)* and the perfusate is oxygenated *(d)* (heart-lung device in clinical settings). Above the tumor, a tight tourniquet is placed that compresses the vessels and prevents leakage to the system. In the experimental setting, the incision is made below the tourniquet, whereas in the clinical setting the incision is made above the tourniquet. In the latter, noncompressible tubing is used to cannulate.

tumor should have a standardized size. Only the outer rim is to be used, because central necrosis strongly affects tumor cell viability.

To implant the tumor fragment a small incision is made, and with the use of a blunt forceps a pocket is created away from the incision, which is closed with sutures. When the tumor is placed too close to the wound, it may break through the skin at that site.

Perfusion was performed at a tumor diameter of 11–14 mm at least 7–10 d after implantation. Animals were anesthetized with Hypnorm (Janssen Pharmaceutica) and 50 IU of heparin was injected intravenously to prevent coagulation. To keep the rat's hindlimb at a constant temperature, a warm-

water mattress was applied. Temperature was measured with a temperature probe on the skin covering the tumor, and was kept at 38–39°C ("mild" hyperthermia). To test the effect of leg temperature on tumor response we also varied between standard temperature, room temperature (24–26°C) and "true" hyperthermia (42–43°C). The femoral artery and vein were cannulated with silastic tubing (0.012 in id, 0.025 in od; and 0.025 in id, 0.047 in od, respectively, Dow Corning). Collaterals were occluded by a groin tourniquet, and isolation time started when the tourniquet was tightened. In the rat perfusion was maintained for 30 min. An oxygenation reservoir and a roller pump were included into the circuit. The perfusion solution was 5 mL Haemaccel (Behring Pharma), and the hemoglobin (Hb) content of the perfusate was 0.9 m*M*/L. Chemotherapeutics (Melphalan or Doxorubicin) and TNFα were added as boluses to the oxygenation reservoir. A roller pump (Watson Marlow; type 505 U) recirculated the perfusate at a flow rate of 2.4 mL/min. A washout with 5 mL oxygenated Haemaccel was performed at the end of the perfusion.

2.3. Assessment of Limb Function

Limb function was a "clinical" observation in which the rat's ability to walk and stand on the perfused limb was scored 5 d after ILP. On this scale a severe impaired function (grade 0) means that the rat drags its hind limb without any function; a slightly impaired function (grade 1) means the rat does not use its hind limb in a usual manner, but stands on it when rising; an intact function of the hind limb (grade 2) means a normal walking pattern.

3. Isolated Hepatic Perfusion

3.1. Rat Liver Metastases Model

To test the activity of TNFα in combination chemotherapy in an organ perfusion setting several methods are available. Next to lung perfusion, perfusion of the kidney and liver in rats can also be performed. The perfusion of the kidney with TNFα is accompanied by high local toxicity, limiting the maximum dosage to ineffective levels ***(14)***. Therefore we will focus on the isolated liver perfusion in which relatively high dose levels can be used. For the IHP we used male inbred WAG/Ri or Brown Norway (BN) rats, weighing 250–300 g. The rats were fed a standard laboratory diet. All animals were housed under standard conditions of light and accommodation.

Three different tumors were used in this study. The weakly immunogenic colon carcinoma CC531 is a 1,2-dimethylhydrazine-induced, moderately differentiated adenocarcinoma transplantable in syngeneic WAG/Rij rats. The estimated doubling in the liver is approx 6–8 d. The spontaneously originated nonimmunogenic osteosarcoma ROS-1 is also transplantable in the WAG/Rij

rat, and in the liver metastases model it has a mean doubling time of approx 4–5 d. The spontaneously originated nonimmunogenic soft-tissue sarcoma BN-175 is the fastest growing tumor of the tumors tested, with an estimated doubling time in the liver of approx 2–3 d and is transplantable in syngeneic BN rats. Following a standardized protocol, small viable tumor fragments of CC531, ROS-1, or BN-175 tumor fragments of 1 × 2 mm were implanted under the liver capsule, one in the left and one in the right side of the left liver lobe, using a 19-gage Luer-lock needle. The donor rat should have a tumor with an approx diameter of 12–14 mm. Comparable to the ILP experiments, we implant tumor fragments rather then injecting cells to increase reproducibility. The tumor fragments are derived from a donor rat which has been injected from a single batch of cells stored on liquid nitrogen. When the tumor is dissected from the donor rat the tumor should have a standardized size. Only the outer rim is to be used as central necrosis strongly affects tumor cell viability. Experiments started at a fixed tumor diameter between 5 and 6 mm. When tumors reached a size of 20 mm in diameter or animals showed obvious signs of discomfort the animals were sacrificed.

3.2. Rat Isolated Hepatic Perfusion Model

This rat isolated liver perfusion model has been described in detail earlier by M. G. A. van Ijken et al. ***(15)*** and B. van Etten et al. ***(16,17)***. Anesthesia was induced and maintained with ether (Merck). During the surgical procedure, with an average duration of 60–75 min, rats were kept at a constant temperature using a warmed mattress. A midline laparotomy was performed and the hepatic ligament exposed. The gastroduodenal side branch of the common hepatic artery was cannulated, positioning the tips of the cannula (0.025 in od, 0.012 in id, Dow Corning) in the proper hepatic artery. Through a small inguinal incision the femoral vein was exposed. To collect hepatic venous outflow a silicon cannula (0.047 in od, 0.025 in id, Dow Corning) was introduced in the femoral vein and moved up into the caval vein positioning the tip of the cannula at the level of the hepatic veins.

Isolation of the hepatic vascular bed was obtained by temporarily ligating the common hepatic artery and the portal vein. The venous outflow limb was isolated by temporarily clamping the suprahepatic caval vein and by applying a temporary ligature around the infrahepatic caval vein containing the cannule, cranial to the right adrenal vein. The mesenteric artery was temporarily clamped in order to reduce splanchnic blood pressure. The circuit was primed with 10 mL Haemaccel (Behring Pharma). Arterial flow of 5 mL/min was maintained with a low-flow roller pump (Watson Marlow type 505 U). Rats were perfused for 10 min with oxygenated Haemaccel in which melphalan and/or TNFα was dissolved. This short perfusion time was used as we observed

rapid clearance of melphalan from the perfusate in this timeframe. Moreover, perfusion of the liver beyond 10 min may increase the risk for tissue damage to the liver, but also to the gut as blood flow to the gut is impaired during the perfusion. Afterward a washout was performed by perfusing with 10 mL of oxygenated Haemaccel. 50 IU of Heparin (Heparine Leo) was added to the perfusate. The perfusate was oxygenated in a reservoir with a mixture of O_2/CO_2 (95%:5%) and was kept at 38–39°C by means of a heat exchanger and a warm-water bath. A temperature probe was positioned in the lumen of the arterial catheter, 5 cm from the catheter tip. Following the washout procedure, the clamps on caval vein, portal vein, hepatic artery and mesenteric artery were released. The gastroduodenal artery and femoral vein were ligated, and the gastroduodenal and femoral cannulas were removed.

3.3. Crucial Factors in Perfusion Experiments

The weight of the rat at the beginning of the experiment is crucial, particularly when a liver perfusion is conducted. When animals are too light it is rather difficult to perform this demanding technique. Monitoring of the animal weights, especially when working with TNFα, is mandatory. Weight loss is typically associated with TNFα-related toxicity and is a rather sensitive parameter for systemic toxicity. Also unusual animal behavior (lethargy), raising of hair, and diarrhea are indications for possible TNFα-related discomfort.

During the perfusion the animal is anesthetized. To prevent body temperature changes the animal is kept on a constant temperature with a warm-water mattress. Especially for the IHP, which demands longer and more intensive surgery, this is of crucial importance. Second, in the IHP setting the rats are anesthetized with ether or other inhalation anesthetics. We found that it is necessary to manipulate the anesthesia as directly as possible in the IHP setting. A surgical microscope is indispensable for the perfusion experiments, in particular for the isolated hepatic perfusion. Also the speed with which the procedure is performed may have a strong impact on the end result.

4. Assessment of Tumor Response

4.1. Assessment of Tumor Response in ILP

In the ILP setting tumor growth can easily be recorded daily after perfusion by caliper measurement. Tumor volume is calculated with the formula 0.4 ($A^2 \cdot B$), where A is the minimal tumor diameter and B the diameter perpendicular to A. Conform protocol animals were sacrificed when tumors reached a size of 25 mm in diameter or animals showed obvious signs of discomfort.

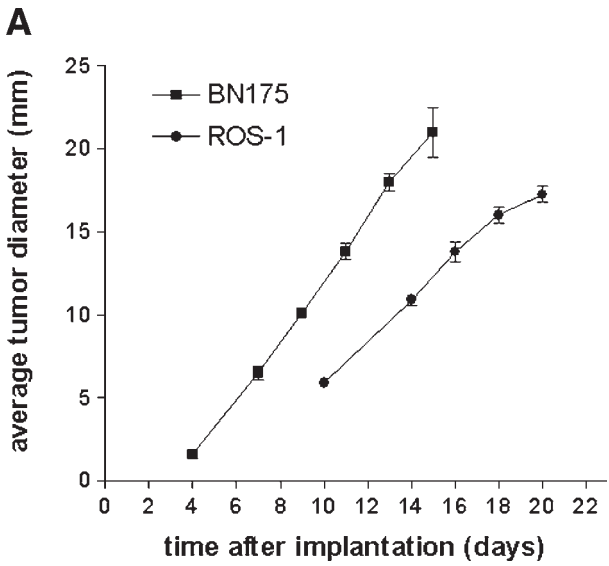

Fig. 2. Standardization of tumor growth in rat liver tumor model. To measure the tumor volume of liver metastases, incision must be made to expose the liver tumors. As these surgical procedures may influence tumor growth, we compared tumor volume after repeated surgery with endpoint measurement and MRI. The growth of both BN-175 and ROS-1 is depicted in **(A)** showing narrow spreading in tumor diameter.
(*continued*)

Classification of tumor response:

progressive disease (PD) = increase of tumor volume (>25%) within 5 d
no change (NC) = tumor volume equal to volume during perfusion (in a range of –25% and +25%)
partial remission (PR) = decrease of tumor volume (–25% and –90%)
complete remission (CR) = tumor volume 0–10% of volume during perfusion or skin necrosis

4.2. Assessment of Tumor Response in IHP

Recording of the size of liver tumors is more difficult. Normally after IHP tumor size was measured with a standardized caliper, via a small midline laparotomy every fourth day. Tumor volume was calculated as described above. As the animals undergo regular surgery an effect on tumor progression may occur. We checked for these effects by two methods. First, the effect of the tumor size measurements was determined by comparing growth rate after regular surgical interventions and one endpoint measurement. Accuracy of measurements was confirmed by MRI (**Fig. 2**). Classification of tumor response is conducted as described in the previous section.

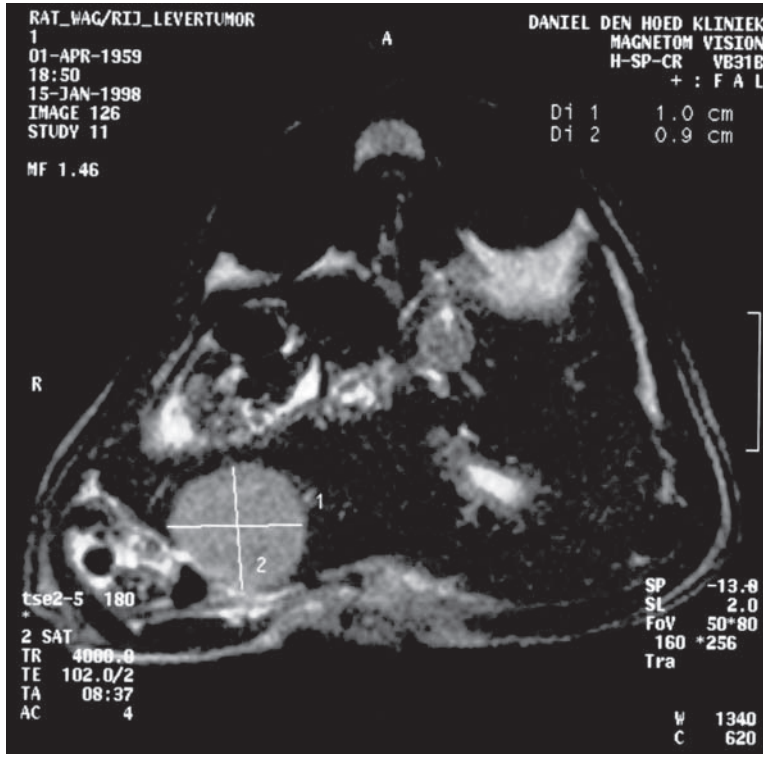

Fig. 2. (*continued*) Tumor growth, which was measured repeatedly, was not different from endpoint measurement. This was confirmed by a noninvasive technique, MRI **(B)**. Tumor volume of a ROS-1 osteosarcoma was measured 14 d after implantation showing diameters of 1.0 and 0.9 cm and a length of 1.5 cm (not shown), that correspond with the tumor size measured with calipers.

5. Measurement of Melphalan and Doxorubicin in Tissue

To evaluate the effect of TNFα on drug distribution, accumulation in the tissue and presence in the perfusate and system were measured. Here we describe the two methods we use for determining the concentrations of doxorubicin and melphalan in tumor tissue.

5.1. Assessment of Melphalan Concentration in Tissues

Five minutes after the restoration of the circulation the perfused tumor and part of the liver were excised. The tissues were immediately frozen in liquid nitrogen to stop metabolism of melphalan and stored at –80°C. Tumor and liver tissues were homogenized in 2 mL acetonitrile (Pro 200 Homogenizer, Pro Scientific) and centrifuged at 2500*g*. Melphalan was measured in the supernatant by gas chromatography-mass spectrometry (GC-MS). P-[Bis-

(2-chloroethyl) amino]-phenylacetic acid methyl ester was used as an internal standard. Samples were extracted over trifunctional C18 silica columns. After elution with methanol and evaporation, the compounds were derivatized with trifluoroacetic anhydride and diazomethane in ether. The stable derivates were separated on a methyl phenyl siloxane GC capillary column and measured selectively by single ion monitoring GC-MS in the positive EI mode described earlier by U. R. Tjaden et al. ***(18)***.

5.2. Assessment of Doxorubicin Concentration in Tissues

To determine the influence of TNFα on doxorubicin uptake in tumors during ILP, tumors (and muscle) were surgically removed after ILP and total doxorubicin content determined as previously described ***(19)***. Briefly, after incubation in acidified isopropanol (0.075 *N* HCl in 90% isopropanol) for 24 h at 4°C, the tumors were homogenized (Pro 200 Homogenizer with 10-mm generator, Pro Scientific), centrifuged for 30 min at 2500 rpm and supernatants harvested. Samples were measured in a Hitachi F4500 fluorescence spectrometer (excitation 472 nm and emission 590 nm) and compared with a standard curve prepared with known concentrations of doxorubicin diluted in acidified isopropanol. Measurements were repeated after addition of an internal doxorubicin standard. Detection limit for doxorubicin in tissue was 0.1 mg per gram tissue.

For perfusate measurements samples were drawn from the perfusion vial at 0.5, 5, 15, and 30 min after ILP was started. Samples were centrifuged for 30 min at 1400*g* and supernatant measured for doxorubicin content as described above. Cell pellets were incubated in acidified isopropanol and doxorubicin content determined as described above.

6. Systemic Treatment Protocol With Low-Dose TNFα

To study the efficacy of TNFα in systemic therapy both rat and mouse tumor models were employed. From the perfusion models we learned, as is described below, that TNFα helps the co-administered drug to enter the solid tumor. However, high local levels are reached in these perfusion settings, whereas in the systemic setting only low levels are allowed. Injection of 15 μg/kg TNFα in a 250-g rat results in a rapid dilution below 1 μg/mL. Moreover, TNFα is thereupon rapidly cleared with a half-life of approx 20 min. In the ILP model, on the other hand, 50 μg TNFα is brought in a circuit of 5 mL giving a concentration of 10 μg/mL. We have observed that this level is maintained throughout the perfusion. As TNFα is greatly diluted and cleared fast in the systemic setting, we designed a protocol in which low-dose TNFα was administered in combination with chemotherapy 5 or 10 times every 2 or 4 d. Because we

hypothesized that TNFα will augment accumulation of the co-administered drug in the tumor, we speculated that this chemotherapeutic drug should have long-circulating characteristics to maximize the chance of extravazation at the desired site. For this purpose we used the Stealth liposomal formulation of doxorubicin (Doxil® or Cealyx® in Europe) ***(20)***. This formulation exhibits a long circulation profile, characterized by a half life of approx 24 h in rats and 48 h in humans and a tendency to preferentially accumulate in tissues with leaky vessels, such as tumors ***(21)***.

In the rat model the already described BN-175 and ROS-1 tumors were used. In the mouse model the B16BL melanoma model is used. The B16BL6 tumor is a high-grade, highly vascularized melanoma which is transplantable to C57Bl6 mice. The progression of this tumor is quite rapid with a doubling time of 6 d.

6.1. Rat Models

Approximately 7–8 d after implantation, tumors reached an average diameter of 8–12 mm when treatment was started. Rats were injected five times intravenously with an interval of 4 d between injections. First injection with Doxil was 4.5 mg/kg followed by 4 injections with 1 mg/kg per injection. 15 μg/kg TNFα was administered to the rats in 0.2 mL volumes. When rats received both Doxil and TNFα these agents were injected separately. Control rats were treated with equivalent amounts of placebo liposomes (i.e., drug-free liposomes) or buffer.

6.2. Mouse Models

The B16BL6 melanoma subline, selected from a spontaneous melanoma B16F10 line, was used in our studies. Tumor cells were expanded in vitro in Dulbecco's MEM containing 10% FCS, 2 m*M* L-glutamine, 1 m*M* sodium pyruvate, MEM-nonessential amino acid, MEM vitamins, 50 U/mL penicillin, and 50 μg/mL streptomycin. On d 0 (the day of inoculation), cells were detached from the culture flask by a short EDTA treatment, washed once in complete medium, and twice in PBS. A total of 6×10^5 cells were suspended in 0.1 mL PBS and injected subcutaneously in the back (just in front of the hind limb) using a 25-gage needle. All mice used in a single experiment were inoculated on the same day using cells from the same suspension.

Treatment started at d 10 when the tumor diameter reached approx 1 cm. The tumor-bearing mice were stratified by tumor size into groups prior to the treatment. All agents were dissolved in endotoxin-free PBS as a single injection solution of 200 μL and administered intravenously via the tail vein. Tumor size was assessed at least every 3 d and expressed as tumor size index (TSI), i.e., the product of the largest perpendicular diameters.

7. Results and Conclusions

The application of TNFα in ILP was pioneered by Lejeune and Lienard in 1988. Addition of TNFα to an ILP with melphalan resulted in very high response rates in all series reported thus far. The results of TNF-based ILP in combination with melphalan with or without IFN have been published since 1992 ***(22–28)***. ILP with melphalan, doxorubicin, and a variety of other drugs was tried in the 1970s and 1980s with poor results and was largely abandoned ***(29–33)***. This changed dramatically with the introduction of TNFα. TNF-based ILP has been established as a highly effective new method of induction biochemotherapy in extremity soft-tissue sarcomas (STS) with a 20–30% complete remission rate and about a 50% partial remission rate ***(26,34,35)***. On the basis of results in a multicenter program in Europe, TNFα was approved and registered in Europe for the treatment of sarcoma by ILP in 1998.

7.1. Efficacy Testing and Possible Improvements of TNF-Based ILP

To gain further insight into the mechanisms underlying the positive results obtained with TNF-based ILP in humans, we developed extremity perfusion models in rats using the BN175 and the ROS-1 sarcomas. As stated above, the application of TNF-based ILP provides a powerful tool for the treatment of limb-threatening advanced sarcoma and melanoma. However, in spite of the high response rates, a number of patients still do not respond to this therapy adequately. Second, although TNF-based perfusions are quite powerful in treatment of tumors confined to the limbs and may also be applied when treating liver metastases, other sites are less easy to treat by this manner, as a result of high local TNF-related toxicity (e.g., kidney) or high leakage (e.g., abdominal perfusion). Therefore, improvements of the TNF-based ILP are sought to conquer these drawbacks. Next to that, the successful application of TNFα in ILP warrants developments towards application of this cytokine in the treatment of systemic disease.

7.1.1. Modification to TNF-Based ILP

In both rat sarcoma models, we could demonstrate that the tumor cells were resistant to TNFα in vitro and that ILP in vivo with TNFα alone had no major impact on tumor growth. TNF alone caused only some central necrosis, and no regression of the tumor was observed, as has been reported for the clinical setting as well. In both models a strong synergistic antitumor effect leading to response rates of 75% was observed after ILP with TNFα plus Melphalan ***(11–13)***. Histopathologically hemorrhagic necrosis was most prominent after ILP with both drugs ***(36)***.

We replaced melphalan by the anthracycline doxorubicin ***(37)***. As anthracyclines are among the most active agents against solid tumors, and

doxorubicin is the most widely used agent of this class, we speculated that doxorubicin could therefore be a suitable cytotoxic agent for ILP in sarcoma-bearing patients. However, we found that in contrast to melphalan, application of doxorubicin in ILP was limited by local toxicity already at suboptimal concentrations. Moreover, five to ten times higher concentrations of this drug were necessary to gain results comparable to melphalan. Also in this setting, where TNFα was added to doxorubicin, strong synergy was observed concerning tumor response. These results demonstrate that the activity of TNFα is drug independent.

The rat ILP model also provides an excellent tool to determine minimal concentrations levels of the drugs to inflict the desired effects. We determined that the standard TNFα dosages of 50 μg per perfusion could be lowered five-fold while maintaining its full activity. At 2 μg all TNFα effects were lost ***(11)***. These observations suggest that the clinically applied dose may be lowered, as is also indicated by the clinical results in the UK ***(23)*** and in Italy ***(38)***.

7.1.2. Addition of Potentially Synergistic Drugs to TNFα-Based ILP

The activity of TNFα toward tumor cells, and also other cells of the tumor stroma such as endothelial cells, can be enhanced by a number of agents. A cytokine well known for its synergistic activity in combination with TNFα is interferon-γ (IFN-γ). In the clinical setting the addition of IFN-γ to TNF-based ILP is disputable. We tested the activity of IFN-γ in our rat ILP model, and the activity of IFN-γ appeared to be minor. We demonstrated a 10% increase in complete response rate and an increase of about 20% in overall response rate ***(39)***, which resembles the situation in the clinic ***(28)***. Although the response rate increased only slightly by adding IFN-γ, local toxicity was negatively affected, resulting in impaired limb function. These observations would argue against the need of IFN-γ in TNF-based ILP.

Actinomycin is also a drug showing strong synergy with TNFα in vitro. However, we observed that in spite of the use of Actinomycin D in some clinics in combination with melphalan, its use is to be avoided in combination with TNFα. We recently demonstrated that the synergy between TNFα and Actinomycin D led to severe toxicity to the normal tissues and amputations in the laboratory setting ***(40)***.

Various vasoactive agents are under study for their potential role in the ILP setting. One of these, the nitric oxide synthetase inhibitors arginine analogs L-NAME and LNA were shown to enhance the antitumor effects of a TNF-based ILP melphalan ***(41)***. Similar observations have been made by us with vasoactive molecules such as histamine and serotonin (manuscript in preparation) which points to the opportunity of identifying different classes of agents that

may be able to change the pathophysiology of tumors and enhance antitumor responses.

7.1.3. Controlling ILP Conditions Favoring Outcome

Using the rat ILP models we have demonstrated that the temperatures as used in the clinic (38–39°C) are essential for obtaining a good antitumor response without damage to the normal tissues in the limb. True hyperthermia (42–43°C) resulted in a marginal increase in response, but was associated with severe damage to the normal tissues, requiring amputations of the limbs. By contrast, all antitumor efficacy was lost when perfusions were performed at room temperature ***(11)***. On this basis and on our experience that tissue temperatures in the clinical setting should be kept at 39°C to avoid any grade IV toxicities to the normal tissues, we recommend avoiding any hyperthermia in the setting of TNF-based ILP. A similar, but less dramatic enhanced toxicity to the normal tissues was observed in an anoxic setting ***(11)***.

In standard rat ILP, the perfusion time (time between tightening of the tourniquet and washout) is 30 min. Reducing perfusion time to 20 or 10 min resulted in decline in response rate; in particular, less complete responses were observed at shorter perfusion durations ***(11)***.

7.2. Mechanisms: Local and Systemic Applications of TNFα

The most important observation for understanding the synergy between TNFα and melphalan in the clinic has come from in vivo experiments in the laboratory. From studies conducted with TNFα in ILP and IHP, but also from systemic application of low-dose TNFα, we learned that TNFα by itself had no or marginal effect on tumor progression. In spite of observed massive hemorrhagic necrosis and obvious signs of tumor vascular disruption in the tumor after TNFα-based ILP, tumor progression was not altered. When an antitumor effect after TNFα-alone perfusion was observed, this effect could be related to a sensitivity of the tumor cells towards TNFα directly ***(13).*** The addition of a chemotherapeutic agent to TNF-based ILP is mandatory. We hypothesized that the synergy observed in TNF-based ILP with melphalan or doxorubicin results from a better availability of the chemotherapeutic drug in the tumor tissue. We demonstrated that the main effect of TNFα, which correlated closely with tumor response, was the induction of augmented accumulation of the co-administered drug specifically in tumor tissue ***(37–42)***. Addition of high-dose TNFα to the perfusate results in a four- to sixfold increased uptake by the tumor of the co-administered cytostatic drug. Both for melphalan and for doxorubicin, it was demonstrated that this uptake was tumor specific and that no increased uptake was noted in the normal tissues, thus emphasizing the selective action of TNFα on the tumor-associated vasculature. Whether the acute drop in interstitial fluid pressure in the tumor after exposure to TNFα, as

reported by C. A. Kristensen et al. ***(43)***, plays an essential role in TNF-based ILP, remains speculative.

Also in the systemic setting, addition of TNFα to chemotherapy results in synergistic antitumor activity ***(44)***. Important, however, is that TNFα be added to an agent with relatively long serum retention times. If TNFα was added to free doxorubicin, no beneficial effect was observed, only some tumor growth delay was achieved, and all treated rats showed progressive disease. When Doxil was combined with TNFα, a strong tumor response was observed with complete and partial responders in most of the rats. Also in this setting, addition of TNFα augmented accumulation of the drug in tumor tissue. To further decrease possible side effect and enhance delivery of TNFα to the tumor site, we encapsulated TNFα in long-circulating liposomes. Comparable to the activity of free TNFα, liposomal TNFα augmented the activity of co-administered Doxil dramatically, resulting in tumor responses in all of the rats ***(45)***. At the same time, liposomal encapsulation resulted in a reduction of the toxicity of TNFα, which increases the therapeutic index of this cytokine.

The central role of TNFα appears to be an effect on the pathophysiology of the solid tumor, resulting in changes that favor chemotherapeutic drug delivery. This indicates that TNFα may have usefulness in a number of local and systemic therapies in which delivery of the agent of choice is not adequate.

Acknowledgments

Part of the research described here was supported by the Dutch Cancer Foundation.

References

1. O'Reilly, M. S., Boehm, T., Shing, Y., Fukai, N., Vasios, G., Lane, W. S., et al. (1997) Endostatin: an endogenous inhibitor of angiogenesis and tumor growth. *Cell* **88,** 277–285.
2. Kerbel, R. and Folkman, J. (2002) Clinical translation of angiogenesis inhibitors. *Nat. Rev. Cancer* **2,** 727–739.
3. ten Hagen, T. L. M., Eggermont, A. M. M., and Lejeune, F. J. (2001) TNFα is here to stay—revisited. *Trends Immunol.* **22,** 127–129.
4. Creech, O. J., Krementz, E. T., Ryan, R. F., and Winblad, J. N. (1958) Chemotherapy of cancer: regional perfusion utilizing an extracorporeal circuit. *Ann. Surg.* **148,** 616–632.
5. Benckhuijsen, C., Kroon, B. B., Van Geel, A. N., and Wieberdink, J. (1988) Regional perfusion treatment with melphalan for melanoma in a limb: an evaluation of drug kinetics. *Eur. J. Surg. Oncol.* **14,** 157–163.
6. Thompson, J. F. and Gianoutsos, M. P. (1992) Isolated limb perfusion for melanoma: effectiveness and toxicity of cisplatin compared with that of melphalan and other drugs. *World J. Surg.* **16,** 227–233.
7. Klaase, J. M., Kroon, B. B., Van Geel, A. N., Eggermont, A. M., and Franklin, H.

R. (1993) Systemic leakage during isolated limb perfusion for melanoma. *Br. J. Surg.* **80,** 1124–1126.
8. Wieberdink, J., Benckhuysen, C., Braat, R. P., van Slooten, E. A., and Olthuis, G. A. (1982) Dosimetry in isolation perfusion of the limbs by assessment of perfused tissue volume and grading of toxic tissue reactions. *Eur. J. Cancer Clin. Oncol.* **18,** 905–910.
9. Eggermont, A. M. M. (1996) Treatment of melanoma in-transit metastases confined to the limb. *Cancer Surv.* **26,** 335–349.
10. OmLor, G., Gross, G., Ecker, K. W., Burger, I., and Feifel, G. (1992) Optimization of isolated hyperthermic limb perfusion. *World J. Surg.* **16,** 1117–1119.
11. de Wilt, J. H. W., Manusama, E. R., van Tiel, S. T., Van Ijken, M. G. A., ten Hagen, T. L. M., and Eggermont, A. M. M. (1999) Prerequisites for effective isolated limb perfusion using tumour necrosis factor alpha and melphalan in rats. *Br. J. Cancer* **80,** 161–166.
12. Manusama, E. R., Nooijen, P. T. G. A., Stavast, J., Durante, N. M. C., Marquet, R. L., and Eggermont, A. M. M. (1996) Synergistic antitumour effect of recombinant human tumour necrosis factor alpha with melphalan in isolated limb perfusion in the rat. *Br. J. Surg.* **83,** 551–555.
13. Manusama, E. R., Stavast, J., Durante, N. M. C., Marquet, R. L., and Eggermont, A. M. M. (1996) Isolated limb perfusion with TNF alpha and melphalan in a rat osteosarcoma model: a new anti-tumour approach. *Eur. J. Surg. Oncol.* **22,** 152–157.
14. Van Der Veen, A. H., Seynhaeve, A. L. B., Breurs, J., Nooijen, P. T. G. A., Marquet, R. L., and Eggermont, A. M. M. (1999) In vivo isolated kidney perfusion with TNF-alpha in tumour bearing rats. *Br. J. Cancer* **79,** 433–439.
15. Van Ijken, M. G. A., van Etten, B., de Wilt, J. H. W., van Tiel, S. T., ten Hagen, T. L. M., and Eggermont, A. M. M. (2000) Tumor necrosis factor-alpha augments tumor effects in isolated hepatic perfusion with melphalan in a rat sarcoma model. *J. Immunother.* **23,** 449–455.
16. van Etten, B., de Vries, M. R., Van Ijken, M. G. A., Lans, T. E., Guetens, G., Ambagtsheer, G., et al. (2003) Degree of tumour vascularity correlates with drug accumulation and tumour response upon TNF-alpha-based isolated hepatic perfusion. *Br. J. Cancer* **88,** 314–319.
17. van Etten, B., ten Hagen, T. L. M., de Vries, M. R., Ambagtsheer, G., Huet, T., and Eggermont, A. M. M. (2002) Prerequisites for effective adenovirus mediated gene therapy of colorectal liver metastases in the rat using an intracellular neutralizing antibody fragment to p21-Ras. *Br. J. Cancer* **86,** 436–442.
18. Tjaden, U. R. and de Bruijn, E. A. (1990) Chromatographic analysis of anticancer drugs. *J. Chromatogr.* **531,** 235–294.
19. Mayer, L. D., Tai, L. C. L., Ko, D. S. C., Masin, D., Ginsberg, R. S., Cullis, P. R., et al. (1989) Influence of vesicle size, lipid composition, and drug-to-lipid ratio on the biological activity of liposomal doxorubicin in mice. *Cancer Res.* **49,** 5922–5930.
20. Gabizon, A., Shmeeda, H., and Barenholz, Y. (2003) Pharmacokinetics of

pegylated liposomal Doxorubicin : review of animal and human studies. *Clin. Pharmacokinet.* **42,** 419–436.
21. Gabizon, A. and Papahadjopoulos, D. (1988) Liposome formulations with prolonged circulation time in blood and enhanced uptake by tumors. *Proc. Natl. Acad. Sci. USA* **85,** 6949–6953.
22. Lienard, D., Ewalenko, P., Delmotte, J. J., Renard, N., and Lejeune, F. J. (1992) High-dose recombinant tumor necrosis factor alpha in combination with interferon gamma and melphalan in isolation perfusion of the limbs for melanoma and sarcoma. *J. Clin. Oncol.* **10,** 52–60.
23. Lejeune, F. J., Lienard, D., Leyvraz, S., and Mirimanoff, R. O. (1993) Regional therapy of melanoma. *Eur. J. Cancer* **29A,** 606–612.
24. Hill, S., Fawcett, W. J., Sheldon, J., Soni, N., Williams, T., and Thomas, J. M. (1993) Low-dose tumour necrosis factor alpha and melphalan in hyperthermic isolated limb perfusion. *Br. J. Surg.* **80,** 995–997.
25. Vaglini, M., Belli, F., Ammatuna, M., Inglese, M. G., Manzi, R., Prada, A., et al. (1994) Treatment of primary or relapsing limb cancer by isolation perfusion with high-dose alpha-tumor necrosis factor, gamma-interferon, and melphalan. *Cancer* **73,** 483–492.
26. Eggermont, A. M. M., Schraffordt Koops, H., Lienard, D., Kroon, B. B. R., Van Geel, A. N., Hoekstra, H. J., et al. (1996) Isolated limb perfusion with high-dose tumor necrosis factor-alpha in combination with interferon-gamma and melphalan for nonresectable extremity soft tissue sarcomas: a multicenter trial. *J. Clin. Oncol.* **14,** 2653–2665.
27. Fraker, D. L., Alexander, H. R., Andrich, M., and Rosenberg, S. A. (1996) Treatment of patients with melanoma of the extremity using hyperthermic isolated limb perfusion with melphalan, tumor necrosis factor, and interferon gamma: results of a tumor necrosis factor dose-escalation study. *J. Clin. Oncol.* **14,** 479–489.
28. Lienard, D., Eggermont, A. M., Koops, H. S., Kroon, B., Towse, G., Hiemstra, S., et al. (1999) Isolated limb perfusion with tumour necrosis factor-alpha and melphalan with or without interferon-gamma for the treatment of in-transit melanoma metastases: a multicentre randomized phase II study. *Melanoma Res.* **9,** 491–502.
29. Stehlin, J. S., Jr., de Ipolyi, P. D., Giovanella, B. C., Gutierrez, A. E., and Anderson, R. F. (1975) Soft tissue sarcomas of the extremity. Multidisciplinary therapy employing hyperthermic perfusion. *Am. J. Surg.* **130,** 643–646.
30. Krementz, E. T., Carter, R. D., Sutherland, C. M., and Hutton, I. (1977) Chemotherapy of sarcomas of the limbs by regional perfusion. *Ann. Surg.* **185,** 555–564.
31. Klaase, J. M., Kroon, B. B., Benckhuijsen, C., Van Geel, A. N., Albus-Lutter, C. E., and Wieberdink, J. (1989) Results of regional isolation perfusion with cytostatics in patients with soft tissue tumors of the extremities. *Cancer* **64,** 616–621.
32. Rossi, C. R., Vecchiato, A., Foletto, M., Nitti, D., Ninfo, V., Fornasiero, A. X. S. G., et al. (1994) Phase II study on neoadjuvant hyperthermic-antiblastic perfusion with doxorubicin in patients with intermediate or high grade limb sarcomas. *Cancer* **73,** 2140–2146.

33. Di Filippo, F., Calabro, A. M., Cavallari, A., Carlini, S., Buttini, G. L. X. M. F., Cavaliere, F., et al. (1988) The role of hyperthermic perfusion as a first step in the treatment of soft tissue sarcoma of the extremities. *World J. Surg.* **12,** 332–339.
34. Eggermont, A. M. M., Lienard, D., Schraffordt Koops, H., Rosenkaimer, F., and Lejeune, F. J. (1993) Treatment of irresectable soft tissue sarcomas of the limbs by isolation perfusion with high dose TNF-alpha in combination with interferon-gamma and melphalan. In *Tumor Necrosis Factor: Molecular and Cellular Biology and Clinical Relevance* (Fiers, W. and Buurman, W. A., eds), Karger, Basel, pp. 239–243.
35. Eggermont, A. M. M., Schraffordt Koops, H., Klausner, J. M., Kroon, B. B. R., Schlag, P. M., Lienard, D., et al. (1996) Isolated limb perfusion with tumor necrosis factor and melphalan for limb salvage in 186 patients with locally advanced soft tissue extremity sarcomas. The cumulative multicenter European experience. *Ann. Surg.* **224,** 756–764.
36. Nooijen, P. T. G. A., Manusama, E. R., Eggermont, A. M. M., Schalkwijk, L., Stavast, J., Marquet, R. L., et al. (1996) Synergistic effects of TNF-alpha and melphalan in an isolated limb perfusion model of rat sarcoma: a histopathological, immunohistochemical and electron microscopical study. *Br. J. Cancer* **74,** 1908–1915.
37. Van Der Veen, A. H., de Wilt, J. H. W., Eggermont, A. M. M., van Tiel, S. T., Seynhaeve, A. L. B., and ten Hagen, T. L. M. (2000) TNF-alpha augments intratumoural concentrations of doxorubicin in TNF-alpha-based isolated limb perfusion in rat sarcoma models and enhances anti-tumour effects. *Br. J. Cancer* **82,** 973–980.
38. Rossi, C. R., Foletto, M., Di Filippo, F., Vaglini, M., Anza, M., Azzarelli, A., et al. (1999) Soft tissue limb sarcomas: Italian clinical trials with hyperthermic antiblastic perfusion. *Cancer* **86,** 1742–1749.
39. Manusama, E. R., de Wilt, J. H. W., ten Hagen, T. L. M., Marquet, R. L., and Eggermont, A. M. M. (1999) Toxicity and anti-tumor activity of interferon gamma alone and in combination with TNF alpha and melphalan in isolated limb perfusion in the BN175 sarcoma tumor model in rats. *Oncol. Rep.* **6,** 173–177.
40. Seynhaeve, A. L. B., de Wilt, J. H. W., van Tiel, S. T., Eggermont, A. M. M., and ten Hagen, T. L. M. (2002) Isolated limb perfusion with actinomycin D and TNF-alpha results in improved tumour response in soft-tissue sarcoma-bearing rats but is accompanied by severe local toxicity. *Br. J. Cancer* **86,** 1174–1179.
41. de Wilt, J. H., Manusama, E. R., van Etten, B., van Tiel, S. T., Jorna, A. S., Seynhaeve, A. L., et al. (2000) Nitric oxide synthase inhibition results in synergistic anti-tumour activity with melphalan and tumour necrosis factor alpha-based isolated limb perfusions. *Br. J. Cancer* **83,** 1176–1182.
42. de Wilt, J. H. W., ten Hagen, T. L. M., de Boeck, G., van Tiel, S. T., de Bruijn, E. A., and Eggermont, A. M. M. (2000) Tumour necrosis factor alpha increases melphalan concentration in tumour tissue after isolated limb perfusion. *Br. J. Cancer* **82,** 1000–1003.

43. Kristensen, C. A., Nozue, M., Boucher, Y., and Jain, R. K. (1996) Reduction of interstitial fluid pressure after TNF-alpha treatment of three human melanoma xenografts. *Br. J. Cancer* **74,** 533–536.
44. ten Hagen, T. L. M., Van Der Veen, A. H., Nooijen, P. T. G. A., van Tiel, S. T., Seynhaeve, A. L. B., and Eggermont, A. M. M. (2000) Low-dose tumor necrosis factor-alpha augments antitumor activity of stealth liposomal doxorubicin (DOXIL) in soft tissue sarcoma-bearing rats. *Int. J. Cancer* **87,** 829–837.
45. ten Hagen, T. L. M., Seynhaeve, A. L. B., van Tiel, S. T., Ruiter, D. J., and Eggermont, A. M. M. (2002) Pegylated liposomal tumor necrosis factor-alpha results in reduced toxicity and synergistic antitumor activity after systemic administration in combination with liposomal doxorubicin (Doxil) in soft tissue sarcoma-bearing rats. *Int. J Cancer* **97,** 115–120.

18

Strategies for Improving the Anti-Neoplastic Activity of TNF by Tumor Targeting

Angelo Corti

Summary

The clinical use of tumor necrosis factor (TNF) as an anticancer drug has been so far limited to loco-regional treatments because of severe dose-limiting toxicity. This chapter intends to review the targeting approaches and the animal models that have been developed in an attempt to improve the therapeutic activity of this cytokine and to enable systemic administration of a therapeutic dose. Using various animal models, evidence was obtained to suggest that the targeting approach could indeed improve the therapeutic properties of this cytokine, either alone or in combination with chemotherapy. Targeted delivery of TNF can be achieved by targeting tumor cell antigens, directly or indirectly by a pretargeting approach, or by targeting antigens expressed within tumor vessels. In both cases the mechanism of the improved antitumor activity appears to be related to indirect effects of TNF on tumor-associated vessels. Thus, targeting markers that are selectively expressed or upregulated in angiogenic tumor vessels seems to be the best choice for developing TNF conjugates with improved activity.

Key Words: Tumor necrosis factor; tumor therapy; tumor targeting; vascular targeting; TNF-antibody conjugates; TNF-peptide conjugates; chemotherapy.

1. Introduction

Tumor necrosis factor (TNF) was originally identified for its cytotoxic activity against some tumor cell lines and for its ability to induce hemorrhagic necrosis of transplanted solid tumors ***(1,2)***. The impressive antitumor activity in animal models raised high expectations for the results of clinical trials in patients. Unfortunately, phase I–II clinical trials showed that systemic administration of TNF to patients was accompanied by prohibitive toxicity, the maximum tolerated dose (8–10 μg/kg) being 10–50 times lower than the estimated effective dose. For this reason, systemic administration of TNF has been essentially

From: *Methods in Molecular Medicine, Vol. 98: Tumor Necrosis Factor*
Edited by: A. Corti and P. Ghezzi © Humana Press Inc., Totowa, NJ

discontinued. Nevertheless, some features of TNF activity, in particular its still unexplained selectivity for the tumor vasculature, which eventually leads to the hemorrhagic necrosis of the tumor, have continued to nourish hopes as regards the possibility of a therapeutic application of TNF in patients. This hope implies, however, the need to find a way to increase the therapeutic index of this cytokine, i.e., to reduce its systemic toxicity and/or to increase its selectivity for the tumor.

Among the various approaches that have been pursued, regional and local administrations have produced the most important results in patients. Regional administration of relatively high doses of TNF, in combination with chemotherapeutic drugs, by isolated limb or hepatic perfusion has produced high response rates in patients with melanoma and sarcoma of the extremities ***(3–5)*** as well as regression of bulky hepatic cancer confined to the liver ***(6)***. These results are of outstanding interest because they show that, in principle, the antitumor effects of TNF can be exploited therapeutically in humans with great success if sufficient dose levels can be attained locally, while shielding the organism from the systemic toxic effects of TNF.

Several lines of evidence suggest that the antitumor activity of TNF depends on indirect mechanisms associated with selective obstruction and damage of tumor-associated vessels and with activation of immune mechanisms, rather than TNF's having toxic effects directly on tumor cells ***(7–10)***. This activity is thought to be caused by the combination of direct toxic effects of TNF on endothelial cells of the tumor vasculature ***(11)*** as well as to a TNF-induced shift from anticoagulant to procoagulant of the hemostatic properties of the same cells ***(9)***. Accordingly, the micro- and macrovasculature of tumors, but not of normal tissue, were extensively damaged after patients were given isolated limb perfusion with TNF in combination with interferon-γ and melphalan ***(4)***. TNF-induced T-cell-dependent immunity, which may contribute to tumor regression ***(10)***, may also be secondary to vascular damage and necrosis. Indeed, recent evidence suggests that tumor necrosis may, *per se*, favor the insurgence of an efficient antitumor response ***(12)*** that could contribute to a positive feedback loop leading to tumor regression. Unfortunately, the same target cells (endothelial cells) that play a pivotal role in mediating the antitumor effects of TNF are also at the origin of hypotension, the almost universal dose-limiting toxicity for systemically administered TNF. This characteristic is an obvious reason why the therapeutic window was found to be so narrow for this route of administration.

These results and considerations provide the rational for targeting TNF to tumors as a strategy for increasing its therapeutic index. This chapter intends to review the targeting approaches and the animal models that have been so far developed in the attempt to improve the therapeutic activity of this cytokine as an anticancer drug.

2. Targeted Delivery of TNF to Tumor Cells With Antibody Conjugates

2.1 Rationale

The therapeutic index of a drug is given by the ratio between efficacy and toxicity. Thus, the therapeutic index of TNF could be increased either by increasing its efficacy or by decreasing its toxicity. Therapeutic strategies based on targeted delivery of TNF to tumors are aimed at increasing the efficacy without changing the toxicity.

It has been estimated on the basis of preclinical and clinical studies that a dose 10- to 50-fold higher than the maximum tolerated dose (200–400 $\mu g/m^2$) is necessary to induce antitumor effects in humans ***(13)***. The targeting approach offers, in principle, the possibility of administering systemically low doses (lower than the maximum tolerated dose) and of achieving effective concentrations at the tumor site.

The most obvious approach that has been pursued to this purpose has been the preparation of conjugates of TNF with tumor-specific monoclonal antibodies (mAb). The concept that a localized action of TNF (at the tumor site or on other cells in close vicinity) could result in efficient antitumor effects is supported by the observation that expression of the TNF gene in tumor cells correlates with reduced tumorigenicity and invasiveness ***(14)***.

2.2. Antibody-TNF Conjugates

The feasibility of producing bifunctional antibody-TNF conjugates is well documented. $F(ab')_2$-like mAb fusion proteins can be constructed by fusing part of the heavy chain gene of an antitransferrin receptor mAb with the TNF gene and expressing the construct in a light chain-secreting transfectoma cell line ***(15)***. The fusion protein is cytotoxic to a human cell line that is resistant to normal TNF at 100-fold higher concentrations. Another genetically engineered hybrid protein was expressed in *E. coli* by fusing the N-terminus of TNF with the C-terminus of the hinge region of a mAb against the tumor-associated TAG72 antigen expressed by colorectal, gastric, and ovarian adenocarcinoma ***(16)***. The same authors reported in another paper the production of a monovalent Fv-TNF fusion protein, and showed that this conjugate is able to form bioactive trimers under nondenaturing conditions ***(17)***.

The tissue disposition, pharmacokinetic, and therapeutic properties of an antimelanoma ZME antibody-TNF conjugate have been reported ***(18)***. Tissue distribution studies in nude mice bearing human melanoma xenografts showed similar tumor localization of the conjugate compared to the free antibody, and slightly higher concentrations in liver and kidney compared to ZME itself. Treatment of nude mice bearing well-developed A375 tumors with the immunotoxin results in a statistically significant suppression in tumor growth rate (fivefold increase) compared to saline-treated controls ***(18)***.

The single-chain recombinant antibody sFv23 recognizes the cell-surface domain of HER2/neu. The cDNA for this antibody was fused to the cDNA encoding human TNF, and the fusion protein was expressed in *E. coli* cells ***(19)***. Cytotoxicity studies against human breast carcinoma cells (SKBR-3-HP) overexpressing HER2/neu demonstrate that the sFv23/TNF fusion construct is 1000-fold more active than free TNF.

2.3. Limitations of the Antibody-Directed Targeting Approach

Despite the promising results of in vitro experiments, the antibody-directed targeting approach may present limitations that must be taken into account when these conjugates are used in vivo. The TNF receptors in normal tissues are likely much greater in number than those in the tumor. Thus, in order to have a reasonable chance to accumulate on tumors rather than on normal tissues, the affinity of the antibody moiety for its target must be significantly greater than that of TNF for its receptors (TNFR-1, Kd $\simeq 0.5 \times 10^{-9}M$; TNFR-2, Kd $\simeq 0.1 \times 10^{-9}M$). Otherwise, the latter would become the rate-limiting step, thereby overcoming the tumor-specific homing effect of the antibody moiety. Indeed, it was reported that a mAb-TNF conjugate with a relatively low affinity for its antigen (Kd = $10^{-8}M$), when administered to animals, is unable to home the cytokine to the antibody-binding site, and is more toxic than TNF, presumably because of its longer half-life ***(20)***. This characteristic may limit the applicability of this strategy, considering the relatively high affinity of TNF–TNFR interactions compared to those of many known antibody–antigen interactions. One possibility for overcoming this problem is, in principle, the development of conjugates that interact simultaneously with both tumor antigens and TNF receptors on tumor cells. Simultaneous binding to both antigens and receptors is expected to result in high-avidity interactions at the tumor site where the antigen is expressed.

Pretargeting strategies, a different approach that will be discussed in the following section, might offer another solution for bypassing this problem.

Another important potential limitation is that targeted tumor cells can internalize antibody-TNF conjugates after binding, thereby preventing the interaction of TNF with other important targets within the tumor, e.g., endothelial cells.

3. Targeted Delivery of Biotin-TNF to Tumor Cells After Pretargeting With Biotinylated Antibodies and Avidin

3.1. Rationale

Tumor pretargeting with biotinylated antibodies and avidin, followed by a delayed delivery of radioactively labeled biotin, is currently used for in vivo cancer diagnosis in patients ***(21)*** and for therapy ***(22)***. Moreover, the same pretargeting strategy was exploited to deliver biotinylated IgE ***(23)***,

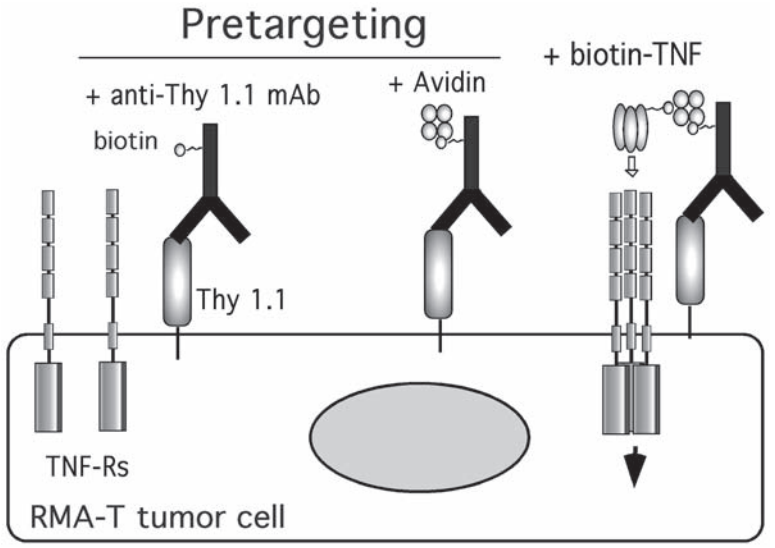

Fig. 1. Schematic representation of tumor pretargeting with biotinylated antibodies and avidin in the RMA-T model. This approach is based on administration of anti-Thy 1.1 biotinylated antibody (mAb 19E12) and avidin to tumor bearing mice, followed by administration of biotin-TNF.

biotinylated B7-immunoglobulin conjugates ***(24)***, or biotinylated cells ***(25)*** to tumors. The good localization of the radiolabeled biotin observed with CEA-positive tumors, cerebral gliomas, ocular melanoma, and neuroendocrine tumors pretargeted with various mAbs ***(21)*** implies that avidin can efficiently localize at tumor sites in patients. Thus, it has been hypothesized that tumor pretargeting with avidin could also be exploited for delivering low doses (non-toxic) of biotinylated TNF to the tumor site, taking advantage of the high affinity of the biotin–avidin interaction.

3.2. In Vitro and In Vivo Models for Investigating the Tumor Pretargeting Approach

To investigate this hypothesis we developed two models for in vitro and in vivo studies based on mouse RMA lymphoma and mouse WEHI-164 fibrosarcoma cells (called RMA-T and WEHI-164-T). These cells were transfected with the *Thy 1.1* allele to create a unique tumor-associated antigen ***(26)***. This antigen can be pretargeted with a biotinylated anti-Thy 1.1 monoclonal antibody (mAb) and avidin. Avidin, in turn, can work as an artificial receptor that increases the amount of biotin-TNF bound to tumor cells ***(26)*** (*see* **Fig. 1** for a schematic representation of the RMA-T model). To perform in vivo experiments, these cells were transplanted, subcutaneously, to C57BL6 or BALB/c

mice *(7)*. Because both animal strains express the *Thy 1.2* allele, the Thy 1.1 antigen enable in vivo tumor avidination by systemic administration of an anti-Thy 1.1 biotinylated antibody (mAb19E12) and, 24 h later, by avidin. In vitro experiments showed that the persistence of biotin-TNF on the tumor cell surface could be increased up to 30 times compared to TNF *(26)*. Furthermore, bound biotin-TNF is able to trigger cytolytic effects in vitro and to decrease the growth rate of tumor cells in vivo, under conditions in which TNF is almost inactive *(26)*. Thus, biotin-TNF bound via the antibody/avidin bridge can interact with natural receptors and trigger biological responses. In vivo experiments showed that the activity of 1 μg biotin-TNF, either murine or human, is significantly increased by antibody/avidin pretargeting and is comparable to that of 5–10 μg on nonpretargeted tumors *(7)*. Pretargeting does not increase the toxicity of biotin-TNF, as judged from animal survival and weight loss after treatment. Thus, pretargeting increases at least fivefold the antitumor activity of biotin-TNF, apparently without changing its systemic toxicity.

3.3. Mechanism of Action

The following considerations suggest that the mechanism of action of biotin-TNF in these models is mainly indirect. First, although biotin-TNF could not kill WEHI-164-T and RMA-T cells in vitro, both tumors can undergo massive hemorrhagic necrosis and growth arrest when targeted with biotin-TNF in vivo *(7,26)*. Second, tumor targeting with biotin-TNF affects well-established and vascularized tumors (older than 6–7 d), but not avascular freshly transplanted tumors *(7)*. This strongly suggests that targeted TNF does not exert critical effects against the antibody-targeted cells themselves, but more likely acts by affecting other targets within established tumors, likely the vasculature.

Biotin-TNF, once bound to neutravidin, slowly disappears from the cell surface, while a relatively large amount of bioactive-TNF is released in the culture medium *(27)*. Dissociation kinetics studies indicated that the mechanism of TNF release is mainly dependent on TNF subunit dissociation from the pretargeting complex, and much less on dissociation of the antibody from the cell surface *(27)*. It is noteworthy that biotin-TNF, after dissociation, can diffuse and interact not only with TNF receptors on the targeted cell, but also with the receptors expressed by bystander cells (e.g., endothelial cells). Thus, the main mechanism underlying the interaction between targeted biotin-TNF and TNF receptors relies on trimer dissociation, subunit reassociation and interaction with TNF receptors located on targeted cells as well as on nontargeted bystander endothelial cells (*see* **Fig. 2** for a schematic representation). The lack of internalization and the capability of affecting bystander cells may overcome one of the major drawbacks of TNF-mAb conjugates discussed above.

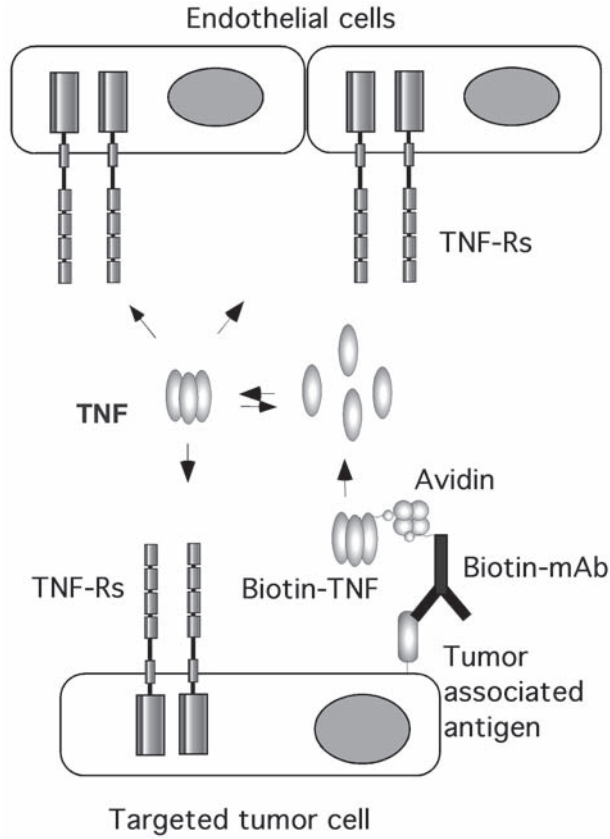

Fig. 2. Schematic representation of the mechanism of action of biotin-TNF, targeted to tumor cells via antibody-avidin bridges, on endothelial cells. Bioactive TNF trimers are slowly released in the tumor microenvironment after dissociation of non biotinylated TNF subunits and reassociation.

3.4. Optimization of Biotin-TNF Conjugate

Biotinylation of TNF can be easily achieved using D-biotinyl-6-aminocaproic acid *N*-hydroxysuccinimide ester. Human TNF contains six lysine residues and one α-amino group that could react with D-biotinyl-6-aminocaproic acid *N*-hydroxysuccinimide ester. Thus, the degree and the sites of biotinylation can vary depending on the reaction conditions.

Structure–activity relationship studies carried out with various biotin-TNF conjugates have shown that the biological activity and the release of bioactive TNF from the targeting complex are strongly dependent on the number of biotins/TNF trimers ***(27,28)***. Biotin-TNF conjugates can be characterized by

trypsin digestion and electrospray ionization mass spectrometry ***(28)***. Typically, these conjugates contain a mixture of trimers made by monomers with 0, 1, and 2 biotins. About a half of these biotins are linked to the TNF α-amino terminus, while the remaining part is linked to the ε-amino group of lysines, distributed in various proportion among Lys^{128}, Lys^{112}, and Lys^{65}. Thus the N-terminal ε-amino group is the most reactive site in the conjugation reaction with biotin-6-aminocaproyl-*N*-hydroxysuccinimide ester, while other sites, including Lys^{11}, Lys^{90}, and Lys^{98} are virtually not modified, even under strong reaction conditions. Biotin-TNF conjugates with more than 1 biotin/trimer (on average), despite being active in cytolytic assays, are inactive in vivo with pretargeted tumors. Apparently, nonbiotinylated subunits must be present in the biotin-TNF trimers for an efficient release of bioactive TNF from the targeting complex. Presumably, hyperbiotinylation increases the binding strength and/or rebinding of subunits to the immobilized avidin and consequently decreases the overall release.

3.5. Tumor Targets

Various antibodies against natural tumor-associated antigens have already been used, in combination with avidin, for delivering biotinylated radiolabeled conjugates to tumors in patients ***(21,22,29)***. These antibodies, in principle, could be exploited also for targeted delivery of biotin-TNF to tumors in patients.

4. Targeted Delivery of TNF to Tumor Angiogenic Vessels

4.1. Rationale and Targeting Ligands

The selectivity of TNF toward the tumor vasculature and the observation that the primary mechanism of action of this cytokine is based on tumor vessel damage provide the rationale for developing a vascular targeting approach to increase the TNF therapeutic index. In view of the marked damage that TNF can cause to endothelial cells of angiogenic vessels ***(30)***, one attractive possibility is the targeting of vascular proliferation antigens, e.g., angiogenesis associated fibronectin isoforms ***(31)*** or angiogenic vessel endothelium markers ***(32–35)***.

In vivo panning of phage libraries in tumor-bearing animals has proven useful for selecting peptides able to interact with angiogenic vessel endothelium markers and to home to tumors ***(36)***. Among the various peptides identified so far, the CNGRC-peptide has proven useful for delivering various antitumor compounds, such as chemotherapeutic drugs and apoptotic peptides, to tumor vessels ***(36–38)***. This peptide is an aminopeptidase N (CD13) ligand ***(39)***. Besides CNGRC, other tumor vasculature targeting peptides containing the NGR motif have been identified, such as linear NGRAHA and cyclic CVLNGRMEC ***(36)***. These and other linear and cyclic NGR-peptides have

been used for targeting viral particles to endothelial cells ***(40,41)***. Both linear GNGRG and cyclic CNGRC, fused with the N-terminus of TNF by genetic engineering technology, can target TNF to tumors ***(38,42)***. However, the antitumor activity of CNGRC-TNF (called NGR-TNF) is greater than 10-fold higher than that of GNGRG-TNF, the cystine flanking NGR residues being critical for the targeting efficiency. Molecular dynamics simulation studies of CNGRC with or without disulfide-bridge strongly support the hypothesis that peptide cyclization is indeed critical for stabilizing the structure of the NGR motif. Thus, CNGRC is the preferred choice as a TNF targeting ligand.

4.2. Production of NGR-TNF and Characterization of Its Antitumor Activity

Human and murine TNF and NGR-TNF conjugates (consisting of TNF fused with the C-terminus of CNGRCG) can be prepared by recombinant DNA technology and purified by ammonium sulfate precipitation, hydrophobic interaction chromatography, ion exchange, and gel filtration chromatography ***(38)***. Because bioactive TNF is a compact homotrimeric protein ***(43)***, only fractions corresponding to trimeric species, i.e., eluted at 40,000–50,000 Mr in the final chromatographic step, must be collected during the purification procedure. The molecular mass of murine TNF and NGR-TNF monomers are 17,386.1 ± 2.0 Da and 17,843.7 ± 2.5 Da, respectively, by electrospray mass spectrometry (expected for Met-$TNF_{1–156}$, 17,386.7 Da; for CNGRCG-$TNF_{1–156}$, 17,844.2 Da). The in vitro cytotoxic activities of TNF and NGR-TNF are $(1.2 \pm 0.14) \times 10^8$ units/mg and $(1.8 \pm 0.7) \times 10^8$ units/mg, respectively, by standard cytolytic assay with L-M mouse fibroblasts, indicating that the CNGRCG moieties in the NGR-TNF molecule do not prevent folding, oligomerization, or binding to TNF receptors.

The antitumor activity of murine NGR-TNF against RMA-T lymphoma or B16F1 melanoma models is 12–15 times greater than that of murine TNF, whereas its toxicity, judged by survival and loss of body weight after treatment, is similar to that of TNF ***(38)***. Tumor regression induced by NGR-TNF is often accompanied by protective immunity, suggesting that targeted delivery of TNF to CD13 may enhance its immunotherapeutic properties and may, therefore, represent a new approach to reduce the tumor burden prior to other therapeutic interventions.

4.3. Mechanism of Action of NGR-TNF

The antitumor activity of NGR-TNF, but not that of TNF, is inhibited by anti-CD13 mAbs ***(38)***. This indicates that CD13 plays a critical role in NGR-TNF's antitumor effects. These effects are unlikely to be related to inhibition of CD13 function by the NGR domain of NGR-TNF, because a CNGRC-peptide

injected alone or in combination with TNF does not induce measurable effects. Notably, RMA-T tumor cells do not express CD13. Nevertheless, the growth of tumors derived from these cells in vivo is affected by relatively low doses of NGR-TNF. This result is in keeping with the original hypothesis that vascular targeting, rather than direct tumor-cell targeting, potentiates the antitumor response of low doses of this cytokine.

In addition to endothelial cells of angiogenic vessels, most cells of myeloid origin, including monocytes, macrophages, granulocytes, and their hematopoietic precursors, express CD13 ***(44–46)***. This peptidase is also abundantly expressed in the brush border of epithelial cells from renal proximal tubules and small intestine, in prostatic epithelial cells, in bile duct canaliculi, in mast cells, and, in some cases, in fibroblasts and smooth muscle cells ***(45,47–50)***. The molecular mechanisms underlying the selective interaction of low doses of NGR-mTNF with CD13 in tumor blood vessels have been partially elucidated. We have recently shown that different CD13 isoforms are expressed in tumor-associated vessels, in epithelia, and in myeloid cells, and that the NGR domain of NGR-TNF selectively recognizes a CD13 isoform associated with tumor vessels ***(51)***. These findings provide a functional mechanism for the tumor homing properties of NGR–drug conjugates and may have important implications in the development of vascular-targeted therapies based on the NGR/CD13 system.

NGR-TNF and TNF behave similarly when used to treat tumors immediately after implantation (i.e., at an "avascular" stage of the tumor) and differently with well-established tumors. This effect is in line with the hypothesis that tumor vessels are important sites of NGR-TNF action, and should be kept in mind when new animal models are developed for testing these TNF derivatives.

Given that tumor vessels as well as normal vessels express TNF receptors, the mechanism of the preferential interaction of NGR-TNF with tumor vessels remains to be clarified. Possibly, low blood levels of NGR-TNF can rapidly interact with CD13-positive endothelial cells because of high-avidity multivalent binding involving both CD13 and TNFRs, and less with CD13-negative endothelial cells of normal vessels, because of lower avidity. A schematic representation of the hypothetical high-avidity interactions of NGR-TNF with membrane receptors is shown in **Fig. 3**.

5. Improving Chemotherapeutic Drug Penetration in Tumors by Vascular Targeting and Barrier Alteration

5.1. Rationale

The addition of TNF to regional isolated limb perfusion with melphalan or doxorubicin has produced higher response rates in patients with extremity soft-tissue sarcomas or melanomas than those obtained with chemotherapeutic

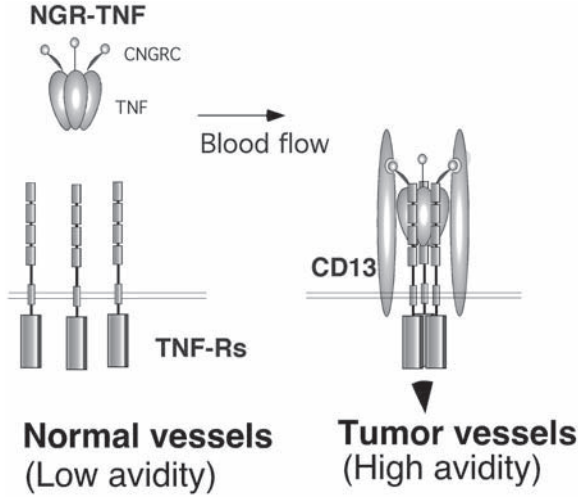

Fig. 3. Hypothetical mechanism of the stronger interaction of a very low dose of NGR-TNF (100 pg) with CD13–positive tumor blood vessels, compared to normal vessels. The expression of CD13 (coreceptor) is expected to increase the avidity of the interaction with membrane receptors.

drugs alone ***(3–5,52,53)***. TNF-induced alteration of endothelial barrier function, reduction of tumor interstitial pressure, and increased chemotherapeutic drug penetration are believed to be important mechanisms of the synergy between TNF and chemotherapy ***(4,52,54–57)***. Indeed, heterogeneous tumor perfusion, vascular permeability and cell density, and increased interstitial pressure could represent critical barriers that may limit the penetration of drugs into neoplastic cells distant from tumor vessels and, consequently, the effectiveness of chemotherapy ***(58)***. Strategies aimed at improving drug penetration in tumors are, therefore, of great experimental and clinical interest.

Homing low doses of NGR-TNF to tumor vessels may represent a new strategy to avoid toxic reactions while preserving its synergism with chemotherapy.

5.2. Animal Models for the NGR-TNF/Cytotoxic Drug Combination Therapy

To investigate the antitumor activity of NGR-TNF in combination with melphalan or doxorubicin, the following murine models, based on subcutaneous RMA-T lymphoma and B16F1 melanoma tumors, can be used: C57BL/6 mice weighing 16–18 g are challenged with subcutaneous injection in the left flank of 5×10^4 RMA-T or B16F1 living cells; 4–12 d later, the mice are treated with TNF or NGR-TNF solutions (100 μL) followed 2 h later by administration of melphalan or doxorubicin solution (100 μL). The tumor growth can

then be monitored daily with calipers. To assess the penetration of doxorubicin in tumors (diameter, 0.5–1 cm), tumor-bearing mice are treated with or without NGR-mTNF (0.1 ng, ip), followed 2 h later by doxorubicin (320 μg, ip). After 2 h the animals are sacrificed and the tumors are excised. Each tumor is then weighed, disaggregated, resuspended in cold phosphate-buffered saline (PBS) and filtered through 70-μm filters. The cells can then be resuspended with cold PBS (50 mL), centrifuged (1500 rpm, 10 min, 4°C), resuspended again in cold PBS (2.5 mL/g of tumor tissue) and mixed with freshly prepared PBS containing 8% formaldehyde (2.5 mL/g of tissue). The cells can be stored in the dark at 4°C overnight, and then analyzed by FACS. The FACScan (Becton-Dickinson) is calibrated with cells recovered from untreated tumors. Each sample is then analyzed using the FL-3 filter and Cell Quest software.

In these models, administration of minute amounts of NGR-TNF (0.01–0.1 ng/mouse, about 10^6-fold lower than the LD50) to tumor-bearing animals potentiates the antitumor activity of melphalan and doxorubicin with no evidence of increased toxicity, as judged by tumor mass reduction, animal survival, and weight loss after treatment ***(59)***. This result suggests that NGR-TNF improves the therapeutic index of these drugs. It is noteworthy that 5×10^4–fold greater doses of TNF (e.g., 5 μg/mouse in the B16F1 model) are necessary to enhance the effect of melphalan to comparable levels, causing marked loss of body weight ***(59)***. NGR-TNF increases both the percentage of cancer cells that can be reached by doxorubicin as well as the intracellular amount of drug, suggesting that NGR-TNF can alter drug-penetration barriers.

5.3. Mechanism of the Synergistic Action of NGR-TNF Chemotherapy

The fact that both melphalan and doxorubicin at doses virtually inactive in the B16F1 model reduce tumor growth when combined with NGR-mTNF indicates that these drugs act synergistically. Studies on the mechanism of action showed that the synergism relies on the interaction of NGR-mTNF with TNFR-1 on stromal cells, most likely endothelial cells, and much less on tumor cells ***(51)***.

Previous studies showed that TNF can rapidly increase endothelial permeability ***(60,61)***, and can decrease interstitial fluid pressure ***(55)***, believed to be important barriers for drug penetration in tumors ***(58)***. Possibly, these mechanisms increase convective transport of drugs through tumor vessel walls and interstitia, finally resulting in increased drug uptake by tumor cells. Besides these mechanisms, other known effects of TNF on endothelial cells could contribute to its overall antitumor activity, including the induction of endothelial leukocyte adhesion molecules, inflammatory cytokines, chemokines, class II molecules, and procoagulant factors ***(1,2)***. These mechanisms are not mutually exclusive and, together with improved chemotherapeutic drug penetration, could contribute to activate inflammatory and immune responses.

5.4. Vascular Targeting and Soluble TNF Receptor Shedding

After infusion in animals or patients, TNF can also induce negative feedback mechanisms that neutralize most of its antitumor effects. For example, TNF, even at moderate doses, can induce the release of soluble p55 and p75 TNF receptors that may prevent its interaction with membrane receptors ***(62,63)***. Although these soluble inhibitors may protect the body from the harmful effects of this cytokine, they may also prevent its antitumor activity and could explain, in part, the need of high doses of TNF for effective therapy.

The hypothesis that vascular targeting could avoid toxic reactions as well as negative feedback mechanisms, usually associated with TNF therapy, is supported by the observation that picogram doses of NGR-mTNF do not induce soluble receptor shedding, while both NGR-mTNF and mTNF rapidly induce the release of sTNFR-2 into the circulation at doses greater than 4–10 ng ***(59)***.

5.5. Potential Clinical Implication of the Vascular Targeting Approach

Molecules containing the CNGRC motif are expected to target murine as well as human angiogenic vessels ***(36,51)***. Thus, human NGR-TNF might be expected to have better antitumor properties than human TNF in patients, based on what we observed with mouse NGR-TNF in animal models. Findings from murine models suggest that doses required for antitumor effectiveness in humans are at least one order of magnitude higher than the maximum tolerated dose. Thus, it is possible that targeted delivery of TNF to aminopeptidase N could contribute to overcoming this problem. Moreover, NGR-TNF cDNA could be used for gene therapy in place of the TNF gene ***(64)***, and biotinylated NGR-TNF could be used, in principle, in tumor pretargeting with biotinylated antibodies and avidin to further increase its therapeutic index. Because tumor debulking with targeted TNF is associated with induction of protective immunity in our models, one appealing possibility is that this approach could be useful to reduce the tumor burden prior to other therapeutic intervention aimed at treating the minimal residual disease (e.g., immunotherapy, antiangiogenic therapy, conventional chemotherapy, and so forth), particularly those relying on a functional immune system.

6. Conclusions

Targeted delivery of TNF either to tumor cells, by a pretargeting approach, or to protein expressed within activated vessels may improve its therapeutic index. In both cases the mechanism of the improved activity appears to be related to indirect effects of TNF on tumor associated vessels. These findings suggest that targeting components of the vascular compartment of the tumor, rather than tumor cells themselves, is a more effective strategy for improving the therapeutic index of this cytokine. Thus, markers of tumor blood vessels

that are selectively expressed or upregulated during angiogenesis could be potential targets for developing TNF conjugates with improved activity. Moreover, the therapeutic properties of NGR-TNF reveal the potential of peptide sequences obtained from the screening of phage display libraries to generate a new class of recombinant cytokines that, compared to immunocytokines, have a simpler structure, could be more easily produced, and are potentially less immunogenic.

Acknowledgments

This work was supported by Associazione Italiana Ricerca sul Cancro (AIRC).

References

1. Fiers, W. Biologic therapy with TNF: preclinical studies. In *Biologic Therapy of Cancer: Principles and Practice* (De Vita, V., Hellman, S., and Rosenberg, S., eds.), Lippincott, Philadelphia, 1995, pp. 295–327.
2. Fraker, D. L., Alexander, H. R., and Pass, H. I. Biologic therapy with TNF: systemic administration and isolation-perfusion. In *Biologic Therapy of Cancer: Principles and Practice* (De Vita, V., Hellman, S., and Rosenberg, S., eds.), Lippincott, Philadelphia, 1995, pp. 329–345.
3. Lienard, D., Ewalenko, P., Delmotte, J. J., Renard, N., and Lejeune, F. J. (1992) High-dose recombinant tumor necrosis factor alpha in combination with interferon gamma and melphalan in isolation perfusion of the limbs for melanoma and sarcoma. *J. Clin. Oncol.* **10,** 52–60.
4. Eggermont, A. M., Schraffordt Koops, H., Lienard, D., Kroon, B. B., van Geel, A. N., Hoekstra, H. J., et al. (1996) Isolated limb perfusion with high-dose tumor necrosis factor-alpha in combination with interferon-gamma and melphalan for nonresectable extremity soft tissue sarcomas: a multicenter trial. *J. Clin. Oncol.* **14,** 2653–2665.
5. Fraker, D. L., Alexander, H. R., Andrich, M., and Rosenberg, S. A. (1996) Treatment of patients with melanoma of the extremity using hyperthermic isolated limb perfusion with melphalan, tumor necrosis factor, and interferon gamma: results of a tumor necrosis factor dose-escalation study. *J. Clin. Oncol.* **14,** 479–489.
6. Alexander, H. R., Jr., Bartlett, D. L., Libutti, S. K., Fraker, D. L., Moser, T., and Rosenberg, S. A. (1998) Isolated hepatic perfusion with tumor necrosis factor and melphalan for unresectable cancers confined to the liver. *J. Clin. Oncol.* **16,** 1479–1489.
7. Gasparri, A., Moro, M., Curnis, F., Sacchi, A., Pagano, S., Veglia, F., et al. (1999) Tumor pretargeting with avidin improves the therapeutic index of biotinylated tumor necrosis factor alpha in mouse models. *Cancer Res.* **59,** 2917–2923.
8. Nawroth, P., Handley, D., Matsueda, G., De Waal, R., Gerlach, H., Blohm, D., et al. (1988) Tumor necrosis factor/cachectin-induced intravascular fibrin formation in meth A fibrosarcomas. *J. Exp. Med.* **168,** 637–647.

9. Nawroth, P. P. and Stern, D. M. (1986) Modulation of endothelial cell hemostatic properties by tumor necrosis factor. *J. Exp. Med.* **163,** 740–745.
10. Palladino, M. A., Jr., Shalaby, M. R., Kramer, S. M., Ferraiolo, B. L., Baughman, R. A., Deleo, A. B., et al. (1987) Characterization of the antitumor activities of human tumor necrosis factor-alpha and the comparison with other cytokines: induction of tumor-specific immunity. *J. Immunol.* **138,** 4023–4032.
11. Clauss, M., Murray, J. C., Vianna, M., de Waal, R., Thurston, G., Nawroth, P., et al. (1990) A polypeptide factor produced by fibrosarcoma cells that induces endothelial tissue factor and enhances the procoagulant response to tumor necrosis factor/cachectin. *J. Biol. Chem.* **265,** 7078–7083.
12. Musiani, P., Modesti, A., Giovarelli, M., Cavallo, F., Colombo, M. P., Lollini, P. L., et al. (1997) Cytokines, tumor-cell death and immunogenicity: a question of choice. *Immunol. Today* **18,** 32–36.
13. Van Ostade, X., Vandenabeele, P., Everaerdt, B., Loetscher, H., Gentz, R., Brockhaus, M., et al. (1993) Human TNF mutants with selective activity on the p55 receptor. *Nature* **361,** 266–269.
14. Vanhaesebroeck, B., Mareel, M., Van Roy, F., Grooten, J., and Fiers, W. (1991) Expression of the tumor necrosis factor gene in tumor cells correlates with reduced tumorigenicity and reduced invasiveness in vivo. *Cancer Res.* **51,** 2229–2238.
15. Hoogenboom, H. R., Volckaert, G., and Raus, J. C. (1991) Construction and expression of antibody-tumor necrosis factor fusion proteins. *Mol. Immunol.* **28,** 1027–1037.
16. Yang, J., Raju, R., Sharma, R., and Xiang, J. (1995) A genetically engineered fusion protein M4/TNF with increased bifunctional activity refolded in the presence of protein disulfide isomerase. *Hum. Antibod. Hybridomas* **6,** 129–136.
17. Yang, J., Moyana, T., and Xiang, J. (1995) A genetically engineered single-chain FV/TNF molecule possesses the antitumor immunoreactivity of FV as well as the cytotoxic activity of tumor necrosis factor. *Mol. Immunol.* **32,** 873–881.
18. Rosenblum, M. G., Cheung, L., Mujoo, K., and Murray, J. L. (1995) An antimelanoma immunotoxin containing recombinant human tumor necrosis factor: tissue disposition, pharmacokinetic, and therapeutic studies in xenograft models. *Cancer Immunol. Immunother.* **40,** 322–328.
19. Rosenblum, M. G., Horn, S. A., and Cheung, L. H. (2000) A novel recombinant fusion toxin targeting HER-2/NEU-over-expressing cells and containing human tumor necrosis factor. *Int. J. Cancer* **88,** 267–273.
20. Pietersz, G. A. and McKenzie, F. C. The genetic engineering of antibody constructs for diagnosis and therapy. In *Monoclonal Antibodies. The Second Generation* (Zola, H., ed.), BIOS Scientific Publishers Ltd, Oxford, UK, 1995, pp. 93–117.
21. Paganelli, G., Magnani, P., Siccardi, A., and Fazio, F. Clinical application of the avidin-biotin system for tumor targeting. In *Cancer Therapy with Radiolabeled Antibodies* (Goldenberg, D., ed.), CRC, Boca Raton, FL, 1995, pp. 239–253.
22. Paganelli, G., Grana, C., Chinol, M., Cremonesi, M., De Cicco, C., De Braud, F., et al. (1999) Antibody-guided three-step therapy for high grade glioma with yttrium-90 biotin. *Eur. J. Nucl. Med.* **26,** 348–357.

23. Reali, E., Greiner, J. W., Corti, A., Gould, H. J., Bottazzoli, F., Paganelli, G., et al. (2001) IgEs targeted on tumor cells: therapeutic activity and potential in the design of tumor vaccines. *Cancer Res.* **61,** 5517–5522.
24. Moro, M., Gasparri, A. M., Pagano, S., Bellone, M., Tornaghi, P., Veglia, F., et al. (1999) Induction of therapeutic T-cell immunity by tumor targeting with soluble recombinant B7-immunoglobulin costimulatory molecules. *Cancer Res.* **59,** 2650–2656.
25. Guttinger, M., Guidi, F., Chinol, M., Reali, E., Veglia, F., Viale, G., et al. (2000) Adoptive immunotherapy by avidin-driven cytotoxic T lymphocyte-tumor bridging. *Cancer Res.* **60,** 4211–4215.
26. Moro, M., Pelagi, M., Fulci, G., Paganelli, G., Dellabona, P., Casorati, G., et al. (1997) Tumor cell targeting with antibody-avidin complexes and biotinylated tumor necrosis factor alpha. *Cancer Res.* **57,** 1922–1928.
27. Corti, A., Gasparri, A., Sacchi, A., Curnis, F., Sangregorio, R., Colombo, B., et al. (1998) Tumor targeting with biotinylated tumor necrosis factor alpha: structure-activity relationships and mechanism of action on avidin pretargeted tumor cells. *Cancer Res.* **58,** 3866–3872.
28. Magni, F., Curnis, F., Marazzini, L., Colombo, R., Sacchi, A., Corti, A., et al. (2001) Biotinylation sites of tumor necrosis factor-alpha determined by liquid chromatography-mass spectrometry. *Analyt. Biochem.* **298,** 181–188.
29. Paganelli, G., Magnani, P., Zito, F., Villa, E., Sudati, F., Lopalco, L., et al. (1991) Three-step monoclonal antibody tumor targeting in carcinoembryonic antigen-positive patients. *Cancer Res.* **51,** 5960–5966.
30. Ruegg, C., Yilmaz, A., Bieler, G., Bamat, J., Chaubert, P., Chaubert, P., et al. (1998) Evidence for the involvement of endothelial cell integrin alpha v beta 3 in the disruption of the tumor vasculature induced by TNF and IFN-gamma. *Nat. Med.* **4,** 408–414.
31. Neri, D., Carnemolla, B., Nissim, A., Leprini, A., Querze, G., Balza, E., et al. (1997) Targeting by affinity-matured recombinant antibody fragments of an angiogenesis associated fibronectin isoform. *Nat. Biotechnol.* **15,** 1271–1275.
32. Essler, M. and Ruoslahti, E. (2002) Molecular specialization of breast vasculature: a breast-homing phage-displayed peptide binds to aminopeptidase P in breast vasculature. *Proc. Natl. Acad. Sci. USA* **99,** 2252–2257.
33. Ruoslahti, E. (2002) Drug targeting to specific vascular sites. *Drug Discov. Today* **7,** 1138–1143.
34. Pasqualini, R., Arap, W., and McDonald, D. M. (2002) Probing the structural and molecular diversity of tumor vasculature. *Trends Mol. Med.* **8,** 563–571.
35. Arap, W., Kolonin, M. G., Trepel, M., Lahdenranta, J., Cardo-Vila, M., Giordano, R. J., et al. (2002) Steps toward mapping the human vasculature by phage display. *Nat. Med.* **8,** 121–127.
36. Arap, W., Pasqualini, R., and Ruoslahti, E. (1998) Cancer treatment by targeted drug delivery to tumor vasculature in a mouse model. *Science* **279,** 377–380.
37. Ellerby, H. M., Arap, W., Ellerby, L. M., Kain, R., Andrusiak, R., Rio, G. D., et

al. (1999) Anti-cancer activity of targeted pro-apoptotic peptides. *Nat. Med.* **5,** 1032–1038.
38. Curnis, F., Sacchi, A., Borgna, L., Magni, F., Gasparri, A., and Corti, A. (2000) Enhancement of tumor necrosis factor alpha antitumor immunotherapeutic properties by targeted delivery to aminopeptidase N (CD13). *Nat. Biotechnol.* **18,** 1185–1190.
39. Pasqualini, R., Koivunen, E., Kain, R., Lahdenranta, J., Sakamoto, M., Stryhn, A., et al. (2000) Aminopeptidase N is a receptor for tumor-homing peptides and a target for inhibiting angiogenesis. *Cancer Res.* **60,** 722–727.
40. Grifman, M., Trepel, M., Speece, P., Gilbert, L. B., Arap, W., Pasqualini, R., et al. (2001) Incorporation of tumor-targeting peptides into recombinant adeno-associated virus capsids. *Mol. Ther.* **3,** 964–975.
41. Liu, L., Anderson, W. F., Beart, R. W., Gordon, E. M. and Hall, F. L. (2000) Incorporation of tumor vasculature targeting motifs into moloney murine leukemia virus env escort proteins enhances retrovirus binding and transduction of human endothelial cells. *J. Virol.* **74,** 5320–5328.
42. Colombo, G., Curnis, F., De Mori, G. M., Gasparri, A., Longoni, C., Sacchi, A., et al. (2002) Structure-activity relationships of linear and cyclic peptides containing the NGR tumor-homing motif. *J. Biol. Chem.* **277,** 47,891–47,897.
43. Corti, A., Fassina, G., Marcucci, F., Barbanti, E., and Cassani, G. (1992) Oligomeric tumour necrosis factor alpha slowly converts into inactive forms at bioactive levels. *Biochem. J.* **284,** 905–910.
44. Chen, H., Kinzer, C. A., and Paul, W. E. (1996). p161, a murine membrane protein expressed on mast cells and some macrophages, is mouse CD13/aminopeptidase N. *J. Immunol.* **157,** 2593–2600.
45. Riemann, D., Kehlen, A., and Langner, J. (1999). CD13—not just a marker in leukemia typing. *Immunol. Today* **20,** 83–88.
46. Drexler, H. G. (1987) Classification of acute myeloid leukemias—a comparison of FAB and immunophenotyping. *Leukemia* **1,** 697–705.
47. Taylor, A. (1993) Aminopeptidases: structure and function. *FASEB J.* **7,** 290–298.
48. Shipp, M. A. and Look, A. T. (1993) Hematopoietic differentiation antigens that are membrane-associated enzymes: cutting is the key. *Blood* **82,** 1052–1070.
49. Razak, K. and Newland, A. C. (1992) The significance of aminopeptidases and haematopoietic cell differentiation. *Blood Rev.* **6,** 243–250.
50. Dixon, J., Kaklamanis, L., Turley, H., Hickson, I. D., Leek, R. D., Harris, A. L., et al. (1994) Expression of aminopeptidase-n (CD 13) in normal tissues and malignant neoplasms of epithelial and lymphoid origin. *J. Clin. Pathol.* **47,** 43–47.
51. Curnis, F., Arrigoni, G., Sacchi, A., Fischetti, L., Arap, W., Pasqualini, R., et al. (2002) Differential binding of drugs containing the NGR motif to CD13 isoforms in tumor vessels, epithelia and myeloid cells. *Cancer Res.* **62,** 867–874.
52. Lejeune, F. J. (1995) High dose recombinant tumour necrosis factor (rTNF alpha) administered by isolation perfusion for advanced tumours of the limbs: a model for biochemotherapy of cancer. *Eur. J. Cancer* **31A,** 1009–1016.

53. Rossi, C. R., Foletto, M., Di Filippo, F., Vaglini, M., Anza, M., Azzarelli, A., et al. (1999) Soft tissue limb sarcomas: Italian clinical trials with hyperthermic antiblastic perfusion. *Cancer* **86,** 1742–1749.
54. van der Veen, A. H., de Wilt, J. H., Eggermont, A. M., van Tiel, S. T., Seynhaeve, A. L., and ten Hagen, T. L. (2000) TNF-alpha augments intratumoural concentrations of doxorubicin in TNF-alpha-based isolated limb perfusion in rat sarcoma models and enhances anti-tumour effects. *Brit. J. Cancer* **82,** 973–980.
55. Kristensen, C. A., Nozue, M., Boucher, Y. and Jain, R. K. (1996) Reduction of interstitial fluid pressure after TNF-alpha treatment of three human melanoma xenografts. *Brit. J. Cancer* **74**, 533–536.
56. Suzuki, S., Ohta, S., Takashio, K., Nitanai, H., and Hashimoto, Y. (1990) Augmentation for intratumoral accumulation and antitumor activity of liposome-encapsulated adriamycin by tumor necrosis factor-alpha in mice. *Int. J. Cancer* **46,** 1095–1100.
57. de Wilt, J. H., ten Hagen, T. L., de Boeck, G., van Tiel, S. T., de Bruijn, E. A., and Eggermont, A. M. (2000) Tumour necrosis factor alpha increases melphalan concentration in tumour tissue after isolated limb perfusion. *Brit. J. Cancer* **82,** 1000–1003.
58. Jain, R. K. (1994) Barriers to drug delivery in solid tumors. *Scientific American* **271,** 58–65.
59. Curnis, F., Sacchi, A., and Corti, A. (2002) Improving the response of tumors to chemotherapy in mice by targeted delivery of picogram doses of tumor necrosis factor-alpha to tumor vessels. *J. Clin. Invest.* 475–482.
60. Brett, J., Gerlach, H., Nawroth, P., Steinberg, S., Godman, G., and Stern, D. (1989) Tumor necrosis factor/cachectin increases permeability of endothelial cell monolayers by a mechanism involving regulatory G proteins. *J. Exp. Med.* **169,** 1977–1991.
61. Goldblum, S. E. and Sun, W. L. (1990) Tumor necrosis factor-alpha augments pulmonary arterial transendothelial albumin flux in vitro. *Am. J. Physiol.* **258,** L57–L67.
62. Aderka, D., Sorkine, P., Abu-Abid, S., Lev, D., Setton, A., Cope, A. P., et al. (1998) Shedding kinetics of soluble tumor necrosis factor (TNF) receptors after systemic TNF leaking during isolated limb perfusion. Relevance to the pathophysiology of septic shock. *J. Clin. Invest.* **101,** 650–659.
63. Sella, A., Aggarwal, B. B., Kilbourn, R. G., Bui, C. A., Zukiwski, A. A., and Logothetis, C. J. (1995) Phase I study of tumor necrosis factor plus actinomycin D in patients with androgen-independent prostate cancer. *Cancer Biother.* **10,** 225–235.
64. Mizuguchi, H., Nakagawa, T., Toyosawa, S., Nakanishi, M., Imazu, S., Nakanishi, T., et al. (1998) Tumor necrosis factor alpha-mediated tumor regression by the in vivo transfer of genes into the artery that leads to tumors. *Cancer Res.* **58,** 5725–5730.